AUTOMATED VISUAL INSPECTION FOR THE QUALITY CONTROL OF PAD PRINTING

by

NICHOLAS DAVID FREEAR

A thesis submitted to

The University of Birmingham

for the degree of

DOCTOR OF PHILOSOPHY

Schools of Engineering

The University of Birmingham

December 2001

Abstract

Pad printing is used to decorate consumer goods largely because of its unique ability to apply graphics to doubly curved surfaces. The Intelpadrint project was conceived to develop a better understanding of the process and new printing pads, inks and printers. The thesis deals primarily with the research of a printer control system including machine vision. At present printing is manually controlled. Operator knowledge was gathered for use by an *expert* system to control the process. A novel *local corner-matching* algorithm was conceived to effect image segmentation, and neuro-fuzzy techniques were used to recognise patterns in printing errors. Non-linear Finite Element Analysis of the rubber printing-pad led to a method for pre-distorting artwork so that it would print undistorted on a curved product. A flexible, more automated printer was developed that achieves a higher printing rate. Ultraviolet-cured inks with improved printability were developed. The image normalisation/ error-signalling stage in inspection was proven in isolation, as was the pattern recognition system.

To Matt and my parents,

your support is everything...

Acknowledgements

The research forms part of the Brite-Euram III Intelpadprint project BE 96-3180, funded through the European Commission. The author would like to thank the EC, and the partners: Maastricht University (NL), Philips CFT and Philips DAP (NL), Marabu GmbH (DE), Tampoprint GmbH and Alfa Tools GmbH (DE), LEGO Group and Lego Engineering A/S (DK).

Particular thanks are due to Calle Scmidt (LEGO), Andreas Reiss (Tampoprint) and Ronald Westra (Masstricht).

Thank you..

David Pycock at the University, for advice and the use of image processing equipment.

Brian Jarvis of Tru-turn Engineering, for making sense of my drawings.

Ken Greening of Greening Technology and Wolfgang Doll at esd-electronics GmbH (DE), for introducing the mysteries of CAN-bus.

Dr. Kevin Howson and Richard White at Kane Computing, for patience in the face of many machine vision questions.

Bob Harrison, Bill Hewitt, Wei Li, etc. formerly in the School of Manufacturing and Mechanical Engineering.

All my friends have supported me, but particular thanks are due to Chris, Steve, Charlotte, Dave Lopes, Mike Wong, Briony, James T., Mel, Will and Luis for being in the front line.

Finally to my principal supervisor, Dr. James Shippen – my biggest thank you.

Glossary of Terms

Pad printing

In the context of pad printing the:

cliché is the plate etched with the graphic, from which ink is taken up to be deposited on the product. In the closed system the cliché must be doubled in length to accommodate the cup. Solid steel, magnetic, and plastic coated clichés are used, and at present chemical etching is employed.

closed cup (also *closed system)* is the inverted ink reservoir pressed against the cliché, and incorporating a *squeegee* rim. Invented by Tampoprint, it minimises solvent loss, reducing health risks, and increasing the stability of the ink viscosity.

Corona (heat) treatment aids ink adhesion to some plastics and is performed prior to pad printing.

doctor-blade (-ring) see squeegee

double print is often required, particularly when printing light colours on dark objects, to give the required opacity. Two or more consecutive print cycles with the same ink may be employed on the same part of an object.

fast when applied to solvents [or inks] means rapid evaporation

gravure is the etched area of the cliché which contains ink

Klischee German spelling of cliché

open system (cf *Closed cup*) uses the original printing process, where a blade scoops ink from an open trough onto the cliché (allowing solvent loss).

pad is the term for a deformable ink-applicator commonly made from silicon rubber. Many geometries and sizes of pads are used for different applications, while pads are also specified in terms of their hardness (*Shore A*) and *quality*.

pre-distortion (compensatory distortion) If a line is to be straight after pad printing but is found to "smile" it can be pre-distorted such that a "frown" on the cliché produces the desired linear effect.

quality (as applied to the pad) suitable for, for example, aggressive inks, high mechanical endurance, or low static charge

raster is an effect used to blend an ink-colour with, typically, the background colour. It is produced by circular depressions in the cliché invisible to the unaided eye which are densely packed near the border of a block of colour, then gradually become less frequent away from the border.

release ink release from the printing pad

Shore(A) is a measure of rubber hardness, the typical range for printing pads being 1 (softest) to 18 Shore A [British Standards Institution BS903, 1995]

substrate is the article on which the decoration is printed. Typically discrete objects are decorated using pad printing, as opposed to the continuous *webs* found in textile and paper printing.

squeegee is a fine rim or blade used to remove excess ink from the cliché prior to ink take-up.

Tampon is the German term for *pad* (above).

Tampoprint-type system On Tampoprint closed-cup pad printers the pad only moves vertically and the cliché moves horizontally under the stationary ink-pot. On some other makes of machine, the

pad moves vertically and is coupled to move horizontally with the ink-pot while the cliché is stationary.

caret arrow head mark indicating to the typesetter where material is to be inserted

flong papier-mâché sheet used for making stereotype moulds; mould made of this

intaglio, gravure technique of printing from a plate in which the images are incised rather than raised

letterpress technique of printing from raised inked surfaces

Linotype machine for setting an entire line of type on a single slug or metal bar

lithography technique of printing from a plate treated so that some areas accept ink while others reject it

logotype single piece of type bearing two or more characters

mackle blur or double impression on a printed sheet

offset printing process in which ink is transferred from the plate to an offset cylinder or other surface and then to the substrate

quoin wedge used to lock type in a chase

registration exact alignment of print an a page

stereotype, cliché printing plate cast from a papier-mâché mould

Plastics

Abbreviations for polymers used in Intelpadprint:

ABS acrylonitrile butadiene styrene (thermoplastic)

Evoprene tradename

Hi-PS high density polystyrene

PA polyamide

PC polycarbonate

PP polypropylene (thermoplastic)

PPO polypropylene oxide

PU polyurethane (thermosetting)

SEBS ?? Styrene-Butadiene-Styrene

Silicone rubber thermosetting elastomer

Photography, image processing and machine vision

CCD charge coupled device, is a semi-conductor matrix of light sensitive elements used in digital cameras

chromaticity see 'HSI'

CMY the cyan-magenta-yellow colour model, cf. 'RGB'

convex hull/ set a collection of values in parameter space whose boundary is not concave at any point

frame-grabber a card attached to a computer bus which synchronises and quantises (digitises) image signals from a camera or other source

HSI the hue-saturation-intensity colour model where the *hue* is the pure colour (blue, green, yellow), *saturation* is the proportion of white in the pure colour, and *intensity*. Hue and saturation constitute the *chromaticity* which is de-coupled from the *luminance* (brightness or intensity)

hue see 'HSI'

luminance see 'HSI'

*L*a*b** CIELAB colour model

mondrian a test image containing a grid of variegated coloured patches

PAL a colour television broadcasting standard used in Europe (phase alternation line)

oclusion occurs where one object obscures another in an image

RGB the red-green-blue colour model uses the additive primaries (mixture of light)

saturation see 'HSI'

Project and other acronyms:

Aloxid aluminium oxide

CFT Philips Centre for Fabrication Technology (Dutch)

CID one-dimensional *cumulative intensity distribution* of the difference between the image and a reference related to the distance to the printed border.

DAP Philips Domestic and personal care products

dms demonstration system: 2nd Intelpadprint system

IPP Intelpadprint project

LCA(-diag) (Fuzzy) linear correlation algorithm developed for Intelpadprint (-diagnosis)

Nd:YAG neodymium: yttrium aluminium garnet laser

OCAP Out of control action plan (Intelpadprint)

ppt pre-prototype: 1st Intelpadprint system

TTL transistor-transistor logic (through the lens)

Contents

List of Figures

Chapter 4: figures

Chapter 5: figures

Chapter 6: figures

Chapter 7: figures

Chapter 8: figures

1 Introduction

1.1 Transfer pad printing

In pad or *tampo-graphic* printing the recessed areas and channels that comprise the graphic on a flat plate or *gravure* called the *cliché* are filled with ink and the excess is removed with a metal *doctor* blade or *squeegee*. A flexible pad or *tampon* deforms onto the cliché to pick up the ink film, which is then released on the product or *substrate* as illustrated in Figure 1.1. Pad printing is used mainly on consumer goods, especially for logos and labelling on electrical appliances such as washing machines and DVD players. It is also applied to toys, bottles and ceramics.

The deformable pad makes this the only printing process that can decorate doubly curved surfaces, and this is its principal advantage over competing printing processes. Other advantages are the ability to print on wet ink (*wet-on-wet*) and fine lines, the high printing rate theoretically achievable, low cost and robustness of the process. However the need to integrate pad printing in automated production lines and to print very fine lines (0.03mm) on small radii substrates has resulted in unacceptably high reject rates of approximately 5 percent, leading to an estimated cost of £120 million (170M euros) per annum [Intelpadprint, 2000]. There has been little research into pad printing so the Intelpadprint project was conceived to maintain and increase the use of pad printing in niche applications and to benefit the European consumer goods industry.

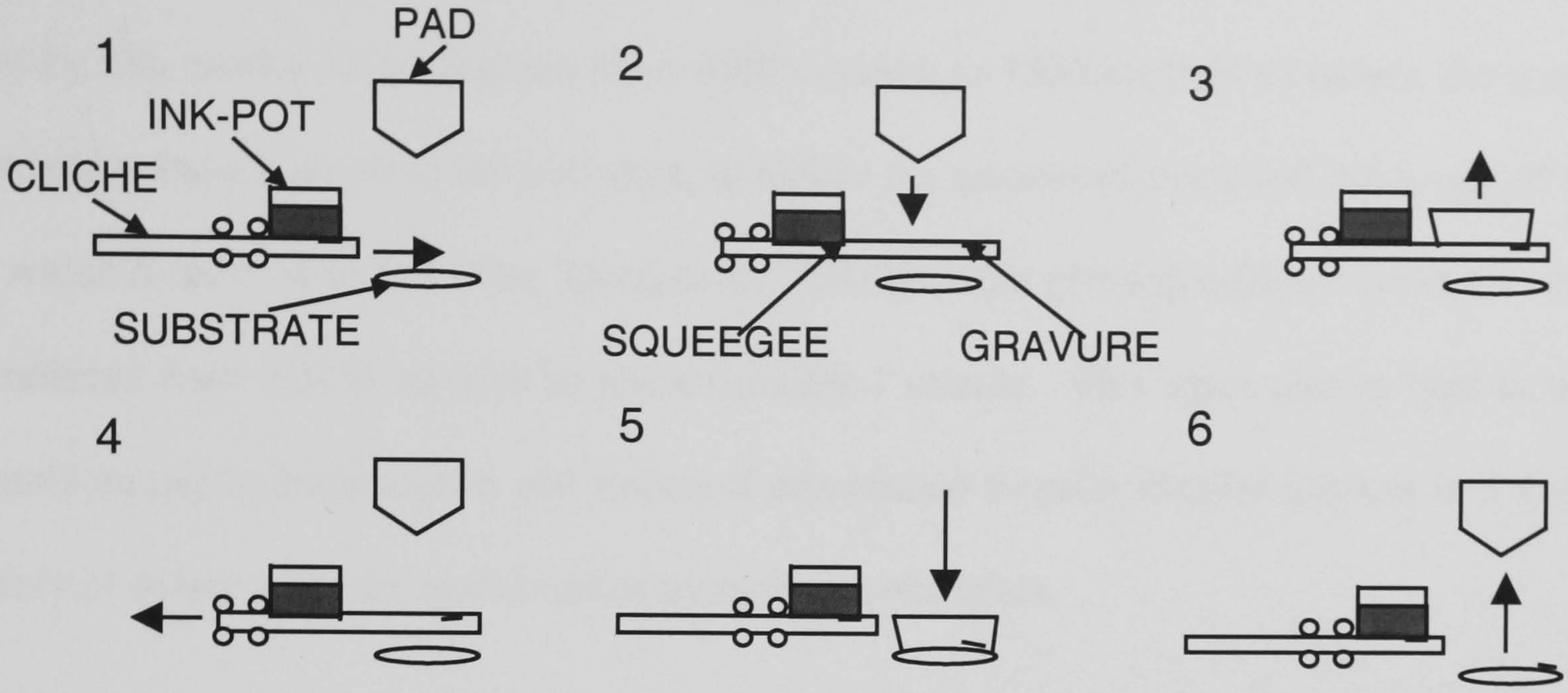

Figure 1.1. The pad printing process (closed system)

1.2 The Intelpadprint project

The full title of the Intelpadprint project was "*Development of an intelligent learning pad printing system.*" It had a duration of three years and started in December 1996. The time-plan for the project was specified in the project programme and defined eleven tasks (see Table 1.3). Tasks one to six lead to the construction and testing of a pre-prototype printing system, while tasks six to ten build on this and culminate in a demonstration printing system. The aims of the European-wide project are to produce a new printing system including pads, inks and clichés, and incorporating intelligent quality control, while undertaking fundamental research into the process.

The objectives of the Intelpadprint project are summarised in Table 1.1. The minimum width of a printed line was to be reduced by a factor of three to 30μm to meet user and consumer demand for fine detail. The maximum dry ink thickness needed to be trebled to approximately 10μm to increase the opacity, particularly of light coloured inks on dark substrates. This

improves the brightness and the overall appearance of pad printed products. The maximum printing rate needed to be doubled from 3600 cycles/h to 7200 cycles/h to reduce the number of printers that are required for a product, to reduce the amount of stock and the length of time for which it must be stored. The 'changeover' time between printing different products was to be reduced from 10–30 minutes to approximately 1 minute. This again allows 'just in time' manufacturing to be practiced and makes it economical to print smaller batches in a greater variety of colour schemes as demanded by modern consumers.

Table 1.1 Intelpadprint project objectives [Intelpadprint, 2000]

Feature	**Current**	**Project target**
* minimum printed line width	100μm	30μm
* ink dry layer thickness	3-5μm	10-12μm
* maximum print rate	3600/ h	7200/ h
* changeover time (including start-up)	10-30 minutes	≤1 minute
* reject rate	5%	0.1%
* ink adhesion (to ISO)	1-3	0
* ink wear resistance	Limited, Rda 1-3	Very good, Rda 0
* ink chemical resistance	Limited, Rhc 1-2	Very good, Rhc 0
* inks	Solvent-based	Little or no solvent
* Other features:	* Operator-assisted, with empirical knowledge * High ink usage * Labour-intensive (expensive)	* Computer-controlled, operator independent process * Low ink use, robust process * Computer controlled, inexpensive process

As Table 1.1 shows the reject rate of 5% must be reduced dramatically to 0.1%. Printing occurs after most other manufacturing stages (except assembly and packing) so the value of the product is high at this stage and it is vital to keep waste to a minimum. Lowering the reject rate reduces material, inspection and operator costs, and allows the high printing rate to be maintained. A lot of waste occurs during or shortly after changeover as the printer is reset by a process of trial and error. The current high-solvent inks are to be replaced with low or solvent-less inks. During drying all solvent is lost through evaporation so reducing the consumption of solvent reduces waste and the impact on the environment and operators. The new inks would also be more wear and chemical resistant to increase the life in service of the product and improve the appearance of the product during its life.

The unit of chemical resistance Rhc is defined for a range of 3 (least resistance) to 0 in Table 1.2. The chemicals used are ethanol and white spirit. The unit of wear resistance Rda is defined for a range of 6 (least resistance) to 0.

Table 1.2 Definitions of chemical resistance and mechanical resistance

Chemical resistance, Rhc	no defect after N abrasions with chemical, N	Wear resistance, Rda	no damage after N rotations with abrasive, N
3	10	6	20
2	25	5	35
1	50	4	60
0	100	3	100
-	-	2	175
		1	300
		0	500

According to Table 1.1 the pad printers will become more autonomous to make them suitable for integrated production lines and to reduce the amount of operator intervention. An operator will be able to supervise more than one machine, the process will be more robust and there will be greater reproducibility in the set up of printing systems. Increasing automation is strongly related to lowering the reject rate and changeover time while increasing the printing rate. Overall the aim was to reduce the cost of pad printing and increase the flexibility and ability to react to consumer fashion.

The parts of the project being addressed in Birmingham were investigating pad geometry and print distortion on doubly curved surfaces, and developing the control hardware and software. These will impact particularly on the reject rate, changeover time, degree of operator intervention and the cost of pad printing.

The aims of the PhD were based on those for the Intelpadprint project: to research and develop a control system with Maastricht University that enabled the project objectives in Table 1.1 to be achieved.

1.3 Partner profiles

The Intelpadprint consortium comprises six European partners and, of those, four are industrial and represent the complete supply chain. The Intelpadprint project was funded by the *European Commission* through the Brite-Euram scheme (project BE 96-3180).

1.3.1 LEGO Group

Lego is a world famous producer of toys with an educational emphasis, for children of all ages. The company was founded by Ole Kirk Christiansen, in Billund, Denmark. In 1998 LEGO had a net turnover of £750 million (DKK 7680 M) and employed ten thousand people. It is an end-user of pad printing and its role was to investigate the prevalence of printing defects and their impact on production, and to test the new pad printing systems.

1.3.2 Maastricht University

Maastricht University was founded in 1976 in the Netherlands, and is a small but thriving university with ten thousand students. Personnel involved in Intelpadprint from Maastricht were from the Mathematics Department and specialised in control through Artificial Neural Networks and Fuzzy Logic.

1.3.3 Marabu GmbH

Marabu was founded in 1859 and originally made draughtsman's products, before moving to industrial inks and specialist paints for artists. It is based in Tamm, near Stuttgart and their turnover in 1999 was £52 million (DM 140 M). Its role in the project was developing, testing and supplying new inks.

1.3.4 Philips

The Dutch company Philips is a leading name in the electronics industry, producing a diverse range of consumer goods and contributing many components to other companies' products. In 1999 Philips achieved sales of EUR 31,459 M and it employs 227 thousand people in sixty

countries. The Intelpadprint project involved the Philips Domestic Appliances and Personal Care Products (DAP) business unit which produces among others the *Philishave* range, and Philips Centre for Fabrication Technology (CFT). Philips-DAP is an end-user of Intelpadprint, while Philips-CFT was the project co-ordinator and performed research for Intelpadprint on pads, inks and clichés.

1.3.5 Tampoprint and Alfa Tools GmbH

Tampoprint and its subsidiary Alfa Tools are German companies that produce standalone pad printers and printing production lines. Their founder transferred pad printing from the watch-making industry where it was used to produce watch-faces, to the expanding plastics industry of the 1960s. Since its inception forty years ago Tampoprint has remained at the forefront of the pad printing industry and today, excluding subsidiaries, it employs 160 people and its turnover in 1998 was £22 million (DM 60 M). Its primary function was to design and implement the new pad printing systems in co-operation with the Universities, and to improve printing pads and clichés.

1.4 Market need: the use of existing printing systems at LEGO and Philips

It is instructive to discuss the contrasts and similarities in manufacturing between the end-users in the project consortium. The scheme for a typical LEGO single-colour pad printing station occupying approximately 3m square is shown in Figure 1.2. It comprises a vibrating and rotating hopper on the left, and this feeds parts onto an indexing carousel, which rotates clockwise. An optical detector ensures that there is a substrate in each product holder on the carousel, before the closed ink-cup printer is reached. After printing the finished component is ejected from its product holder onto a conveyor belt where the operator can inspect it prior to

it being deposited in a collector. It is important to LEGO to increase the capability of its printing systems from 3600 to 7200 cycles per hour, the project target. It produces many small parts and so often prints four to eight components using special pads or a pad cluster attached to one printer. At present one operator supervises two printing stations, and this fact plus the printing rate means that a fraction of the output is inspected here, and exhaustive manual sorting is performed separately.

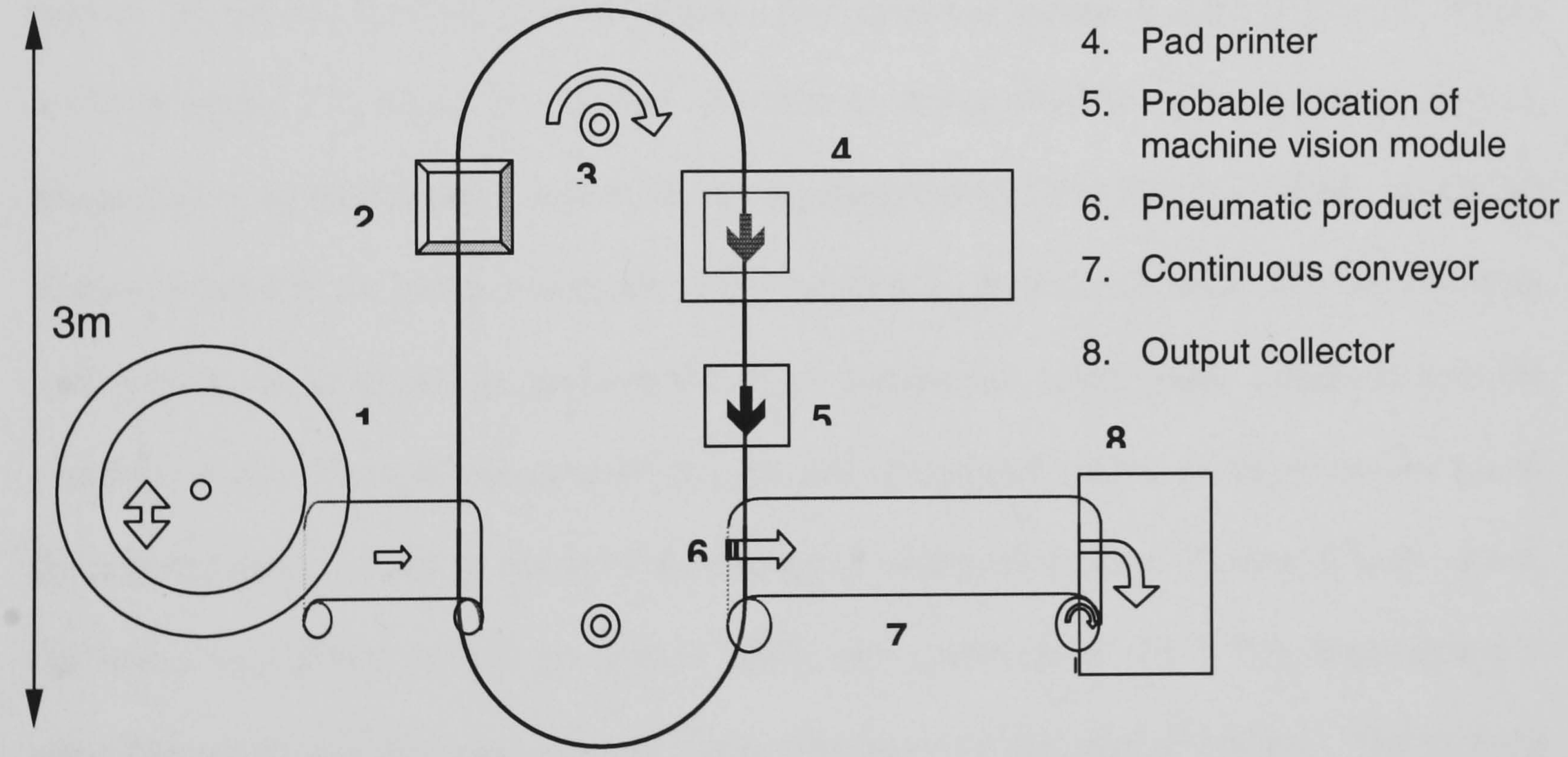

Figure 1.2. Plan view of a typical LEGO pad printing station.

Philips uses printing cells approximately 4m square like the one illustrated in Figure 1.3 to print logos on kitchen and bathroom products (shavers, kettles) and hi-fi equipment. The operator sits at point 1 on the left and places substrates on an eight-holder indexing carousel.

Prior to pad printing some plastics are *corona* heat-treated to change the chemical structure of the product surface in order to improve adhesion of the ink. After any required pre-treatment occurs the part is decorated, and individually inspected and unloaded at position 4. At present Philips achieves approximately the same production rates as LEGO, and wants a more modest increase to approximately 5000 parts/h as a result of the project.

The use of printing at LEGO provides a number of contrasts with production at Philips DAP. The LEGO stations are designed to be compact, fast (3600 cycles/ h) and semi-automated. LEGO would prefer to use them as the basis for the next generation of automated inspection and control pad printing systems, and this presents significant challenges to the Intelpadprint project. At present the only possible position for inspection hardware is the gap on the station at (5) in Figure 1.2, which is cramped. In order to decide whether parts should be rejected, image data must be processed, which can be expected to take from 500 to 2500ms. As LEGO wishes to increase its pad printing rate to 7200 cycles/ h, then it is possible that the conveyor will need to be extended to position the reject mechanism before parts disappear into the container at (8). Furthermore parts are not precisely positioned on the conveyor as they are on the indexed table, so that to discard the correct and minimum number of parts, if faults occur, the reject mechanism should be placed before the conveyor at (5). This requirement is contradictory to the previous one and needs flexibility on the part of LEGO. The printing stage can be moved further back, perhaps to position (2), with the substrate checker immediately before it and the camera immediately after. This will give the required time to process the inspection-image and decide whether to 'pass' the part before the product ejector at (6).

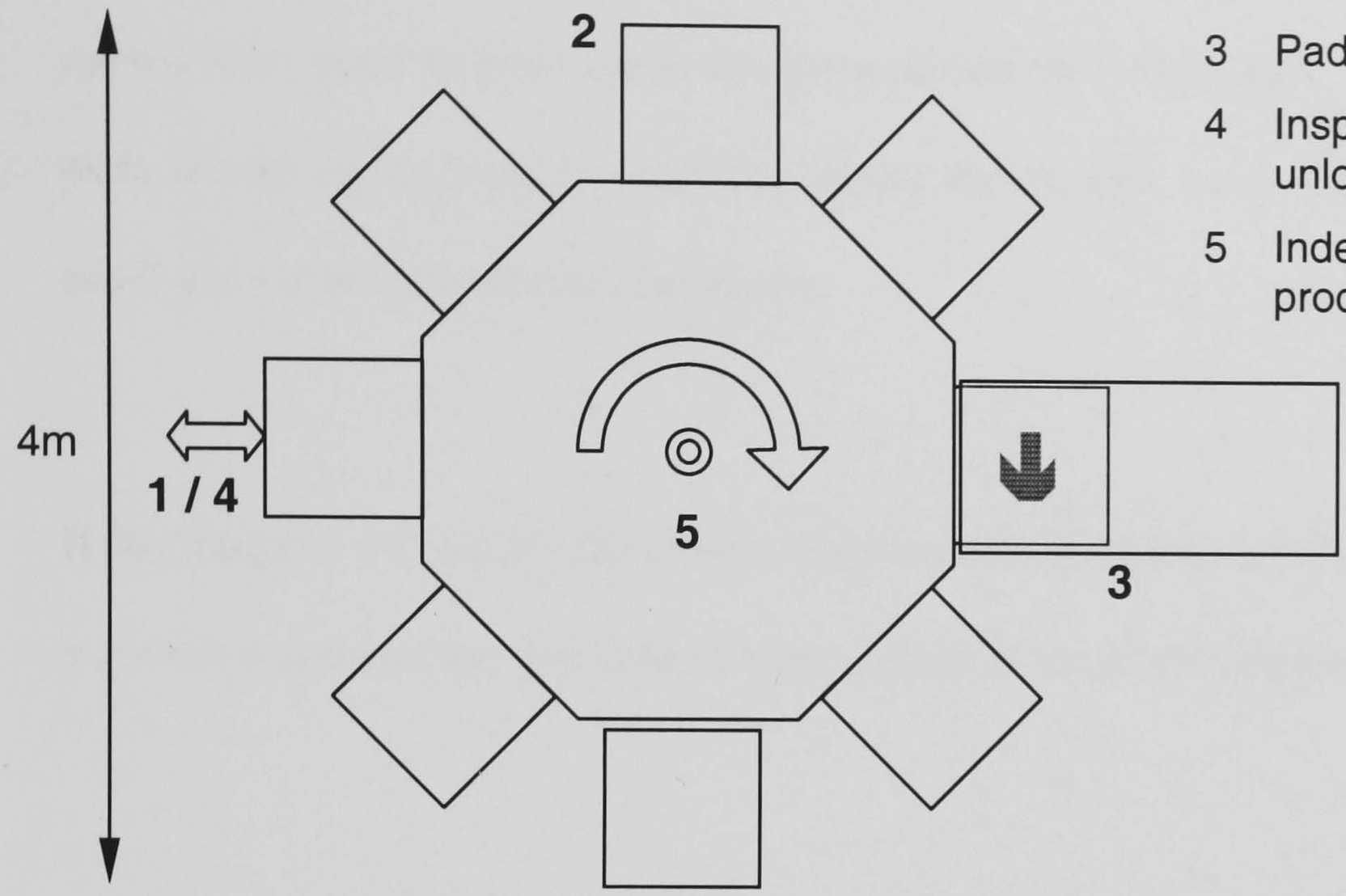

Figure 1.3 Diagram of a typical Philips DAP printing cell.

Finally, LEGO and Philips are arguing for the development of solvent-less inks as part of the Intelpadprint project, to reduce the health and environmental impact, and minimise waste. These inks must be cured using UV light, in a post-printing treatment at space (5) on the station in Figure 1.2. UV cured inks do not at present meet mechanical or chemical resistance criteria, but when they are introduced inspection should occur after curing in order to monitor the post-printing treatment.

Pad printing is used to decorate the majority of LEGO's products, with transfers employed occasionally. LEGO prints large batches, and up to six colours are printed using consecutive printers on the same production station. The majority of their components are flat, exceptions

include the heads on their figures, whose small radius presents difficulties. LEGO employs *'gang' printing* where one printer holds several pads or segmented pads, and a number ink pots and clichés. The pots and clichés may print different colours in which case the parts are moved from point to point under the same printer after each cycle. For monochrome printing parts are moved as a batch under the printer during each cycle. Gang printing allows many small parts to be printed simultaneously.

If Intelpadprint can satisfy the contrasting demands of LEGO and Philips it will have produced a system that meets the demands of most end-users in the worldwide market.

1.5 Structure of the thesis

Chapter 2 is a literature survey, which explains why and how the pad printing process can be developed through automation. There is a review of the control techniques that may be useful in Intelpadprint and the need for automated visual inspection is discussed. Machine vision is introduced and the chapter concludes with a commentary on the past and current image processing research that is relevant to the Intelpadprint project. Chapter 3 starts with a discussion of the models and tools that were useful in designing and implementing the Intelpadprint inspection and control system. Operator knowledge about pad printing is classified and a specification for the Intelpadprint system is formulated, and this corresponds with the University of Birmingham's tasks 1 to 3 in the Intelpadprint schedule (Table 1.3).

In chapter 4 the reasons for choosing the hardware and software used during the project are discussed. The pre-prototype algorithm and interfaces are designed, implemented and evaluated, leading to the completion of project-tasks 4 and 6. Chapter 5 encompasses tasks 7 to 10 in table 1.2, which involves the design, implementation and testing of the demonstration system for Intelpadprint. In chapter 6 a different research area within the project is assessed: the analysis and elimination of print distortion in pad printing. Chapter 7 looks at contributions by the other partners to Intelpadprint: ink, cliche and printer research. Chapter 8 concludes the thesis and discusses future work.

Table 1.3 The Intelpadprint project task list

Task 1 Define specifications and test methods for the system

1.1 define the software and the reliability of the complete pad-printing system

UoB 1man-month months 1 - 6

T 2 Develop adaptive/intelligent network algorithms for system software

2.1

2.2

UoB 5 man-month months 3 - 9

T 3 Investigation and development of new pad-printing process

3.1 investigate the mechanical aspects of the pad-printing process

3.3 find conditions for a high-yield pad-printing process

UoB 0 months 3 - 9

T 4 Development of a pre-prototype pad-printing system (inks, hardware, software)

4.3 develop control software ..

UoB 12 man-month months 9 - 18

(T 5 Evaluation of developed inks on existing pad-printing equipment **)**

UoB 0 months 9 - 18

T 6 Evaluate pre-prototype pad-printing system

6.3 evaluate the software control ..

UoB 10 man-month months 18 - 24

T 7 Preparations for the realisation of the pad-printing demonstration model system

UoB 2 man-month months 18 - 24

T 8 Evaluation of the new inks, sub-assemblies and software routines on the pre-prototype pad-printing system

UoB 4 man-month months 24 - 30

T 9 Realisation of the pad-printing demonstration model system

9.1 integrate the results from Tasks 6 & 7

UoB (MU 9 man-months) months 24 - 30

T 10 Alpha-testing of the demonstration pad-printing system in a pilot production line

UoB 2 man-months months 30 - 36

T 11 Project co-ordination and exploitation measures

UoB 2 man-months months 0 - 36

TOTAL UoB 38 man-months

2 Literature review

2.1 Introduction

The thesis deals primarily with research into the *control* of the *pad printing* process using *machine vision*. In the pad printing section we assess the present and future value of the decoration industry, the importance of pad printing in relation to other decoration processes, the state-of-the-art in pad printing. The possible control solutions are then explored with respect to pad printing. Finally, the literature on machine inspection, image segmentation, pattern recognition and imaging hardware is surveyed.

2.2 Pad printing

2.2.1 The benefits of pad printing

In 1965 Tampoprint produced the first automated pad printers based on the existing hand-presses. This was the first and most important step on the path from a craft technique used to label the faces of watches to a modern industrial process. The gelatine pads, which were unstable in the face of ambient conditions including humidity, were replaced in the late sixties by silicone rubber applicators, which are more stable and elastic. In the mid-seventies hollow pads were introduced for plastics printing. Hollow pads made from pig's bladders were replaced by gelatine, then silicone rubber in the ceramics industry.

The moulding process allowed complex forms to be produced for the growing domestic goods industry and pad printing was the only way of decorating these curved products. Against this are the cost and wear of clichés and squeegee rims/ blades, the inflexibility of clichés and the need to periodically clean and refill the ink-pot preventing continuous operation. A high

degree of skill is required during set-up when there is a lot of waste, operator supervision is high and because it is fundamentally a robust, high quality process there has been little research into the pad printing process.

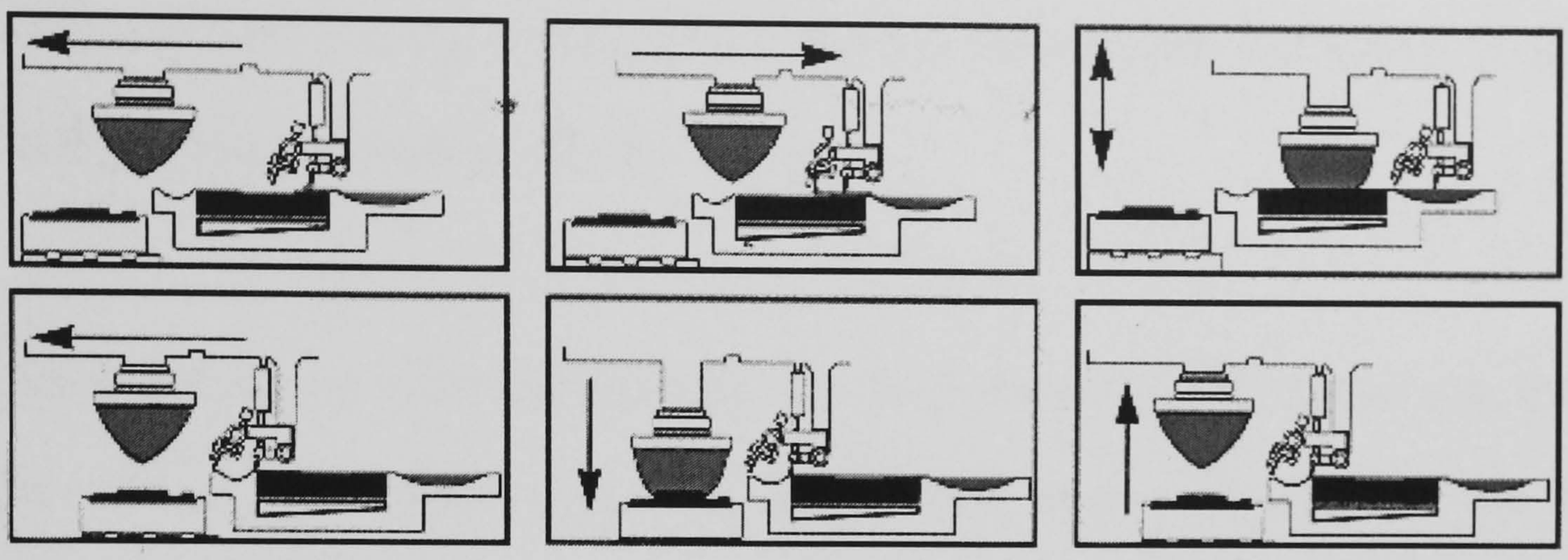

Figure 2.1 Open system pad printing [Tampoprint]

Initially pad printing machines used an open trough to hold the ink as shown in Figure 2.1. The main disadvantage of this arrangement is the loss of solvent from the ink, leading to a change in ink viscosity over time, and loss of graphic quality. In addition, the mechanism that moves the scoop to lift ink onto the cliché and moves the squeegee to remove excess ink is complex. Primarily because of the problem of solvent-loss, in 1983 Tampoprint introduced a sealed or closed system represented in figure 1.1, where the ink-cup is upside down and pressed against the cliché, which is doubled in length to accommodate it. The doctor-blade seals the ink in and scrapes the excess ink from the cliché as it slides. The sealed system was an important advance as it reduces the emission of *volatile organic compounds* (VOC) by approximately ninety percent [Sherman, 1996] making the ink more stable and longer lasting, and less harmful to the operator and the environment. The reduction in solvent consumption is an important economy for end-users. Additional benefits are a simplified mechanism, increased flexibility and a potentially higher printing rate compared with the open system, although the sealed ink-cup requires a mechanism to press it with even pressure against the

cliché. In the open system the ink-cup and cliché are typically stationary so that the pad must move horizontally as well as vertically. In the closed system the ink-cup can be stationary with the cliché sliding horizontally and the pad moving vertically, and this is referred to in the thesis as a *Tampoprint-type* machine. The resulting printer can be more rigid, and another aspect of the increased flexibility of the sealed system is that it can be mounted upside down to print the under-side of objects in production lines.

There are disadvantages to the sealed system: the rim of the cup and the cliché wear unevenly and the cost of replacement cups and double-length clichés is high. Some printer manufacturers have developed mechanisms to rotate the ink-pot a quarter-turn with each print-cycle to attempt to make the rim wear evenly, while others produce ink-pots with separate rims. The claimed 24 hour operation and high printing rates do not always occur in practice [Kiddell, 1996]. Shrouded open systems similar to the open pad printer shown in Figure 2.1 are a compromise that allows large areas to be printed while reducing solvent loss and together with closed systems these account for ninety percent of sales. A conservative printing rate of 4000 cycles/ hour is a great improvement on the 1400 cycles/ hour possible with open systems.

The Intelpadprint project commenced in 1996 and at this time the state-of-the-art in pad printing was sealed ink cups, stepper-motor drives giving increased reproducibility and limited machine visual inspection [Sherman, 1996] [Collard, 1995].

Machine vision solutions have been found for specific pad printed products, for example switch casings, and the system developed by Truchetet and Cholley only distinguishes between four classes of defect [Truchetet *et al*, 1997]. It is unclear if the system uses image data to control the printing system, or whether the operator provides feedback.

2.2.2 Pad printing versus other decoration processes

Pad printing is a process used mainly on plastic and domestic ceramics. This thesis will consider non-paper printing with emphasis on the decoration of plastics. Pad printing is ideally suited to the complex curved surfaces possible with plastic moulding so it is useful to summarise the value of the plastic and printing sectors. There has been an exponential growth in the world consumption of polymers from 1 million tonnes in 1939 to just under 100 million tonnes by 1996, as demonstrated by Figure 2.2 [BPF, 1996]. The consumption of thermoplastics in Western Europe has shown approximately linear growth from 14 million tonnes in 1985 to 24 million tonnes in 1996 and this is forecast to approach 30 million tonnes by 2005 [AMI, 1997]. Printing on non-paper products in Europe was worth approximately £370 million in 1996 and was forecast to exceed £460 million by 1999 [Howitt, 1995] [Howitt, 2000].

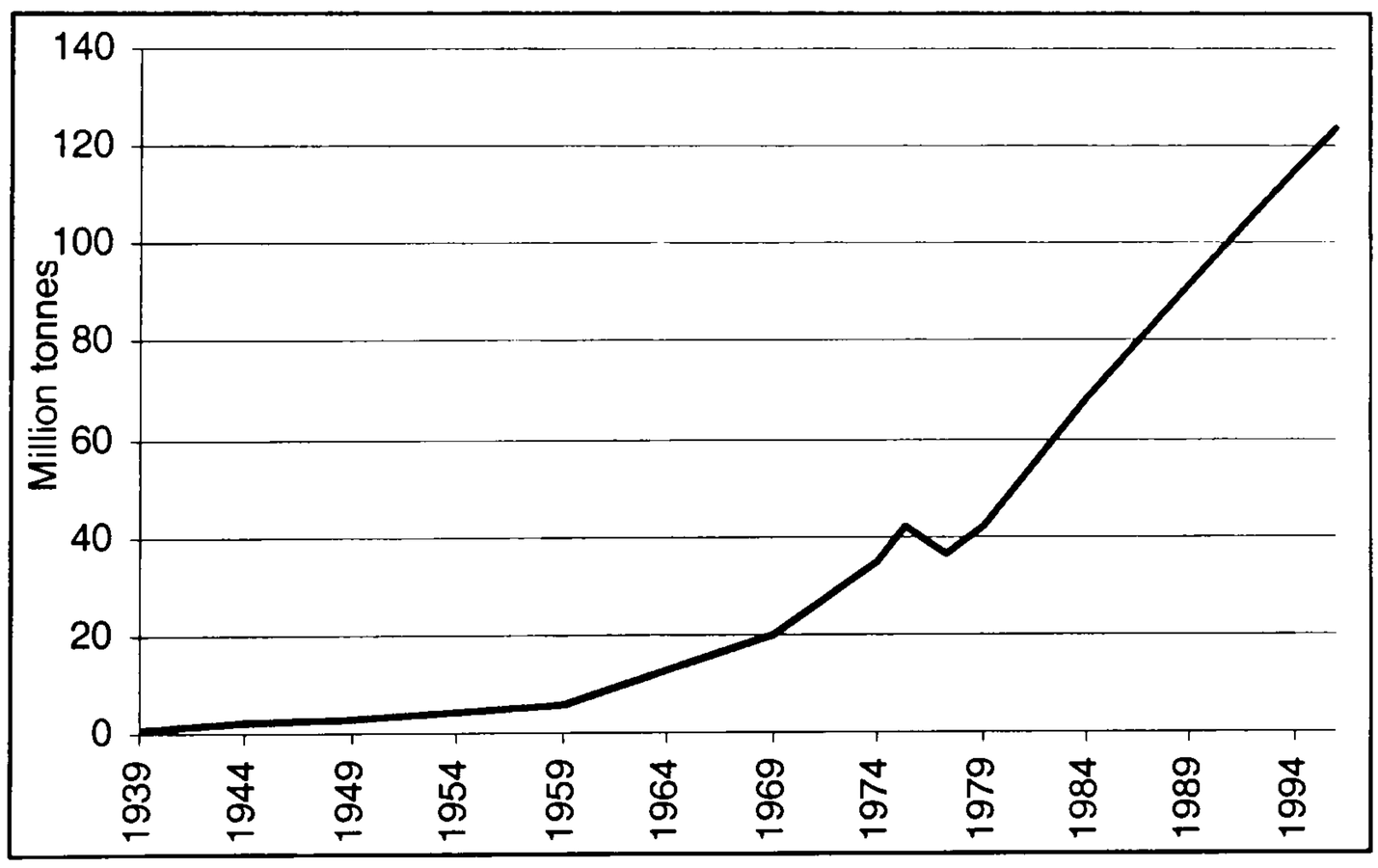

Figure 2.2 World polymer consumption, 1939-1995 [BPF, 1996]

Pad printing is in competition with in-mould and out-of-mould decoration. Decoration in the mould uses heat and pressure, and can involve "Insert" moulding where one or two pre-printed

films are placed in the mould prior to injection of the polymer and they become part of the product [Griffin, 1999] [Beyer *et al*, 2000]. The alternative is "In mould" decoration or "Heat transfer moulding" which uses a pre-printed paper sheet in the mould, the ink is transferred to the substrate using sublimation, or the Nisha or Kurtz process and the transfer sheet is then discarded [Zepf, 1995] [Griffin, 1999]. "Heat transfer" can also be performed after moulding and this is a variation on the Hot-stamping process, and the films can be printed using screen, ink-jet or offset printing. Transfers are used extensively in the domestic ceramics industry.

There are various painting processes where most or all of the surface is coated (as distinct from printing where the material is applied to select areas), but these are not relevant to our discussion. Other out-of-mould techniques recounted by Hillestad are electro-plating, vacuum metalizing, and decals and appliqués can be applied [Hillestad, 1998].

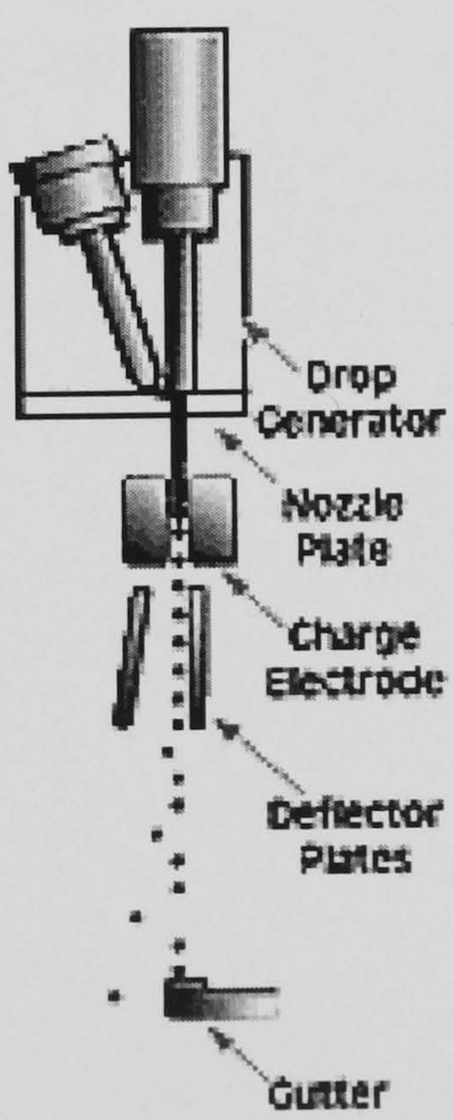

Figure 2.3 The parts of an ink-ject printing head [Domino, 2001].

During laser printing, typically with a CO_2 laser, the product is irreversibly marked. On paper or card the laser beam vaporises a toner and the surface, on glass and PET the surface is

chemically altered or the surface of certain plastics and thermal-coatings can change colour [Domino, 2001]. Laser printing is low maintenance as there are few moving parts, no consumables (except toner on paper) and artwork can be changed between consecutive prints. This makes laser suitable for printing, for example barcodes and 'best before dates' for the food industry. However the scope for and quality of colour printing is limited and the substrate must react correctly with the laser.

The head of an ink-jet printer is shown in Figure 2.3. The *drop generator* receives ink under pressure [Domino, 2001]. Ultrasonic waves are produced in the ink by a drive rod and it emerges from the *nozzle plate* as finely separated drops. An electrostatic charge is created in each droplet by an electrode and, like in a cathode-ray tube, a voltage across deflector plates directs the droplets to the required position on the substrate. Ink-jet printing produces vibrant colours on a wide variety of substrates, but resolution is limited by the size of the nozzle. The substrate can only be curved in one dimension. Ink-jet printing consumes volumes of ink and fine pipes and nozzles in the printer must be cleaned during a change of colour. Like laser-printed artwork, ink-jet prints can be changed rapidly.

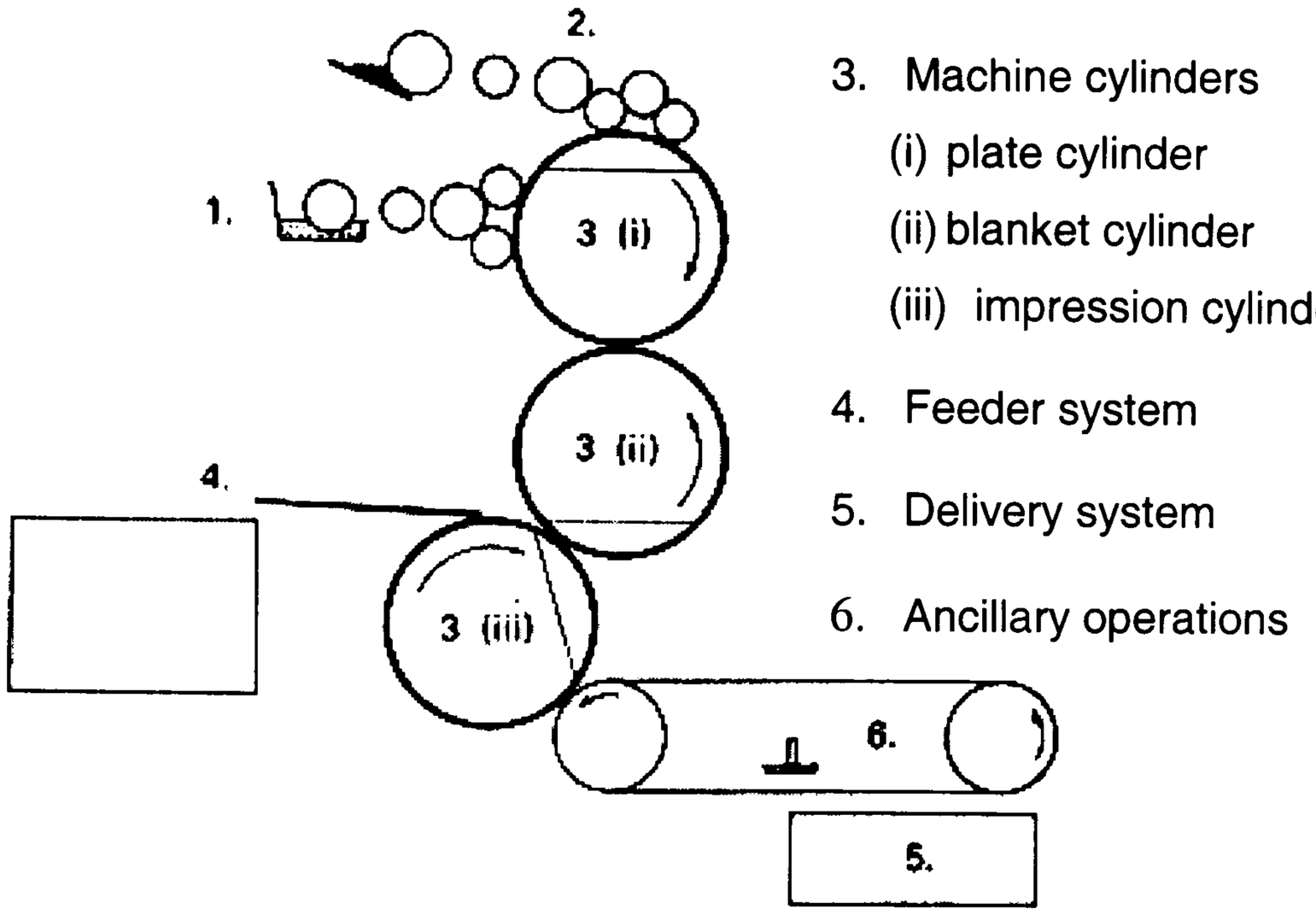

Figure 2.4 Components of a small offset (lithographic) printer [Rowlatt, 1986]

In lithography, illustrated in Figure 2.4, an electro-static charge holds the ink on part of the plate, while flexography uses raised areas and a gravure offset process uses recessed areas to hold ink [Chambers, 1979]. These methods were developed for paper and later textile printing and are suited to continuous media. Rotary pad printing is an offset roto-gravure process. In screen printing ink is forced through a silk or steel mesh onto the substrate. A squeegee like the one pictured in Figure 2.5 is used. Finally "Tampo-graphic" or transfer pad printing which is hereafter called simply pad printing is an offset plano-gravure process.

According to Janco, the processes most commonly used on plastics are screen and pad printing, hot stamping and heat transfer [Janco, 1996]. Other methods in competition with pad printing are offset lithography, ink-jet and laser printing – these are now considered further.

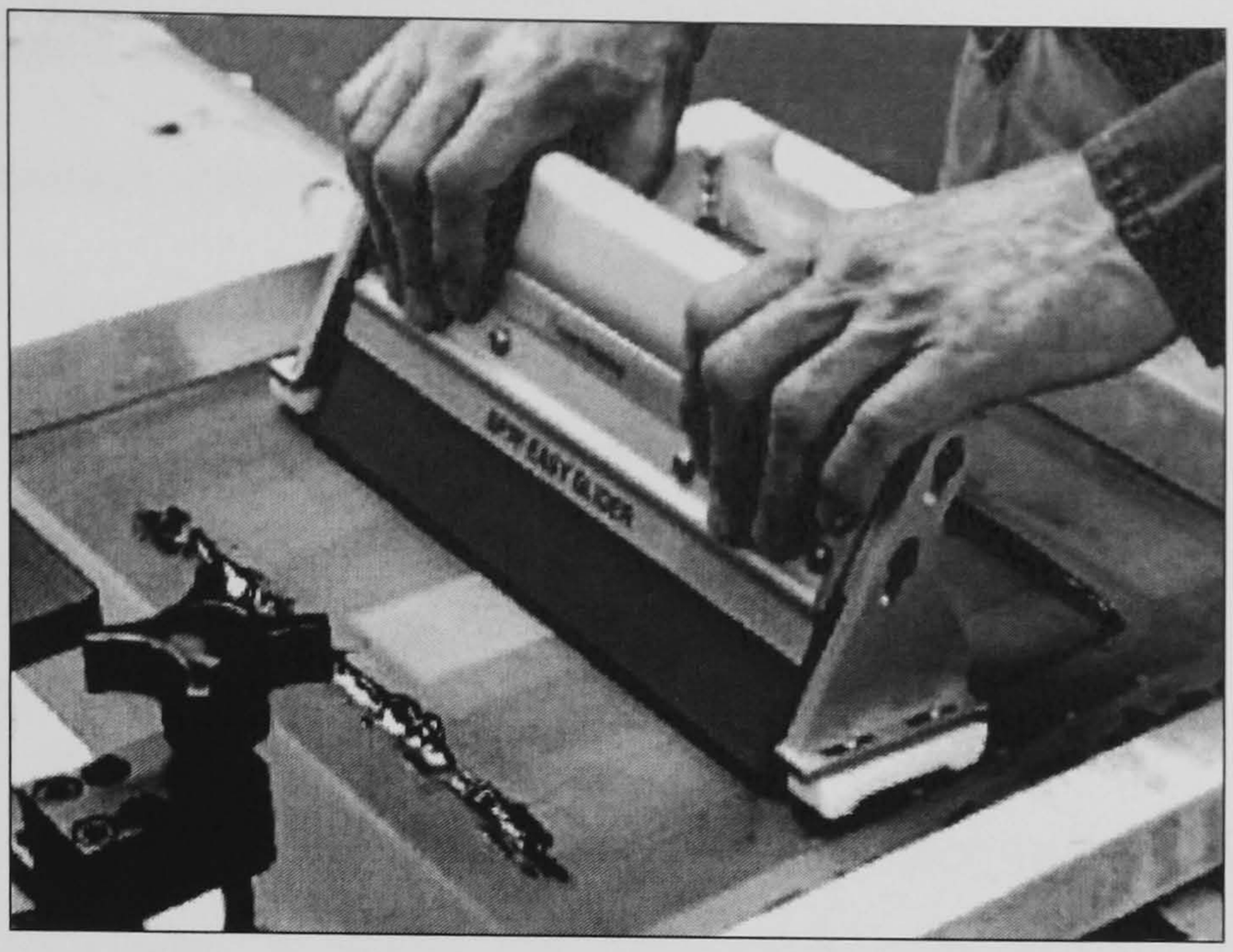

Figure 2.5 Manual screen printing with the Easy Glider squeegee holder [Hunt, 1999]

Criteria on which a decoration technique can be judged are:

- Cost per part – including equipment and materials. Dependent on batch size.
- Reject rate
- Required operator skill and level of supervision
- Ink type: economic and environmental cost (VOC volatile organic compounds regulations) and curing requirements
- Ease of integration into production line
- Printing rate
- Changeover time
- Print resolution
- 2/ 3-dimensional capability
- Depth of colour of ink
- Multi-colour printing capability
- Ink abrasion and chemical resistance
- Stability of process
- Possible graphic size

Janco reports that screen and pad printing have a lot of limitations in common: both require skilled setup and operation, costly training compared with hot stamping and heat transfer, and both use wet inks where viscosity is critical [Janco, 1996]. Ultra-violet cured inks are increasingly used in screen-printing, reducing the cost of curing and the environmental impact, and increasing the printing rate from 3500 to 7000 parts/ hour. As yet pad printers have not successfully used UV inks because of poor image quality and their abrasion resistance is not proven [Sherman 1996]. By contrast hot stamping and heat transfer are dry and therefore stable processes. Set-up and operation require only semi- and un-skilled personnel respectively lowering the cost of training. Foil decoration, for instance using polyamides, provides a more wear resistant finish than inks or paints, however the film needs to be carefully matched to the substrate [Beyer and Lohmar, 2000].

Hot foil marking allows metallic finishes to be applied, but they are more expensive than inks according to Reichmann [Reichmann, 2000]. Colour is important and most of the methods under discussion here give a good depth of colour except laser marking which is largely a black and white process at present.

Table 2.1 Summary of the limitations of competing printing processes

Process	2D/ 3D	Colour	Stability	Resolution	Reject rate
Laser	2D+	Poor	Very good	Fair/ good	~0.1%
Ink-jet	2D+	Fair/ good	Fair/ good	poor	~1.0%
Silk screen	2D	Very good	Fair/ good	Fair/ good	~2.0%
Offset	2D	Very good	Fair/ good	Fair/ good	~1.0%
Traditional pad-printing	3D	Very good	Poor	Fair/ good	~5.0%
Adaptive/ intelligent pad-printing	3D	Very good	Very good	Very good	~0.1%

It has been shown that there will continue to be a steadily widening demand for plastics and their decoration. There are many decorating options and most of them are competitive with pad printing. However pad printing is still the only technique that will cope with complex curved and irregular surfaces. As Table 2.1 demonstrates traditional pad printing is better than ink-jet printing for resolution, better than laser printing for colour and in many respects equals screen and offset printing. It has poor stability and the highest reject rate, but it is the only 3-dimensional process.

2.3 Control

2.3.1 Control and Intelpadprint

When analysing the control aspect of the Intelpadprint project it was instructive to consider what actuators might be included in the printer, how they would be used and what data would be available to make control decisions. A number of methods have been employed in existing printers to move the pad and cliché: electro-mechanical cams, pneumatic rams and servo-motors driving machine-screws. It is likely that servo-motors would be selected as the *primary* actuators to provide flexibility in the print cycle, cope with the high printing rate demanded by Intelpadprint and rapidly apply the high loads required to deform the printing pad. There might be a second actuator to rotate the cliché to compensate for printing inaccuracies, perhaps caused by an uneven substrate surface; and there would be an actuator to press the ink-pot against the cliché. As a printing process is being discussed there will probably be automated valves to add solvent or ink, in order to alter the viscosity of the ink. It will be demonstrated that it can be beneficial to warm the ink, and this can be achieved using a coil embedded in the cliché.

The primary actuators are cyclic and the positions to move between and times or speed in which these movements are to be achieved are used to re-compute the velocity-time curves each cycle. The user inputs a change in speed, or requests a variation in part of the cycle. The change in cycle detail can also be decided by the system to improve the quality of printing. The secondary actuators affect incremental changes, for example cliché orientation, or maintain a constant value, for example the pressure between the ink pot and cliché.

2.3.2 Artificial Neural Networks

Artificial neural networks are sometimes referred to as parallel distributed processing models or connectionist models. They are models based on our current understanding of biological nervous systems and are composed of many simple highly interconnected elements or nodes [Lippmann, 1987]. The nodes take the form demonstrated in Figure 2.6 where a bias θ is subtracted from the weighted sum of *n-1* inputs and with the simplest *Heavyside* or step function, f_h, the output y is either 0 or +1 if the result is greater than 0:

$$y = f_h [\sum w_i x_i - \theta] \qquad (1.)$$

$$f_h(x) = 1, \quad x > 0$$

$$f_h(x) = 0, \quad \text{else}$$

Artificial neural networks can be characterised by the type of non-linear function used to produce the output, whether the inputs are binary or continuous, the manner in which nodes are connected and the learning algorithm that is used. Figure 2.6 is a McCulloch-Pitts model which was given the name 'perceptron' by Rosenblatt in 1962 [McCulloch *et al*, 1943] [Rosenblatt, 1962]. It is a *feedforward* system as inputs are passed through the node to produce the output and the inputs are analogue or continuously-valued [Beale *et al*, 1992].

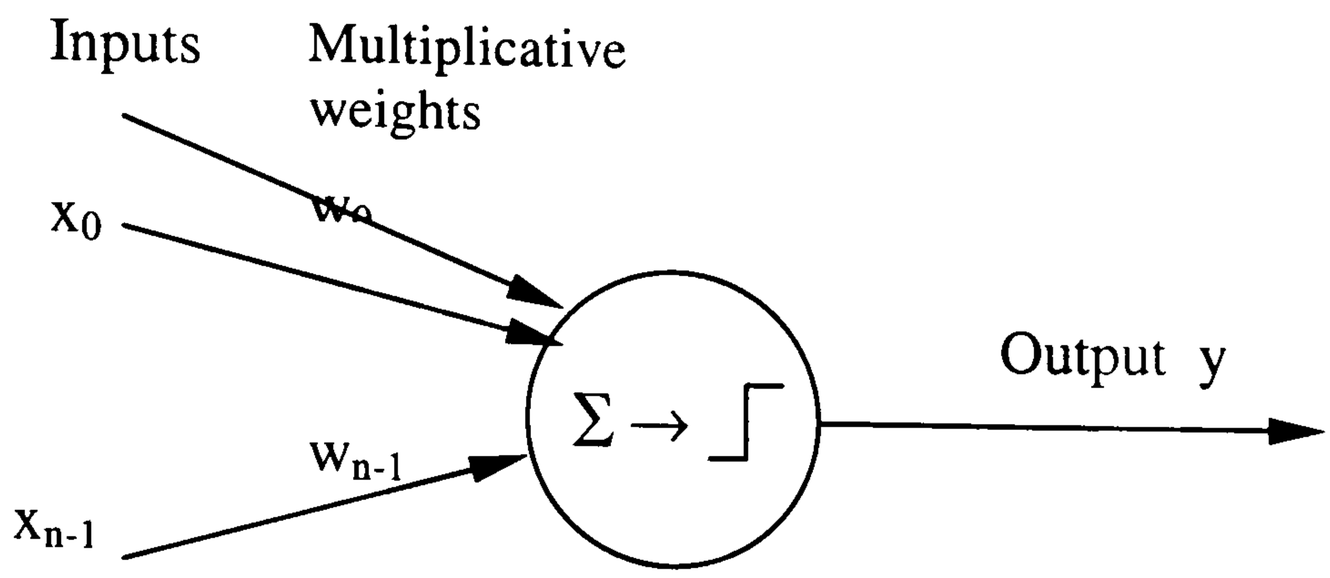

Figure 2.6 Computational node in an artificial neural network

A simple learning paradigm based on Hebbian learning is presented in Beale and Jackson [Hebb, 1949] [Beale *et al*, 1992]:

- Initialise the weights and thresholds randomly.
- Present an input.
- Calculate the actual output by taking the thresholded value of the weighted sum of the inputs.
- By comparing the desired output with the actual output alter the weights to reinforce correct decisions and discourage incorrect decisions, ie. reduce the error.

In using the desired output this is termed *supervised* learning. Artificial neural networks can be implemented in a parallel hardware architecture [Shippen *et al*, 1998] or they can be simulated using a Von Neumann serial computer such as a PC.

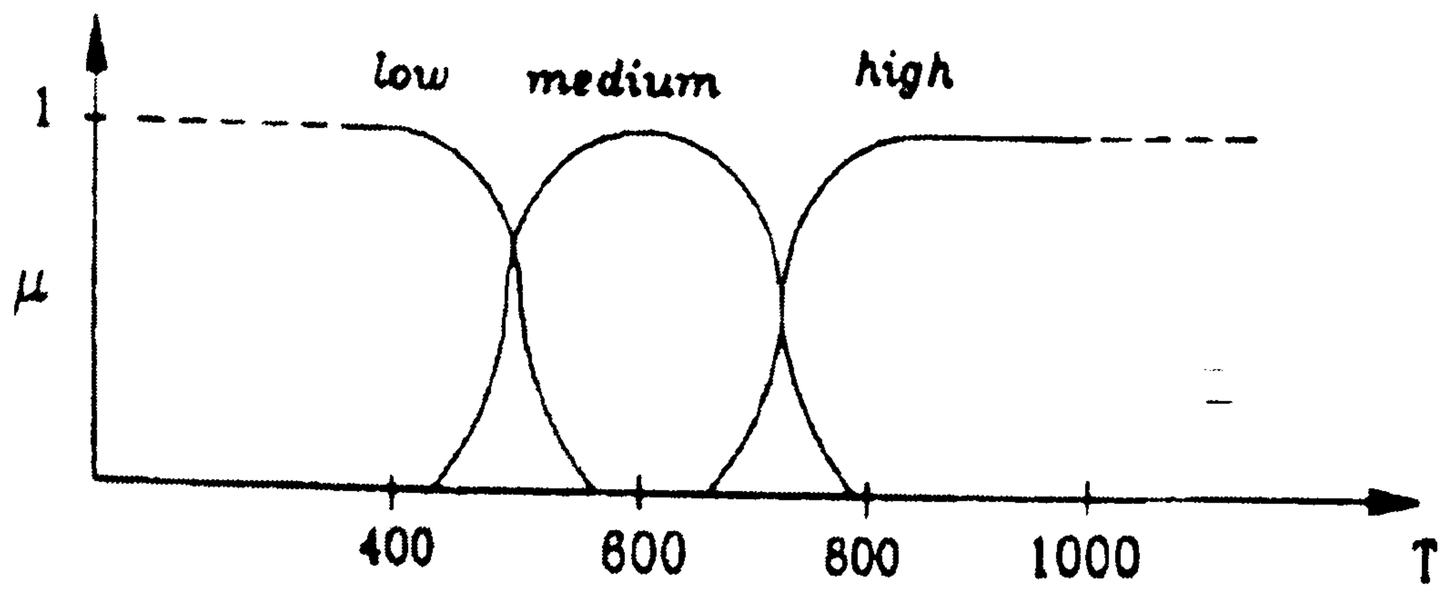

Figure 2.7 Illustration of fuzzy membership functions.

2.3.3 Introduction to Fuzzy control

In conventional set theory the membership of a set is a binary function: a value is either in the set or it is not. *Fuzzy sets* have a membership function that varies between zero and one, that is, a fuzzy set *A* typically has elements with membership $u_A(x) = 0, 0.5, 1, 0.3$. The first element is not a member, the third is most fully a member while the remaining elements have a degree of membership [Zadeh, 1965]. The fuzzy sets try to model human responses and are given linguistic descriptors such as 'very small', 'small', 'medium' and 'large'. A value is typically a member of two sets and control actions can be calculated from a rule base for both memberships, with the results being combined afterwards. Since its conception, the involved mathematics of fuzzy set theory has been defined, and the principles applied to control and pattern recognition.

Before fuzzy logic can be applied, data undergoes a '*fuzzyfication*' stage to produce *linguistic* variables as demonstrated in Figure 2.8. A principal advantage of fuzzy control is that a precise mathematical model of the system is not required. The challenge is in determining the rule base for a problem, and this can be achieved following interviews with the operators of the system, though they can forget to explain shortcuts found through trial and error. The control engineer can determine the rules heuristically from his knowledge of the system, or the rule

base can be determined by a fuzzy *self-organising controller* (SOC), which uses feedback in the same manner as self-tuning and adaptive control. The latter strategy was used to good effect to control the non-linear yaw of a warship (rotation about an axis through the earth's centre) [Sutton *et al*, 1991]. The ship changed and maintained course satisfactorily, and the accuracy of the system model and experimental analysis were less significant. A fuzzy self-organising controller to maintain the attitude of a satellite was studied in comparison with a proportional-differential controller [Daley *et al*, 1989]. The fuzzy solution was as effective as the more complicated PD one, and the fuzzy controller was able to damp the articulation of the satellite despite having no direct knowledge of it. Once optimal performance of the system has been attained the controller constantly deteriorates then re-corrects because of the feedback, but this was found acceptable.

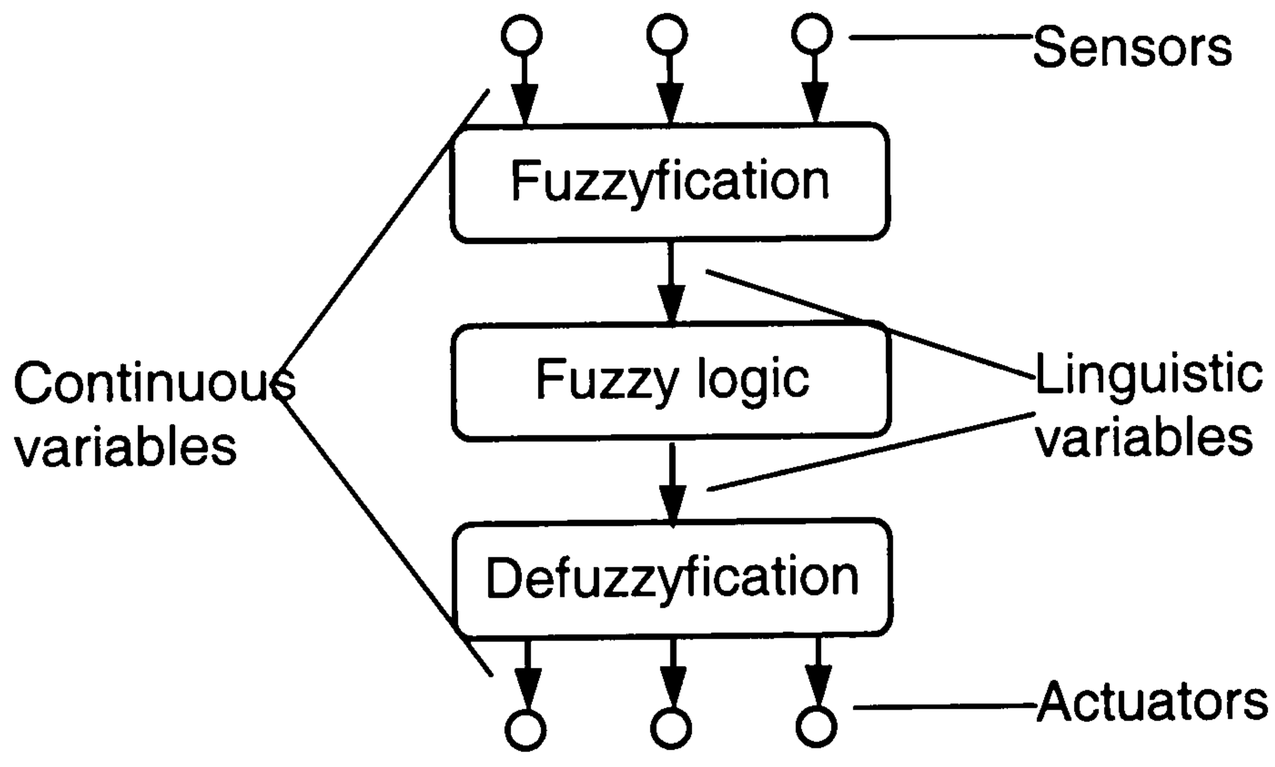

Figure 2.8 A fuzzy logic controller [Astrom *et al*, 1992].

2.3.4 Examples of Intelligent Control

Recently, there has been renewed interest in proportional-integral-derivative (PID) controllers and their optimisation [Chen *et al*, 1999] [Vrancic *et al*, 1999]. It is reported that load disturbances greatly affect the response of a PID-controlled servo system, so that it requires re-tuning [Mishra *et al*, 1999]. A fuzzy logic controller used for position control was found to be robust over a wide range of system parameters, both in simulation and implementation.

Another study compared fuzzy logic, proportional-integral (PI) and *model reference adaptive control* (MRAC) of a servomotor [Li *et al*, 1989].

In the context of supervisor control of hydro-electric power generation to match consumption, the PID family of controllers was thought to lack stability and give a sluggish response [Vinor Kumar, 1999]. Fuzzy logic, artificial neural network and hybrid fuzzy neural network solutions were investigated and the latter was found to provide the better dynamic response, in terms of reduced frequency transients, minimal errors and higher speed.

An interesting discussion of various intelligent control solutions and their commercial viability can be found in a paper from Rockwell [Chiu *et al*, 1995]. A fuzzy self-organising controller was used to control a motor and gave comparable performance to PI and PID controllers at low loads, and a faster response and lower overshoot under high load. However, as high powered motors are generally chosen to provide over-kill and PID controllers are inexpensive and more widely understood there is little commercial need for this higher performance. Fuzzy logic control is best marketed in this context as enabling smaller, cheaper motors to be used, and providing online adaptive control (PID controllers need down-time for re-tuning to new parameters).

Fuzzy logic is an obvious way to model the behaviour of an aircraft pilot, and this was achieved for automated level change and throttle control. The level change solution was better than the existing controller, comparable with a new one and more easily understood than either. Fuzzy self-organising throttle control reduced the incremental root-mean-square (RMS) change by half giving a smoother ride, and gave equal performance to the conventional controllers on other criteria. However standard stability and robustness tests for fuzzy logic controllers

(FLCs) are not yet established, so safety critical inner stability loops on aircraft are unsuitable applications of FLCs at present [Chiu *et al*, 1995]. The low-level control of the pad and cliché on the Intelpadprint system is similarly safety critical, but high-level supervision is a suitable arena for fuzzy logic.

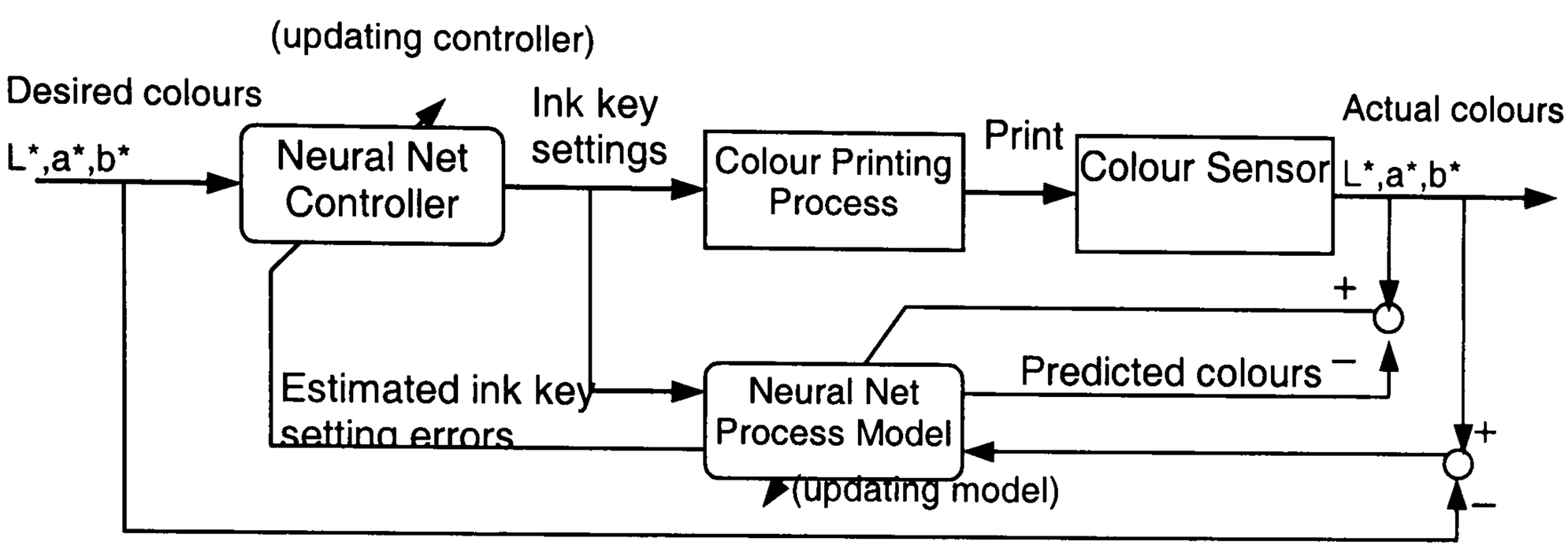

Figure 2.9 Neural network-based control architecture for lithographic colour printing [Chiu *et al*, 1995].

In contrast, a fuzzy logic tuner for aircraft inner loops was a viable industrial application as manual tuning is time-consuming, subjective and inconsistent and the method is easily understood in relation to the manual process. Artificial neural networks were successfully used at Rockwell to model the process and control it in lithographic offset colour printing, as shown in Figure 2.9 [Chiu *et al*, 1995] [Lan *et al*, 1994]. Like pad printing, this is a non-linear multi-variable system which can be set-up by skilled operators with the loss of time and materials. During printing the operator makes adjustments to a row of multiple ink-keys for each colour across the width of the paper while observing the results. Fuzzy techniques were unsuited because of the difficulty of translating the human-based rules to use the CIELAB $L^*a^*b^*$ colour triplet produced by a spectrophotometer. The neural network controller reinforces and adapts online to printing conditions such as humidity and paper quality, and commercial realisation is probable [Chiu *et al*, 1995].

Predictive control models the future trajectory of a process parameter. Various adaptive and linear predictive control algorithms have been applied in industry but non-linear modelling gives better results. A non-linear first order differential equation was used for predictive control of a robotic grinding system [Kurfess *et al*, 1992]. Simulation achieved complete levelling of a weld bead, and tests on a PUMA 560 robot were successful in the face of dynamic modelling errors and measurement noise; the bead was reduced in cross section. The use of non-linear programming methods is complex and not suited to real-time control. Neural networks are a simple non-linear alternative to minimising the performance function for non-linear systems [Liu *et al*, 1998]. A least-squares technique for online weight learning was proposed, and one and two step ahead predictors were studied. The weights and estimation error were found to converge over infinite time. More work was proposed to analyse the stability and implement the networks in the real world.

Deadbeat control occurs where the response matches and continues to track a reference signal after a finite time [Zak *et al*, 1993]. Discrete deadbeat describes the condition where matching occurs at sampled intervals, and when the tracking error is continuously zero ripple-free control prevails. The ripple-free deadbeat condition was achieved by Zak et al for a single-input-single-output (SISO) servo system with a linear second order function. The model gave minimum overshoot and rapidly tracked step and square wave signals when a 20% variation in parameters was input.

Most controllers including PID regulators are tuned heuristically, but the large number of 'if-then' statements this entails are cumbersome. Rule-based expert control was conceived to provide a framework for expressing operator knowledge about a process. An expert system

comprises a database to store sensor tolerances, operating thresholds, hypotheses and goals; a rule base similar to that in a fuzzy self-organising controller; and an inference engine to decide which rules to use. Initially it was difficult to implement expert systems in real-time [Åström *et al*, 1986] [Åström, 1989]. An architecture was proposed for a closed loop algorithm running concurrently with an expert system, in a manner similar to a real-time operating system [Årzén, 1989]. Rapid prototyping often entails using integrated software tools in a graphical environment and is related to Rapid Application Development as discussed in Chapter 3. It is suitable here and with advances in computer power and integration with other control methods, this is a growth area.

A useful review of intelligent control which comprises expert, artificial neural network and fuzzy logic control is provided by Shoureshi [Shoureshi, 1993]. A structure for a general intelligent control architecture is proposed, that relates well to conventional feedback systems. It contains a hierarchy of local controller, coordinator and supervisory control, and is applied to the problem of building climate control. Another study takes the view that control engineering has dealt almost exclusively with low-level machine control and more emphasis should be placed on process control, which is the coordination level in the control structure after Shoureshi [Hardt, 1993].

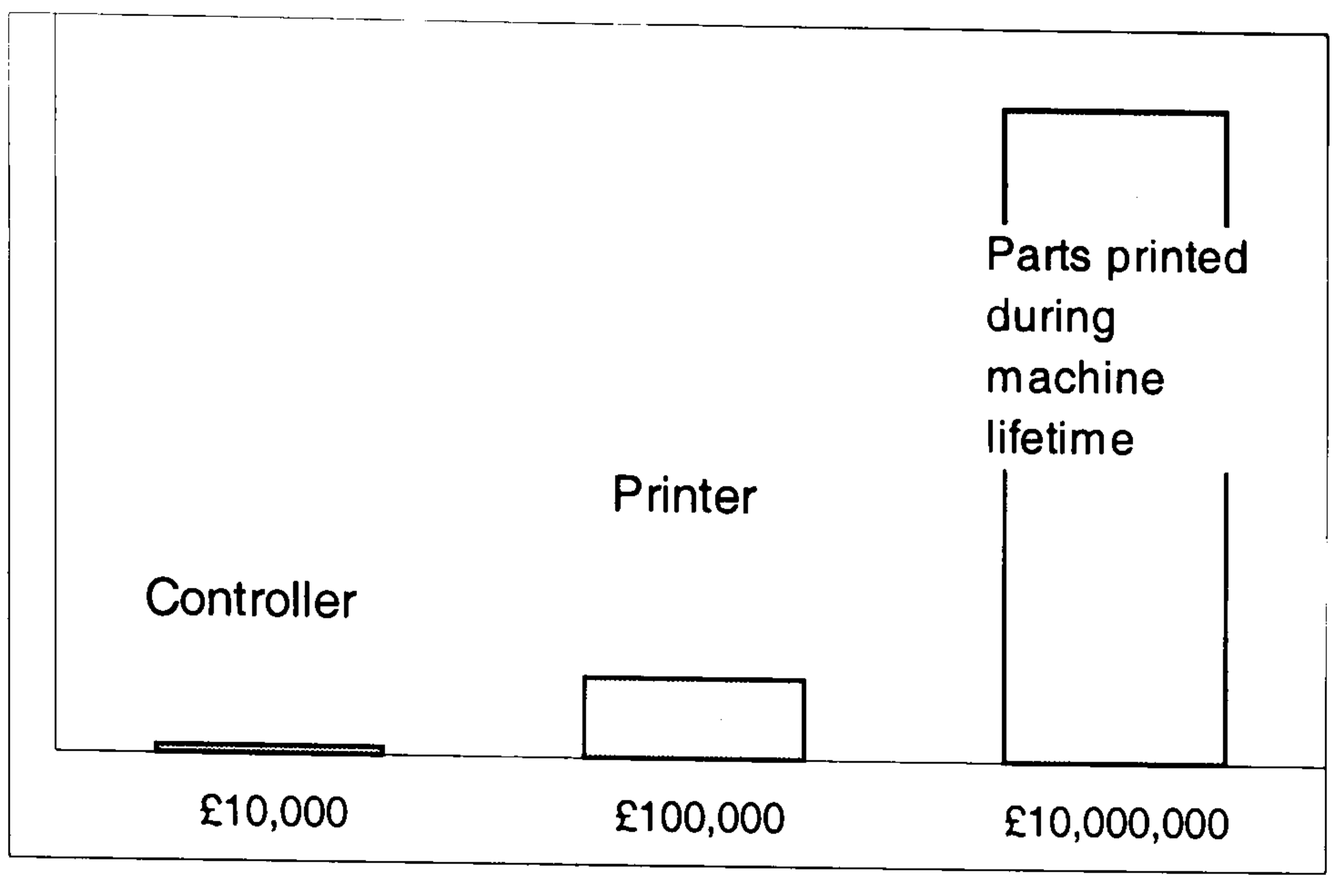

Figure 2.10 The case for investment in process controllers [after Ulsoy *et al*, 1993]

Another survey discusses a three-tier control hierarchy, and though it deals with the control of machining processes much of the paper is pertinent to pad printing [Ulsoy *et al*, 1993]. Servo control for pad printing involves computing pad velocity curves, and the level of ink in the ink-pot constitutes process control. Supervisory control includes such things as machine monitoring and integrating different sources of sensor data. Better high-level control reduces the complexity of machine-level control, for example visual data which suggests an incomplete print can signal that the pad is not being deformed onto the cliché sufficiently. Ulsoy points to negative early industrial experiences, difficulties in integrating and upgrading the system and ease of use, as impediments in the application of non-conventional techniques like adaptive control. There is a good economic case for using process control in Figure 2.10. An investment of 10% in a controller, leading to say, a 10% increase in productivity, can produce a 100-fold return on investment.

2.4 Machine Vision

"From the patterns of stimulation on the retinas we perceive the world of objects, and this is nothing short of a miracle" [Gregory, 1972].

2.4.1 Introduction

The power of the human brain can be illustrated by our understanding of cartoons. A face is represented by a simple collection of lines, which are sensed as areas of dark and light at the retina. The vast amounts of data in the image are compressed at the visual cortex so that it is again recognisable as a collection of lines, but because of the brain's learned experience a face containing expressions and emotions is perceived.

It is estimated that the optical nerves continuously transmit 10Mb/ s of visual data, but this is quickly reduced to a fraction to be analysed abstractly by the higher level regions of the brain. It still constitutes a data-stream far larger than that from any of the other senses, and yet we 'see' almost instantaneously. This is due to the massively parallel nature of the brain, which contains 10^{10} computing elements or neurons each with up to ten thousand connections to other elements. Most man-made computers contain 10^{8} elements (transistors) each connected to less than ten other elements and are essentially serial devices [Davies, 1997].

2.4.2 Digital image fundamentals

An image suitable for manipulation by digital processors must be stored in memory as an array of numbers representing pixels. A *pixel* is an element, usually rectangular which has spatial coordinates relative to the origin in the top-left corner of the two-dimensional image, and can be described by upto four numbers representing colour (chromaticity) and brightness or intensity (luminance). A *grey-level* or monochrome image can be thought of as a quantised three-dimensional bar chart where the first two dimensions are spatial coordinates and the bar represents intensity.

The RGB colour model is a hardware-oriented representation where the visible spectrum of colours is represented by the additive primaries (mixture of light) *red, green* and *blue*. It is useful for display on monitors and its mathematical representation is a unit cube so that each component is in the range 0-1. By contrast, the HSI model separates the *hue* or pure colour, from *saturation,* which is the proportion of white in the pure colour, and *intensity*. Hue and saturation constitute the chromaticity which is de-coupled from the luminance, and the HSI model is close to the response of the human eye [Gonzalez *et al*, 1995].

For the purposes of visual inspection images can be input to a computer using a camera, and the obvious choice at present is a digital camera containing a semi-conductor *charge coupled device* (CCD). Being mass-produced it is economical and gives a more linear and stable response than the imaging tube, so it has become the pre-eminent digital imager [Theuwissen, 1994]. The CCD is typically a third or half an inch square (8.5, 12.5mm) and is composed of an array of light-sensitive elements which produces a signal which is already spatially quantised. An on-board processor or remote card in the computer, called a *frame-grabber*, converts the internal camera signal to a standard colour model and quantises the signal so that a grey-level pixel is typically represented by one of 256 levels, as an eight-bit integer.

2.4.3 Convolution and the point spread function (PSF)

Convolution is an important tool in most image processing tasks, and it is illustrated in Figure 2.11 with a one-dimensional slice from an image and a three-term operator. Initially the mask is placed over the image so that the first terms of each are super-imposed. The product of the co-incident pixels is found and accumulated. The process is repeated so that for an N-pixel image and an m-pixel template $N - m + 1$ one-dimensional convolutions are performed.

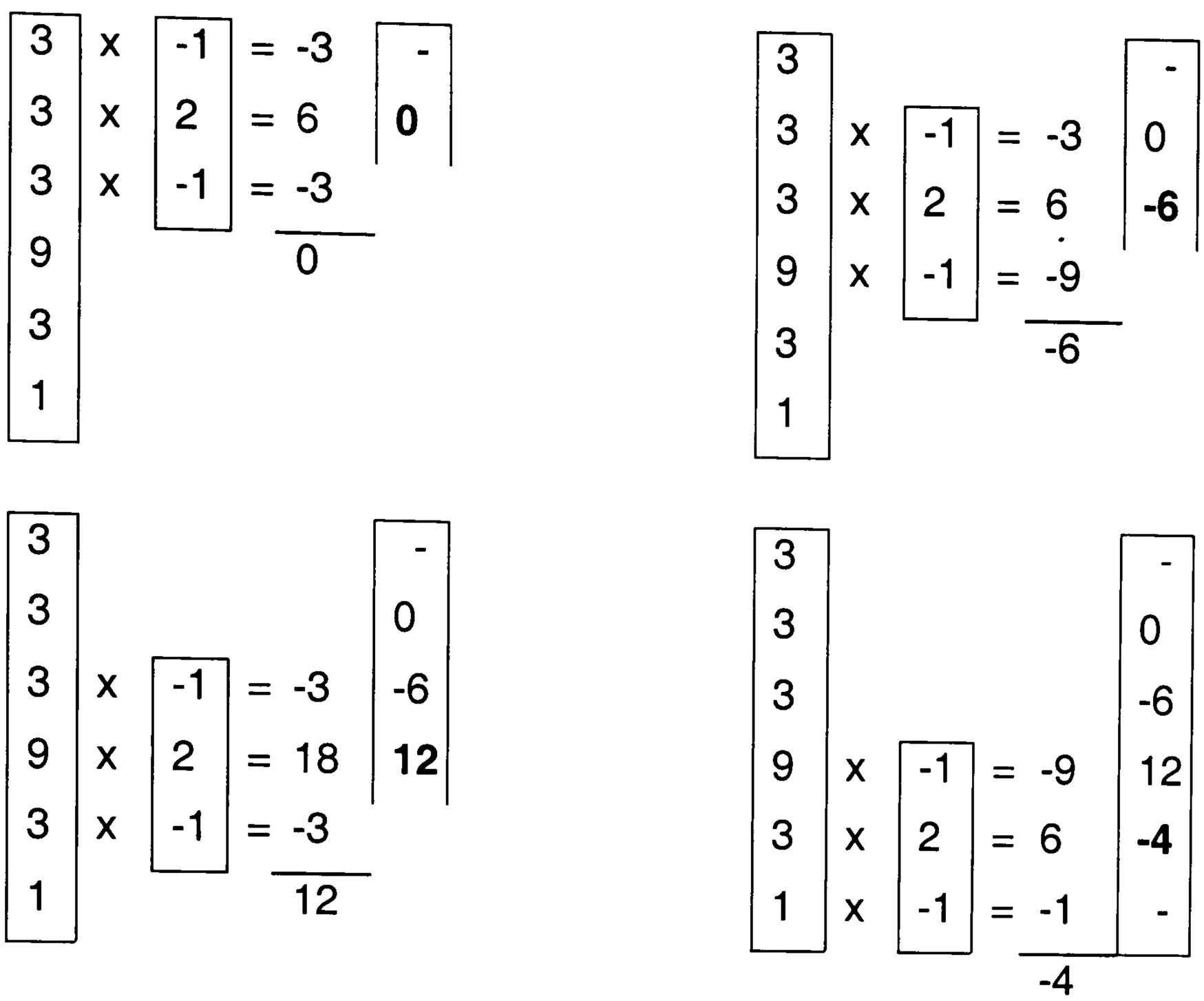

Figure 2.11 One-dimensional discrete convolution [Leavers, 1992].

The convolution operator is denoted $\times$ and the 2-dimensional discrete convolution can be written formally as:

$$I(x, y) \times g(x, y) = \sum_i \sum_j I(i, j)\, g(x-i, y-j) \qquad (2.)$$

Convolution of an image with a suitable mask, such as the Sobel edge operators, can be used to effect edge detection (section 2.4.10). A useful extension of convolution theory is the *point spread function* [Gonzalez *et al*, 1992]. The convolution of an image $f(x, y)$ with a linear position-invariant operator $h(x, y)$ is

$$g(x, y) = h(x, y) \times f(x, y) \qquad (3.)$$

In the frequency domain the following relation holds true

$$G(u, v) = H(u, v)\, F(u, v) \qquad (4.)$$

where are G, H and F are Fourier transforms of g, h and f. In image processing theory $H(u, v)$ is the *optical transfer function,* and if a unit impulse function is applied to the system, where for this input the Fourier transform is 1, then equation 4 becomes

$$G(u, v) = H(u, v) \qquad (5.)$$

That is, the inverse transform of $G(u, v)$ is $h(x, y)$ which is the *impulse response* or in optics the *point spread function*. This term holds because the effect of the system transfer function $H(u, v)$ on a point of light, or impulse, is to blur it. The transfer function and point spread function of an optical system are therefore Fourier transforms of each other.

2.4.4 Visual inspection

Machine vision can be used at two stages in manufacturing, assembly and inspection. In assembly a vision system can provide a robot with the locations and orientations of components in real time. This is now particularly significant for flexible manufacturing as production lines can react more rapidly to new demands. The second application is inspection where following a production process data is collected and a decision is made whether to accept the part or reject it.

2.4.5 Lenses and illumination

There are many confusing terms to describe the branches of photography relevant to the Intelpadprint project. *Close-up photography* and *photomacrography* (or macrophotography) use cameras and lenses at less than their normal focusing distance, and whereas close-up photography occupies the magnification range of approximately 1:20 to 1:1, photomacrography can be used for the range of 1:2 to 30:1. Photomacrography uses a simple microscope, which contains one objective lens or a combination of lenses. By contrast

photomicrography uses a compound microscope with an objective lens and an eye-piece, and because of the greater resolution available is commonly used where a great magnification is required. For completeness, *microphotography* should not be confused with photomicrography as it uses a microscope in reverse, to produce small images of large objects [Williams, 1984] [Vetter, 1984]. As the graphics produced by pad-printers are commonly in the range of 5 × 5mm to 130 × 130mm and a visual inspection system should be as compact as possible Intelpadprint requires the use of close-up photography.

Zoom lenses, close-up filters, extension tubes, bellows and fixed-focal-length lenses may all be applicable to the system being developed for Intelpadprint. Most lens cause errors in refraction and image formation or *aberrations* and lenses are designed with multiple elements to minimise these imperfections. In order to cope with graphics of different sizes a zoom lenses can be considered, though caution must be taken. It is known that zoom lenses can produce field curvature where a flat object produces an image focussed on a curved plane and distortion [Ray, 1984].

The light source for visual inspection has often been an after-thought, but with applications demanding higher speeds and resolutions and the use of colour, lighting has been rapidly improved. Important considerations are uniform spatial intensity, constant intensity over short time periods and over the lifetime of the element, and *cold* (white) light. Regulated direct current supplies are now at the same prices as unregulated alternating supplies were until recently. The resulting current contains less ripple and noise [Smith, 1997].

2.4.6 Template matching

Difference template matching is one of the fundamental and oldest image processing techniques. In its simplest form the absolute difference between a test image and a smaller reference image is computed for points in the test image. If the sum of the differences exceeds a threshold there is considered to be a mis-match at that point. Depending on the size of the template and the test image this computation can be costly so various techniques have been proposed to speed up the process.

Instead of computing the difference row by row, it is possible to select the order for the calculation [Nagel *et al*, 1972]. It is also possible to select the order in which the template positions are tested but this was not explored. One ordered search strategy is to test the template points in the order (highest to lowest) of their expected difference from a randomly selected picture point. As the cumulative sum can be tested against the threshold at each cycle the routine can be stopped for that location as soon a mis-match is achieved. A second strategy is to test points in order (lowest to highest) of joint probability of occurrence in the template and picture. The second strategy can be up to three times faster than the row by row method on complete images.

A second method for increasing the speed of computation is to use coarse and fine templates [Rosenfeld *et al*, 1977]. The block means of the template and test picture are found and matched together first. When the correlation is below a given threshold in localised areas the fine template is then used on those areas. It was found in some cases that the minimum computational cost resulted from a very coarse first template.

Another method has been proposed which is two-stage template matching. Here sub-templates are used first to find possible locations of features, such as edges or corners in the image,

before the overall template is used to confirm a possible match for the object. An advantage of using sub-templates is that they are less affected by the orientation or scale of the object in the image [Vandebrug *et al*, 1977].

The time taken to perform a template matching procedure depends on the number of pixels in a two-dimensional image, and as the size of the image increases to improve resolution the computational load increases as the square. Difference template matching is also sensitive to noise, and orientation and scale variations.

2.4.7 The Hough transform

An alternative is the Hough transform which was first developed for the study of particle tracks [Hough, 1972]. The *classical* Hough transform can be used to search for regular curves and ellipses in noisy images, where an equation for the line can be found. The *generalised* Hough transform (GHT) is used to analyse arbitrary shapes where their boundaries cannot be specified in parametric form. Due to its simpler nature the *classical* Hough transform is reviewed first.

The initial work used the slope-intercept model for a line which produced an infinite parameter space, leading to computational difficulties. The alternative proposed by Duda and Hart has been generally adopted and is the parametric description of a straight line given by:

$$x \cos \theta + y \sin \theta = r \qquad (6.)$$

where r is the length of the normal between the origin and the line and θ is the angle of r with respect to the X-axis [Duda *et al*, 1972] [Fisher *et al*, 1994]. In relation to image processing, xi and yi are the coordinates of candidate edge segments resulting from edge detection, while r and θ are unknown. The Hough r-θ parameter space yields curves corresponding to points,

and points on the same line segment produce intersecting curves. The Hough transform is useful for locating shapes in noisy images and is scale and orientation invariant. Referring to Figure 2.12, rotating the square in part a) by 45 degrees would result in a shift in the transform-space (b) by $\pi/4$ along the θ axis. A change in scale alters the height of the 4 peaks in the p-θ plot.

An implementation of the Hough transform involves quantizing the parameter space into accumulator cells. Each point xi, yi which may form part of a line segment is transformed to a discretised curve and the elements of the accumulator array corresponding to that curve are incremented. Thresholding isolates points where there is strong evidence of a line, in the form of peaks in the array.

Deans related the Hough transform to the earlier development of the Radon transform, and this made the wealth of analytical work undertaken for this transform available to developers of the Hough transform. The use and properties of the Radon transform for lines and pixels was developed, and the Hough transform was generalised to extract arbitrary shapes in their entirety, as opposed decomposing them into line primitives [Deans, 1981] [Ballard, 1981]. Implementations of the *generalised* Hough transform define the relationship between the boundary conditions, orientations and Hough parameters in a look-up table (R-table). A preparatory step uses a template or prototype shape to calculate the values in the look-up table [Fisher *et al*, 1994].

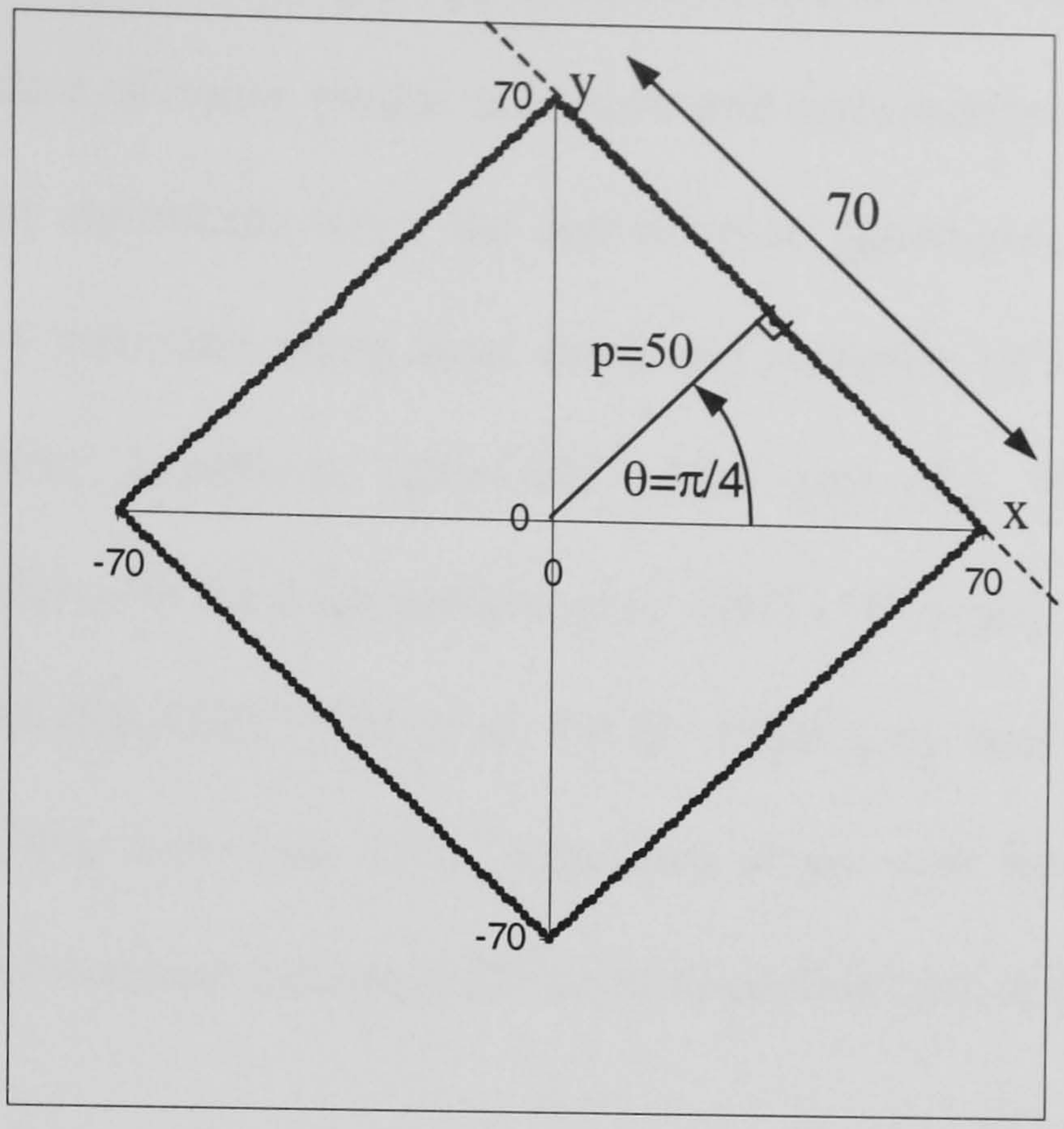

(a)

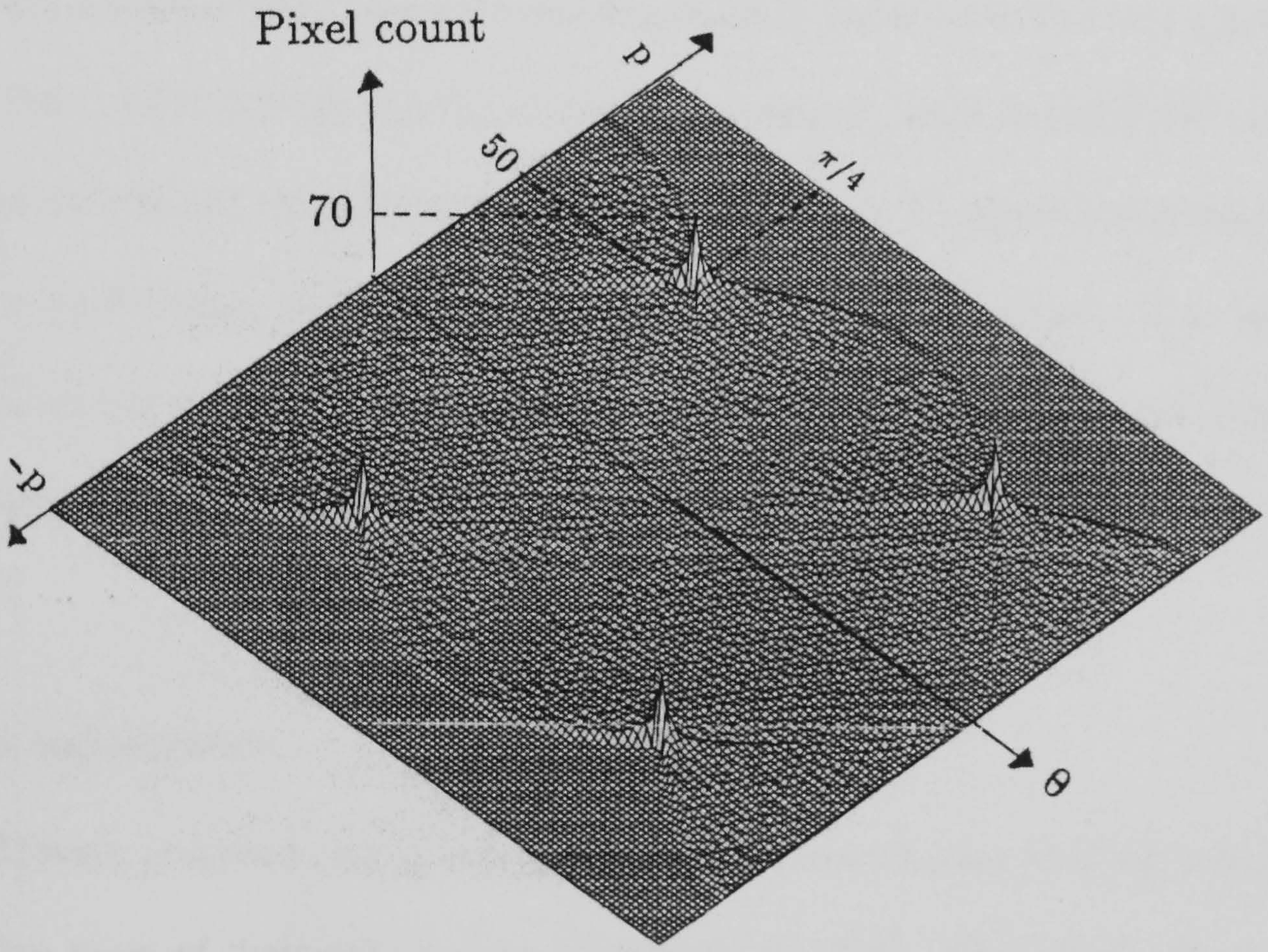

(b)

Figure 2.12 a) A square and b) the 4 peaks of its Hough transform [Leavers, 1992].

The principal disadvantages of the generalised Hough transform are the amount of processing and the size of the memory required. Many variations of the GHT, which aim to reduce

computational load, have been developed by practitioners and they have been compared for their robustness in the face of noise, partial occlusion and scale-rotation variations [Kassim *et al*, 1997]. The different algorithms were: the conventional generalised Hough transform (C-GHT) [Ballard, 1981]; a transform using local slope and curvature (SV-GHT) [Ma and Chen, 1988]; a relative-gradient transform (RG-GHT) [Ser and Siu, 1992]; one employing displacement vectors relative to the edge gradient (DV-GHT) [Thomas, 1993]; and an *edge-as-reference* point transform (ER-GHT) [Lee *et al*, 1992]. Finally, the *scale-orientation invariant* transform (SOI-GHT) [Jeng and Tsai, 1991] describes shape with the aid of half lines and circles in the point spread function (see page 35) and this replaces the R-table.

The ER-GHT was reported as the most complex scheme with the C-GHT having approximately a third of the complexity and the SC, RG and DV-GHTs being appreciably less complex. The C-GHT had the greatest memory requirement, while the ER-GHT required little memory and the rest fell virtually halfway between these two. Comprehensive tests by Kassim and Tan for performance under conditions of object overlap (*oclusion*), noise and multiple objects showed that the edge-as-reference parametric transform performs well even though it has a low computational load [Kassim *et al*, 1997].

2.4.8 Image segmentation

Ballard and Swain proposed *colour indexing* which can be employed to identify objects within images on the basis of their colour alone [Swain *et al*, 1991]. The scheme is geometrically robust in that partial oclusion, a change in orientation, viewing position and even the shape of the object make little difference to its success. This makes it an interesting alternative to template matching, the Hough transforms and other methods, which employ the geometric properties of objects.

In a preliminary step RGB (red-green-blue) triples of images containing model objects are converted to an opponent-theory based colour space which defines the axes: black-white, red-green and blue-yellow, and their histograms are stored in a database. During a test, the camera RGB triples are similarly converted and the resulting colour histogram is compared with the database to find the closest correlation. The method crucially accounts for the area covered by each colour in the object. Computation time is proportional to the number of pixels in the image.

However colour indexing can be limited by spatial and chromatic variations in the illumination. Two solutions to this are pre-processing to achieve colour constancy, or the use of histograms.

It has been proposed that histograms containing the ratios of RGB values from neighbouring pixels be used in place of the absolute colours as these are invariant to changes in incident illumination [Funt *et al*, 1995]. Successful tests were performed on synthetic and real images with spatially varying lighting.

The alternative approach established by Forsyth uses the supposition of a *canonical gamut,* whereby red-green-blue responses from imaging all reflectances under an illuminant that is spatially invariant form a convex hull (that is, their boundary in parameter space is not concave at any point) [Forsyth, 1991]. The original algorithm was successful with the provisos that the illumination was spatially uniform in chromaticity and intensity, the surfaces were planar and there were no specularities. A *RGB* image of a scene under these conditions and with an otherwise unknown illuminant can be mapped to the image that would be produced by the standard *canonical* illuminant. Refinements by Finlayson made the process more robust, so that the constraints could be relaxed and the algorithm applied to real-world scenes; and further

work produced a method to select the best estimate for the illuminant from the feasible set [Finlayson, 1996] [Finlayson *et al*, 1999].

There are two components of light reflected from a surface: diffuse and specular. Specular reflections occur when the angle of incidence equals the angle of reflection, and results in highlights localised around the specular direction. These are generally undesirable as they can cause image processing procedures to fail.

Diffuse reflection is the result of many reflections and refractions from light in a sub-surface layer. The reflections change slowly over the surface; are distributed in a wide range of directions giving the surface a *matte* appearance; and in an ideal *Lambertian* surface they do not change with viewing perspective.

A method was proposed to separate specular and diffuse components which uses polarisation to produce local estimates of the colour of specular reflections [Nayar *et al*, 1997]. The local diffuse component must lie in a subspace produced by the colour estimates and this is employed in the image neighbourhood to find the diffuse component. It was reported that unlike previous separation techniques this algorithm copes with gradual variations in diffuse reflectance, different material properties and specular reflection on textured objects.

2.4.9 Noise in images

A problem usually inherent in noise reduction by smoothing is blurring of the image. Improving on previous methods, an algorithm was proposed which detects areas where edges do not occur by virtue of a small variance and uses the minimum variance pixels to average the homogeneous neighbourhood [Nagao *et al*, 1979]. The technique works well on real scenes, preserves the detail at boundaries and can be used to sharpen blurred images.

2.4.10 Line, edge and corner detection

An important topic in image segmentation is finding edges, or local changes in image intensity, using template matching (TM) or the *differential gradient* (DG) approach. Both aim to accentuate borders for selection and so have been termed enhancement/ thresholding edge detectors, and because they use the perimeter as opposed to the area of objects later processing is reduced. Both techniques use convolution, but whereas template matching employs typically 8 to 12 masks for different edge-directions and takes the maximum response, only x and y differential gradient operators are required and the outputs are summed vectorially:

$$g = (g_x^{\,2} + g_y^{\,2})^{1/2} \qquad (7.)$$

To save computation expressions of this form are often simplified in image processing to:

$$g = |g_x| + |g_y| \qquad (8.)$$

or

$$g = max(\,|g_x|, |g_y|) \qquad (9.)$$

Roberts, Sobel and Prewitt proposed differential gradient masks, while Prewitt, Kirsch and Robinson have developed well-known template matching operators [Robinson, 1977] [Davies, 1997].

Detecting narrow lines, as opposed to edges, is a distinct problem, and as pad printing is often used to produce fine lines it is particularly significant. Operators which find line segments often fail at junctions and line-ends, so building on the work of Vandebrug, three variations were proposed and evaluated [Paton, 1979] [Vandebrug, 1976]. They use various sampling configurations to choose unconnected pixels in a 9 by 9 neighbourhood; criteria against which evidence of a line in a given direction is assessed; and a further rule to filter evidence of lines in different directions in a given region. The performance was discussed in the context of

noise, competing structures in the proximity of lines and scope for line-building from segments. False negatives and positives occurred especially in the presence of noise.

-1	-2	-1
0	0	0
-1	-2	-1

-1	0	-1
-2	0	-2
-1	0	-1

Figure 2.13 Sobel differential gradient convolution operators[1]

Corner detection is another interesting topic and uses the supposition that a local area round a corner contains ordered grey levels corresponding to the object, the edge region and the background respectively [Paler *et al*, 1984]. The sharpness and contrast of a grey-level histogram of a candidate area were examined to provide evidence of a corner. The algorithm works well under noisy conditions but does not find the orientation of the corners. This is a common problem among corner detectors which recent work attempts to solve [Chabat *et al*, 1999]. Based on a scheme proposed by Yang *et al*, the operator calculates the anisotropism at all points in the image where edges occur and removes those points, which are strongly anisotropic as they are not corner points [Yang *et al*, 1996]. The procedure finds the direction of corners using the edges in their local area and worked well in the presence of noise.

Abdou and Pratt developed performance criteria for edge detectors based on a) deterministic calculation of edge sharpness, b) comparison of probabilities of correct and false edge detectors and c) figure-of-merit computation [Abdou *et al*, 1979]. When applied to a variety of edge detectors it was found that the 3x3 Prewitt and Sobel masks performed better than other 2x2 or

---

[1] Note that all mask coefficients sum to 0, indicating a response of 0 in constant areas, as expected of a derivative operator [Gonzalez and Woods, 1991].

3x3 differential masks; the best DG and TM operators performed comparably in respect of edge direction and signal-to-noise ratio; and amplitude tuning of extended size edge detectors is preferable.

An important topic for many feature extraction routines (including edge detectors) is optimising the threshold and detectors to overcome noise and other real-world features. Wilkinson extended the use of a *robust automatic threshold selection* (RATS) algorithm which uses a weighted mean of an arbitrary areas in an image, and eight detectors were examined. Criteria were used to select the best detector for curves, and the 3x3 Sobel differential masks gave the best performance against noise in synthetic images.

The tension between speed and accuracy in two-stage template matching, as introduced by Nagel, Rosenfeld and Vandebrug, was examined in the context of the generalised Hough transform [Davies, 1988]. Davies used a criterion-function solution to optimisation, but also found that random sampling of images sometimes gave the best results. A method was formulated to decide when ordered searches should give way to random ones.

It was argued that though edge detection and region growing appear unconnected they are identical problems [Haralick, 1980]. The proposed solution determines edges as points of significant slope between regions of adequate homogeneity. A later approach models edges at sub-pixel accuracy using the *local energy* function [Kisworo *et al*, 1994]. It uses the property that, the components of the Fourier expansion of intensity across various types of edges (step and ramp for example) exhibit phase congruency. Local energy is a complex function, which is defined as the difference of the Fourier function and its Hilbert transform, but these can be replaced with simpler quadrature functions too. The algorithm improved on an earlier method

by considering various edge models and it was found to work robustly on real images of two and three-dimensional edges.

Curves in images can be described elegantly using a quadtree, where the line is segmented at multiple resolutions depending on its local degree of curvature [Calway *et al*, 1994]. The *multi-resolution Fourier transform* (MFT) is used, and problems of redundancy and computational load are addressed. Preliminary work was encouraging. An alternative approach puts forward a paradigm for curve description which views curves as unique geometric entities, and does not seek to model them as line segments [Forsyth *et al*, 1991]. It is demonstrated on planar and three-dimensional objects under different camera perspectives.

A problem with applying template matching to real objects in images is the large numbers of models required to successfully handle all possible projections of the three-dimensional object [McQueen, 1981]. The difficulty was surmounted by using context and generalising the template to a class of objects, as opposed to a particular member of the class. A twenty-sided polygon was used as a model for bubbles in a biological sample but intense computation was reportedly necessary so this method is most suited to image processing as opposed to machine vision and inspection.

It was argued that the scale at which images are processed can have an impact on the information that can be extracted from them [Lindeberg, 1998].

Implementation of the generalised Hough transform can require: 1) edge enhancement and detection, 2) edge thinning, 3) edge linking, 4) accumulation of data in parameter space (GHT), and 5) extraction of significant peaks in parameter space; though removal of steps 2 and 3 can be tolerated.

2.5 Summary

It was demonstrated that pad printing has improved significantly during the past century and there is still a large market for pad printed products, primarily because of the ability of the pads to decorate doubly curved surfaces. Improvement and automation of the process would secure the European share of world printing capacity.

Low level or inner-loop control of actuators is best achieved using classical control theory. The pad and cliché actuators particularly require proven and robust technology as there is the potential for collision, with the associated safety risk [Chiu *et al*, 1995]. The pad printing process is non-linear, complex and difficult to model. Intelligent control techniques incorporating neural networks and fuzzy set theory are suitable to model and control the process at a higher level.

Machine vision will be an important tool to achieve quality control of the pad printing process. Object location will be achieved by means of the Hough transform, coarse-fine template matching or another convolution technique will be used to locate the print. Pattern recognition will be used to identify specific printing errors.

3 Development of the Intelpadprint algorithms

3.1 Introduction

In chapter 1 the needs of the market were identified and objectives of the project to satisfy those needs were explained. This chapter is concerned with producing a design specification to meet those objectives. Then the design methodology and experiments to find a solution for Intelpadprint are presented. Finally the concept for the pre-prototype printing system is developed and a survey that was used to collect data from pad-printer operators is discussed.

3.1.1 Product Design Specification (PDS)

It is useful to discuss the overall design process for Intelpadprint. Pugh defines *total design* as *"the systematic activity necessary, from the identification of the market/user need, to the selling of the successful product to satisfy that need..."*, and he goes on to contrast this with partial design which involves for example mechanical analysis in isolation to market need [Pugh, 1991]. Technical rigour must not be sacrificed, but the success of a product can best be achieved by fitting this into the framework of total design. Intelpadprint requires the design of a number of sub-systems: new inks, pads, printer, software, hardware, and these can be considered as modules as well as one inter-connected entity. As this thesis describes the research and development of the inspection and control system this part will be considered on its own.

The total design methodology proposed by Pugh involves the specification of a product design (PDS) which follows next. A linear flow-chart is presented whose core is market analysis, specification, concept, detail design, manufacture and sell. This simple model is similar to the linear waterfall model in Figure 3.1 in contrast to the Intelpadprint programme, which lends itself to the iterative process proposed in Figure 3.2.

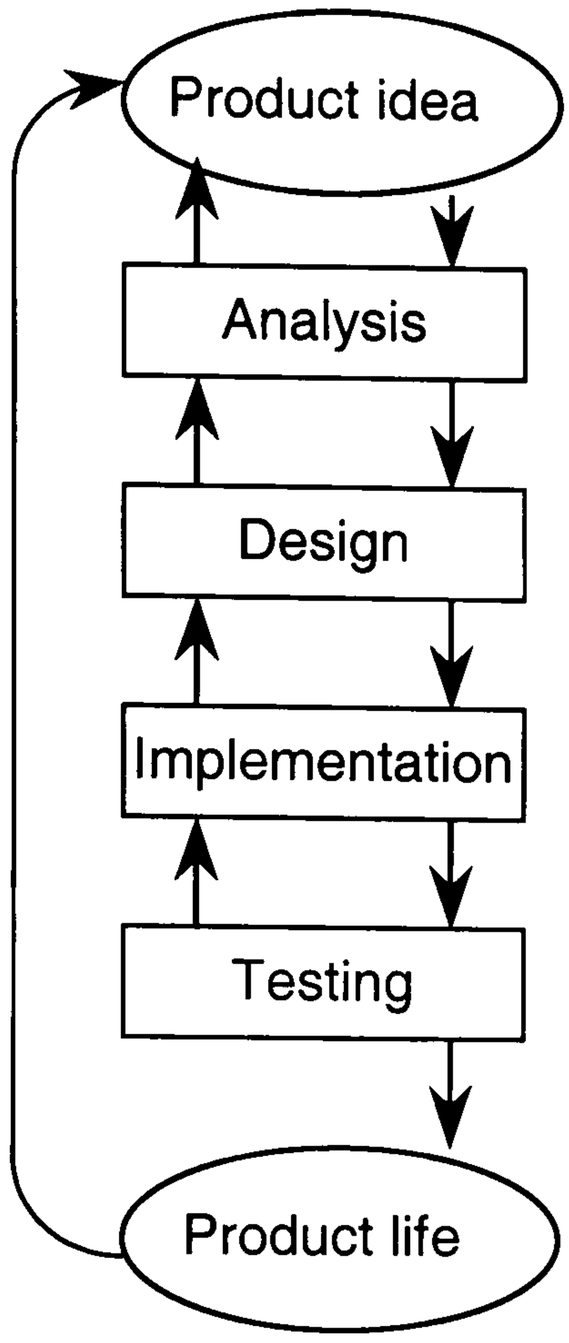

Figure 3.1 Linear waterfall software design model.

The product design specification in Table 3.1 for the Intelpadprint inspection and control system (software and hardware) is based on the objectives laid out in the introductory chapter. This is not a fixed document but rather the first version of a specification, which will guide the author and evolve as the project progresses.

Table 3.1 Product design specification for the Intelpadprint printer including inspection and control systems

1. Purpose	To reduce the pad printing reject rate from 5% to 0.1% by identifying and controlling printing errors, and to automate the process.
2. Performance	Real-time image processing for pad printing at 2 cycles/ s, successful inspection is initially more important than speed.
3. Environment	Factories in European and other climates: electrical noise, vibration, inks and other chemicals, dust, static electricity.
4. Life in Service	Hardware: 5 years, software will be upgraded approximately once every

		two years.
5.	Maintenance	Hardware should be low maintenance; software can be upgraded infrequently.
6.	Target cost	Unknown.
7.	Competition	Manually controlled standalone printers, semi-automated one-off printing lines.
8.	Quantity & Market	Low volume, 100s/ year. Market: large manufacturers of consumer goods.
9.	Size & Weight	Sensors: miniature but not micro; photographic system: within 1(h) x 0.5(d) x 0.3(w)m.
10.	Aesthetics	Functional.
11.	Materials, manufacturers	New software (Maastricht, Birmingham, contractor), off-the-shelf hardware, new and existing printer parts, new pads (Tampoprint), inks (Marabu).
12.	Product life span	20 years plus: once automation is adopted it will exist as long as the pad printing process is used.
13.	Quality & Reliability	High reliability is essential to minimise downtime on a production line.
14.	Ergonomics & User	Graphical user interface for use by trained system operator.
15.	Timescale	Three year Intelpadprint project: 1997 – 1999, see project programme and discussion of Rapid Application Development.
16.	Company constraints	Control by Universities of Birmingham and Maastricht, and overall strategy decided by the Intelpadprint consortium: Philips, LEGO, Tampoprint, Marabu and the Universities.
17.	Processes	System design and programming, control engineering.
18.	Product literature	Half yearly, mid-term and end of project technical reports (confidential), minutes (confidential), papers and user help documents.
19.	Social implications	System requires more skilled operators so that the workforce becomes more highly trained, more uniform print quality on consumer goods, and

	see 'political implications'.
20. Patents & Legal	Patents can be filed by individual project partners. Third-party software may be used under license.
21. Shelf-life	Software, hardware, printer, pads: unlimited. Inks: approximately 1 year.
22. Political implications	Greater automation reduces the number of operators required, but increased competitiveness of the European printing industry safe-guards jobs.
23. Installation	By Tampoprint.

Disposal, other standards: not relevant

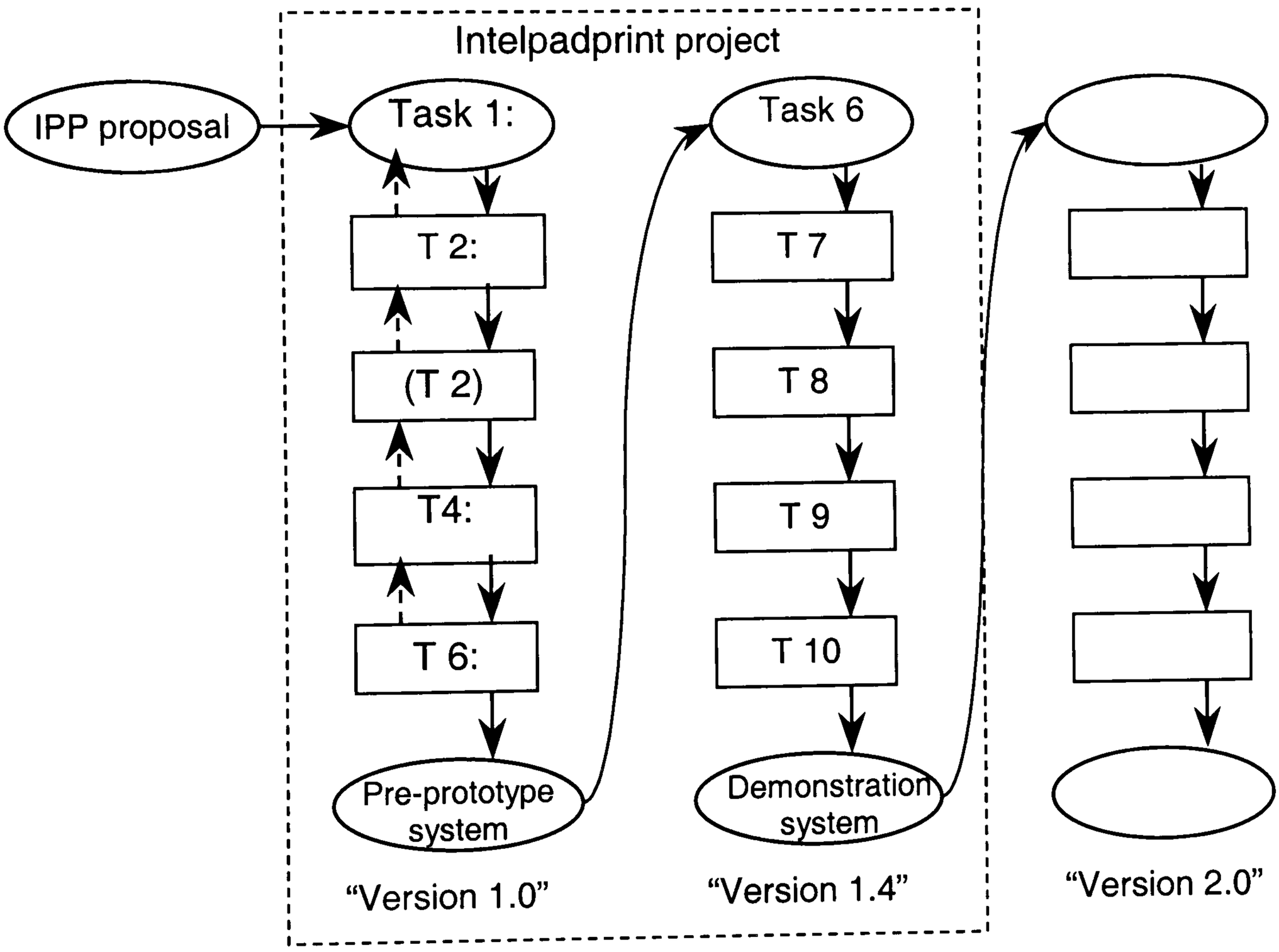

Figure 3.2 Incremental linear waterfall model related to the Intelpadprint tasks introduced in Chapter 1 (table 1.3).

3.1.2 Software engineering risk management

The contributions of the Universities of Birmingham and Maastricht demand appreciable amounts of software development and as Karolak [1999] argues software engineering is still

perceived as a high risk activity when compared with more traditional engineering activities. Risk can be separated into budget, schedule and technical areas. Research has shown that projects typically cost between 50 and 300 percent more than the budget and are 100 percent over schedule [Suding, 1977] [Putnam, 1980] [Karolak, 1985]. Davis' study of nine United States Government projects showed that nearly 30 percent of the budgets was spent on undelivered products, 47% of the software by cost was not successfully used, while only 2% was effective first time [Davis, 1990]. The remainder required minor or major changes. On this evidence it is important to analyse and control risk from the outset to ensure the success of the Intelpadprint project.

3.1.3 Rapid Application Development (RAD)

Rapid Application Development is a flexible software design strategy that balances schedule, economy and product quality to find the right compromise for a given project, and it was considered for the Intelpadprint project. As Maner explains *"in certain situations a usable 80%* [sic] *solution can be produced in 20% of the time..."*, which means that peripheral features and usability may be sacrificed while maintaining core functions [Maner, 1997]. This is the measure of quality in this context, though higher defect rates may also result from RAD and this can also be described as lower quality.

The customer conventionally receives the complete product at the end of the software development process, but RAD involves the release of working prototypes during production followed by evaluation by the customer and further development. This reduces risk and fits well with the Intelpadprint project programme.

A key tool for Rapid Application Development is a "visual" environment such as Borland Delphi, Microsoft Visual Basic, or Microsoft Visual Studio for C/C++, where user interface elements, for example windows, buttons and text boxes can be manipulated as if they were

graphics. This significantly reduces the time and effort required to produce a user interface allowing more time to be devoted to the core problem. Visual tools are easy to learn, reducing the cost of training, they ease the construction of a more effective user-interface and can encourage good design. However, if care is not taken 'quick and dirty' application development can result as planning, coding standards and help documentation are sacrificed. Other tools are *wizards*, code generators, working prototypes and reusable components. An example of a wizard is the series of dialog windows that are displayed during a set-up process that software suites such as Microsoft Office employ, where the user is asked questions and the program uses the responses to effect installation. Reusable components are libraries of functions that different programs or later versions of the same program can utilise, and that can be updated in the field without affecting these programs. They share a common *application programmer's interface* (API) which can be thought of as a blueprint for communication between the library and the application. Typical reusable components are the parts of a Microsoft Windows operating system, which allow a piece of software to have a Windows graphical user interface.

Rapid Application Development is effective when components (for example re-usable components) already exist and when the system can be divided into modules. . It is less appropriate when the product is safety critical, the performance and reliability of the software is of paramount importance, or there are high technical risks. RAD is not a panacea that will automatically prevent time and cost overruns.

Whatever methodology is employed to produce a piece of software there needs to be a model for the stages in the design process and how they interact. A simple one is the linear waterfall model, shown in Figure 3.1, which contains the steps: product idea, analysis, design, implementation and testing. Implementation is the stage at which the computer program is

actually 'written' and each of the steps is performed once before moving on to the next. However this is not a realistic model as most development processes entail re-design of the product in the light of analysis of a prototype. Therefore a more realistic model is the incremental one shown in Figure 3.2 (the Intelpadprint tasks introduced in chapter 1 are related to steps in the design process). After the first release of the software (the Intelpadprint pre-prototype) for use by the project partners there is a process of reanalysis, redesign and re-implementation.

It can be seen that the philosophy of Rapid Application Development fits closely with the Intelpadprint project and an incremental waterfall model can usefully be used to plan the development of the Intelpadprint software. However as we will probably use innovative, high-risk solutions and may produce computationally intensive code which should be efficient we needed to be cautious in using RAD for this project. An extreme implementation of rapid application development where a lower than average quality was tolerated would be incompatible with Intelpadprint, but a more moderate philosophy where faster than average implementation and better than average quality are maintained would be compatible. The latter interpretation of RAD was followed for the development of control software for Intelpadprint.

3.2 Analysis: concept design

At the outset of the project there was no explicit intention to use machine vision for the Intelpadprint project and the project programme merely states that during the project we will *"investigate the use of multi-sensor assisted Adaptive/ Intelligent computer control of the pad-printing process."* Advantages and disadvantages of using direct sensing, machine vision and other process data will be discussed in the following section.

By direct sensing we mean measuring for example the temperature of the ink or the position of the pad. These measurements yield relatively small amounts of data: at most one temperature reading is required per printing cycle, while several hundred position measurements may be needed to calculate velocities and accelerations for a printing cycle. This is time dependent data, and the system can take as many readings as required without the need to filter unwanted data. The small amount of data can quickly be processed into information such as the viscosity of the ink and in this sense it is direct. It indicates the state of the system and it can be compared with a model to enable parameters to be changed to correct printing faults. However an ink viscosity that is too high does not 'contain' the defect '*hairs*' (ink filaments stretched from the printed boundary). It can only imply the defect to an expert system, and as shall be demonstrated in the next section there are a number of causes of hairs and an incorrect ink viscosity can result in a number of printing faults. Sensor data can therefore be considered circumstantial evidence.

By contrast, machine vision yields one image per printing cycle, but the image will contain 442,368 (576 x 768 is the size of image produced by a standard frame-grabber – see chapter 4) pixels and if it is a colour image each pixel has three values (for example red, green and blue). This raw data has no meaning to the computer and so requires a lot of processing to extract useful data and to identify printing errors. It will be difficult to identify which of the printing defects is present in real-time with existing hardware and algorithms. A significant time lag would mean that the product had been lost. However, images contain direct evidence of printing faults if they occur, so the Intelpadprint system would use both visual and indirectly sensed data.

3.3 *Analysis of printing faults*

The Out of Control Action Plan (OCAP) was produced as part of the Intelpadprint project and lists pad printing faults by name and a picture, their causes and corrective actions. There are 18 faults and a good graphic defined. Multiple causes and corrective actions is a common trait among the faults defined in OCAP and this is one of the reasons that direct identification of the printing fault is not sufficient to correct the underlying problem. A control system also needs knowledge of the printing parameters, such as ink temperature to effect control of this complex system.

The OCAP document is based on the knowledge of printing experts and it is instructive to present what independent authors have said regarding decoration faults, though the literature deals with painting as opposed to printing much of it is still valid.

3.3.1 Hairs Hairs are ink filaments stretched from a printed boundary into a non-printed area. They can be caused by a build up of static electricity on the pad or product, which can be solved by blowing ionised air. They can be the result of ink that is too viscous and this can be eradicated by adding thinner, a flow agent or increasing the temperature of the ink by heating the cliché.

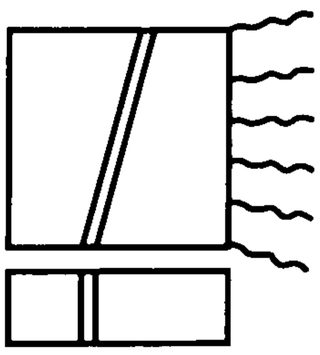

Another cause is a cliché that is too deep, and this can be replaced by one with the correct depth (and raster if applicable). Hairs can result from incomplete ink transfer from the pad, which can be solved by increasing the dwell time of the pad on the product, air-blowing the ink on the pad, using a faster evaporating ink on the pad, increasing the ink viscosity or decreasing the printer speed.

3.3.2 Air-bubbles/ pinholes Air bubbles are the result of air trapped during the release of ink from the pad to the product. They can be caused by use of the incorrect shape or hardness of pad and the solution is to use a "steeper" (more pointed) pad or one with a greater hardness respectively. Air bubbles can be the result of using ink that is too viscous in which case one of the solutions outlined in

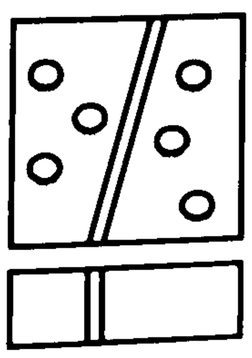

section 3.3.1 is appropriate.

If the doctor-blade (rim of the ink-pot) moves too quickly in relation to the cliché air-bubbles can form in which case the doctor-blade speed should be reduced.

3.3.3 Constriction A constriction (not to be confused with recess) is the result of ink missing from the edge of a printed graphic. Where the graphic is not taken up completely from the cliché or not transferred completely from the pad to the product the pad should be compressed further onto the cliché or product respectively. A constriction can also be caused by dirt on the pad, in which case it should be cleaned.

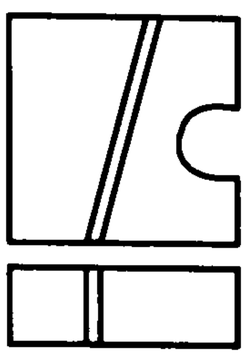

3.3.4 Recess A recess takes the form of extra ink at the border of a printed graphic. It can be caused by a damaged pad, cliché or doctor-blade (the rim of the ink-pot on a closed system) and the defective part should be replaced.

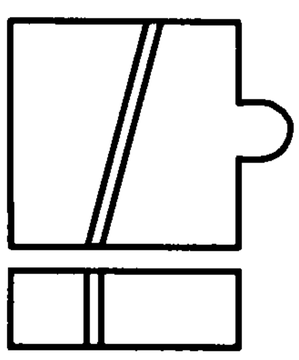

3.3.5 Ink missing Ink can also be missing from inside the graphic. This can be caused by ink that is too viscous in which case the appropriate solution from section 3.3.1 should be applied. Ink may be missing because there is dirt on the pad in which case it should be cleaned. It may be because the solvent evaporates too fast in which case use a slower evaporating solvent, or because the process is too slow in which case the printing rate can be increased. The graphic can be too small for pad printing in which case the artwork and cliché can be changed.

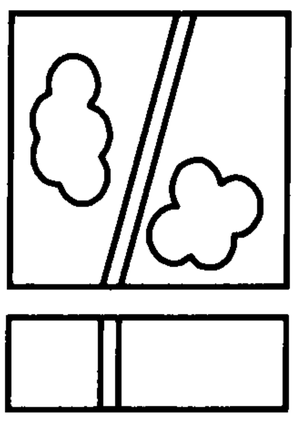

If the surface of the pad is too rough or damaged then the pad should be replaced. Too much or irregular air blowing can lead to missing ink and this can be solved by reducing the air blowing. Finally, if there is insufficient ink on the cliché ink can be added to the ink tray or pot, and in the case of open pad printing the spatula can be adjusted to a deeper position.

3.3.6 Mis-registration of double printing It is sometimes desirable to pad print a part of a graphic twice to increase the opacity of the ink (especially when printing white on black) and mis-registration of double printing describes the mis-

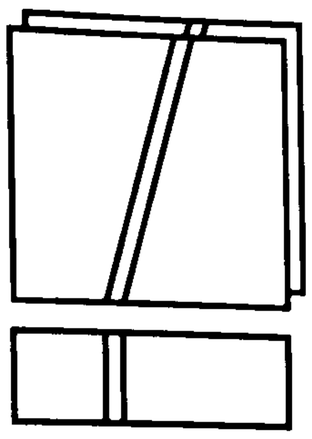

alignment of the second print relative to the first. This can be caused by not pressing the product sufficiently onto the jig, by using the wrong jig or by the jig or pad not being well fixed. The solutions are to use the correct jig and to secure the relevant part.

The mechanical tolerances on printer may be too large in which case the printer should be reviewed or replaced. If the mis-registration is due to the build up of a "ghost" print on the pad then the pad should be renewed. The fault is specific to pad printing and is not mentioned in the literature.

3.3.7 Dirt particles Dirt can be found on the product, in the ink or on the pad. The solutions

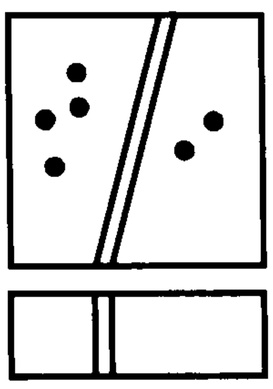

are to clean the product or blow ionised air over it, to change the ink or the pad respectively. D*irt particles* is listed as a fault by Margolis and is possible during any decoration process [Margolis, 1986].

3.3.8 Edge roughness Edge roughness can be caused by the etching process used to produce

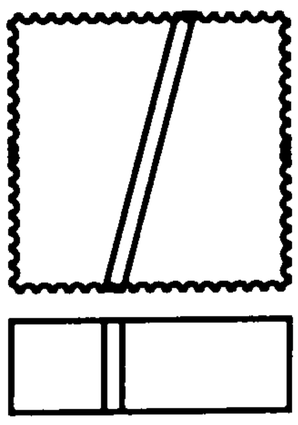

the cliché in which case the cliché should be replaced, possibly using a different material. It can be the result of using a pad with a rough surface and the solution here is to replace the pad. If edge roughness is caused by using the wrong raster size the cliché should be replaced with one containing the correct raster.

If a UV-curable ink is used local (de)wetting of the ink on the product can occur and the solution is to decrease the time between printing and UV exposure. If the fault is caused by the drying of ink on the pad then the time between ink uptake and release on the product should be reduced. Another cause is a textured product in which case a more viscous ink or a product with a reduced texture should be used. Finally, edge roughness can be the result of a poor outline in the film used to produce the cliché and the film should be replaced.

3.3.9 Ink-flow Ink flow results in a straight edge of a printed area becoming convex. It can

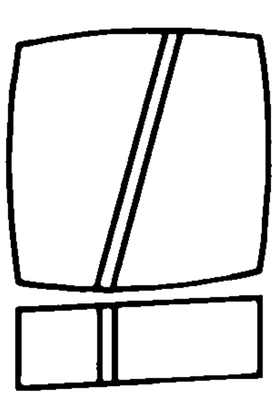

only be caused by too low an ink viscosity and the ink can be replaced or made more viscous to solve it.

3.3.10 Smearing Smearing can be caused by too much or irregular deformation of the pad.

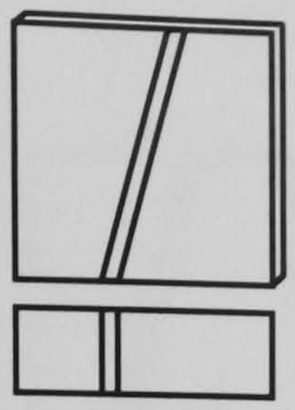

Possible solutions are using a larger pad, decreasing the pad compression, changing the pad position, changing the hardness of the pad and improving the support of the pad.

If the surface of the product is too smooth the graphics can adjusted to compensate or the graphics can be printed in smaller segments or with double printing. Smearing can be caused by an incorrect doctor-blade (rim of the ink-pot in closed pad printing) in which case it should be replaced.

3.3.11 Fine line flow together Narrow gaps between printed areas can be obscured if the ink viscosity is too low in which case ink can be added to increase the viscosity, or the ink can be replaced. The pad may be too soft or the wrong shape for the application in which case it should be replaced. If the thinner evaporates too slowly then a faster evaporating thinner can be added, air blowing can be increased or the printing rate can be reduced.

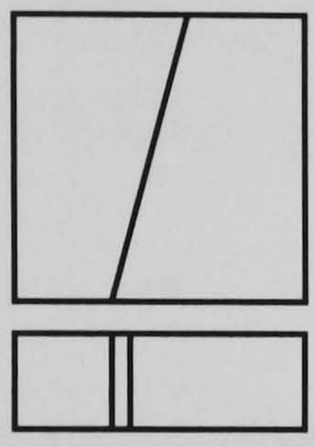

The cause may be a build up of ink on the pad in which case the pad should be cleaned and automatic cleaning apparatus should be installed. If fine lines flow together because a badly designed or fixed product holder (jig) is being used then the holder must be redesigned or re-secured. If the fault is due to a cliché that is too deep or that has rounded etched edges then the cliché should be replaced.

3.3.12 Colour differences Colour differences within a area that should be printed uniformly can be caused by insufficient ink transfer from the pad to the product and one solution is to clean the equipment. When insufficient ink transfer is caused by irregular drying or an ink with insufficient viscosity the air blowing can be improved/ increased or the ink can be changed. If it is due to an ink that is too viscous then thinner can be added to it.

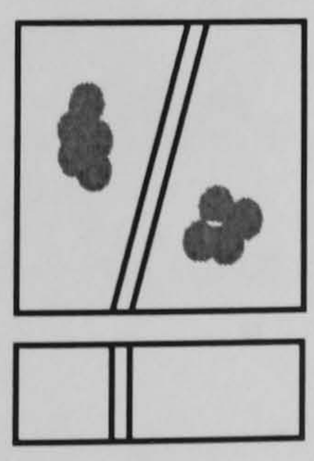

Colour differences can be caused by dirt on the product in which case it should be cleaned prior to printing. If they are caused by the doctor-blade (the rim of the ink-pot in closed pad printing) then a more rigid doctor blade should be used, or the pressure on the blade should be decreased.

3.3.13 Raster points visible A *raster* is a pattern of points at the edge of a recessed (and therefore printed) area that are flush with the upper surface of the cliché. It reduces the density of an ink in order to blend it with a non-printed area or another coloured ink. The points can be visible if the wrong raster is used, in which case the artwork should be changed and the cliché replaced. If they are visible because the cliché is too shallow then it should be replaced with a deeper one.

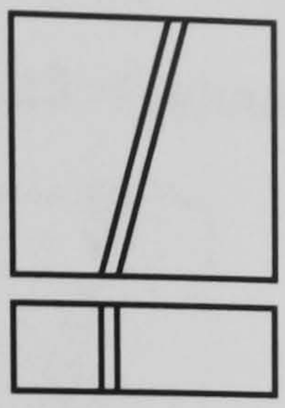

3.3.14 Colour mis-registration Colour mis-registration is distinct from mis-registration of double print (OCAP 6) and describes the misalignment of one printed feature relative to another. Like OCAP fault 6, colour mis-registration can be caused by the product, the product holder, the pad or the cliche not being well fixed or being out of alignment in which case the requisite part should be adjusted and secured. The wrong product jig may be in use or the dimensions of the artwork may be incorrect.

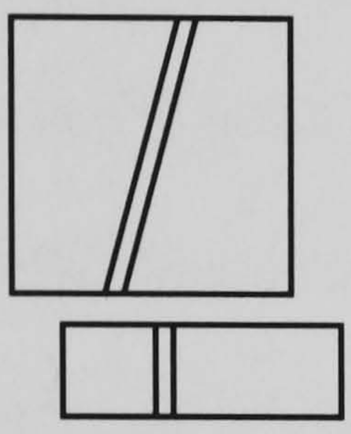

3.3.15 Streaks/ lines Streaks, lines and droplets of ink on the product can be the result of dirt on the doctor-blade, a worn doctor-blade or dirt in the ink. The latter problem can be cured by renewing the ink, protecting the printing station against dirt and cleaning the products. Other possible causes are too viscous an ink and a worn cliché. Thinner can be added and the cliché replaced as necessary.

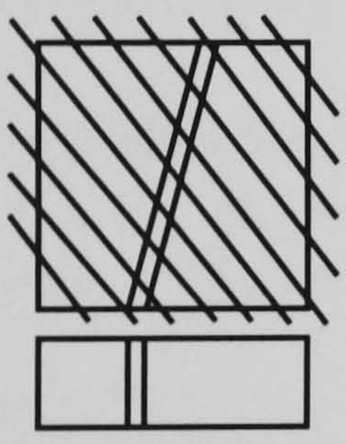

3.3.16 Haze A 'haze' on printed and non-printed areas of the product can be caused by an incorrectly installed doctor-blade. The blade should be refitted and if necessary the pressure on it increased. Other causes are a blunt doctor-blade or a damaged cliché. Haze can be the result of too high a printing rate in which case the rate should be decreased. It can be caused by solvent that evaporates too slowly and in this instance a faster evaporating solvent should be used.

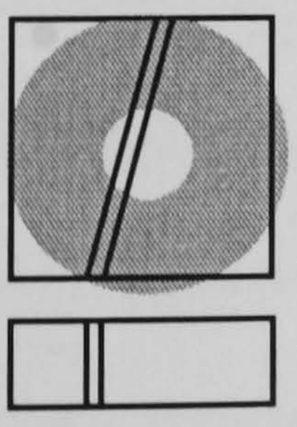

3.3.17 Orange peel Orange peel is the description for an area of print that does not have a uniform depth. It can be caused by a cliché that is too deep in which case it should be replaced. If the printing pad is too new it should be cleaned to remove the excess silicon oil added during the moulding process. Orange

peel can be caused by too flat a pad in which case a 'steeper' (more conical) pad should be used.

3.3.18 Colour match wrong An incorrect colour match is generally the result of an incorrect setup. It can be caused by using the wrong ink, using double printing when single-cycle printing is appropriate, or using single printing when double-cycle printing is specified. Finally, a wrongly coloured product may be in use.

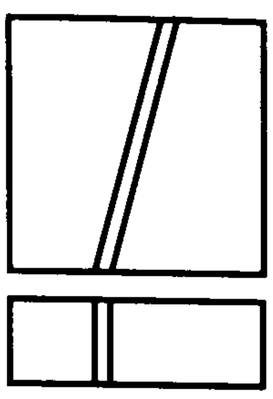

There is no mention in the literature of errors like hairs, *constriction*, *recess* or *edge roughness* (OCAP 1,3,4,8), and what these have in common is that they occur at the boundary of the printed area and could be specific to pad printing. *Air bubbles* (2) (pin-holes) may appear similar to 'pops' or 'fisheyes' described by Margolis but whereas air bubbles are attributed to mechanical causes by OCAP, Margolis cites chemical causes [Margolis, 1986].

Ink-flow, *smearing* and *'fine lines flow together'* (OCAP 9, 10, 11) are not faults mentioned by the literature, because they occur at the ink-boundary and so are printing as opposed to painting errors. The OCAP error *colour differences* (12) within a printed area is similar to Margolis' 'blush' and he attributes this to application of the ink/ paint below the ambient dew point.

The analysis of the OCAP document shows that a number of assumptions were made. A number of authors [Margolis, 1986] [Hess, 1979] allude to errors arising from an adverse reaction between ink and substrate, but this is not covered by OCAP probably because a limited number of plastics are pad printed and these are known through extensive testing to be inert with the inks. Two assumptions about pre-processing are that the mould and substrate are good quality, and that the substrate is not mis-handled so as to be not present or damaged prior to printing.

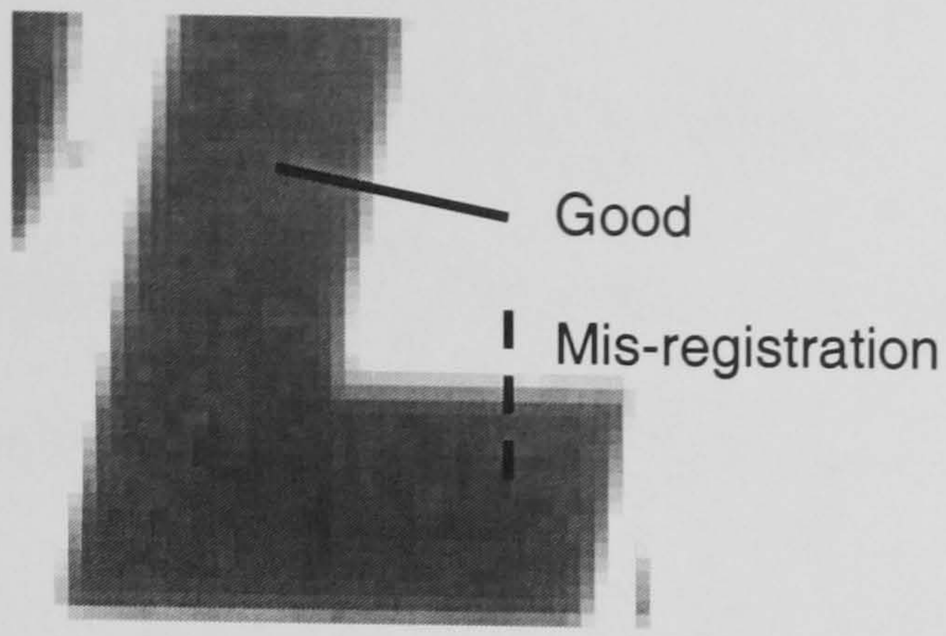

(a)

13	0	17	7	213	207	212	211	…
7	17	13	8	216	213	204	211	
3	19	1	7	215	205	215	207	…
4	20	5	15	209	218	209	218	
0	14	5	16	212	211	212	205	…
5	11	18	10	205	203	208	211	
7	9	4	3	217	219	200	211	…
16	13	1	8	220	209	216	209	
…		…		…		…		…

(b)

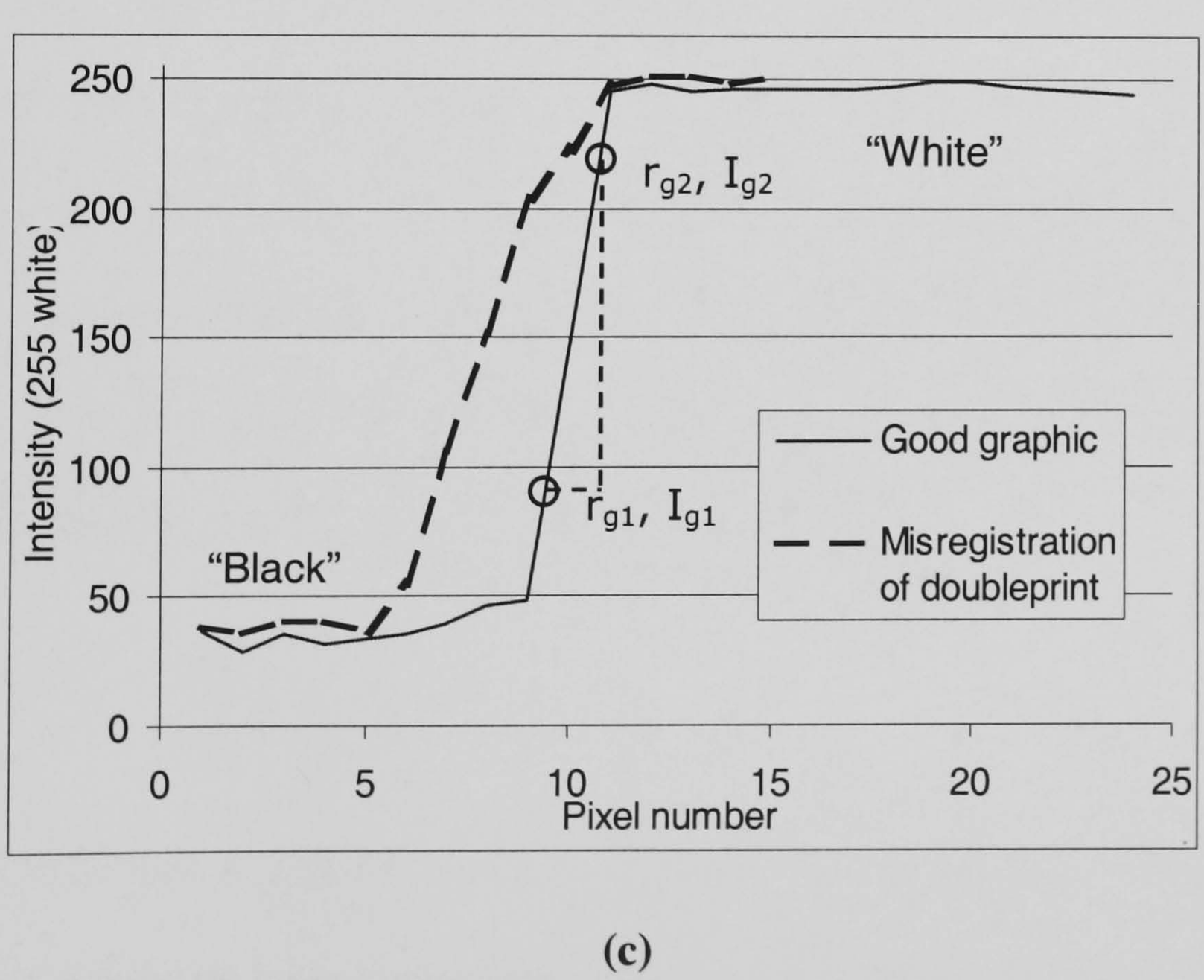

(c)

Figure 3.3 Example of mis-registration of double print (OCAP 6)

Figure 3.3 a) Example of mis-registration of double print (OCAP 6), b) a part of the image matrix showing the good edge (vertical) and a perpendicular path along which pixel values are extracted, and c) a graph of a good and mis-registered edge.

3.4 Early experiments on 1-dimensional image profiles

Experiments were conducted to test ways of differentiating the OCAP printing faults using visual data. The results would be used to formulate algorithms to solve the problem set by Intelpadprint.

Samples of products containing faults were provided by the project consortium, and grey-level images of the faults were taken with a Kodak DC120 digital still camera in natural light. The MATLAB mathematical software package was used to manipulate the images. These were eight-bit images, that is each pixel could have an integer light-intensity value in the range 0 to 255 ($2^8 - 1$). In MATLAB a grey-level image is represented by a 2-dimensional matrix and a part of one is shown in Figure 3.3 b) (the images are 768 columns wide by 576 rows high). The 4 columns of numbers on the left represent a dark grey area while those on the right are a white printed area with a sharply defined 'good' edge in between. The row of pixel values indicated in Figure 3.3 b) can be extracted and plotted on a graph against the position of the pixels. The gradient of the edge is the change in intensity, $I_{g2} - I_{g1}$, divided by the change in position, $r_{g2} - r_{g1}$. As these changes tend towards zero (become infinitesimally small) the gradient can be represented by a *differential* expression, dI_g/dr_g:

$$\frac{I_{g2} - I_{g1}}{r_{g2} - r_{g1}} = \frac{dI_g}{dr_g} \quad \Delta \to 0 \qquad (1.)$$

However, the finite size of a pixel in a digital image limits the changes to finite values so the expression on the right in 1 can be replaced by $\Delta I/\Delta r$. The mean gradient of an edge in a mis-registered double-printed graphic (OCAP error 6) was found and this was less than the gradient for a good edge:

$$\frac{\Delta I_e}{} < \frac{\Delta I_g}{} \qquad (2)$$

Δr_e Δr_g

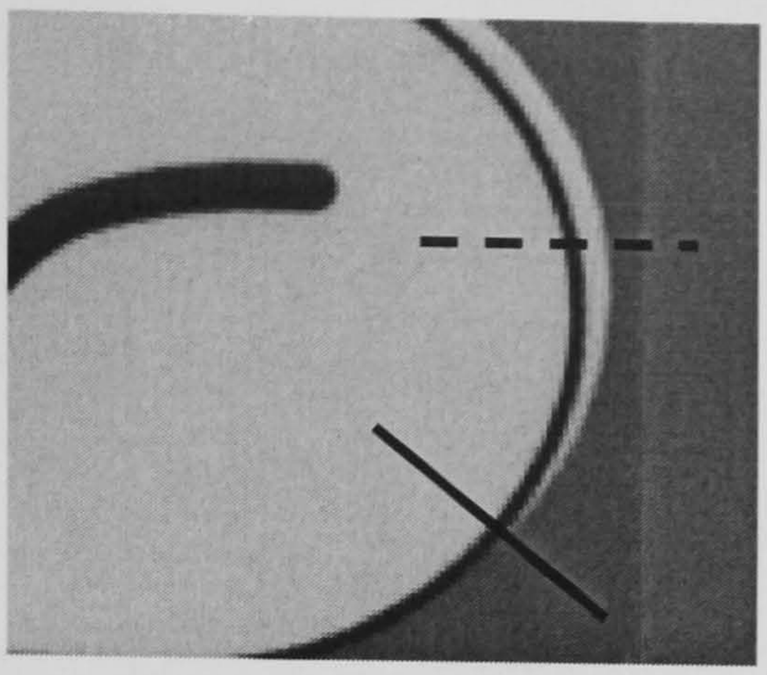

(a)

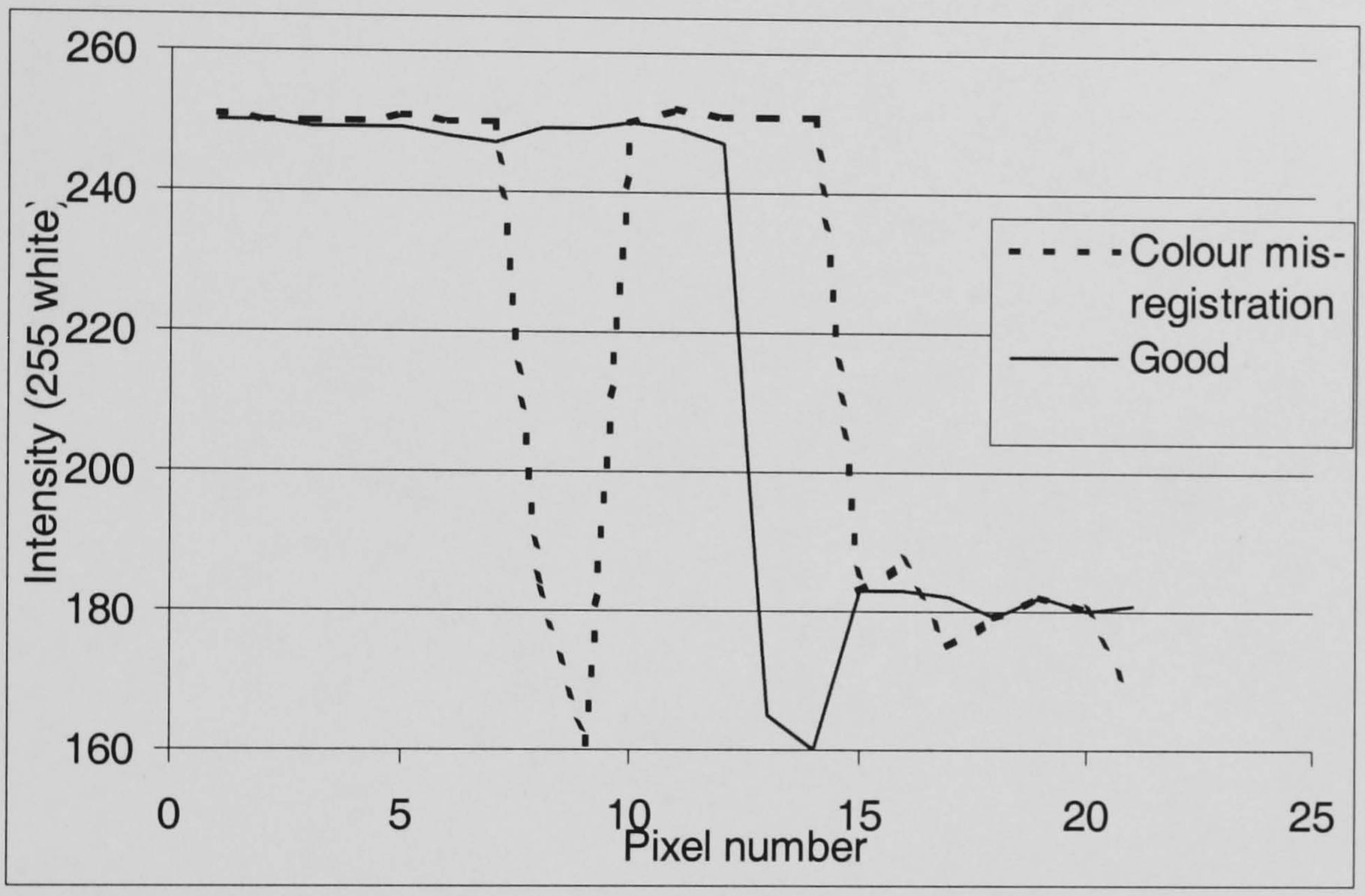

(b)

Figure 3.4 a) Example of colour mis-registration (OCAP 14), and b) graphs of good and faulty edges

Another test was performed on the image in Figure 3.4 of a sample containing a black line that is mis-aligned with respect to the white print it should separate from the red black background (OCAP error 14). Contiguous pixel values (*profiles*) were again extracted along paths perpendicular to good and erroneous edges. The graph of the good edge contains three regions (white, black and grey), while the graph of the error contains an extra white region between the black line and the red background.

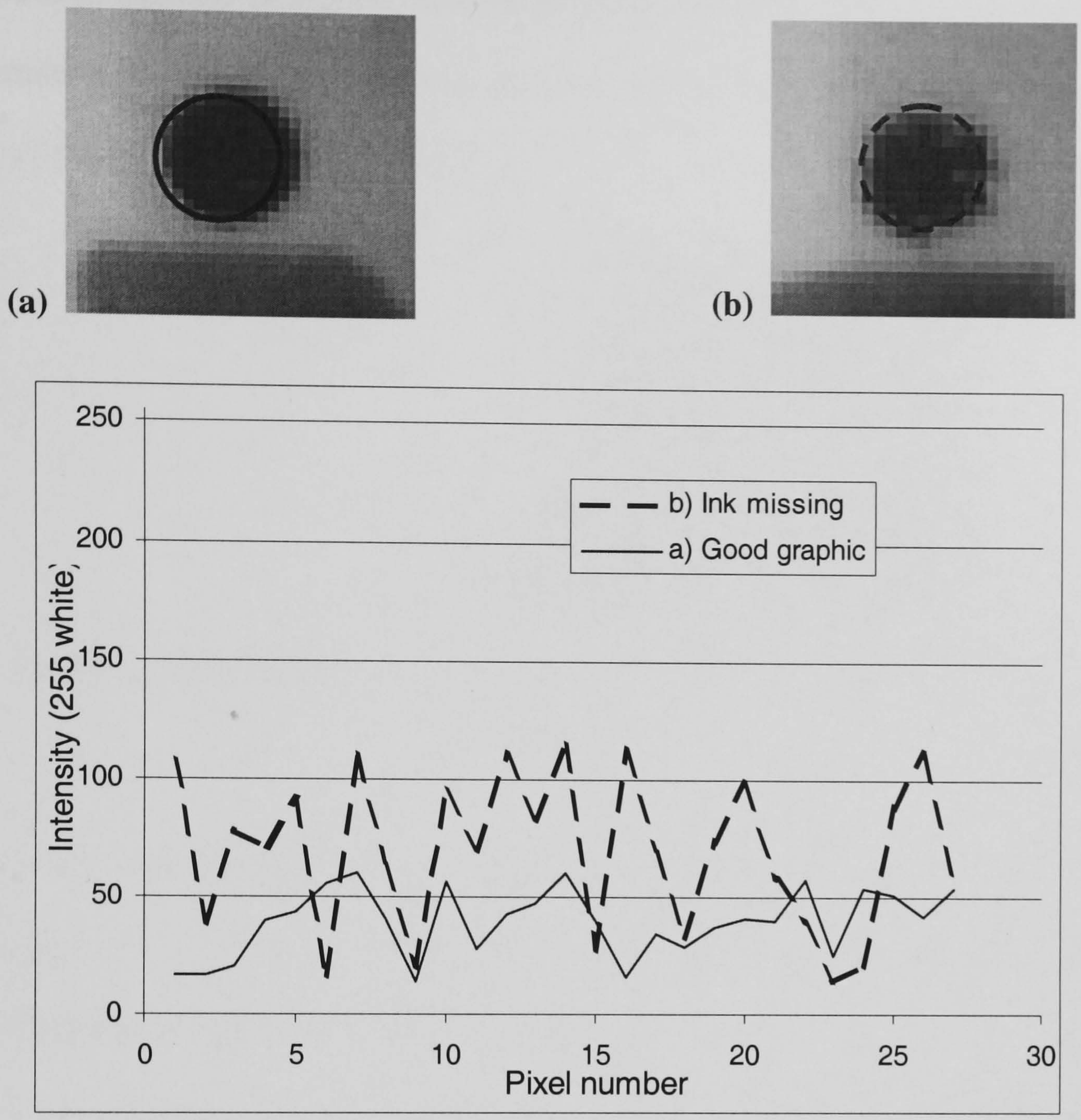

Figure 3.5 Example of a) a good print and b) a print with ink missing (OCAP 3/ 5), with c) graphs.

The final example (Figure 3.5) contrasts an acceptable print of a round black dot with a print containing *constriction* and missing ink (OCAP errors 3 and 5). Circular profiles taken just inside each perimeter demonstrate that there is a wider distribution of grey-levels for the constricted print (grey-levels 115 to 250) compared with the good print (levels 95 to 175). The mean difference in intensity between neighbouring pixels is greater in the bad than in the good graphic.

The conclusion from this small set of tests is that statistical measurements directly on one-dimensional profiles extracted from an image can be used to recognise OCAP errors.

However, large numbers of profiles would need to be extracted. What became apparent from the experiments was that the OCAP faults can be broadly separated into classes based on where they occur in relation to a printed boundary.

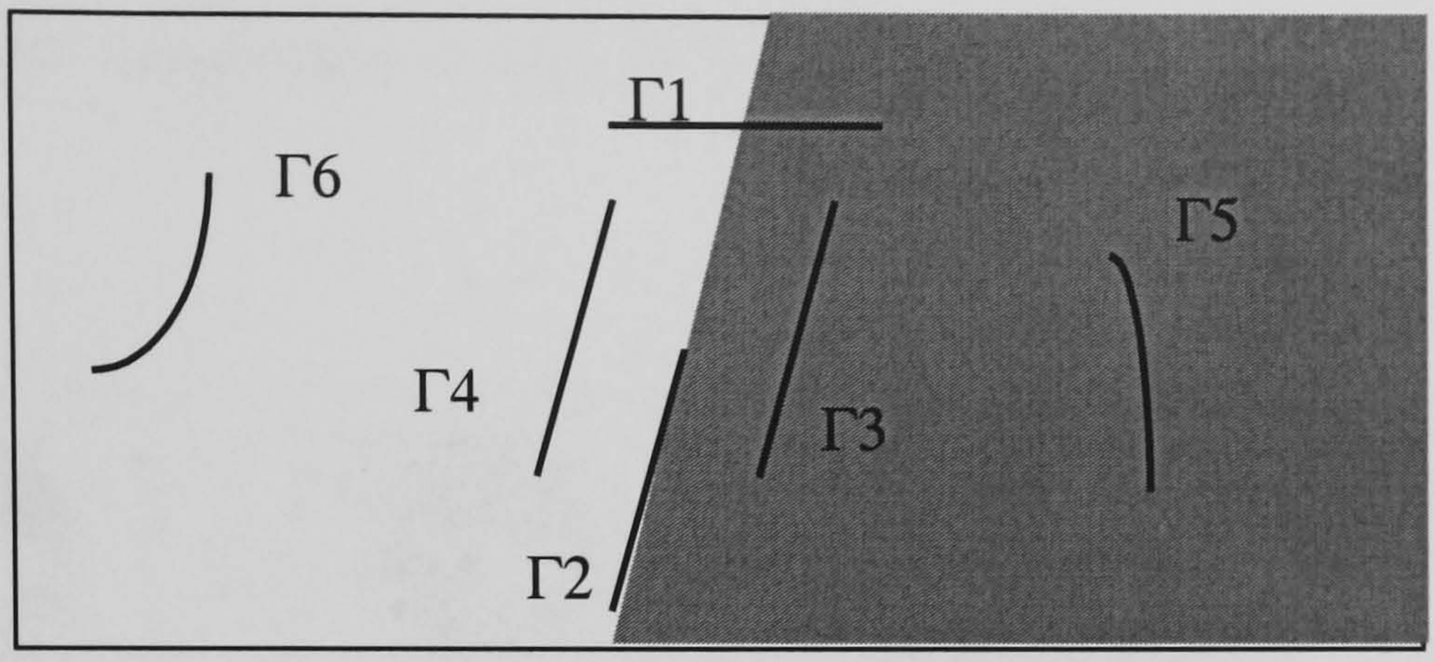

Figure 3.6 The 6 possible curve locations Γ1 to 6 in relation to printed and non-printed areas.

This lead to the identification of six generalised locations (denoted *Γ1* to *Γ6)* where useful one-dimensional profiles, or collections of contiguous pixel values can be extracted relative to the area and boundary of a print, as illustrated in Figure 3.6.

Γ1 Perpendicular on the area (⊥): a set of contiguous pixels spanning and perpendicular to the border of a printed area.

Γ2 * On the border of an area (‖): a contiguous set of pixels parallel to and on the border of a printed area.

Γ3 Parallel to the border, close inside the area (‖ i): a contiguous set of pixels parallel to and 2 to 5 pixels inside a printed area.

Γ4 Parallel to the border, close outside the area (‖ o): a contiguous set of pixels parallel to and 2 to 5 pixels outside a printed area.

Γ5 In the interior of the area (⊙): a contiguous set of pixels more than 5 pixels inside a printed area.

Γ6 (far) outside the area: a contiguous set of pixels more than 5 pixels outside a printed area.

For example, *Γ4* is the most suitable location to identify the printing fault, hairs. The problem is to determine where the profiles should be extracted and this can be achieved using a matching process.

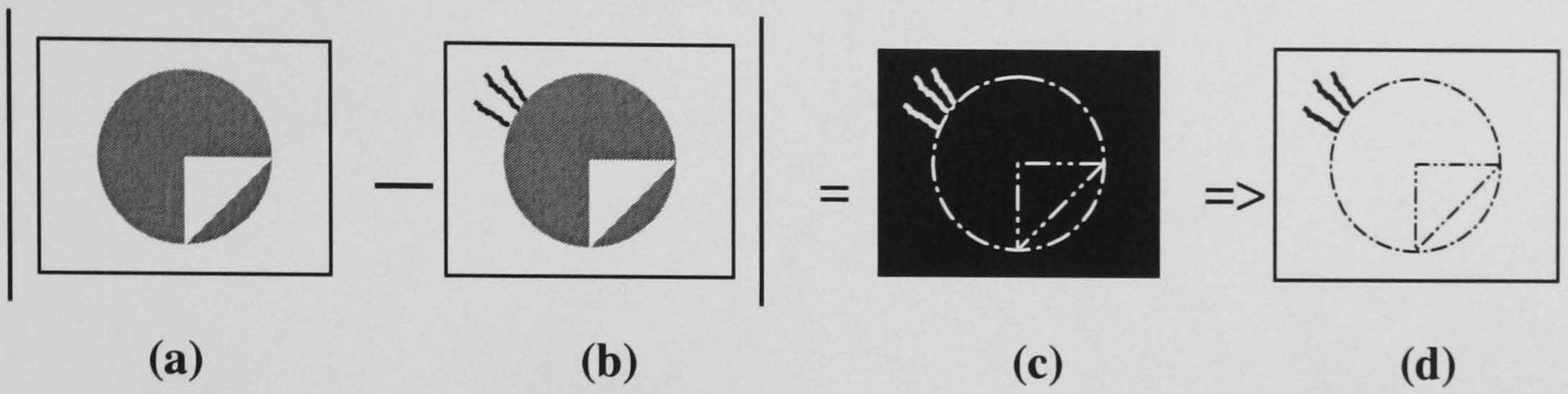

Figure 3.7 Absolute difference of 'well aligned' images [1]

Figure 3.7 shows a simple representation of a reference image containing a graphic without errors (a good graphic), R_{ij} and an image of a graphic that is 'well-aligned' with the reference image and contains OCAP error 1, hairs, I_{ij}. *i* denotes the row and *j* the column starting from the top-left corner. The *absolute difference* of two numbers is the size of the difference irrespective of direction and is always positive:

$$|a - b| = \sqrt{(a - b)^2} \geq 0 \qquad (3)$$

If the two images are treated liked matrices the absolute difference produces a ghost image, G_{ij}, which is mostly black but contains faint light grey outlines of the printed areas, *noise* and any printing faults picked out in grey.

$$G_{ij} = |R_{ij} - I_{ij}| \qquad (4)$$

---

[1] The absolute difference of a) a reference image and b) an image containing hairs (OCAP 1) that is 'well aligned' with respect to the reference produces c) a ghost image which is mostly black. d) It may be inverted (see text) and the resulting image is predominantly white and contains noise, the faint outline of the graphic and the printing error picked out in dark grey.

Though the human eye sees an object that is smooth and red as being red, a digital image will contain an area of pixels whose intensity varies around 'red' and this is one explanation of noise in this context. Noise can also be caused by electrical interference in the image signal while it is still in analogue form. For ease of display this can be inverted by subtracting every pixel value from 1 (assuming the ghost image contains pixel values *normalised*, that is converted, to the range 0 to 1):

$$V_{ij} = 1 - G_{ij} = 1 - |R_{ij} - I_{ij}| \qquad (5)$$

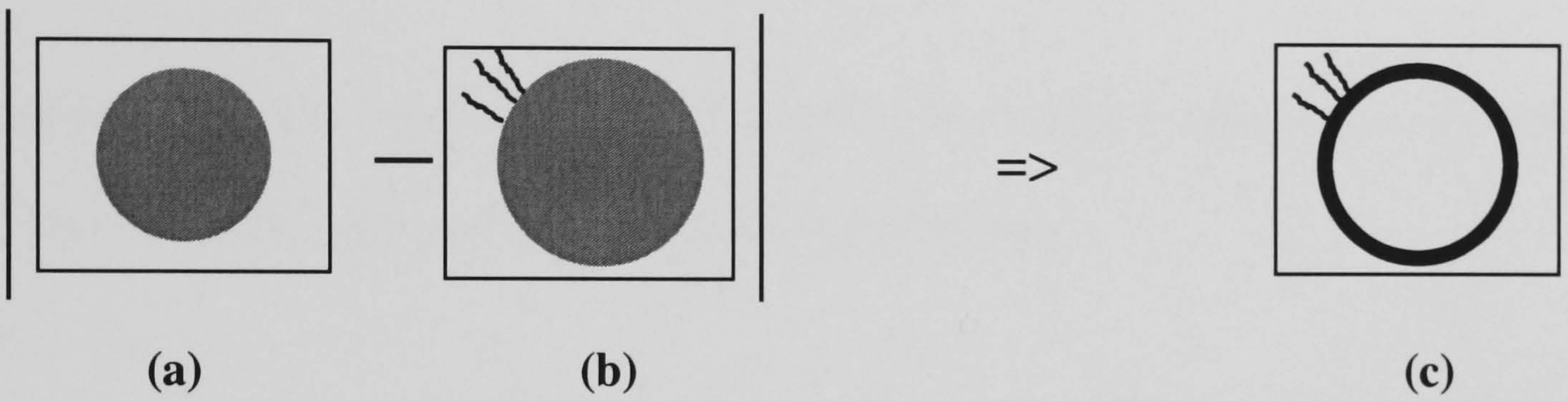

Figure 3.8 Absolute difference of 'mis-aligned' images [2]

An example of an inverted ghost image for hairs is shown in Figure 3.7 d). The ghost image and the inverted ghost image can be used to reveal the position of printing errors in a graphic, but the difficulty is in producing the ghost image. The reference image and the one that may contain printing errors (I_{ij}, the *suspect* image) must contain the printed graphic at the same position, scale, orientation and intensity, and this is defined as a *well-aligned* or *coincidental* suspect graphic. Otherwise a situation like that illustrated in Figure 3.8 c) occurs. A mis-alignment between the size of the graphic in the reference image and that in the suspect image

---

[2] The absolute difference of a) a reference image and b) a suspect image containing hairs that is 'mis aligned' – the suspect image has not been scaled correctly to compensate for differences in camera setup between it and the reference image. In c) the resulting inverted ghost image the printing error is less noticeable than the error caused by bad image processing.

produces a ghost image that contains a wide black band that is larger than the printing faults. The mis-alignment in this case is because the suspect image has not been scaled correctly to compensate for differences in camera setup between it and the reference image. Such *imaging* errors can obscure printing faults that occur at the border of a printed area, or detract from the printing faults. The pre-prototype inspection system designed by Birmingham and Maastricht builds on the ideas described above, and is illustrated in Figure 3.9. This is the initial concept design and the details of each stage are not shown. The process in the flow-chart performs one loop for each printing cycle.

Acquire image: a suspect image of a printed graphic (one that may contain printing faults) is acquired using the camera and placed in the computer's memory.

Match 1: the suspect image is compared with a reference image of the desired graphic without faults (a good graphic). The details of how the comparison is performed were unknown at this stage (see Chapter 5). Treating the comparison as a black box the desired outputs from it are:

- The X and Y position of the suspect graphic in its image compared with the position of the good graphic in the reference image.
- The X and Y scale of the suspect graphic in its image compared with the scale of the good graphic in the reference image.
- The orientation (angle) of the suspect image in its image compared with the orientation of the good graphic in the reference image.

Geometric transformation: using the outputs of the comparison stage the suspect image undergoes a geometric transformation to scale, rotate and shift the graphic in the X and Y direction. This produces a well-aligned suspect image.

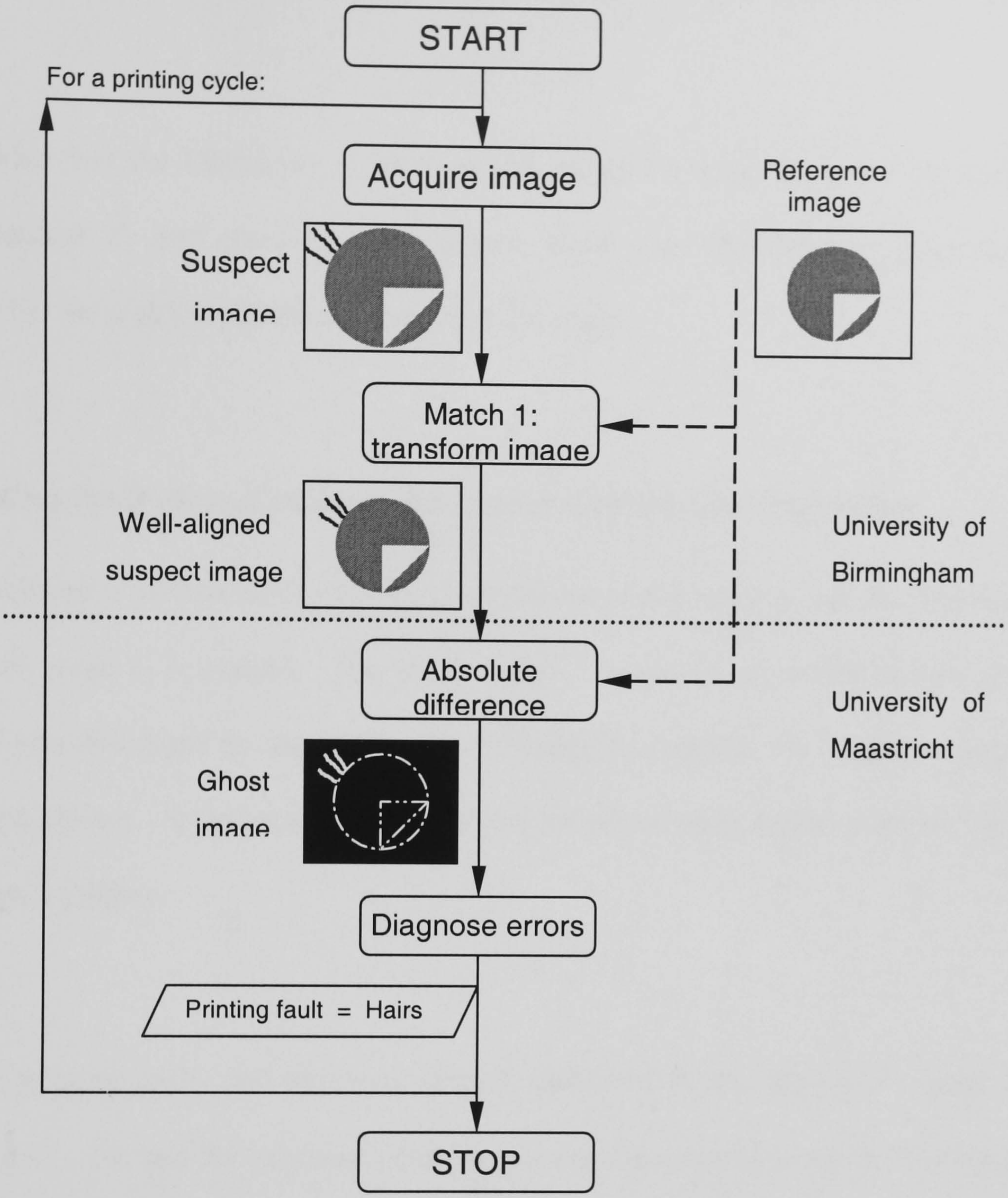

Figure 3.9 A flow chart for the pre-prototype visual inspection system, showing the division of labour between the Universities of Birmingham and Maastricht.

Absolute difference: the ghost image can now be found by computing the absolute difference of the well-aligned suspect image and the reference image. Because the images were well-aligned the ghost image is mostly black and contains a faint outline of the printed graphic and any printing faults in light grey.

Diagnose errors: the ghost image which contains clear evidence of any printing faults is then used in an as yet unknown diagnosis stage that determines which printing faults are present.

It was decided that the University of Birmingham would be responsible for the acquisition, matching (match 1) and transformation stages, while the University of Maastricht was responsible for the absolute difference and diagnosis stages.

3.5 Printing fault classification: the Linear Correlation Algorithm

Having developed a concept design for the complete inspection system, the detailed design for the diagnosis stage is presented. The fuzzy *linear correlation algorithm* (LCA) shown in Figure 3.11 was developed by the University of Maastricht to fulfill the diagnosis stage in the pre-prototype system. It determines which of the OCAP printing faults is present in a well aligned suspect graphic.

The OCAP printing faults and the *good* graphic identified in the section 3.3 (page 59) are denoted by k=1…19, and the locations of extracted one-dimensional profiles Γi are i=1…6 as defined in the previous section. The *ideal* expected outcome for a one-dimensional scan in the image at locations $\Gamma 2$ to $\Gamma 6$ is *E1*; a constant intensity as shown in Figure 3.12 a). The expected profile at $\Gamma 1$ is a step function, *E2*, which is defined to go from high (whiter) to low (blacker). The actual profile must fit one of a finite number of models, *Rj, j=1…n*. *R2* to *R6* are possible outcomes for an expected constant profile *E1*, and are illustrated in Figure 3.12 b). *R7* to *R10* are possible outcomes for a profile spanning a printed border *G1*, and can be considered two distinct regions, and the models *R1* to *R6* can be used to represent each. This gives n=30 permutations, examples of which are illustrated in Table 3.2.

Table 3.2 Models of possible outcomes, *Rj*, for 1-dimensional constant and step functions in images.

Name	Short	Applies to	Description
R1	'OK'	All	Absolute difference between the two profiles is below a predefined threshold $\Delta 1$: $\sum \lvert I_1(\lambda) - I^*(\lambda) < \Delta 1$
R2	'too high'	**E1**	$I_1(\lambda)$ is systematically too high, almost constant and featureless: $I_1(\lambda) \approx I^*(\lambda) + C,\ C > \Delta 2$
R3	'too low'	*E1*	As R2, but too low: $I_1(\lambda) \approx I^*(\lambda) - C,\ C > \Delta 2$
R4	'bump'	E1	A single bump ('up' or 'down') in the otherwise nearly constant profile $I_1(\lambda)$
R5	'twist'	*E1*	$I_1(\lambda)$ is a sigmoid torque ('left' or 'right')
R6	'oscillation'		$I_1(\lambda)$ alternates irregularly
R7		E2	
R8		E2	

The linear correlation process comprises two parts: the correlation *Mij* of the actual profile with the set of possible models *Rj*, and the computation of the membership function over the set of OCAP faults, *k*.

$$P_k = \sum_j S_{ijk} * M_{ij} \qquad (6)$$

The Linear Correlation Algorithm (LCA) employs one-dimensional discrete convolutions between the actual profile *A*, and the set of match types *R*j, compared with corresponding convolutions between the expected outcome *E* and *R*j. The resulting vector, match *M*ij, is image invariant. Linear cross correlation of the match against a support matrix, *S*ijk, gives a probability *P*ijk for each fault. The support matrix, *S*, is pre-defined from training samples.

The absolute difference between the reference image (template) and the aligned image is thresholded to produce a binary image:

$$Gij = 1, \quad |Rij - Iij| > t \qquad (7)$$

Gij = 0, else

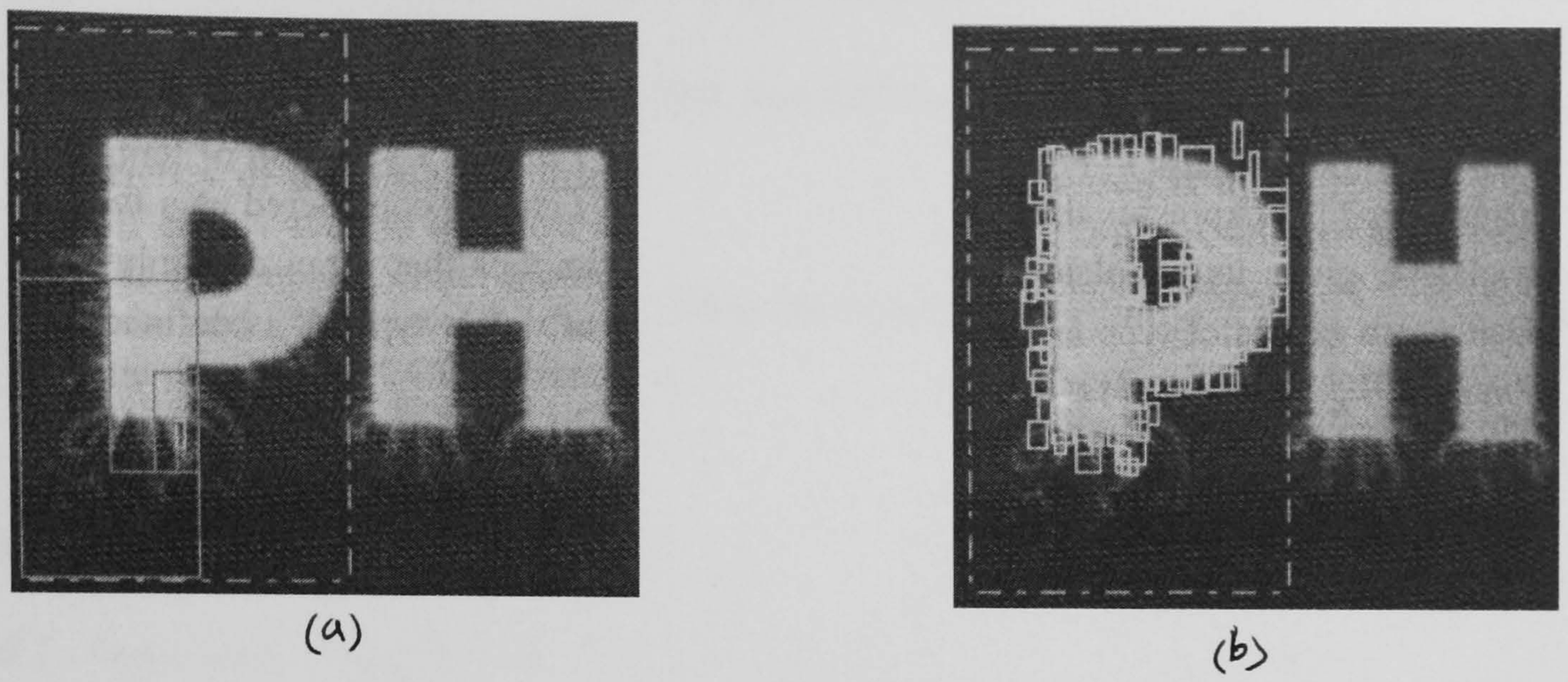

Figure 3.10 a) The computation of 1 search-box and b) finding 75 search-boxes with FindAreas [Westra, 2001].

A sub-algorithm, FindAreas, iterates and uses dividing search boxes to decompose regions in the image which contain discrepancies into unions of areas (2). The function, GenerateCurve, extracts contiguous grey-level pixel intensities at locations and orientations defined by *Γ1...6* within the search boxes (3). The curves are approximated using a multi-resolution wavelet representation [Malat, 1989] [Debauechies, 1990]. Unlike a Fourier series which is infinite, wavelets have the ability to describe a large set of waves using one finite waveform and a collection of scaling and shift factors. The linear correlation is computed as described above to produce one membership distribution *Pk* (4), and the program decides whether to perform another iteration (5). The reasoning is as follows:

- If the cumulative membership of one OCAP fault is high compared with the rest, the conclusion is that this is the fault and the algorithm stops.
- Else if none of the cumulative memberships are converging to a conclusion, stop
- Else if the present number of cycles is greater than a threshold, stop with no conclusion
- Else, perform another iteration

Performing a new iteration can entail using another curve type, Γ, in the search box used previously, or establishing a new search box in a different part of the image.

In the following example the set of possible outcomes is constrained and redefined as R1 to R6:

R1	'equal'	$M_{41} = 0.02$
R2	'high low'	$M_{42} = 0.01$
R3	'low high'	$M_{43} = 0.35$
R4	'no no'	$M_{44} = 0.00$
R5	'oscillating'	$M_{45} = 0.91$
R6	'the rest'	$M_{46} = 0.04$

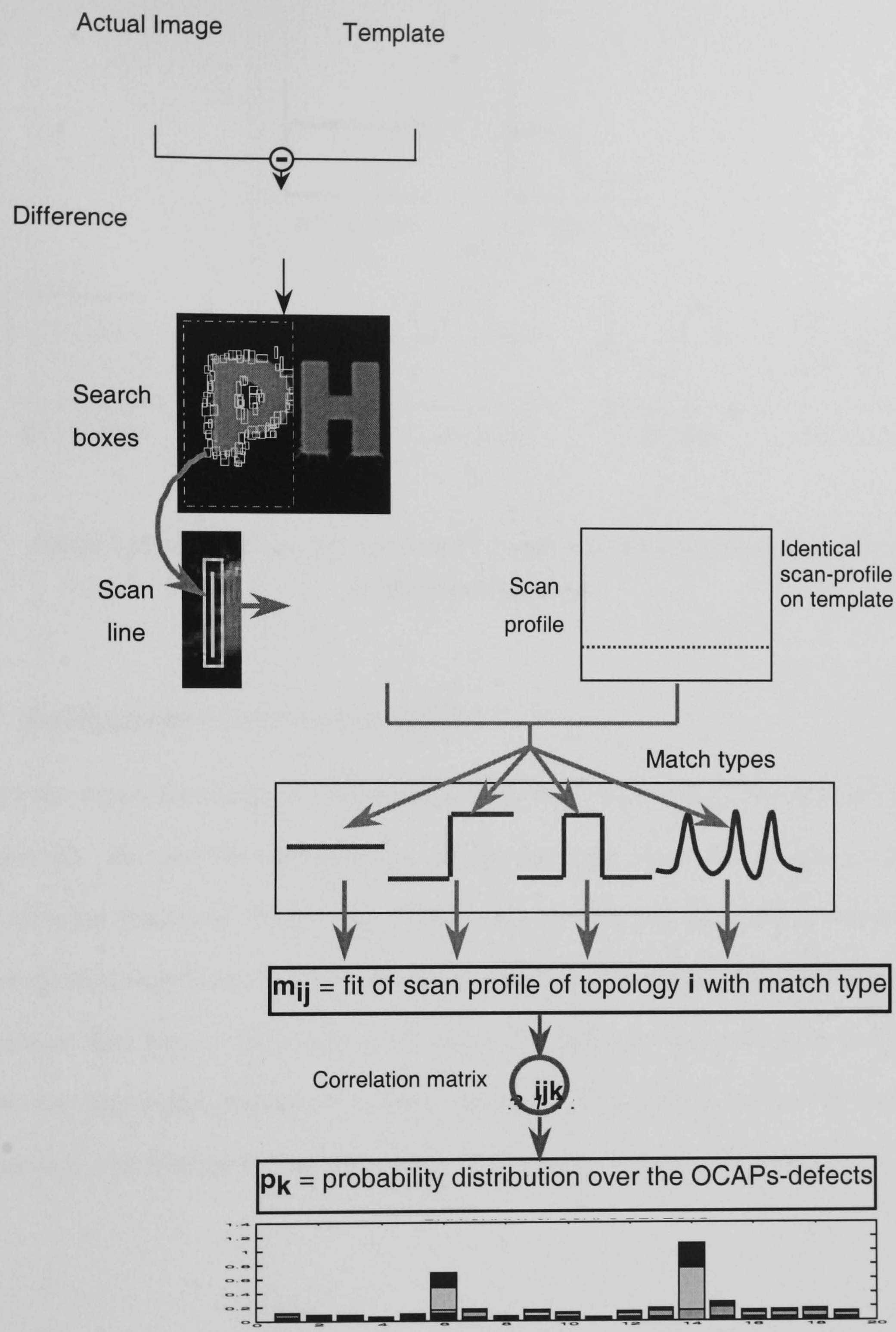

Figure 3.11 The fuzzy linear correlation algorithm (LCA).

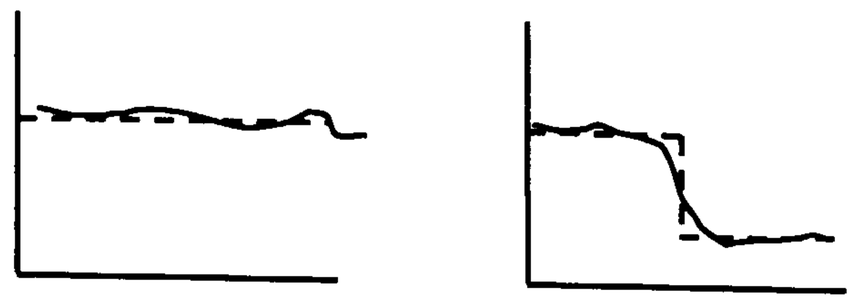

E1: constant

E2: 'Hi-lo' step

(a)

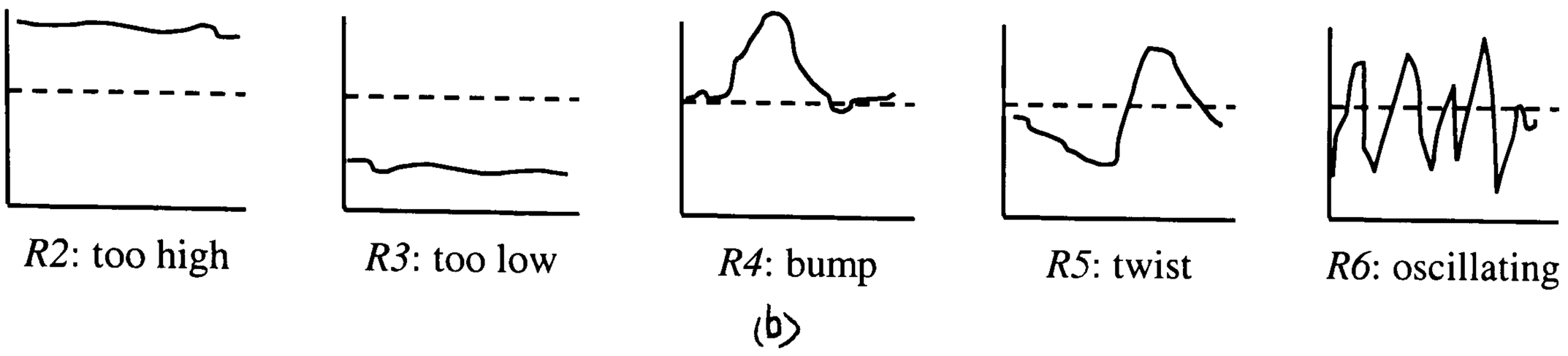

R2: too high *R3*: too low *R4*: bump *R5*: twist *R6*: oscillating

(b)

Figure 3.12 a) Ideal expected outcomes *E1,2*, and b) possible outcomes *R1* to *R6*, for 1-dimensional profiles

3.6 Intelpadprint Best Practice Survey

Important expert knowledge is encapsulated in the Out of Control Action Plan discussed in section 3.3. However for each printing error several causes and control actions are proposed and these are qualitative. Furthermore OCAP is the result of consensus after group discussion and individual experience. What is required in addition to these subjective rules is statistically significant data from a large number of pad printer operators and experts. It is sometimes useful for the control engineer to conduct interviews with experts, but in this case it was considered most efficient to conduct a survey by means of a Visual Basic program.

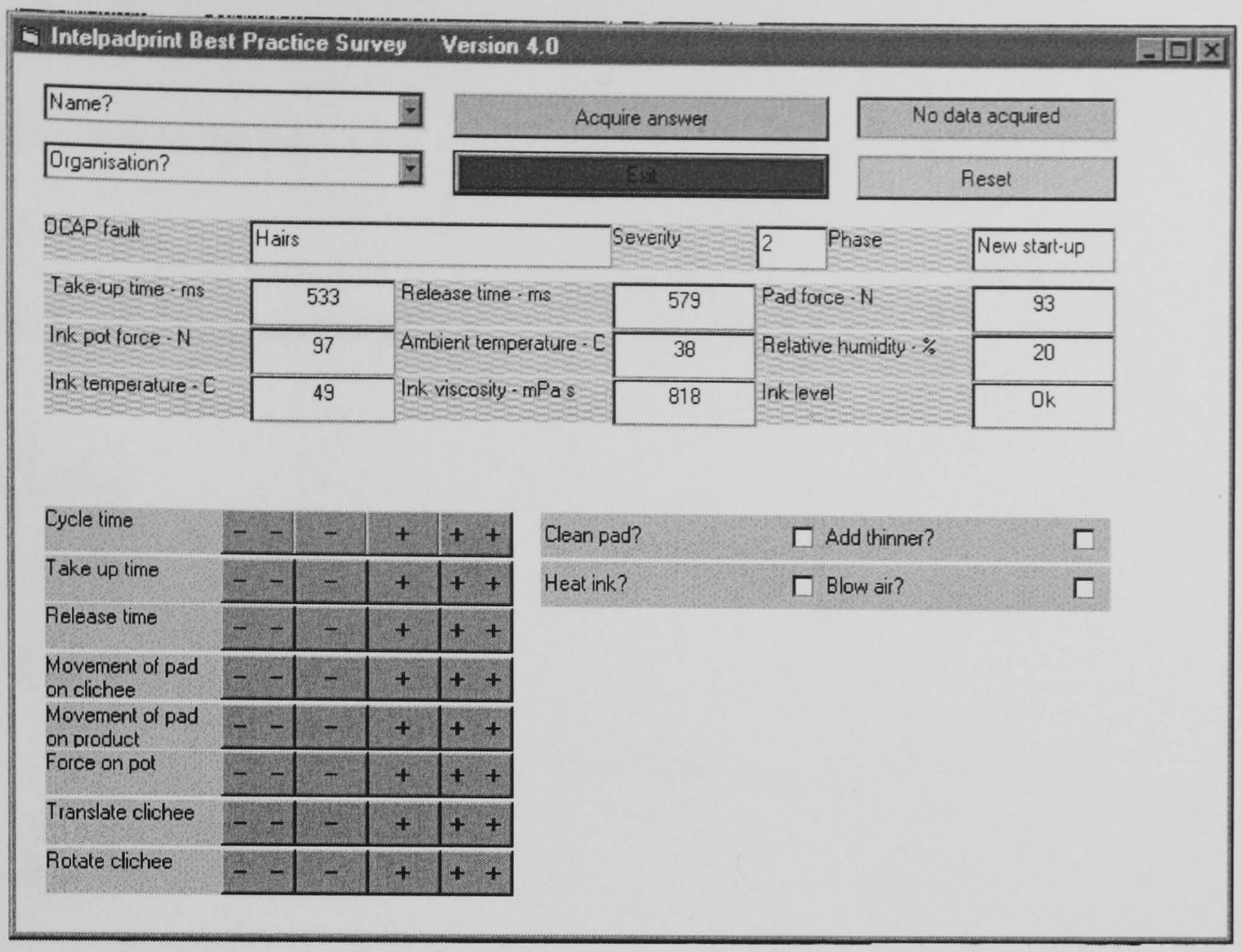

Figure 3.13 A screen-shot of the Intelpadprint Best Practice Survey program.

The main window of the Best Practice Survey (version 4) contained a form with three sections shown in Figure 3.13 [Shippen, 1998]. The control section allows the user to select or enter their name and organisation, and contained 'Acquire answer', 'Reset' and 'Exit' buttons. The sensor section presents the user with a randomly chosen OCAP fault and severity (1 not serious, 5 very serious), 9 sensor values randomly chosen between limits defined after consultation with the consortium and the printing phase (startup with a new product, startup with an existing product or running). The operating conditions section presents the user with 4 'binary' actions which he can either select or not and 8 continuous adjustments. A large ('- -') or small ('-') reduction or a small ('+') or large ('++') increase can be selected. The order in which corrective actions are selected is significant and the test can be run multiple times by the user selecting the Acquire data button.

'Binary' and continuous adjustments:

- Clean the pad
- Add thinner to the ink
- Heat the ink
- Blow ionised air onto the pad (to clear a static charge)

- Cycle time
- Take-up time
- Release time
- Movement (deflection) of the pad on the cliché
- Movement of the pad on the product
- Force of the ink-pot on the cliché
- Translate cliché
- Rotate cliché

The survey software was distributed to LEGO, Philips and Tampoprint with instructions to collect data from as many printer operators as possible. The response was disappointing, with 126 analyses from 17 individuals (an average of 7 per OCAP fault). This is not a statistically significant amount of data: 100 tests for each of the 18 OCAP faults would be just about acceptable. The importance of collecting a lot of useful data had been stressed to the consortium, but apparently too much was left to individuals at each partner company to organise. An alternative way of collecting data will be proposed later.

3.7 Summary

1 If the Intelpadprint project can satisfy the contrasting demands of LEGO and Philips it will meet the needs of most end-users in the world.

2 The OCAP document and printing fault library is supported by published literature and is the starting point for the Intelpadprint control system.

3 Real-time inspection is central to the system and a novel approach using the position of a printing fault in relation to the border of a printed area was proposed by Birmingham. Experiments on test images supported this proposal and with Maastricht University the Linear Correlation Algorithm was formulated to use this approach. This required the automated capture and pre-processing of an image by software to be developed by Birmingham University, while the LCA would be implemented by Maastricht.

4 The Best Practice Survey was conceived as a means to capture expert knowledge. However, because the project partners were unable to give it enough support a statistically significant quantity of data was not collected and a different approach would have to be used.

4 The pre-prototype printing system

4.1 Introduction: hardware and software selection and configuration

This chapter presents the criteria for the selection of hardware including the camera, lenses, illumination, the *frame-grabber* computer card and control sensors. The selection of off-the-shelf software and the writing of the pre-prototype inspection program is discussed. The results of the evaluation of the pre-prototype inspection system are presented, then solutions to a number of problems in the pre-prototype system are explored in preparation for the demonstration system.

4.1.1 Criteria for camera selection

It has been established that a digital CCD (charge coupled device) camera provides the best option for the Intelpadprint system. Compared with imaging tubes, charge-coupled devices have lower power consumption; because they are solid-state devices they are unaffected by electro-magnetic fields; they are small, light and robust; they do not require voltage-tuning; there is no image-lag or burn-in; and because of mass-production they are cheaper. The advantages of size and robustness make CCDs particularly suitable for the industrial inspection environment, which can contain dust, vibration and electro-magnetic noise. Charge coupled devices achieve the same static resolution as tubes, do not require set-up or warm-up time and produce repeatable results [Theuwissen, 1994] [Vernon, 1991].

The criteria for selection of a model of camera for the project were:

- access time and integration with the computer
- resolution
- colour capability
- cost

- suitability for the pad printing process

Still digital cameras typically need no additional hardware and plug into the serial port of a computer. However, the time required to access the image can be minutes, so they are unsuited to pseudo-real-time applications like industrial inspection. Video digital cameras allow real-time acquisition of images and this is the option that will be considered further for Intelpadprint.

The required resolution of the image can be ascertained from the following equation. f_u is the smallest dimension of the smallest feature (desirable or erroneous) in the object, g_u is the size of the graphic as printed, and f_v and g_v are the size of the feature and the graphic respectively in the image.

$$\frac{f_u}{g_u} = \frac{f_v}{g_v} \qquad (1)$$

$$g_v = g_u \cdot f_v / f_u \qquad (2)$$

The finest line in the Intelpadprint test graphic (figure 4.8) has a width of 100 μm (0.1mm) and to be visible in the image should have a minimum width of one pixel. The test graphic is 45mm square so from equation 1 this would occupy at least 450 pixels in the image. The finest pad printing errors are 'hairs' which are typically 180 microns, so they are visible. The maximum image size possible with a standard frame-grabber card is 576 x 768 pixels, and this is suitable for the test graphic.

There are two configurations of CCD: *line-scan*, and *area* or array. A grey-scale (monochrome) line-scan device contains a single line of photosensitive cells and a two-dimensional image is created by moving the device relative to the subject and assembling the one-dimensional intensity signals side-by-side. The line-scan camera is an obvious choice for inspection of continuous webs of cloth or paper, or objects on a continuously moving

conveyor. Line-scan sensors are typically 1024 pixels wide allowing large images to be assembled. The area CCD contains a two-dimensional grid of cells and in the context of automated inspection is better suited to imaging stationary objects. The question of which is more suitable for the Intelpadprint project is discussed in the next section (section 4.1.2).

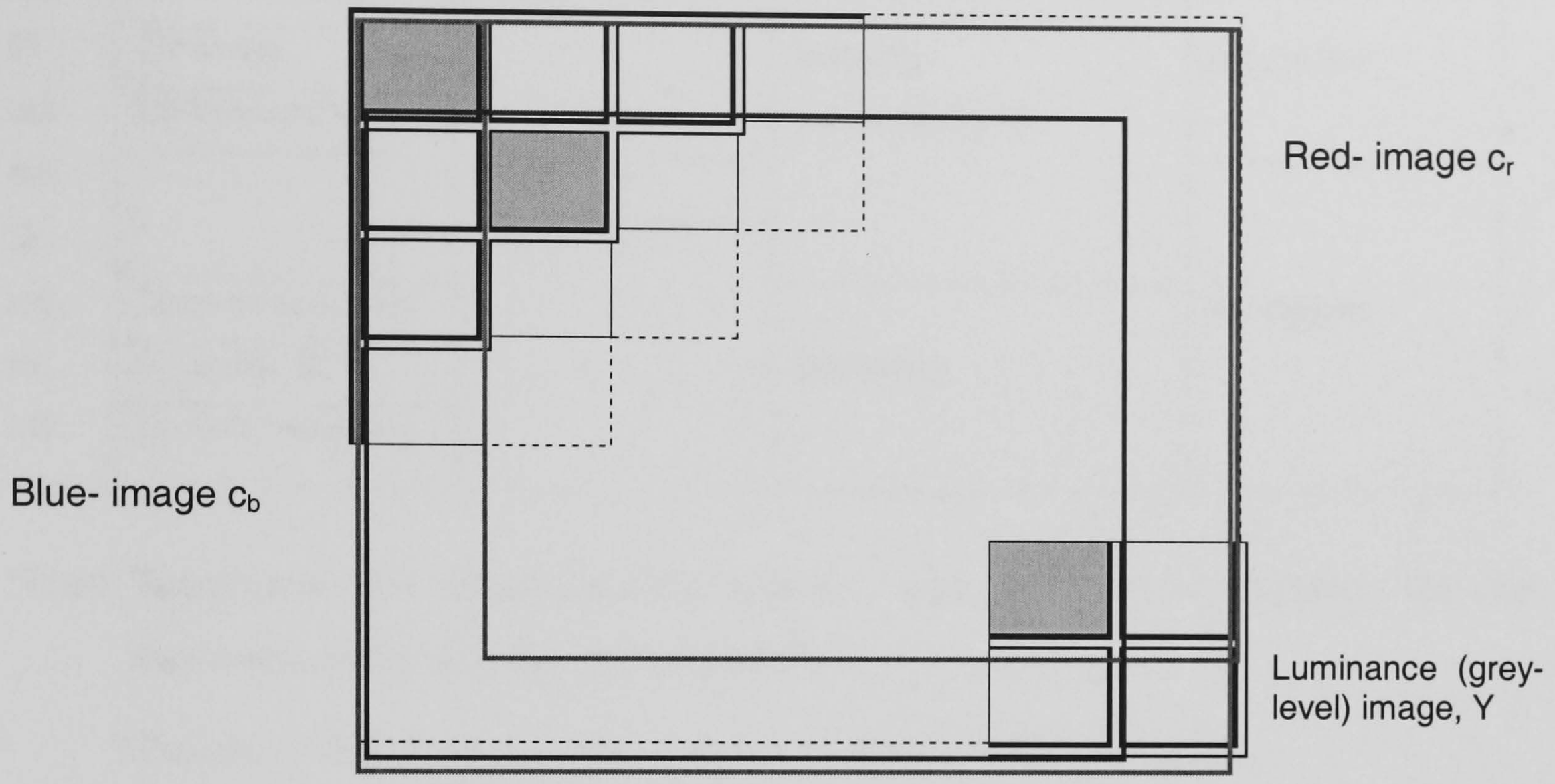

Figure 4. 1 Part of a single array colour CCD, showing the resultant offset nature of the different component images

There are two types of area colour digital cameras: single chip and three chip. The single chip option is cheapest with models at about £600, and uses one large (1/3 inch) CCD array with individually filtered photo-sensitive cells. Typically as shown in figure 4.2, half the cells are unfiltered to detect luminance, a quarter are filtered to detect red-green and a quarter to detect blue-cyan. The main disadvantage of this arrangement is that the images for the three components are offset from each other. The alternative uses a special prism to separate the spectral components of the light, and three small (1/2 inch) CCDs filtered to detect red, green and blue. Quality of manufacture ensures that the spectral components of the image from this sensor are not offset relative to each other, but the price is very high at approximately £3000. On a cost criterion the single-chip colour option is preferable.

Table 4.1 The pad printing process on a Tampoprint-type closed system

	Pad, Z	Cliché,	Carousel, θ	Process
m1		Out		
t1	*			
m2	Down to cliché			
t2	On cliché		Indexing	Ink uptake
m3	Up from cliché		(potentially **)	
m4		In		
t3	*			
m5	Down to substrate		Stationary	Ink release
t4	On substrate			
m6	Up from substrate			

Notes- Tampoprint-type closed printing system: pad only moves vertically, ink-cup is stationary, cliché only moves horizontally

* Pauses, *t1* and *t3* are optional, depends on results of IPP research

** Carousel can potentially move except during printing: ie. potentially in *m1 – t3*.

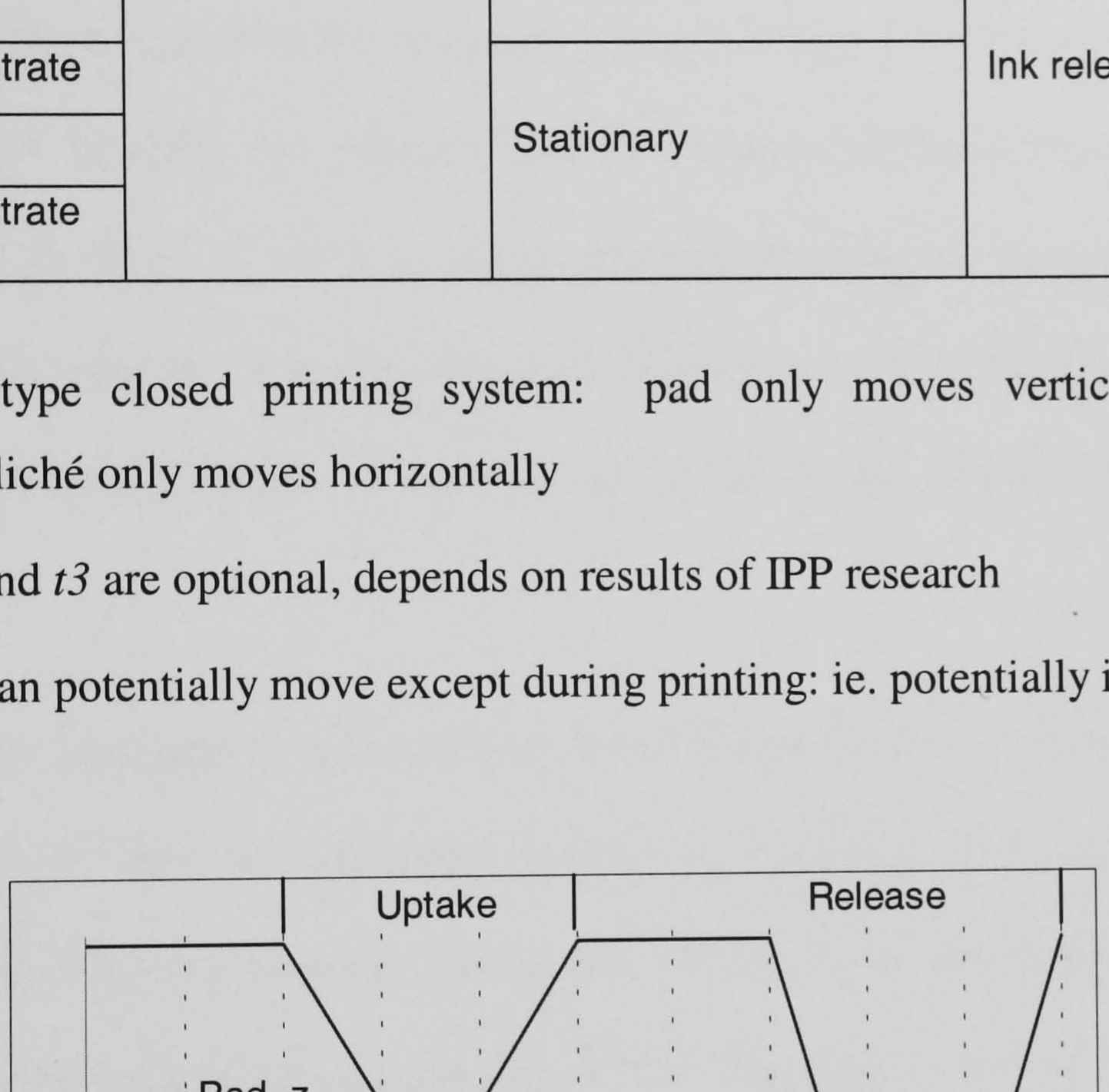

Figure 4. 2 A graph of positions of the pad, cliché and carousel during the pad printing cycle

4.1.2 Position and configuration of the CCD camera in the pad printing line

Table 4.1 is based on Philips CFT's formal description of the pad printing cycle for a Tampoprint-type closed system. The cycle is divided into 6 motions, *m1* and *m4* are the movement of the cliché out and in, *m2, 3, 5* and *6* are the movements of the pad onto the cliché and the product. Between each all the motions except *m3/m4* pauses, *t1* to *t4*, are defined. The time that the various movements and pauses should occupy for optimal pad printing was the subject of Philip's research and pauses *t1* and *t3* are optional depending on the results of their research. The positions of the pad, cliché and carousel holding the product during the printing cycle can be represented graphically as in Figure 4. 2. The carousel can rotate one place (index) anytime during motions and pauses *m1, t1, m2 ,t2 ,m3 ,m4* and *t3*.

One constraint on the Intelpadprint printing line is that it should be as compact as possible. A consequence of this is that the automated inspection system should occupy little space. Another result is that following printing, which ends with motion *m6* in table 4.1, there should be the smallest possible delay before image-acquisition. The significance of this statement can be illustrated with the typical pad printing cell illustrated in figure 1.2, which LEGO wants to use as the basis for its implementation of the Intelpadprint system. During printing the component is in a product-holder on an indexed carousel. If a decision is made to reject the component whilst on the carousel it is straightforward to re-direct it as its precise location is known. However, if the component is ejected using compressed air onto the conveyor-belt before the reject decision is made, the location is lost. Automatic re-location on the fast moving conveyor is difficult and inefficient.

Table 4.2 Different camera sites related to the motion of a non-Tampoprint-type printing line.

		Pad, Z	Pad/ ink-cup/ camera,	Carousel	Camera-site 1	Camera-site 2
Printing cycle	*m1*		In (pad to cliché)			
	t1	*				
	m2	Down to cliché				
	t2					
	m3	Up from cliché				
	m4		Out (pad to			
	t3	*	substrate)			
	m5	Down to substrate				
	t4			(Stationary)		
	m6	Up from substrate				
Image acquisition cycle	*m1*			*[a]*	Line-scan	Line-scan
	t1	*				
	m2			*[b]* Indexing **	Area type	
	t2					
	m3					
	m4			*[c]*		
	t3	*			Acquisition	
	m5				not possible	
	t4			Stationary		Area type
	m6					

This led to two concepts for siting the camera on a closed-cup pad printing production line. Consider first Table 4.2, which is based on Figure 4. 2. The table considers one component, which is decorated during its *printing cycle* and photographed during its *image acquisition cycle* while the next component is being printed. The first camera-site relies on a non-Tampoprint-type (non-TP-type) machine, where the cliché is stationary, the pad and ink-cup move horizontally as one, and the pad also moves vertically onto the cliché and substrate (see Figure 4. 3). A camera can be mounted on the same structure as the ink-cup and pad sub-assembly, such that the camera is directly above the substrate when the pad is over the inked-area of the cliché (table 4.2: camera-site 1). The camera can contain either a line-scan sensor

and use the horizontal motion *m1* to produce a two-dimensional image of the printed graphic, or an area sensor. In this case image-acquisition can occur during printer stages *t1* to *m3*, but the carousel cannot index during the periods denoted *[a]* and *[b]* in table 4.2.

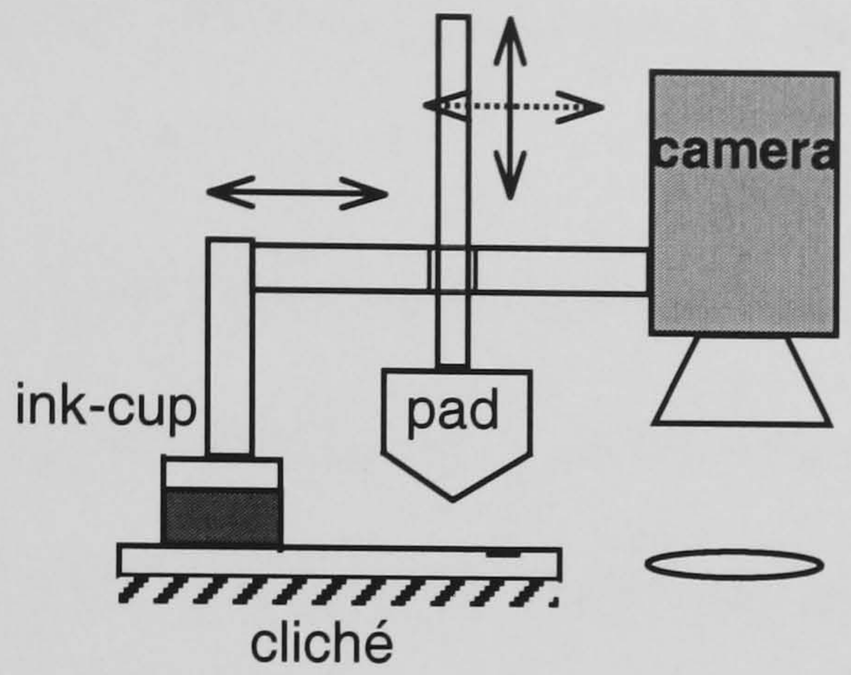

Figure 4. 3 Non-TP-type pad printer, showing an integrated camera

The other position for the camera (table 4.2: camera-site 2) is separate from the printer and above the next indexed position on the carousel. Again the camera sensor can be of the line-scan variety and use the motion of the carousel to move the graphic across the path of the camera to build up the image. Alternatively, an area CCD can be employed and the image is then acquired when the graphic is at rest, definitely by the time of printer motion *m5* but possibly earlier.

The advantages of camera site 1 are the small space occupied by the inspection system and the opportunity to acquire an image as early as possible. However this idea makes the design of the printer, and the motion of the printer and carousel more complicated. The idea relies on Tampoprint accepting a design of closed-cup pad printer that it would not normally choose, partly because the printer can be potentially less rigid, and frame-grabbers capable of line-scan acquisition are more costly. Finally, there may not be space for lighting in such close proximity to the printing pad; and the camera is subjected to jerky movements and vibration,

which may affect image quality and damage the camera over time. Camera site 2 is a safer, simpler option that separates the inspection hardware from the printer. This makes it easier to test as a standalone system before integrating it with the printer, and it was the option chosen for the Intelpadprint pre-prototype. The inspection system occupies more space and if an area camera is used acquisition occurs later, but for an initial concept these are less important.

The choice of a line-scan or area CCD (defined in the previous section 4.1.1) is dictated by the motion of the carousel. If the motion immediately after the printer is linear then a line-scan camera can be used. However if a rotary carousel is employed then the motion of the graphic will not be linear and an area sensor must be used. At the time when the inspection hardware was being selected it was not known what type of carousel Tampoprint would design into the pre-prototype system. The rotary option is simpler so this was the assumed choice, and on this basis an area camera was chosen.

The *frame-grabber* interfaces between the camera and the image processing software. It is a computer card like a graphics card. It quantizes the intensity signals from the camera and places the image in a buffer in memory prepared with the use of software drivers. Criteria for selection of a frame-grabber are compatibility with the camera, compatibility of the drivers with computer languages and image processing software, and the type of computer-*bus*. The term bus is adopted from the power-generation industry and refers to a collection of parallel metal tracks on the main board of the computer and the communication standards used to connect peripheral devices like a frame-grabber with the central processing unit. There are more and generally better quality products suitable for PCs than workstations running the UNIX family of operating systems, and the PCI (*peripheral component interconnect*) bus is the economical high-speed choice. Other selection criteria are image quality, image size and the availability of I/O (input/output) control lines to trigger image acquisition.

4.1.3 Imaging errors

The various parts of an image acquisition system can give rise to 'imaging' errors either through the choice of unsuitable or incompatible hardware, incorrect set-up, deterioration. The source of errors can be classified into illumination, position and synchronisation, lens and filter aberrations, acquisition (camera) and transmission, digitisation and processing. The 'imaging' errors can obscure or have the appearance of printing faults.

Illumination errors include specular reflection (highlights) caused particularly by glossy or curved surfaces and direct illumination. Source spikes caused by power surges, deterioration of light intensity and change in the spectral response of the light source over time. Light conditions can change because of light pollution, a change in power settings or 1 bulb in a multi-bulb light source failing. Dirt (particularly in a manufacturing environment) or oxidation of reflective surfaces, lenses and bulbs. Illumination errors can be minimised by using single halogen light sources, diffuse and indirect illumination, regulated and smoothed power supplies, enclosures around the light subject and camera.

Position and synchronisation errors include vibration (particularly in processes with rapid and discontinuous movements) and mis-timing image acquisition so that the product is moving, distorted or not completely visible. Incorrect position or angle relative to all 3 axes can be caused by accidental knocks by the operator, or incorrect adjustment.

High quality, modern compound lenses are designed to minimise aberrations. Most acquisition errors are prevented by the use of charge coupled device (CCD) cameras [Theuwissen, 1994]. In general, imaging errors can be minimised by the secure attachment of components, automatic set up and recording of positions and power settings, regular servicing

and cleaning. The image acquisition system should be sited away from sources of vibration, electrical interference, dirt and bright light. Calibration samples of known size, colour and shape can be used to test and adjust the set-up of the system.

4.1.4 Survey of sensors

As part of the development of the pre-prototype a survey of commercially available sensors and actuators was undertaken. The parameters that were to be measured were:

- Displacement, velocity
- Load
- Temperature
- Humidity
- Static charge
- Viscosity
- Fluid-level
- Print quality

The criteria on which sensors and actuators were selected were cost, size, the availability of an external signal, for example via an RS232 serial connection. Most importantly, the sensors must operate on the machine during production.

The displacement of the cliché and pad are the most fundamental parameters in the pad printing process. Particularly at the high printing rate specified for Intelpadprint, the relative position of the components must be known to prevent collision. One option is to use LVDTs (*linearly variable differential transformers*) to measure the displacements and provide feed-back to the user and to separate actuators. The LVDTs with sufficient range (800mm) were

too long to fit in the space. Also, external feedback is too slow at this printing rate, and the servo-motors proposed by Tampoprint incorporate internal feedback.

The load exerted by the ink-pot on the cliché must be monitored to prevent excessive wear of the cliché or rim of the pot, and to prevent ink leakage. The force between the pad and cliché, and the substrate is a function of the stiffness of the pad and its displacement onto each surface. The forces can be measured using a piezo-electric or strain gauge load-cell and altered using the servo-motors. In order to prevent twisting an annular shaped sensor, or load-washer of between 40 and 60mm diameter. Several piezo-electric models from Kistler and RDP costing approximately £500.

The temperature of the air and the ink effects the uptake, release and drying of the ink. A thermocouple was proposed to measure the temperature of the air and a thermocouple or non-contact infrared sensor were possibilities to measure the ink temperature. A coil operating under closed loop control and embedded in the cliché was proposed to heat the ink.

The humidity of the air around the printer affects the ink in a similar way to the temperature, and can lead to a poor quality print. Various probes with hand-held meters are available for approximately £250, but it would be difficult to interface with these devices. A Farnell PCB module was favoured because of its low cost (£100) and the ease of integration into the Intelpadprint system.

Static charge can build up on the pad and cause the printing fault *hairs*. The Intelpadprint printer required a sensor to detect static build-up and a means to dissipate it. A non-contact sensor from John Chubb is available with a liquid crystal display and an RS232 output, but the price at over £1000 is prohibitive. The visual inspection system needs the ability to detect the

fault caused by static electricity, so it was decided that this was the best sensor and ionised air is blown over the pad or product to correct the build up of static charge.

Ink viscosity is one of the hardest parameters to measure on a production line. Laboratory viscometers are established tools that measure the power required to drive a rotating disc or paddle in the liquid in close proximity to a stationary plate, at a given speed. A typical device is the portable meter produced by Bohlin, which costs approximately £3000. Results from one model are not repeatable with another because they depend heavily on the design of the machine, as well as on the fluid.

A particular requirement for the viscosity meter was undisturbed ink flow past the sensor. This was made more probable by the stationary ink-pot to be used in the Intelpadprint system, but the high-velocity of the cliché in contact with the ink would inevitably cause some ink flow. Other requirements were that the meter's spindle be vertical, the ink-pot should be easily removable, that bearings and seals must withstand corrosive solvents and inks, and that it should be straightforward to clean the ink-cup and sensor. It was decided that on-line measurement of viscosity had to occur in the ink-pot as tubes exiting and entering the pot would clog up and be difficult to clean. It was conjectured that a meter, such as that produced by Bohlin, could be modified and mounted on a bracket. The measuring spindle would be detachable from the meter and located by bearings in the ink-pot. However the cost would be high so it was decided by Tampoprint to produce a viscosity meter built into the ink-pot. A viscometer was implemented on the pre-prototype and improved for the demonstration model, but no data exists so its effectiveness was not established.

Another difficult quantity to measure is the level of liquid in the ink-cup, but it is desirable to have a warning that the ink is low before incomplete prints occur, resulting in waste. No

commercial level meters were discovered and there was insufficient time in the project schedule to create a solution.

4.1.5 First attempt IPP template matching algorithm

As the literature survey shows a technique developed by early image processing practitioners was template matching, either using the cumulative absolute difference or convolution to find the location of the best match between a whole object contained in a template and the image. The disadvantages of this method in general were found to be the number of templates required to cope with different sizes and orientations of objects, the limitations on object pose; and the dependence of the time for computation on the area of the image and template. In general global template matching is unsuited to machine vision and various refinements were reviewed: coarse-fine and local template matching. In contrast to many machine vision applications the results of pad printing are constrained. Provided the substrate is in its product-holder, the location of the graphic is known to within a tolerance of several millimetres. Similarly, faulty printing will only lead to variations of ±5% in the scale and orientation of the graphic within the image.

The Local Corner Matching algorithm described below was devised to take advantage of the constraints in the imposed by a printing environment to reduce computation and cope with any printing faults which occur. A demonstration of the algorithm is presented in figure 4.4. The algorithm contains three phases: a "preparation" phase which can be performed at any suitable computer and generates data for a reference (that is, "good") graphic, substrate and inks. The "changeover" phase, is performed at the printer and sets up the inspection system for a new product; and an "on-line" phase encompasses the steps required to find a graphic on a product during printing.

Figure 4. 4 Demonstration of the Local Corner Matching algorithm

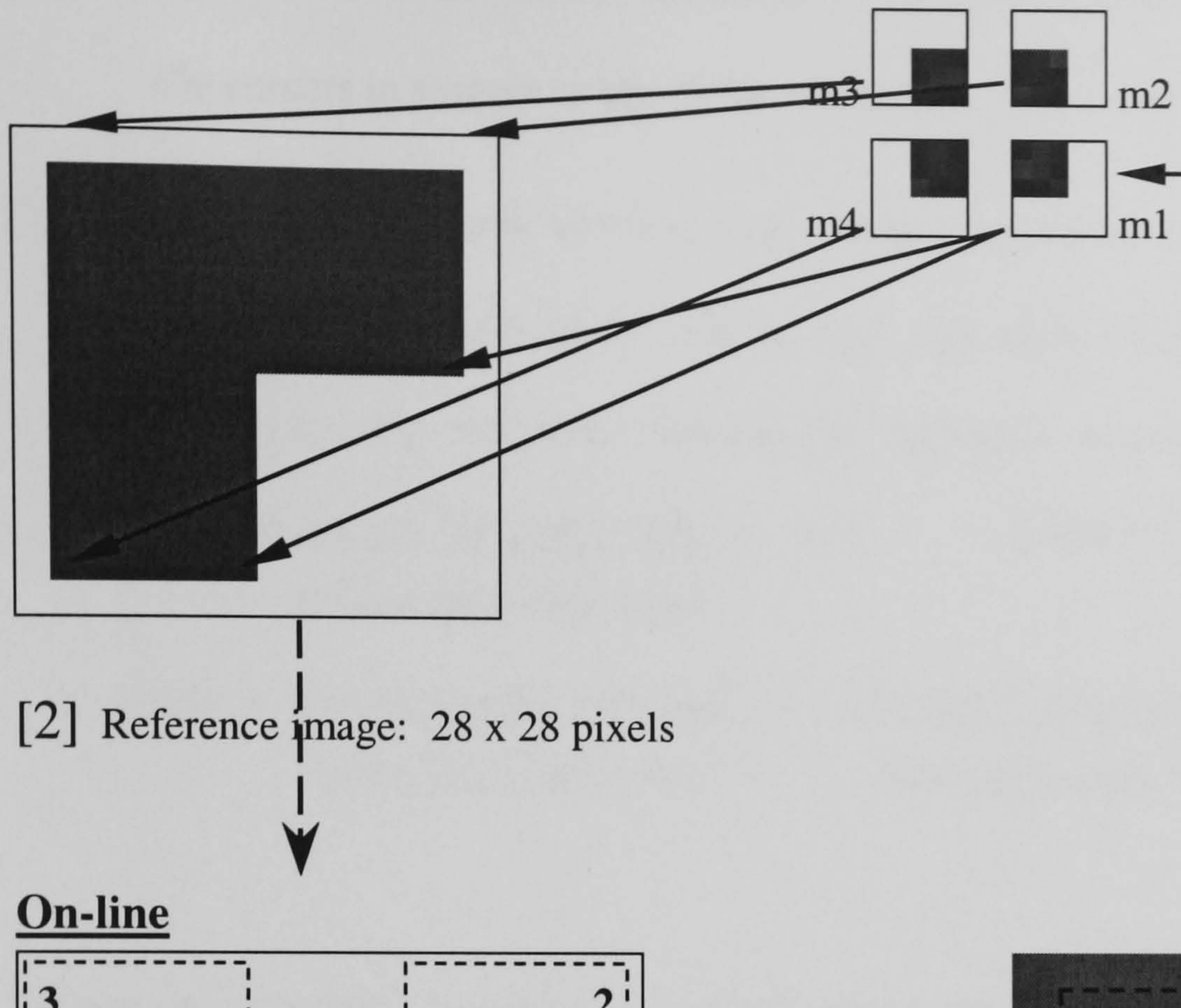

[6] "Chain" differences between corners..

Corner in suspect image	Mask used	Expected corner row, rg	Expected corner column cg	Suspect corner row, re	Suspect corner column ce	Expected column "chain" difference	Dg *	Suspect column "chain" difference	De *	Error Dg - De
C1	m1	20	32	20	29	cg2 - cg1	**0**	ce2 - ce1	**7**	-7
C2	m2	9	32	9	36	cg3 - cg2	**-23**	ce3 - ce2	**-23**	0
C3	m3	9	9	9	13	cg4 - cg3	**0**	ce4 - ce3	**0**	0
C4	m4	32	9	32	13	cg5 - cg4	**11**	ce5 - ce4	**10**	1
C5	m1	32	20	32	23	cg1 - cg5	**12**	ce1 - ce5	**6**	6

* Expected and suspect row "chain" differences not shown

[7] Are more "chain" differences required (ce5 – ce3,…) ? No

Are corners in suspect image within tolerance? No: C1, C5 | Yes: C2, C3, C4.

[8] Calculate suspect graphic position, scale, orientation relative to reference:

X = mean(ce2, ce3, ce4) – mean(cg2, cg3, cg4) =*4.0 pixels*

Y = mean(re2, re3, re4) – mean(rg2, rg3, rg4) = *0.0 pixels*

scaleX = $\frac{\text{mean(ce2, ce3, ce4)}}{\text{mean(cg2, cg3, cg4)}}$ = *0.0* scaleY = …*0.0*

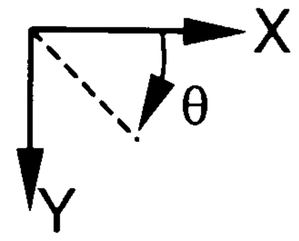

angle = tan($\frac{\text{sum(re2, re3, re4)}}{\text{sum(ce2, ce3, ce4)}}$) – tan($\frac{\text{sum(rg2, rg3, rg4)}}{\text{sum(cg2, cg3, cg4)}}$) = *0.0 radians*

During the preparation stage 5 x 5 pixel masks are generated and stored to model corners in the reference graphic. In the case presented in Figure 4. 4 [step 1] the graphic is a black square with a corner "cut away" printed on a white product. The masks (m1 to m4) representing the 5 corners contain black (0s) on white backgrounds (255 on an unsigned 8-bit integer scale) with the corner taken to be the middle pixel (represented by MASK(row=3, column=3) in the MATLAB). The 6th corner – in the middle of the reference image is white-on-black but is ignored in this demonstration. The reference graphic is placed at the expected position, typically the centre, in an image (not shown) that is the same size as the one obtained from the inspection camera (40 x 40 in the demonstration). The coordinates of the expected corner locations are found for this image (columns 3 and 4 at step [6]), given a label (C1 to C5 anticlockwise) and stored for the on-line stage. The sizes of the reference image, R_{ij}, a mask $m1_{ij}$ and the expected image, E_{ij}, are compared to find the dimensions of a search-box, S_{nij}, to be centred on each expected corner position:

$$Sni = Ei - Ri + m_{ni} - 1 \qquad (3)$$

The search-box size is 16 x 16 pixels and this is stored.

During changeover the inspection software loads data for the desired product. A "suspect" image is acquired on-line and a part of the image is shown in [3]. In this instance the graphic contains the printing error 'Constriction' (OCAP 3) on corners C1 and C5 while C2 to C4 are acceptable. The difference image A_{nij} for each search-box at the expected corner location and the required corner-mask is computed. This comprises the 2-dimensional means of the absolute difference of the mask with the suspect image as the mask is traversed across the search-box.

$$Anij = \frac{1}{I\,J} \sum \sum | m(y, x) - g(i-y, j-x) | \qquad (4)$$

In the difference images at step [4] the most likely locations of corners are dark areas. These images are 12 x 12 because of the size of the mask. The matrix for a part of image D2 is shown in [5]. The 2-dimensional minimum equals 1 and is located at A1(7, 10) which when offset by the location of the original search-box and the size of the mask is I(9, 36) (columns 5 and 6 at step [6]).

Continuing the on-line computations, the principal "chain" differences are calculated between the suspect-image corner coordinates at step [6] (only the column chain differences are shown). The expected-image corner coordinates are also known (calculated during changeover) and the error between the expected and suspect column differences is found. In step [7] the row and column errors are used to decide which corners are valid and which are modified by printing errors. With a tolerance of 1, corners C2, C3 and C4 are acceptable, while C1 and C5 are errors and because a conclusion can be made there is no need to find more chain differences (for example *ce5 – ce3*). In step [8] the X and Y positions, scale and the orientation of the suspect graphic in relation to the reference graphic are computed. The

suspect graphic is 4.0 pixels to the right of its expected position, and at the same scale and angle as the reference image.

The suspect image can then be transformed as required (not shown). The basic steps to be performed by the pre-prototype image processing system were:

1. Acquire a good quality image of a graphic
2. Locate the graphic in the image.
3. Geometrically transform the graphic such that it and an instance of it in a reference image are coincident. This requires the scale, orientation and position of the graphic relative to the reference.
4. Present the transformed image for fault diagnosis

An algorithm such as that described above could have been implemented with the minimum of programming tools for Intelpadprint. However, it would require a significant amount of time to code, debug, evaluate and develop to reach a satisfactory result. The algorithm is novel and with the time constraint imposed by the project this option was considered to present too great a risk.

4.1.6 Software and hardware selection

The alternative was to purchase commercial image processing software libraries that could be integrated into the Intelpadprint system, and various selection criteria were considered. The libraries should locate an object in an image and geometrically transform the image for further processing in a time commensurate with *quasi* real-time applications (0.5 to 2s). They should contain housekeeping functions that for example write image files, and general image enhancement and manipulation tools. It should be possible to call (that is, access) the functions within the libraries from a program written in one of the available languages: Microsoft Visual C or C++, Visual Basic or MATLAB, and complement the frame-grabber

drivers (software). The software should be cost effective and in order to exploit the results of the project it must be possible to sell it under licence as part of a commercial product. Finally, there should be technical support, and it should be reasonably predictable that new versions of the libraries would become available during the lifetime of the project to take advantage of advances in hardware and software.

As has been demonstrated there are dependencies between the lens, frame-grabber, software and programming languages. Furthermore, the illuminant is an important element, so it was considered important to select the components as a complementary package.

The Euresys Picolo was the frame-grabber chosen for Intelpadprint, because it is a low-cost (approximately £500) high-quality solution. It acquires colour or grey-scale images with a maximum resolution of 768x576 pixels from an area CCD and uses the PCI bus. It contains 4 TTL input-output lines and came with a range of library functions for Visual C++.

The JVC TK-C1380E camera contains a good quality single-chip area CCD with a resolution of 768x575. Illumination was provided by a Schott KL 1500 Electronic regulated DC cold light source with a fibre-optic ring-light.

A motorised zoom lens was selected for the pre-prototype because it was envisaged that during changeover the system would automatically adjust itself to the new product and graphic. If the new graphic was larger than the previous one the lens would zoom in to show the print at the maximum resolution. It was considered important to choose this option at the outset so that the lens aberrations or other difficulties could be resolved at the outset, even if automated changeover was not implemented. The Cosmicar Pentax lens gives a range of 100-250mm, which with +1, +2 and +4 close-up filters is sufficient to adjust between graphics with

a diameter of between 30 and 120mm. The zoom lens contains an automated *iris* to optimise the exposure. A Dennard unit was purchased for manual control of the zoom lens during the early stages of the project.

The EasyMatch library is part of the Euresys 'EasyLib' range of machine vision software. At the time the pre-prototype was being developed version 4.0 was available and this is 32-bit software coded in C++ and compiled for various platforms including Windows NT 4. The range comes with the EasyAccess prototyping application, which can be integrated with the Picolo frame-grabber's test program, EasyGrab. The frame-grabber drivers contain their own image data types, but they can also use the 'EasyLib' image objects, allowing seamless software integration.

EasyMatch performs grey-level pattern matching. This entails a preparatory learning stage using a reference image, which must be performed once each time the software is run, and the main matching process that can be performed on as many images as desired. EasyMatch is based on a proprietary algorithm, which is at present un-patented and so the details are not published. The information in the public domain indicates that the routine uses *pyramidal* processing involving a quick first-pass on a coarse sample of the image with subsequent matches at higher resolutions. This is in the spirit of coarse-fine template matching [Rosenfeld *et al*, 1977]. When rotation and scaling are allowed the image is re-sampled, and the position of the object relative to the reference object can be found to sub-pixel accuracy. Similarly, the scale and angle are found to a high accuracy.

The routine computes a standard correlation between the reference and the image, or it can compensate for variations in intensity (offset) or intensity and offset (offset and gain) to allow for non-uniform illumination. Many parameters in the EasyMatch library can be set and these

as well as other factors affect the performance. It was claimed that on an Intel Pentium II 166MHz processor an object in a 128x128 pixel reference image could be located in a 512x512 pixel image in 45ms, and when ±45° degrees of rotation was allowed in 760ms.

4.2 Pre-prototype implementation of IPPimage

The initial Intelpadprint image pre-processing application was created using Microsoft Visual C++ 5.0 in Developer Studio 97. Developer Studio is a programming application that combines the basic functions of text editing, compilation, debugging, and application building with visual tools. The *visual* tools allow new icons to be created, toolbars to be edited and the visible part of the user interface to be implemented on a what you see is what you get (WYSIWYG) basis. Visual programmes operate in a similar manner to graphics software using the mouse and Windows drag-and-drop and resize interaction, to manipulate objects on screen.

The Visual C++ example applications that came with the Picolo frame-grabber and the EasyLib software libraries were created by the Visual C++ software wizard AppWizard and amended by Euresys. They were a useful aid to learn how to use the frame-grabber and function libraries, and contained classes derived from the Microsoft Foundation Class (MFC) mainframe, view and document classes. The FirstEasyBW8 example was chosen as it demonstrates the complex procedure to initialise the frame-grabber and a buffer in memory, and point an EasyLib image object to the buffer:

1. Start the Picolo (*P*) driver and return a handle to the frame-grabber
2. Select the type of video signal input: composite BNC and PAL standard (P)
3. Choose the Picolo image format: grey-scale unsigned 8-bit integer, Y8 (P)
4. Fetch the image dimensions in pixels (P)
5. Get the size of the acquisition buffer to be allocated in memory (P)

6. Call the constructor to create a grey-scale EasyLib (*E*) image object: EImageBW8

7. Use the standard C memory virtual-allocation function to initialise buffer and return a pointer: VirtualAlloc

8. Register the buffer with the driver, and the Picolo buffer-list (P)

9. Set the EImageBW8 pointer to the aligned buffer (E)

10. Initialise the driver for image acquisition by registering an 'end of image', and setting refresh and live acquisition to false (P)

Before the application exits a reverse procedure must be followed to return resources to the operating system. (The application must end image acquisition if required, release the Picolo driver from the buffer, free the memory allocation, stop the Picolo driver and delete the image object.) The Picolo driver calls are made using low level functions, and the EasyLib libraries comprise low-level functions and object-oriented classes.

Coding of the Intelpadprint development application proceeded by adding member functions to the document class in the example application. Each function performed a small number of related operations and the executable was named 'IPPimage'. As mentioned previously, many parameters in the EasyMatch library can be adjusted so, to increase flexibility these values were read from a text file by the member function OnLearn(). The following lines from OnLearn() set the amount of rotation that is allowed in revolutions. The default is no rotation and in that case matching will not indicate the angle between the objects in the image and the ideal copy in the reference.

```
m_pMatch->SetMinAngle( –f32DegAngle / 360 )

m_pMatch->SetMaxAngle( f32DegAngle / 360 )
```

The routine OnLearn() then calls the function that processes the template prior to matching:

```
m_pMatch->LearnPattern( m_pRefImage )
```

Two functions were created each implementing the core acquire-match-transform-save algorithm, and each timing the process. The function 'OnImageTest()' performs the algorithm once, contains an option to use a low-pass filter, and images can be presented from the frame-grabber or from a file. The alternative 'OnImageOnline()' uses the frame-grabber exclusively and calls no filters or non-core functions. The algorithm loops for a maximum number of 'runs' selected by the user to allow testing during production. The geometric transform is produced with the EasyImage library function ImgScaleRotate(...) and the scale, angle and position parameters input from EasyMatch(). The 'test' and 'online' functions save the run-number, number of milliseconds elapsed, the 'EScore', and the angle, scale and position of the print in the image relative to the reference image. Data is saved in a text file for analysis. EScore is the strength of the match produced by the EasyMatch library and lies on the interval –1 to 1. 1 indicates a perfect match between the reference and the image, while –1 is for a perfect mis-match: that is, pixels that are black should be white and vice versa.

4.2.1 Integrating IPPimage/ diagnose

The pro-processing routine *IPPimage* was being coded in C++ and simultaneously the classification routine *IPPdiagnose* was being developed in MATLAB. It was necessary for IPPimage to pass the processed image to IPPdiagnose, and the most efficient way would be to pass the address of a buffer in memory that the applications could share. However, due to the project schedule and the challenge of interfacing programs written in different languages a simpler approach was sought for the pre-prototype. A *check-for-file* algorithm was specified. It works on the basis that IPPdiagnose finishes its previous computation and goes into a waiting state. Each loop it pauses then tests for the existence of an image file in a predefined

location. IPPimage performs its processing and writes its image to this location whereupon IPPdiagnose finds the file, reads it into memory, deletes it and starts its processing.

4.2.2 Triggering image acquisition

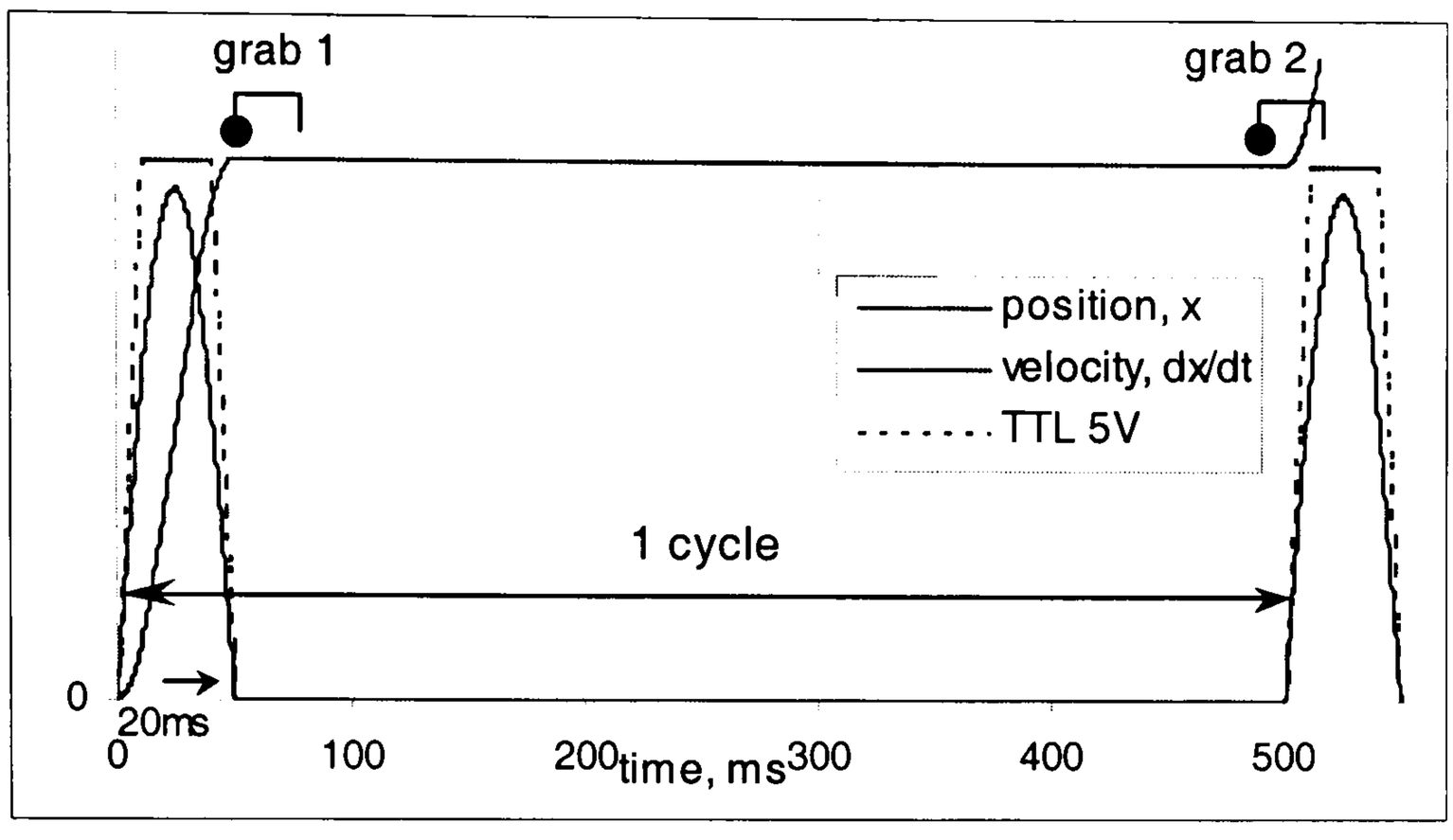

Figure 4. 5 Carousel motion triggers image acquisition during printing at 7200/h (see figure 3.16)

As section 4.1.2 (siting the camera) demonstrated, for the pre-prototype system image acquisition should occur while the substrate is stationary and as early in the cycle following printing as possible. The concept graph in Figure 4. 2 shows the relative position and velocity of the carousel during one cycle, with the carousel following path *A* in Figure 4. 2. The Picolo frame-grabber contains four *transistor-transistor level* (TTL) voltage input-output lines, and the first one can be used by the software driver to control image acquisition. An external source dictates whether the TTL voltage is at five volts or at ground voltage, and there are tolerances specified for these binary levels. An interrupt can be caused by a falling or rising edge, or a high or low level TTL signal. A falling edge can be used to trigger acquisition as shown in figure 4.5 ('grab 1'), but this assumes that inspection and printing occupy the same amount of time and are synchronised. The pre-prototype printer achieved a printing rate of

5100 cycles/h (section 5.2.2). The pre-prototype inspection system was expected to operate at 900 to 1800 cycles/h, so printing and inspection occur asynchronously.

A high-level TTL signal was chosen to trigger image acquisition. As acquisition occupies a finite time, it was accepted that during production a small proportion of the many images will be triggered so that acquisition occurs while the carousel is in motion ('grab 2' in figure 4.5) and the resulting image will not contain the whole graphic. The input-output frame-grabber functions can be configured to prevent this problem. The Intelpadprint software was coded to configure the input-output module when the 'online' and 'test' functions were initialised:

```
PicoloEnableIO( m_hPicolo, INT_HIGH_LEVEL)
```

where 'm_hPicolo' identifies the Picolo card. Each acquisition is 'armed' then triggered when the carousel is next stationary:

```
PicoloAcquire( m_hPicolo, PICOLO_ACQUIRE_ARM+PICOLO_ACQUIRE, 1)
PicoloTriggerEvent( m_hPicolo, PICOLO_EV_IO_INTERRUPT)
```

4.2.3 Evaluation of pre-prototype *IPPimage*

The pre-prototype imaging system was debugged and briefly evaluated at Birmingham. The project program dictated that the system was then evaluated with the diagnosis software from Maastricht and the printer by the end-user LEGO. The computer used was an Intel Pentium II 233 MHz supplied by LEGO, and the camera was mounted above the next station on the pre-prototype system after the printer.

Image acquisition could be triggered on-line by the printing process as detailed above. Due to the speed problem mentioned below the trigger was a manually operated switch and the 'test' function was used in place of the 'online' function.

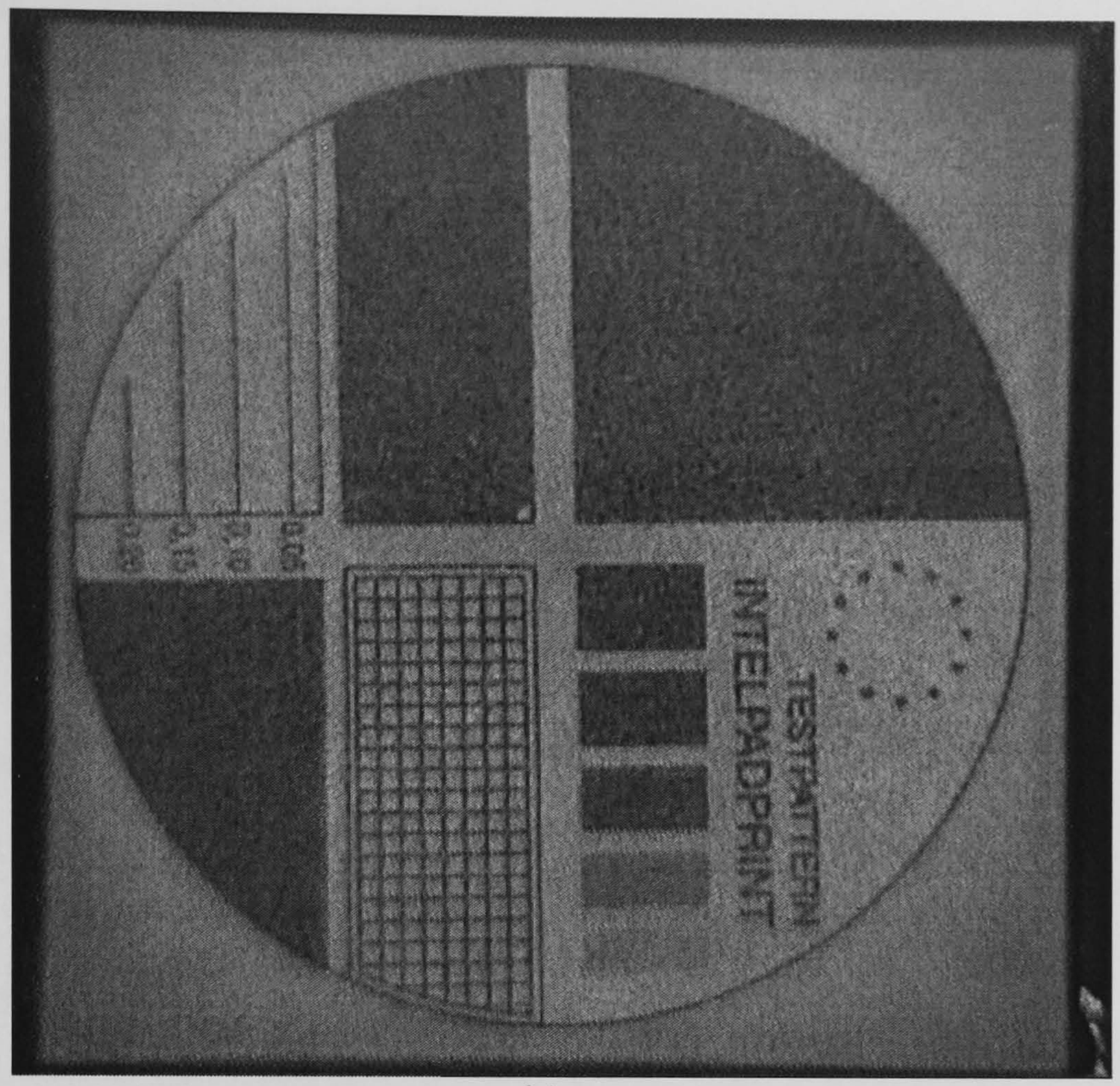

(a)

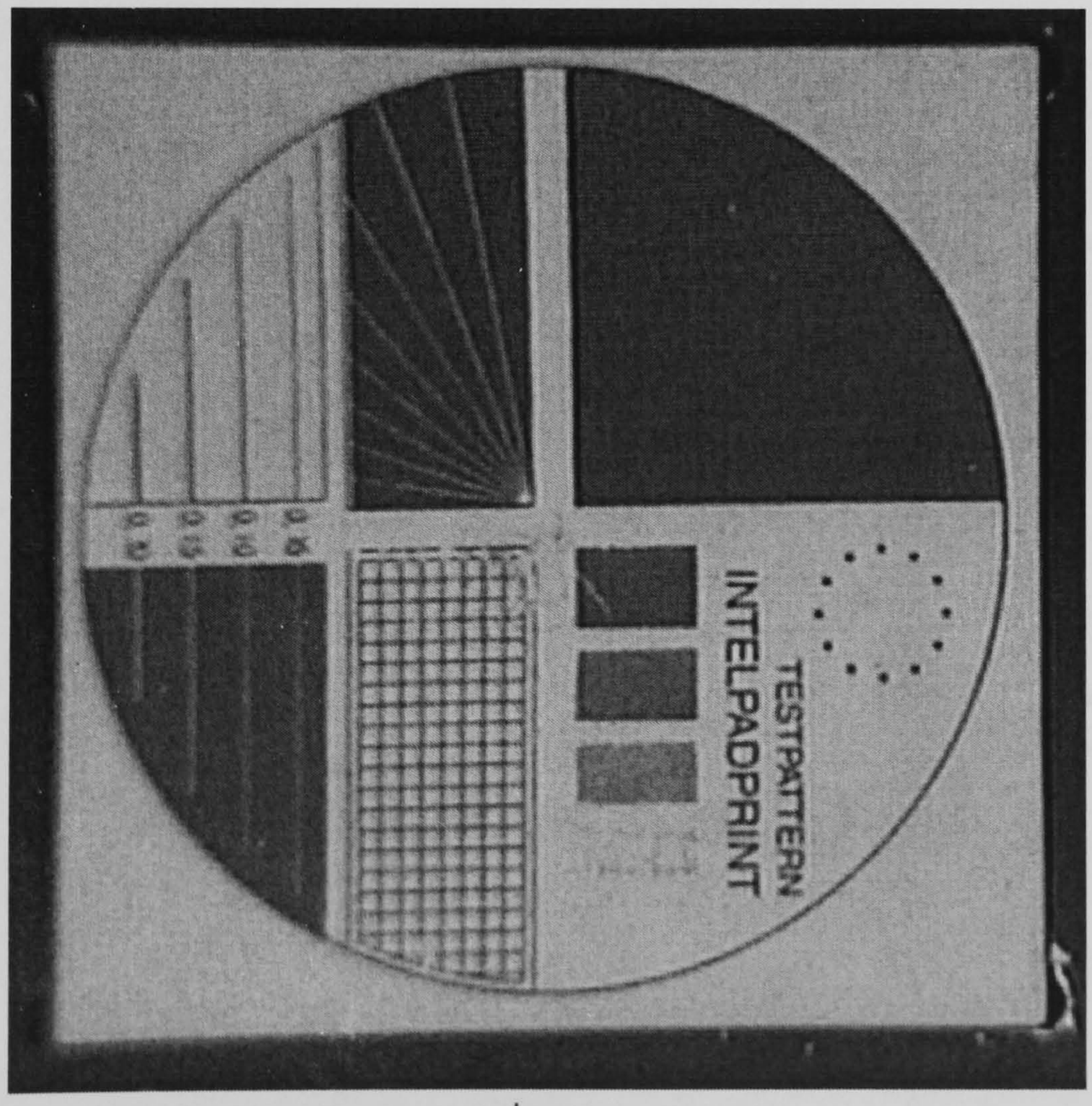

(b)

Figure 4. 6 Images of a red print on a grey substrate under a) direct lighting and b) the new diffuse illumination, demonstrating the improvement in image quality

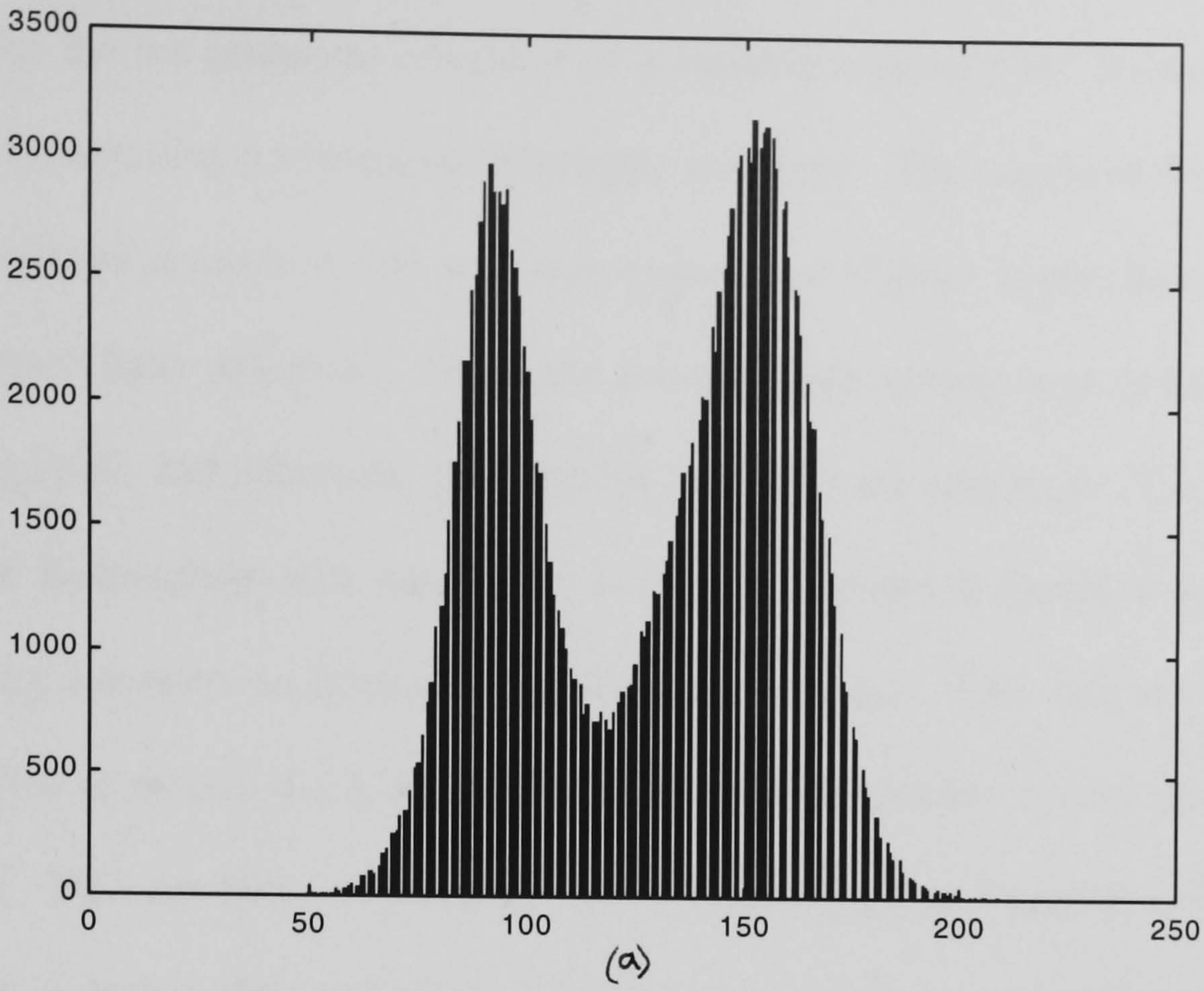

(a)

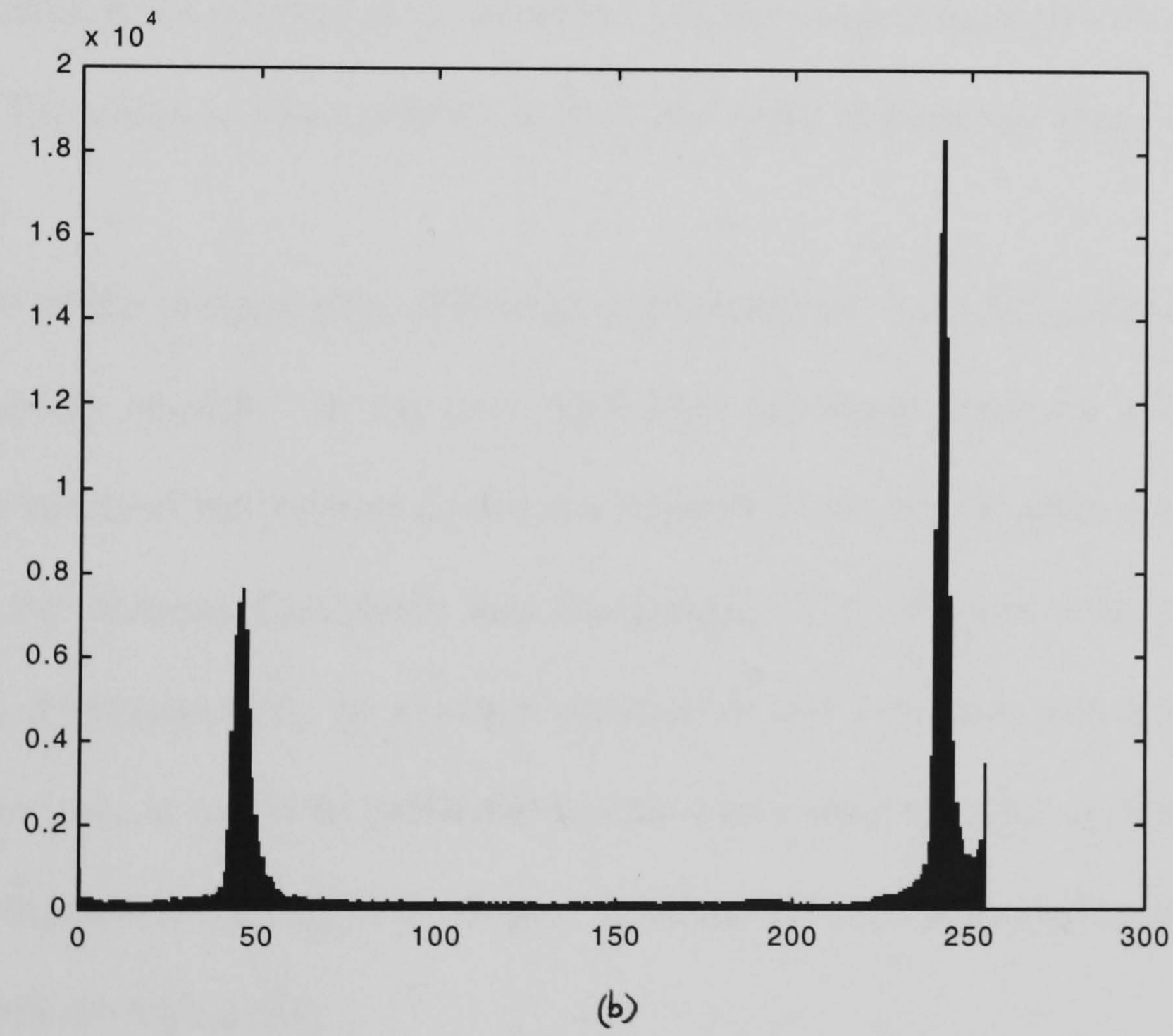

(b)

Figure 4. 7 Histograms of the distribution of pixel-intensity [1]

---

[1] Histograms for a) a red print on a grey substrate under direct lighting and b) a black print on a white product under the new diffuse illumination

The lighting for the pre-prototype consisted of a variable regulated DC power supply and a halogen lamp illuminating a continuous fibre-optic ring-light. The ring-light shone directly on the substrate and the inspection area was surrounded by a 400mm square black enclosure to eliminate external light pollution. When the pre-prototype system was evaluated with the Intelpadprint graphic and substrate, poor quality images were acquired. The problem was investigated at Birmingham and was found to give the images a speckled appearance and spatially-varying intensity, as demonstrated in Figure 4. 6 (a). This was one of the image defects identified in section 4.1.3, and would prevent the inspection system from identifying printing faults. The correlation of an image of the correctly printed graphic with its template would lead the system to diagnose printing faults that were not present. Also, printing faults would be obscured when comparing an erroneous graphic imaged under this illumination with the template. The solution to this problem is discussed in the next section (page 113).

The evaluation of the pre-prototype IPPimage at Birmingham and LEGO showed that it did not operate rapidly enough. In the user application IPPimage there are few instructions making up the kernel of the program so that the majority of the time is spent on computations performed in the libraries EasyMatch and EasyImage. The software written for the pre-prototype was developed from an example application and is loosely structured making it difficult to maintain. It would be preferable to create new demonstration IPPimage software, however with the time remaining in the project schedule writing a new application in C++ was judged to present too high a risk.

Part of the solution was to use the new version of the Euresys libraries: eVision 5, which replaced EasyLib 4.1. The new libraries uses the multimedia extension (MMX) that is built into the Pentium generation of Intel processors to accelerate operations on arrays of numbers.

Microsoft's ActiveX technology allows the libraries written in C++ to be used by applications written in C++, Microsoft Visual Basic or Delphi. Visual Basic 5 was available at Birmingham and it can promote high levels of productivity making it suitable for low-risk *rapid application development* (RAD). It is a compiled language yet it is possible to quickly run and debug a program prior to compilation. There is only a minor speed penalty over "low/ high" languages such as C++, which is reduced further as intense and critical computation is performed by the function libraries.

Alongside a new version of the Picolo software, Euresys released the alternative MultiCam drivers for the Picolo family of frame-grabbers. Like eVision, the MultiCam software uses ActiveX so that it can easily be linked to from applications written in Visual Basic, and as it has a different structure to the Picolo driver several applications can access the frame-grabber simultaneously. A disadvantage is that MultiCam cannot co-exist on a computer with the Picolo software, so development of the pre-prototype software would have to cease. At the time that preparations for the demonstration software were being made in parallel with use of the pre-prototype software this was a problem.

New hardware was the main solution to the low-speed encountered on the pre-prototype. For the pre-prototype a computer with a Pentium II 233MHz processor and 64MB of memory was purchased by LEGO. To give Birmingham control over the demonstration system computer a 450MHz Pentium III with 256MB of RAM was chosen. A computer contains a memory hierarchy: internal cache on the CPU-chip is the most expensive but has the lowest access time, the external cache, random access memory (RAM) and virtual memory on the hard drive are progressively slower but cheaper. The components of a computer must be balanced to minimise bottlenecks, but at a reasonable cost.

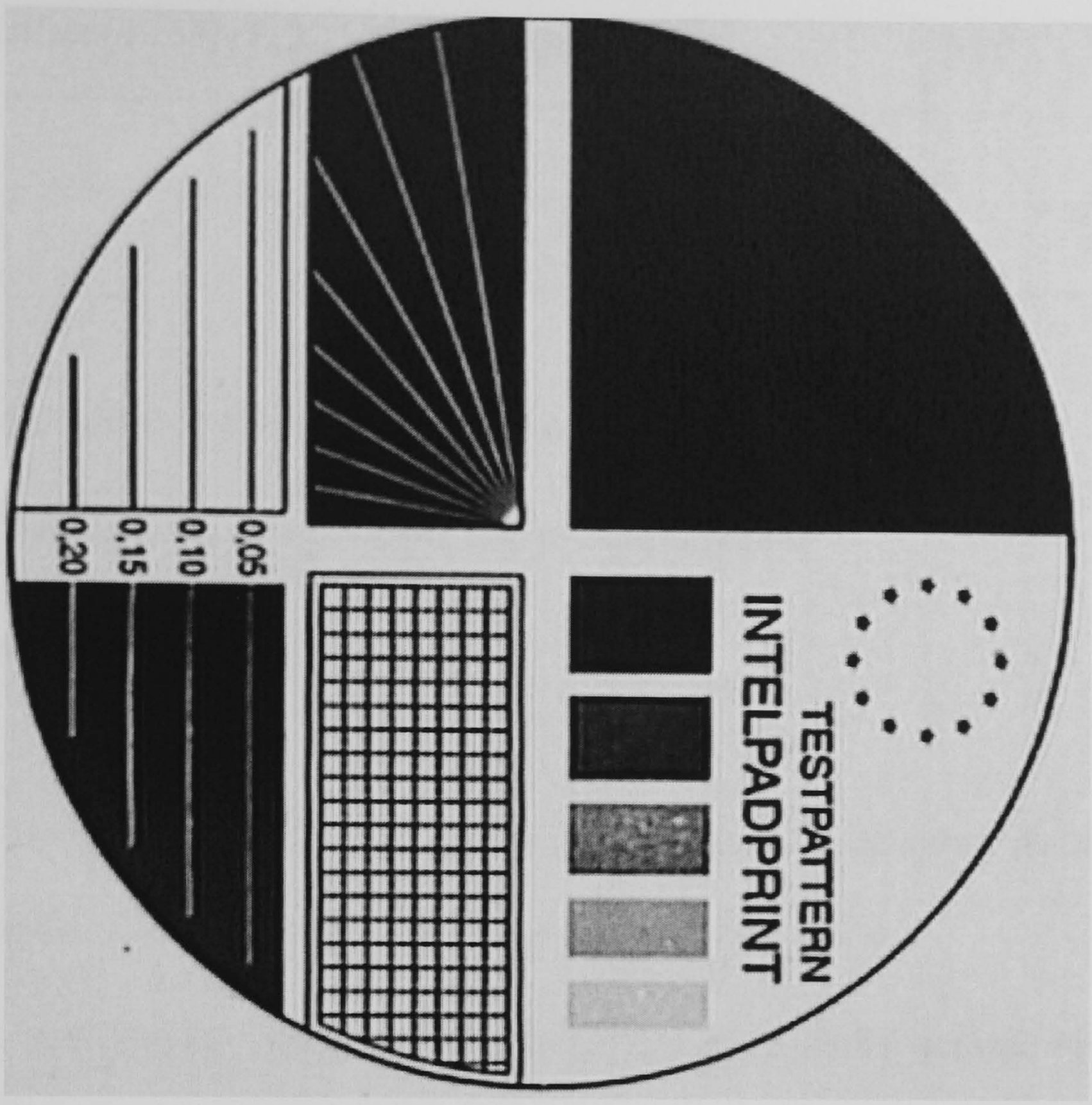

Figure 4. 8 Intepadprint testpattern image

The initial template or reference image used by the IPPimage software was the design for the cliché and was the Intelpadprint test pattern as shown in Figure 4. 8. It contains a representative sample of fine lines, raster areas, text ("INTELPADPRINT TESTPATTERN") and large areas, and when printed is approximately 45 mm in diameter. It was extracted from an Adobe Acrobat PDF document supplied by LEGO, had an arbitrary size (less than 768 x 576 pixels) and included the whole graphic. It was ideal in that it contained no noise and it comprised grey-levels that corresponded to the colours in the graphic: black, white and a number of tones in between. A *real* good-quality image of a print of this cliché would contain some unpredictable noise and a "compressed tonal range." This is systematic in that white is transformed to a very light grey and black a dark grey.

$$P_r = m\,P_i + c \qquad (5)$$

Gain~0.96, Offset (0:255)~5 (0:1)~0.0195	Ideal	Real
Black	0 | 0	5 | 0.0195
White	255 | 1	250 | 0.9795

There are three ways to produce the real template:

1. A moving average reduces noise (assumes no camera shake)

$$ax = ax + \frac{x(i) - ax}{i} \qquad (6)$$

2. Apply the transform in equation 5 to produce a geometrically equivalent real template from the ideal template. This requires the calculation of the gain and offset.

3. Produce a real template using multiple thresholds based on the average over connected regions in a real image of a good graphic. (This is done to find the gain and offset for 2.)

A mosaic of sub-templates was considered, but a single template is more useful to IPPdiagnose. The third option was chosen as this accounts for lens distortions and acceptably small print distortions that might occur. IPPdiagnose required a fixed size of template for a given graphic and this was chosen to fit in boxes between ninety and ninety-five percent of the available image size (576 x 768 pixels).

Of the two parts of the computer vision system for Intelpadprint: IPPimage and IPPdiagnose, IPPimage occurs first in a cycle and presents a lower risk. The matching routine used by IPPimage produces a 'score' which is a measure of the correlation between the template and an image (though the sum of the absolute difference is not calculated by EasyMatch). For a high quality image of a good graphic matched with a good quality template the score will lie between a threshold and one ($t < EScore_G \leq 1$) and this represents a 'pass'. However, for a

graphic containing printing defects the match will be less than the threshold ($-1 \leq EScore_E < t$) which represents a 'fail'. The threshold is expected to fall between 0.95 and 1.0, and can be found from experiments. As the pass state is the more probable outcome when the system operates correctly it is implied. The fail or *red-light* state will be indicated to the operator by the demonstration software and can be used to stop the printer producing more faulty parts.

The pre-prototype vision hardware was integrated with the pad printer and image capture could be triggered by the printing process. However, LEGO did not perform image acquisition under production conditions and it was agreed that initially the demonstration vision system would be standalone, with only IPPimage and IPPdiagnose integrated. Connection of the vision system with printer would occur when both parts were operating satisfactorily.

The pre-prototype interface between IPPimage and IPPdiagnose operated well. Based on the requirements of Maastricht University for compatibility with MATLAB the JPEG image file format was specified with a quality of 100%. However, even with at the highest quality or lowest compression the image degrades, so an alternative file format was sought. A commonly used lossless format compatible with eVision and MATLAB is TIFF (tagged image file format) and this was specified in version 2 of the interface for the demonstration system. As a template based on a real image was to be used, the interface specification demanded that the current template was saved to the buffer directory prior to the operation of the vision system.

4.2.4 Illumination

In order to solve the problem of low quality images described previously an alternative *evaluation* light-source was borrowed, comprising a ring-light of 8 halogen lamps shining

radially outwards and a reflective white annular-screen, as represented in figure 4.8. The light produced by this system was approximately spatially uniform and diffuse. As a result the slight texture on the plastic substrate did not produce the specular reflection which resulted in the poor quality encountered earlier.

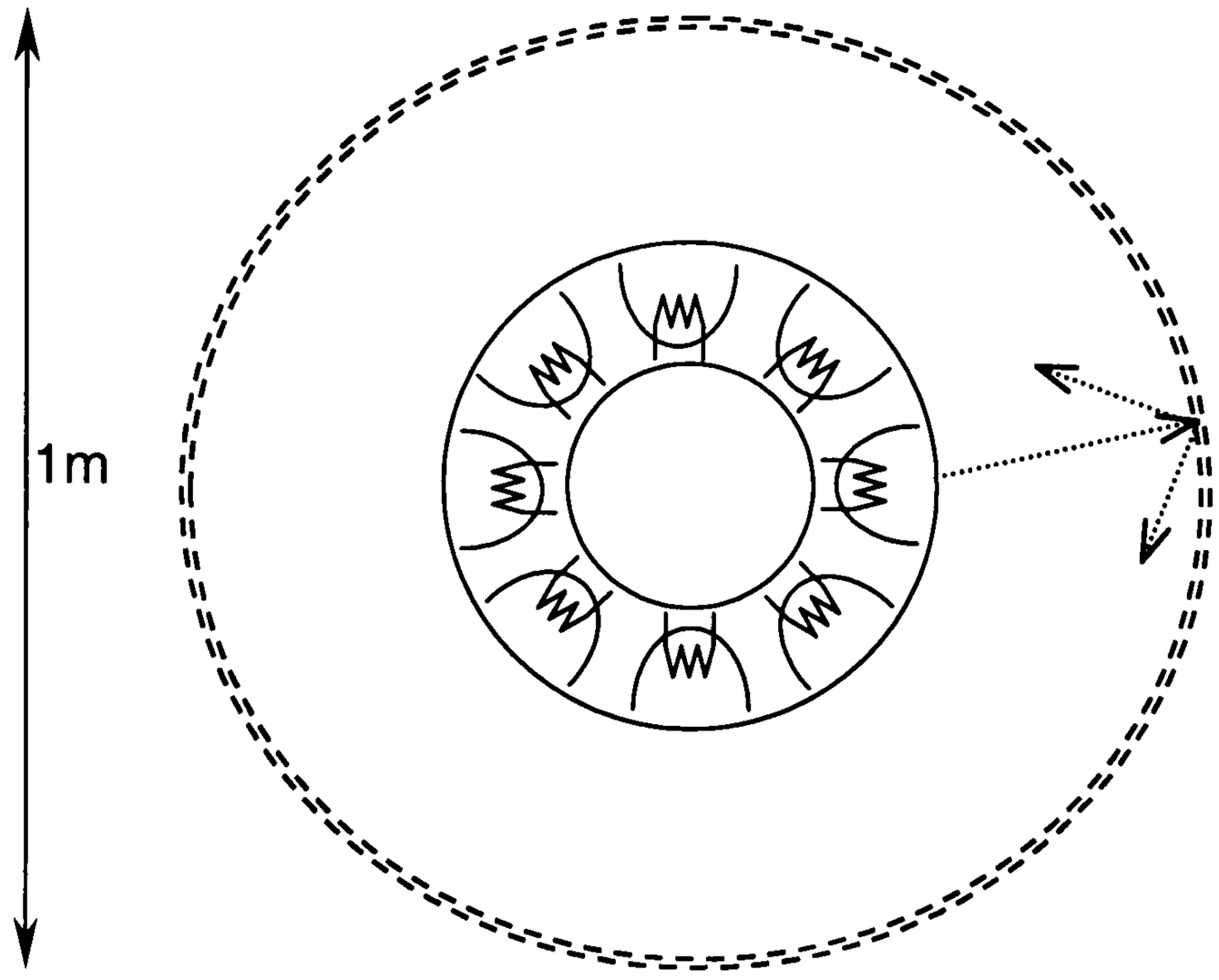

Figure 4. 9 Laboratory diffuse illumination, comprising a ring-light of 8 halogen lamps shining radially out, a white annular-screen and a regulated power supply

The evaluation system illustrated in figure 4.8 is quick and inexpensive to produce and gives good-quality illumination, making it ideal for laboratory tests. However, it would have drawbacks in a production environment. The screen is approximately 1m in diameter and the ring-light 0.5m, so it is not compact. Also, the 8 halogen bulbs consume a substantial amount of power and heat up the air around the printer which could affect the print-quality; and replacing the bulbs is awkward and disruptive. A solution combining the single, easily accessible lamp and cold, compact ring-light of the pre-prototype with the diffuse concept of the evaluation system would be ideal.

Such a lighting system was developed around the existing Schott source and ring-light, and the main innovation was the conical reflective adapter . The adapter screws into the thread on the ring-light and the height of the resulting unit is adjustable by means of slotted brackets attached to the adapter. Aluminium was used for ease of fabrication and the highly polished surface (*A*) deflects the axial beam from the ring-light radially outwards. The beam reflects off a surrounding white annular screen 260mm in diameter to create diffuse, uniform illumination over the area of the product holder. Light emerges from the Schott ring-light in a narrow beam through a narrow 0.5mm slit at a diameter only 1mm greater than the diameter of the thread. This makes the reverse conical section, minimum diameter and small radius at *B* in figure important to minimise loss of light. Other points to note in the figure are the matt black inner surface at *C* to prevent unwanted light entering the camera, and the knurled outer edge, *D*, to facilitate easy attachment of the adapter. The new unit could be mounted with the Schott ring-light uppermost, but best results were found with the conical adapter at the top and the base of the unit approximately 250mm above the substrate. The new diffuse light system for Intelpadprint gives ample illumination with the Schott source and the images are a significant improvement over those from the pre-prototype system as they are clear with good contrast, as demonstrated by Figure 4. 6. The system is compact and simple, and will work well with curved and glossy substrates. The only drawback is that in a dirty production setting the polished reflective surface will oxidise and dull resulting in a gradual change in illumination over time. The adapter and the light-slit in the need to be wiped clean occasionally and the problem can be reduced by coating the reflective surface.

4.3 Summary

1. The next indexed position after printing was chosen as the camera site on the pre-prototype printer's carousel. This reduced the dependency of the imaging system on the printer, but there was an alternative that would allow earlier image acquisition.

2. A novel template-matching algorithm was developed for *IPPimage* (the image pre-processing stage) which used local feature masks, reduced the matching time and ignored erroneous features in the printed graphic.

3. To reduce time and technical risk third-party image processing software libraries were employed in the pre-prototype software for IPPimage. This system used a *'check-for-file'* algorithm to interface with the *IPPdiagnose* printing fault diagnosis software. Image acquisition in IPPimage was triggered by the printing-cycle.

4. The pre-prototype IPPimage system written in C++ was too slow (processing 1 image typically occupied 10-15s), in part due to the use of an older, lower-specification PC. This resulted in it being evaluated separately from the printer at LEGO.

5. The pre-prototype system used directed illumination which was found to produce poor quality images. A compact diffuse lighting system was developed. From the histograms in Figure 4. 7, only 0.1% of pixels occupy the 2 peak intensities under poor lighting (pixel-intensity is widely distributed) while approximately 10% of pixels occupy the peaks under the new lighting.

5 Demonstration model

5.1 Introduction

The objectives of this chapter are to explain the evaluation of the printing fault visual diagnosis software (IPPdiagnose), the development of the demonstration inspection system (IPPimage). The method and results from the evaluation of IPPimage are discussed.

5.2 Evaluation of the printing fault visual diagnosis software

The fuzzy linear correlation algorithm implemented for the Intelpadprint pre-prototype was found to identify the correct printing error on laboratory specimens in 85 to 90% of cases. The quality of diagnosis or performance was defined as the highest correlation with an OCAP class over the second highest correlation:

$$q = \frac{max(P)}{2nd\_largest(P)} \qquad (1)$$

The results for 268 specimen faults were averaged by OCAP fault. Sixteen of the nineteen faults resulted in $q > 1$ and 74% gave a value of $q > 2$.

However there are a number of drawbacks to the LCA software. It is sequential and having waited for the pre-processing system to present an aligned image its computation takes substantially more time than a printing cycle (12-15s). The steps to produce a one-dimensional profile are relatively fast, but the correlation stage is slow. The algorithm is subject to cumulative errors starting with finding the most relevant parts of the image using the Search-box routine, then extracting the most applicable curve. The reasoning system only looks at data from the image and does not take account of pad printing expertise. Finally, the

algorithm only identifies one type of printing error on a sample, and though at the pre-prototype stage it was only presented with single errors by its nature it finds the membership over the whole class of OCAP errors. The samples are presented on the judgement of the human operator and if several errors obtain comparably high scores this may be because elements of both errors are present in the graphic.

a: Image with defect 'ink missing',
b: Image with defect 'air bubbles',
c: intensity profile compatible with a and

Figure 5.1 Demonstration of the ambiguity between some printing faults resulting from 1-d scans

The LCA software uses one-dimensional data segmented from the image and though this significantly reduces the amount of data to be processed at the next stage it can lead to ambiguity. Figure 5.1 shows examples of ink missing (OCAP error 5) and air bubbles (OCAP 2). The one-dimensional profiles from either can in principle result in the intensity graph illustrated. Information about the shape of the error is limited in one-dimensional data.

The final difficulty with the pre-prototype system was the availability of real printed errors. Initially this was caused by difficulties experienced by Philips in producing samples. Printing

errors were forced by deliberately producing the required wrong printing conditions, for example ink-viscosity that was too high. The next factor was that the pre-processing and fault diagnosis systems were developed in parallel by Birmingham and Maastricht, as demanded by the project time-schedule. The fault diagnosis program used MATLAB and its Image Processing Toolbox, and these tools were already familiar to developers at Maastricht. A lot of mathematical processing was coded in the diagnosis software, but MATLAB is user-friendly, un-compiled and relatively straightforward to debug. In contrast, the software developed at Birmingham interfaced with the frame-grabber hardware and used off-the-shelf function libraries. The use of commercial tools was considered to present lower risk to the project. The tools required familiarisation and the pre-prototype software required development in C++, while there was example code for a Windows user interface and this would produce a more user-friendly product. The Windows interface classes available in Visual C++ are however complex and the penalty was that the compiled program required more debugging. Most of the bugs in software developed at Maastricht had been fixed and pre-processed real images were required to evaluate and develop the algorithm, and the software produced by Birmingham could not at that stage supply them. When the software coded at Birmingham was ready it was tested in the field and it only became apparent then that the images it produced were not of sufficient quality.

The LCA is a good starting point and its performance is satisfactory for this type of pattern recognition system. However, the technical goals and research that were needed to achieve the demonstration system would explore different pattern recognition techniques.

5.2.1 Pattern recognition experiments in preparation for the demonstration system

Proof of principle experiments were performed with neural networks replacing individual parts of the LCA. They all used feed forward three-layer networks with momentum back-propagation learning, and the networks were implemented using the Neural Network Toolbox in MATLAB on a serial computer.

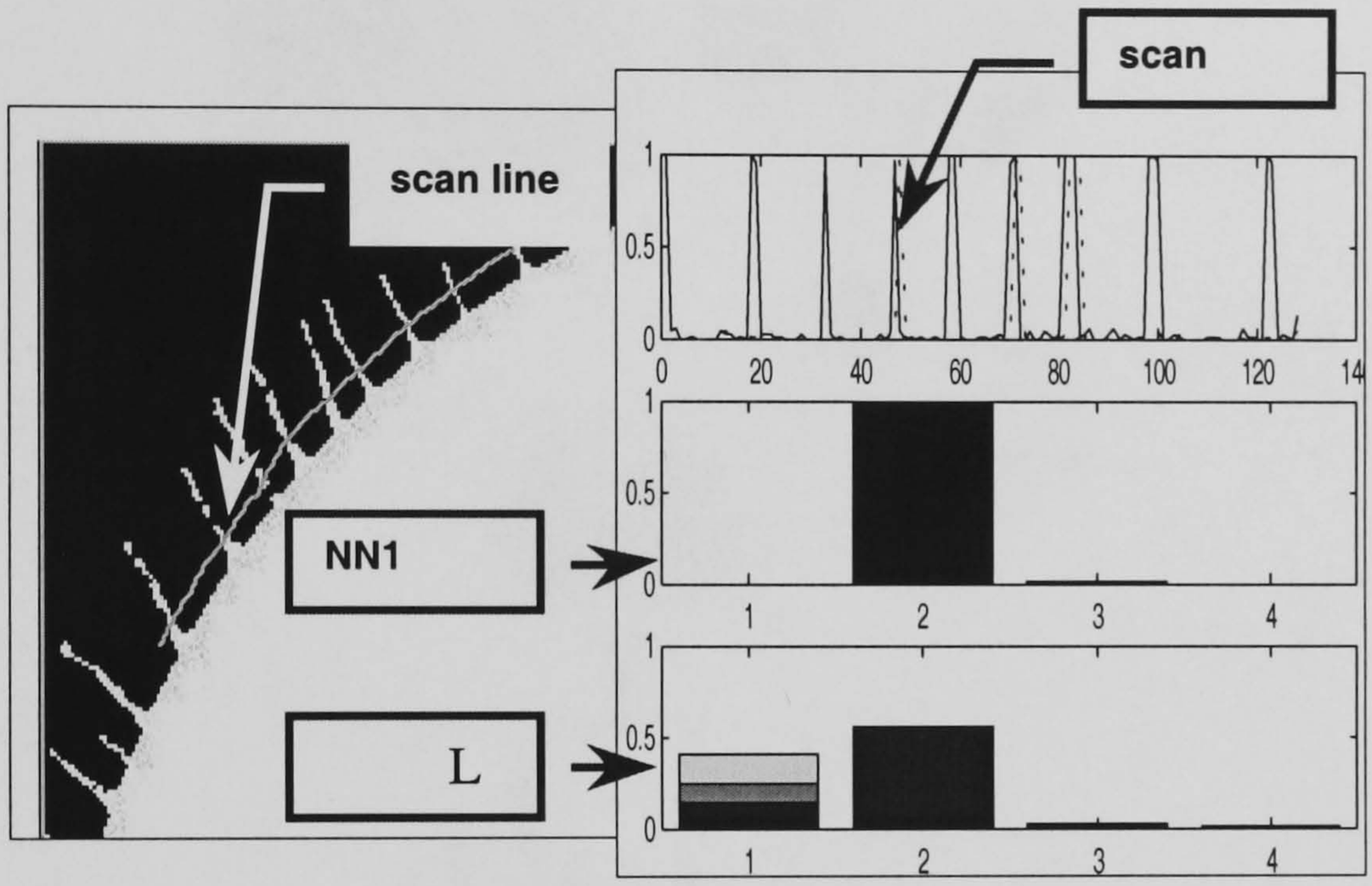

Figure 5.2 Comparison of the first stage of the LCA with neural network 'NN1' in classifying a scan-profile to the classes '*line*', '*hairs*', '*step*' or *'the rest'*. In this example a profile for the fault '*hairs*' is offered, to give the intermediate match *M*ij.

To facilitate comparison, the first neural network ('NN1') only performs the first task of the linear correlation algorithm to find the intermediate match vector *M*ij [Freear *et al*, 1999]. Then the subsequent mapping using *S*ijk to probability of faults *P*ijk can be performed with the original linear correlation algorithm, but for the proof-of-principle this was not done. A feed-forward three layer net was used with a logarithmic sigmoid transfer, and trained using the back propagation with momentum. To speed up training, the match types *R*j are restricted to four models: '*straight line*', '*step*' and '*oscillatory*' functions, and '*the rest'*. Initial results

were encouraging with the neural network giving a higher proportional of correct fault classifications than the LCA. A logarithmic sigmoid transfer function was used.

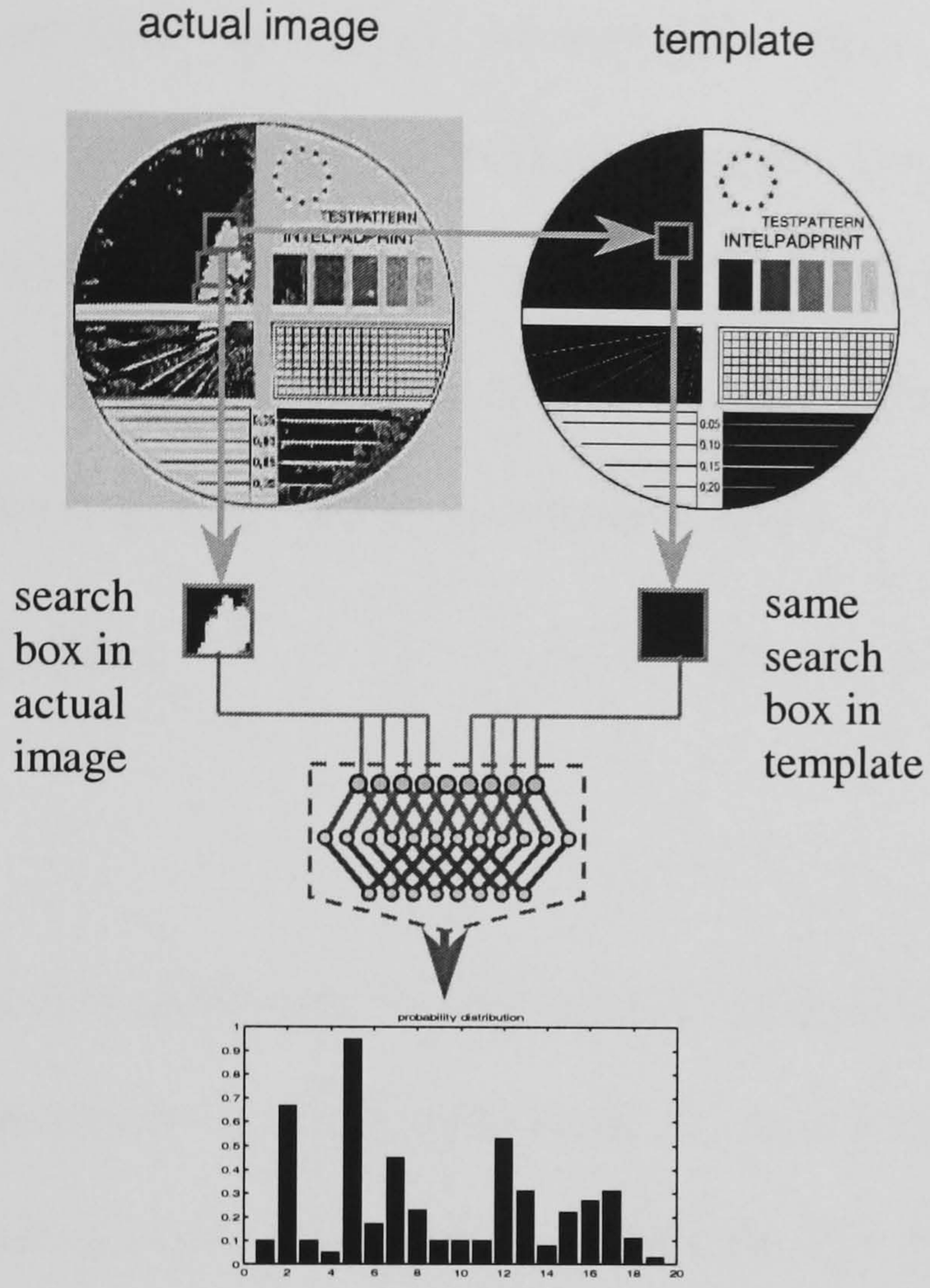

A neural network is trained to compare a 16x16 searchbox automatically generated on a relevant spot on an defect image with the same searchbox on the template. In controlled experiments the approach works satisfactory.

Figure 5.3 Neural network 'NN2'

Another neural network replaces both parts of the LCA-kernel and used 16 x 16 patches extracted from the image by the search-box routine of the LCA [Westra *et al*, 1999]. A coincident two-dimensional region was taken from the template and each of the 512 pixels intensities from the two sub-images ($2 \times 2^4 \times 2^4$) was presented to a neuron of the input layer. The hidden layer contained twenty neurons, and because five classes of OCAP defect were available in a training set of 260 images the output layer comprised five neurons. The network

was large so many areas were selected on each image resulting in a training set of 25000 sub-images.

Template-invariant observables, or direct measurements from the image, were also investigated in preparation for implementing the demonstration system. The first study was on the size of the defect, which is a function of the size of the difference between individual image and a reference pixels and the number of pixels which show a substantial difference. The size of a printing fault is given by the correlation measure:

$$\delta = \frac{1}{N} \cdot \Sigma_v \Sigma_u |I_{uv} - R_{uv}| \qquad (2)$$

where $N = \Sigma_v \Sigma_u 1$

The means and standard deviations over five examples of each OCAP fault were calculated. OCAP fault 6 ('mis-registration of double-print') had the largest characteristic size, and its error-bar was the only one not to overlap others. It was clear that *d* did not provide a strong correlation with the defect.

An alternative is the one-dimensional *cumulative intensity distribution* (CID) of the difference between the image and a reference related to the distance to the printed border, which is denoted $\Lambda(z)$. A four-band filter can be used to sample the difference in the area far outside the border $\xi 1$, close to but outside the border $\xi 2$. Two images of each OCAP defect were pre-processed and filtered.

Artificial neural networks were found to improve on the LCA in two cases and the third had comparable performance. The networks were implemented quickly and they allowed the

system to adapt to changing images. However, neural networks require long training times, large, consistent training sets, tuning of many parameters, and they were black-boxes which did not consistently produce converging results. Westra decided to use the cumulative intensity distribution approach with ξ and L1L2-clustering.

Even after the sub-pixel geometric transformation the test-graphic could still not be precisely coincident with the reference, so a filter was used to disregard a strip of pixels around the border. Fine defects such as hairs can potentially be lost in this 'don't care' region. The demonstration system using CID methods was implemented in MATLAB.

5.3 Interfacing and the Intelpadprint system encyclopaedia

The *Component Object Model* (COM) is a Microsoft specification that allows user applications or clients and server objects to interact across process and host computer boundaries with *location transparency*. Location transparency means that the mechanics of connection across an intranet or the Internet are hidden, and the software operates as if it is all resident on one machine. It is now an essential tool for maintaining and extending large software systems, and it employs binary reuse which is more efficient than code reuse. Binary reuse allows vendors to protect proprietary algorithms and makes individual components independent of the computer language. COM uses the *object-oriented programming* paradigm to give higher levels of reuse than other models and separates the interface between different components from the implementation of those components. The Euresys eVision and MultiCam libraries used in Intelpadprint rely on COM in the form of *ActiveX* so that client-applications can be written in C++, Visual Basic or Delphi and the library files can be updated in the field without altering the clients.

5.4 Development of the demonstration IPPimage software

During the development of the demonstration IPPimage various test applications were produced, for example a program to test triggering of image acquisition from the printing cycle.

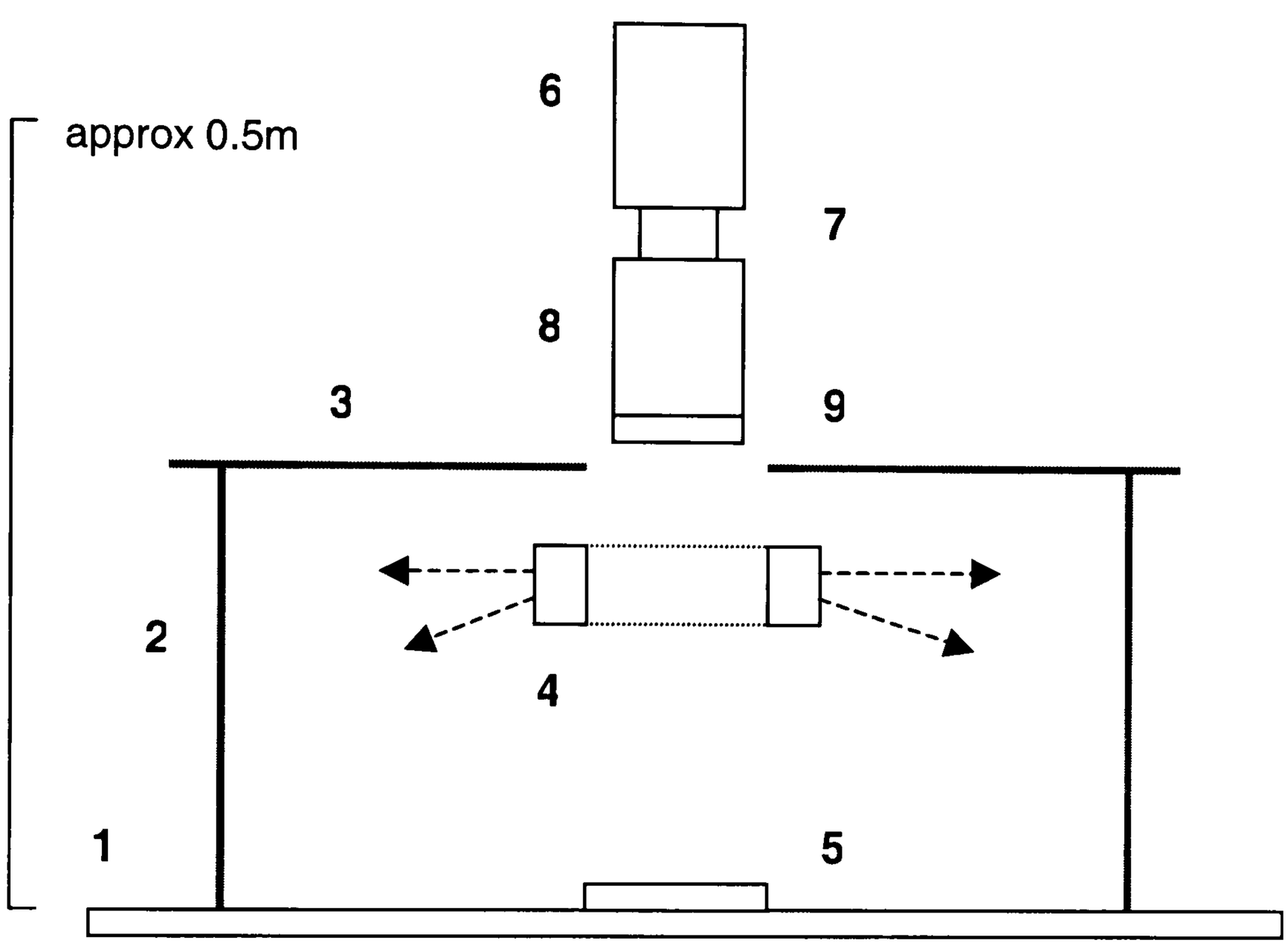

Figure 5.4 The components of the *Intelpadprint* standalone demonstration inspection system

Component	Ver	Cost, £	Comments
1. Table II and holder	D	3.00	Lego sheet – matt BLACK
2. Diffuse ring reflector	D	1.00	WHITE inside dia. approx 350mm
3. Top reflector	D	1.00	WHITE lower (inside) surface, centre hole dia. 70mm
4. Ring light assembly	D	370.00	Polished aluminium outer reflector, matt BLACK inner surface
5. Substrate	P D	–	-
6. CCD video camera	P D	636.00	JVC TK-C1380 colour, C-mount

7. C-mount extension tube(s)	D	36.00	Cosmicar set giving range 0.5–76.5mm
8. C-mount zoom lens II	D	255.00	Computar , 10:1, 8-80mm
9. Support for camera	D	100.00	[*] Jessops 3500 enlarger
10. Light source	B	860.00	[*] Schott: KL1500 electronic, fibre-optic ringlight (06414)
11. Frame-grabber	P D	433.00	[*] Euresys Picolo includes driver software
12. Computer II ('IPP-server')	P D	990.00	[*] PIII 450MHz, NT, 256MB, network card
13. C-mount zoom lens I	P	1200.00	Motorised
14. Filter(s)	P	60.00	+1, +2 close-up
15. Table I	P	690.00	Heron, Tampoprint & custom componennts
16. Computer I	P		PII 266MHz, NT, 64 MB

Notes: [*] – NOT SHOWN in schematic

P – pre-prototype model only

D – demonstration (standalone) model only

Cost – approximate, EXCLUDING tax (VAT), correct at August 1999

White screen: dia 255 x H 310mm

Ring-light: dia~ thread 77mm, slit 79.5mm, diff 1.5mm | slit-W 0.5mm

Black enclosure: W 250 x H 360mm

As additional functions were added different versions of the application were produced. Progress reports from Tampoprint at Intelpadprint meetings indicated that the demonstration printing system would not be operational in time for testing with the vision system, before the final project meeting in January 2000. Therefore, the final version for Intelpadprint (IPPimage-d 1.7) was a standalone version which only interfaced with IPPdiagnose. It was designed to demonstrate that the algorithm works and to allow user-controlled tests to be performed.

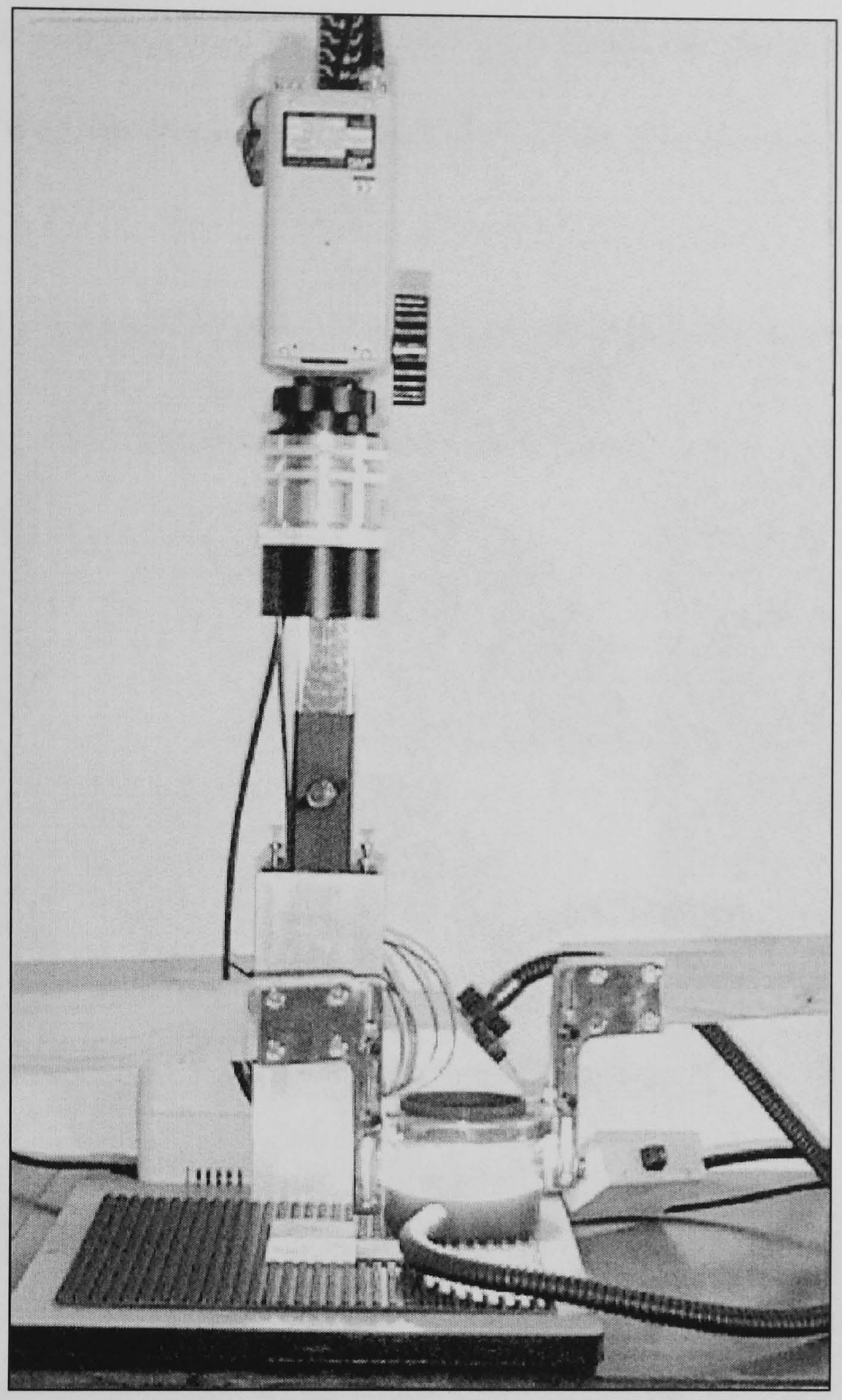

Figure 5.5 The *Intelpadprint* standalone demonstration inspection system (photo)

When IPPimage-d starts it tests whether a Picolo frame-grabber is installed: if one is not the image acquisition buttons 'live' and 'grab' are disabled and images are only available from file. The main window then opens, and it contains a row of buttons and four tabs: 'camera', 'process', 'template' and 'data' as shown in Figure 5.6. The camera tab shows the most recently acquired image from the camera or from file, while the process tab shows the transformed and then difference images after matching. The Visual Basic form which specifies the main window contains the Eurecard camera ActiveX control and routines to

rescale the images, resize objects with the window, grab single images and perform matching. The live routines provide feedback to the operator while the camera, lens or lighting is adjusted.

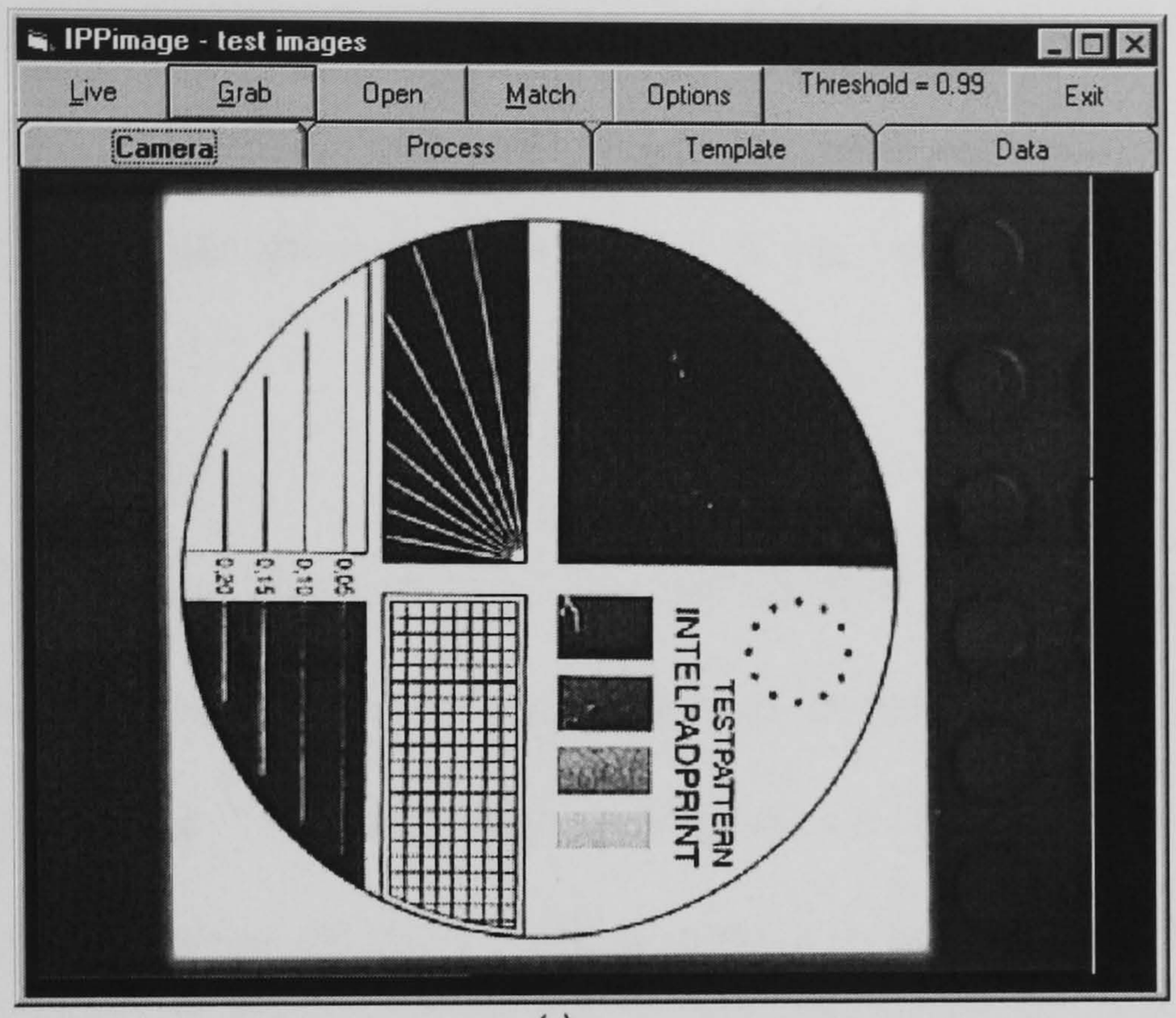

Figure 5.6 Screenshots of the demonstration version of IPPimage, a) 'Camera' tab and b) 'Redlight' dialog

The Eurecard controls include the EDisplay control which allows live acquisition, but it does not include the ability to draw lines on the image. A pseudo-live capability was achieved using an instance of the built-in timer control to acquire an image, draw a cross-hair and a box at 90% on the image and refresh it at 1ms intervals. A template is loaded by double clicking the template tab in the main window to create a standard 'open' dialog box , followed by a an image preview window with the option to go back to the open box or 'OK' the choice of image.

Visual Basic Form1 contains the "red-light" window which by default is not displayed. The form contains the routines to initialise EasyMatch as in the C++ pre-prototype software. Visual Basic projects can be re-compiled quickly and more had been learnt about the EasyMatch library, so the value for parameters such as the minimum and maximum scale were compiled in, as opposed to being read from a text file. A match is instigated from the main window, but is performed by Form1, which

5.5 Evaluation of the IPPimage demonstration system

5.5.1 Objectives

The purpose of the evaluation exercise was threefold: to produce test images to be used by Maastricht in their testing, to determine the efficacy of the IPPimage system and to produce threshold data for future tests.

There are many useful measures of the quality of the system, where quality is a corner of the time-cost-quality triangle mentioned in the discussion of Rapid application development (section 3.1.1). The primary criterium is, does it deliver the correct images to IPPdiagnose?

Correctness includes the orientation, scale, position and distortion of the graphics after processing by IPPimage. More important are the correct dimensions for the delivered image and the correlation of the image with the template.

Other criteria are the ability to determine useful thresholds for the red-light condition, the reliability, speed, ease of use, and ease of integration in the production system.

5.5.2 Materials and design

The main material for the tests was a set of identical substrates printed with the same graphic. Ideally each sample would have one or more examples of a single OCAP printing fault, all the OCAP classes would be represented by a number of samples and the samples would be classified and labelled. The samples were provided by Philips CFT and the faults were induced artificially by alterations to the set up of a printer by a skilled operator. An image of the graphic was supplied as an Adobe PDF document and this could be scaled and manipulated to produce an ideal template as described in chapter 4.

There are a lot of potential variables in this type of evaluation and an important principle is to only vary one parameter at a time. A variety of graphic designs would eventually need to be tested, but initially the Intelpadprint 'testpattern' graphic was used as shown in figure 4.8. Eventually the IPPimage is required to cope with more than one ink colour, but the preliminary tests would involve black ink on a white substrate for maximum contrast. The system is required to cope with a variety of substrates: flat and curved, glossy, matt, smooth and textured, but initial work would use flat textured substrates.

Identical and optimal illumination without light-pollution were used throughout the initial tests. Similarly, the same camera, hardware and software setups were employed, and in order to collect meaningful speed-data the same processes were left running on the test computer. Based on experience gained while evaluating the pre-prototype, the demonstration system was tested in isolation in non-continuous operation. Depending on time constrainsts and the availability of other parts of the Intelpadrint system later experiments, for instance the Alpha tests specified as task 10 of the project, can determine reliability under continuous, integrated operation. Similarly, tests involving degraded and fluctuating illumination and camera setup will be used to assess the robustness of IPPimage.

5.5.3 Method and results

The first task was to label the reverse of the samples with the batch letter, the OCAP fault they were classified under and the example number. The standard adopted for naming the images produced by the tests also included an optional test number. An example is "IPPtestB-01-02": a deliverable image of a batch B sample, implied as test 1, OCAP fault 'hairs', second example. *Deliverable* indicates that the image is suitable for use by IPPdiagnose: the graphic has been transformed to match the template and the image is the same size as the template.

The lighting, camera and lens were adjusted by eye using the 'live' facility in IPPimage. An image of a good graphic was matched with the ideal template by IPPimage and this was manipulated using method 3 explained in section 4.2.3. to produce a real template to be used for the remainder of the test. The test program IPPimage-t used in the evaluation of 10 October was identical to the version described in section 5.4, but the 'red-light' messages were

suppressed to speed up the work and the emphasis in the software was on automated data collection.

The moulded samples in test A1 were pushed firmly onto the holder in the correct orientation, while the cut substrates of test B1 were placed against the jig. The light-reflector was replaced around the rig and the sample code was entered in the program. The test was run, and the transformed and ghost images, and data were examined on screen. The sample was removed and the method was repeated for the next sample. Occasionally the test was rerun for a sample and observations were noted.

5.5.4 Results and observations

The samples provided by Philips for test A were close to what was required in the following respects. The same substrates and ink had been used throughout. To test the effectiveness of thresholding half the samples should be good graphics and the remainder should be divided evenly among the eighteen OCAP faults. Instead there were ten examples of good graphics and ten samples for each of nine OCAP faults. Philips experienced difficulty in inducing some of the printing faults.

The reliability of the software can be judged from the proportion of the time that it produces reasonable data and an image that to the naked eye is better than or the same as the raw image. The EasyMatch score must always be in the range of –1 to +1 and the tests would provide evidence to predict narrower ranges. During test A the software was found to be very reliable (98.8%) with only one sample from 81 requiring repeat processing.

Table 5.1 Summary of conditions for two evaluations performed at the University of Birmingham in August and October 1999.

	Test A1	**Test B1**
Date	11 August	10-11 October
Hardware/ operating system	Intel PI-166MHz, 64MB RAM, Microsoft NT4, FAT(16) file system, 128-256MB pagefile (virtual memory)	As for test A1
IPPimage	Version vb1.0	IPPimage-t (test) vb-1.0.4
3rd party	Multicam driver 1.3, Eurecard ActiveX 1.1, eVision libraries 5.1	As for 'A1'
Camera, etc	JVC camera, Cosmicar motorised lens, +2+1 filters, Picolo f-grabber	JVC camera, Computar manual lens, 5mm extension, Picolo f-grabber
Light	Temporary 2 arm fibre optic, Schott level '2'	IPP-2 ring-light/ reflector, Schott level '3.5'
Object distance	350 mm	330 mm
Samples	IPP testpattern, black ink, produced artificially by Philips CFT	IPP testpattern, black ink, produced artificially by Philips CFT (7 Oct)
Substrate	48 x 48 x 3.2mm moulded textured white [] plastic	White 70 x 50 x 1.8 cut white smooth gloss [], except B-12-13 to B-12-18, 48 x 48 moulded textured coloured*
Rig	Pre-prototype IPPimage rig	NEW Jessops-3500 w/o extension
OCAP classes represented	10]: 0, (1), 5, 6, 7, 9, 10, 11, 12, 17 (10 examples of each) (OCAP 1: hairs dealt with separately)	9]: 0, 1, 2, 5, 7, 10, 15, 16, 12 (10 examples of each, except OCAP 12:)
Unavailable	2, 3, 4, 8, 13, 14, 15, 16, 18	3, 4, 6, 8, 9, 11, 13, 14, 17, 18
Template	From real good graphic #7. T-	From real good graphic B-00-00, T-

	ipp9aug9.jpg, 437 x 433 pixels	ipp11oct.jpg
Graphic	'Intelpadprint testpattern'	As for 'A1'
Image name example	ipp_pa17.jpg	IPPtestB-00-01.jpg

The computing equipment used was slow compared with what was typical at the time, and this was reflected in the time to process the images. Between 16 and 27 seconds was required per image, and when the algorithm failed it occupied an extra 2 to 4 seconds. The outlying points are evident in figure 5.8. As figure 5.9 demonstrates the failure was reflected in the results for scale as well as orientation and position compared with the template.

<OCAP #: FF, -- from 00 to 18>	00
<sample #: SS, -- from 00 to (99)>	00
<Process timer, milliseconds>	23572
<EMatch score: -1 to +1 [perfect]>	.9468126
<Angle, revolutions>	1.89928E-03
<Centre X, pixels>	389.1233
<Centre Y, pixels>	284.2
<Scale X>	1.19544
<Scale Y>	1.193571
<-BLANK LINE->	

Figure 5.7 An example record from the plain text file produced by IPPimage.

Table 5.2 Summary of results for a) test A and b) test B.

10 Aug – A	**Minimum**	**Mean**	**Maximum**
Time, s	16.2	20.0	26.9
Orientation, degrees	-1.91	-0.09	10.0
Centre X, pixels	-14.9	1.80	13.1
Centre Y, pixels	-2.65	0.34	4.81
Scale X, %	-1.87	0.00	2.51
Scale Y, %	-5.94	0.00	3.63

10-11 Oct – B	**Minimum**	**Mean**	**Maximum**
Time, s	23.6	29.4	39.5
Orientation, degrees	-0.82	-0.08	0.96
Centre X, pixels	-23.12	0.70	13.88
Centre Y, pixels	-12.80	13.19	32.80
Scale X, %	-3.29	-0.54	2.33
Scale Y, %	-3.11	-0.77	3.15

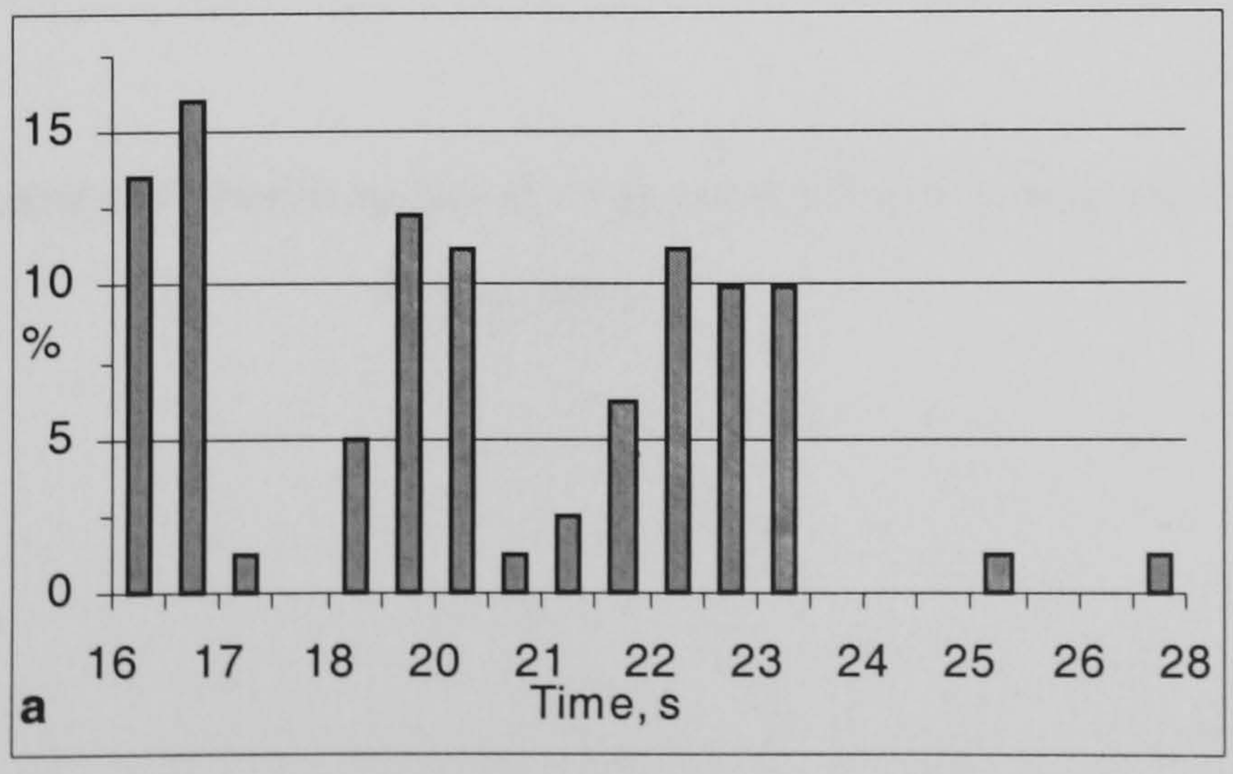

Figure 5.8 A histogram representing the distribution of processing times for all test-A graphics

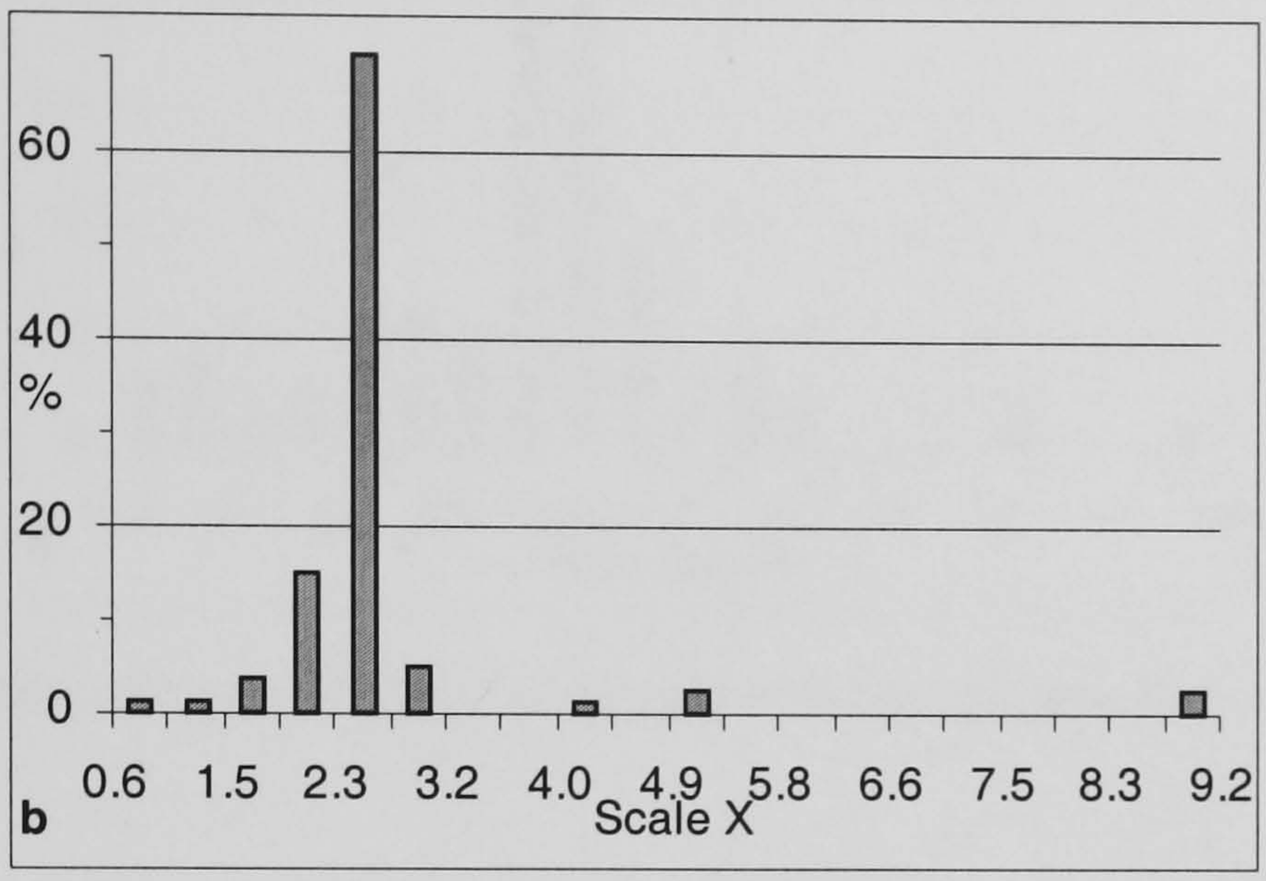

Figure 5.9 The deviation in scale from the template for all test-A graphics

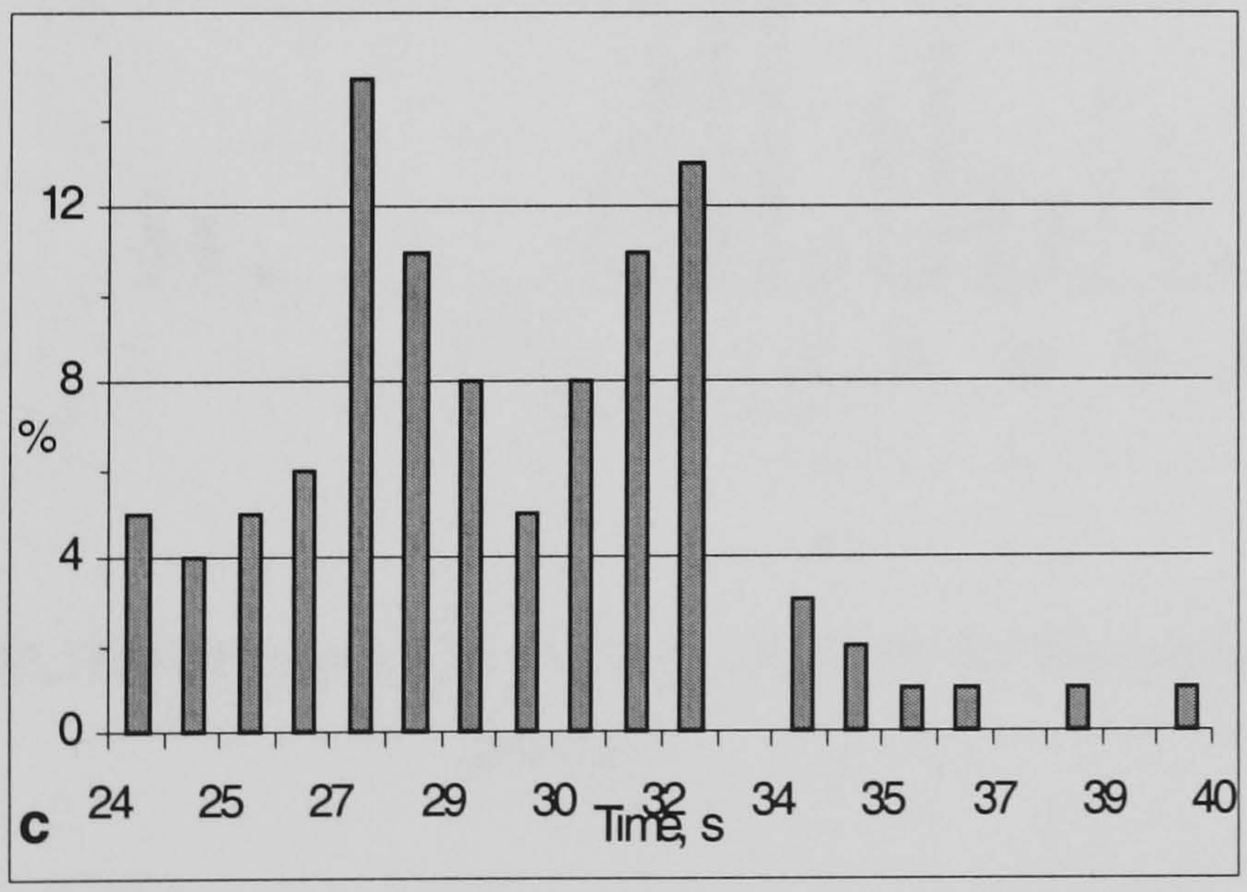

Figure 5.10 A histogram representing the distribution of processing times for all test-B graphics

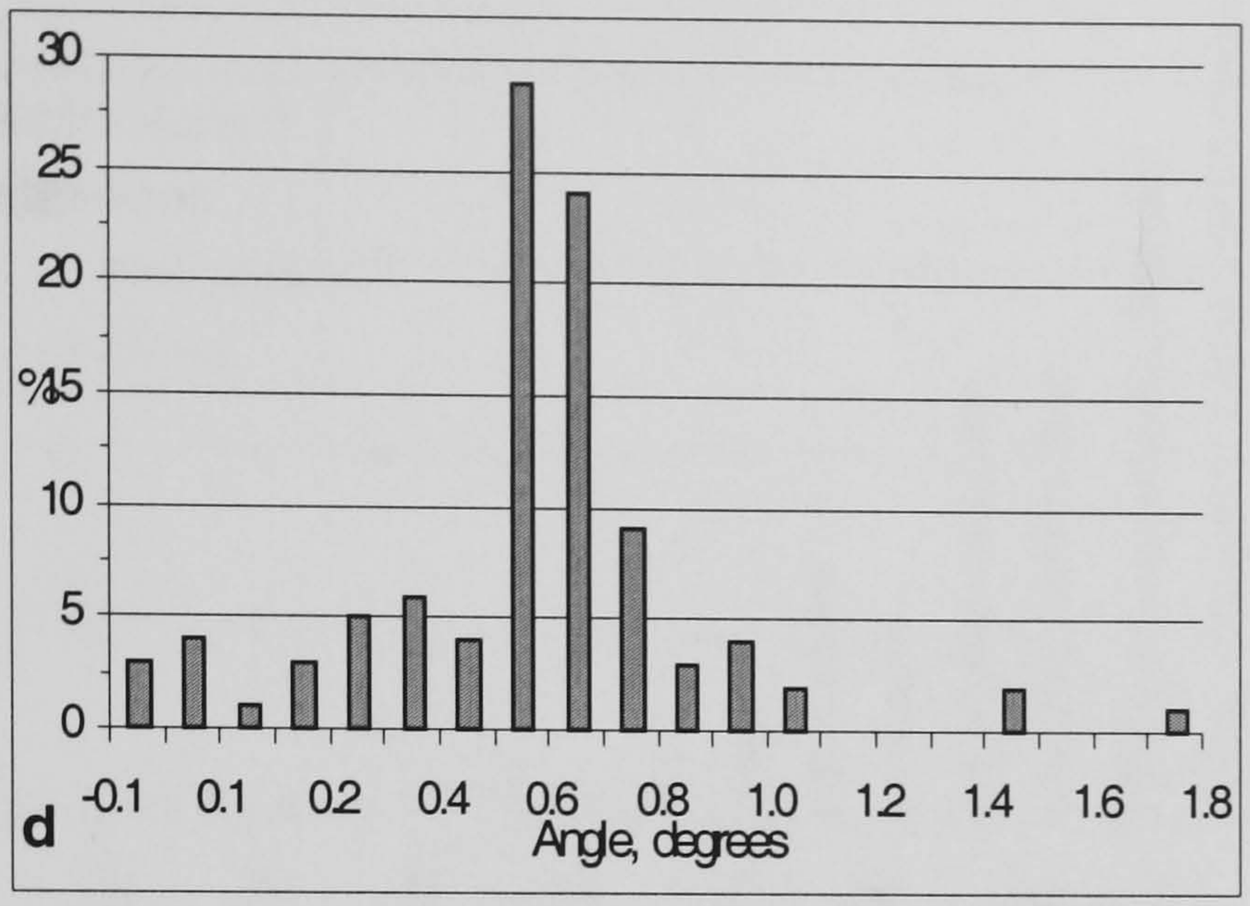

Figure 5.11 The distribution of angular deviation from the template for test B

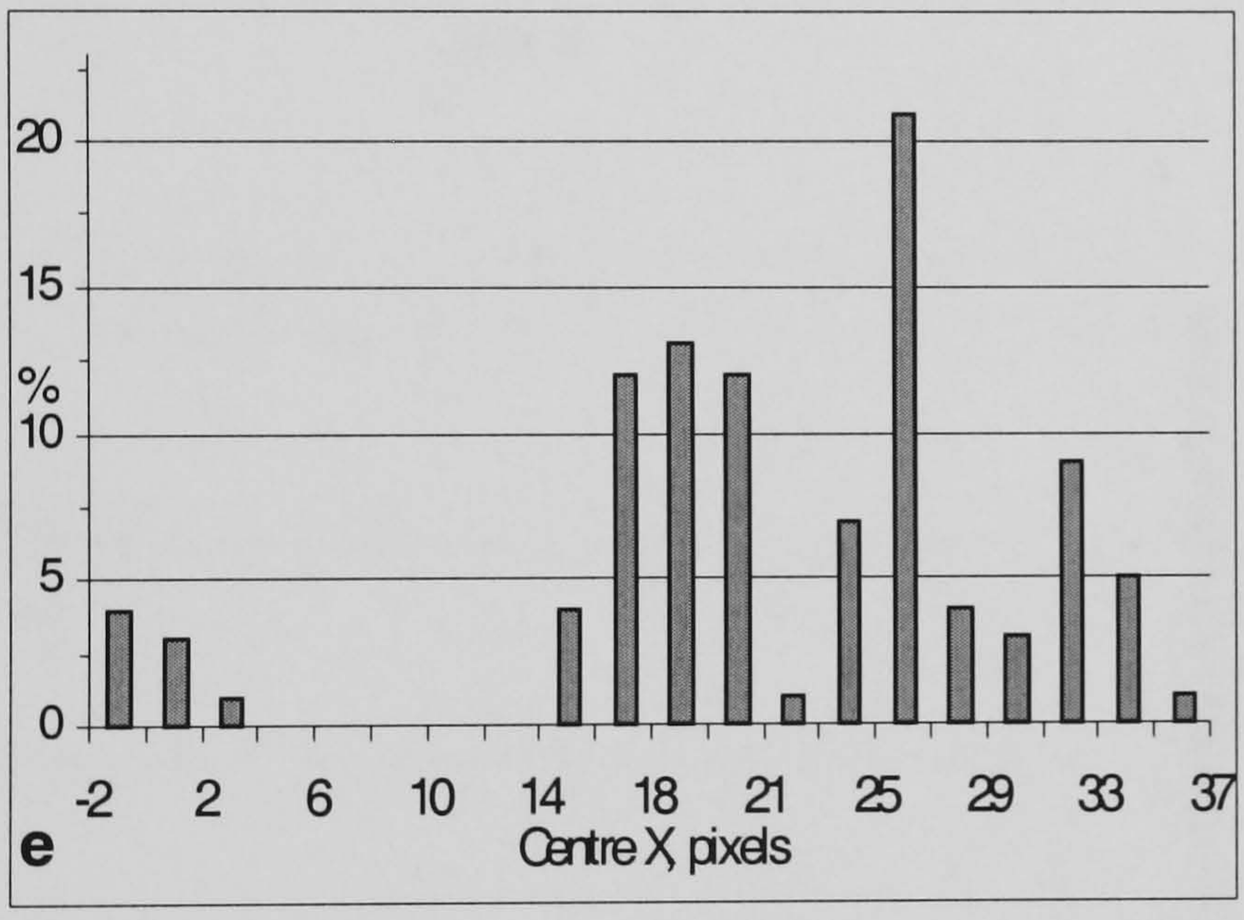

Figure 5.12 The distribution of positional deviation from the template for all test-B graphics

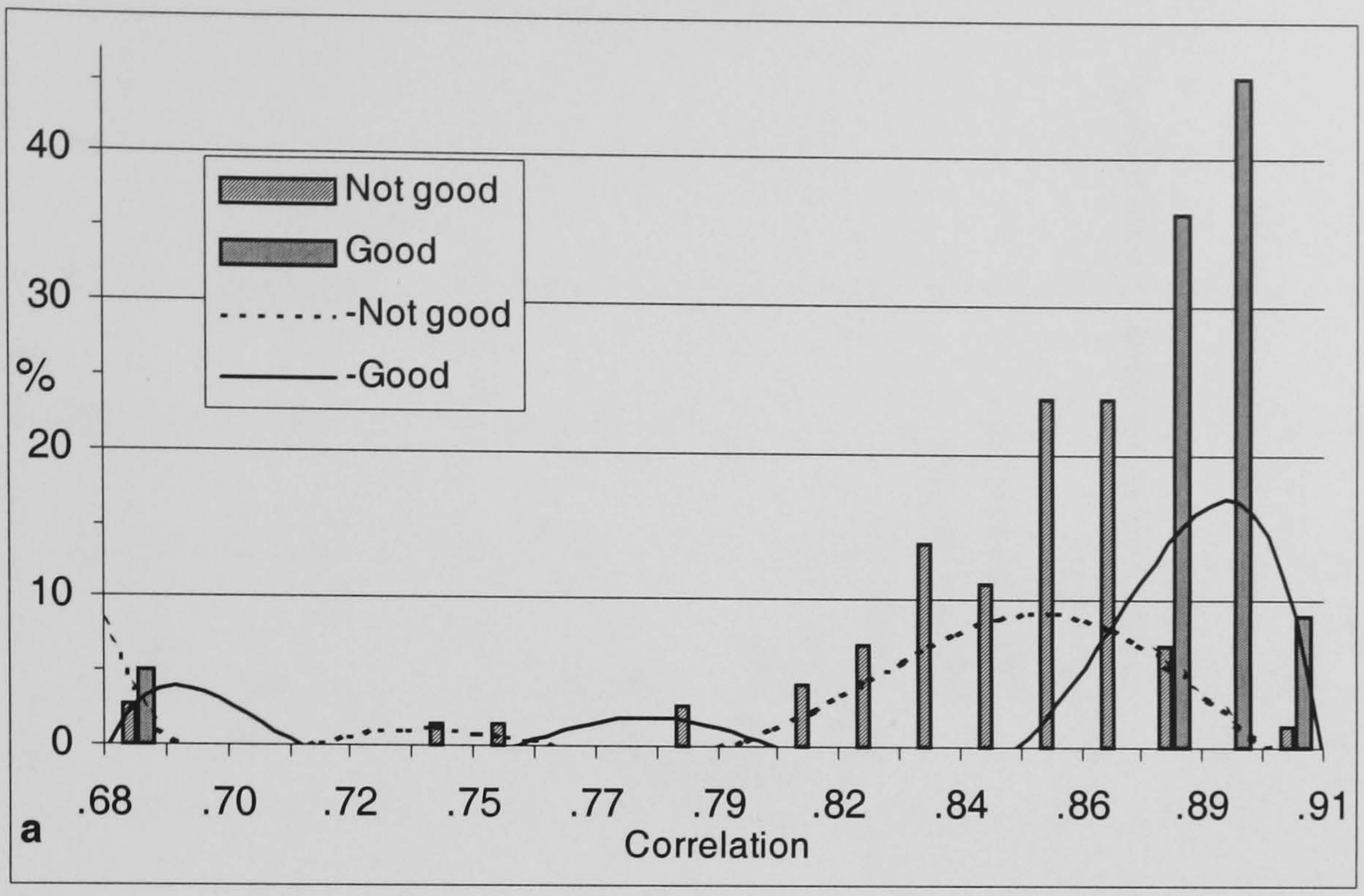

Figure 5.13 The partitioning of good and bad graphics by template-correlation for test A

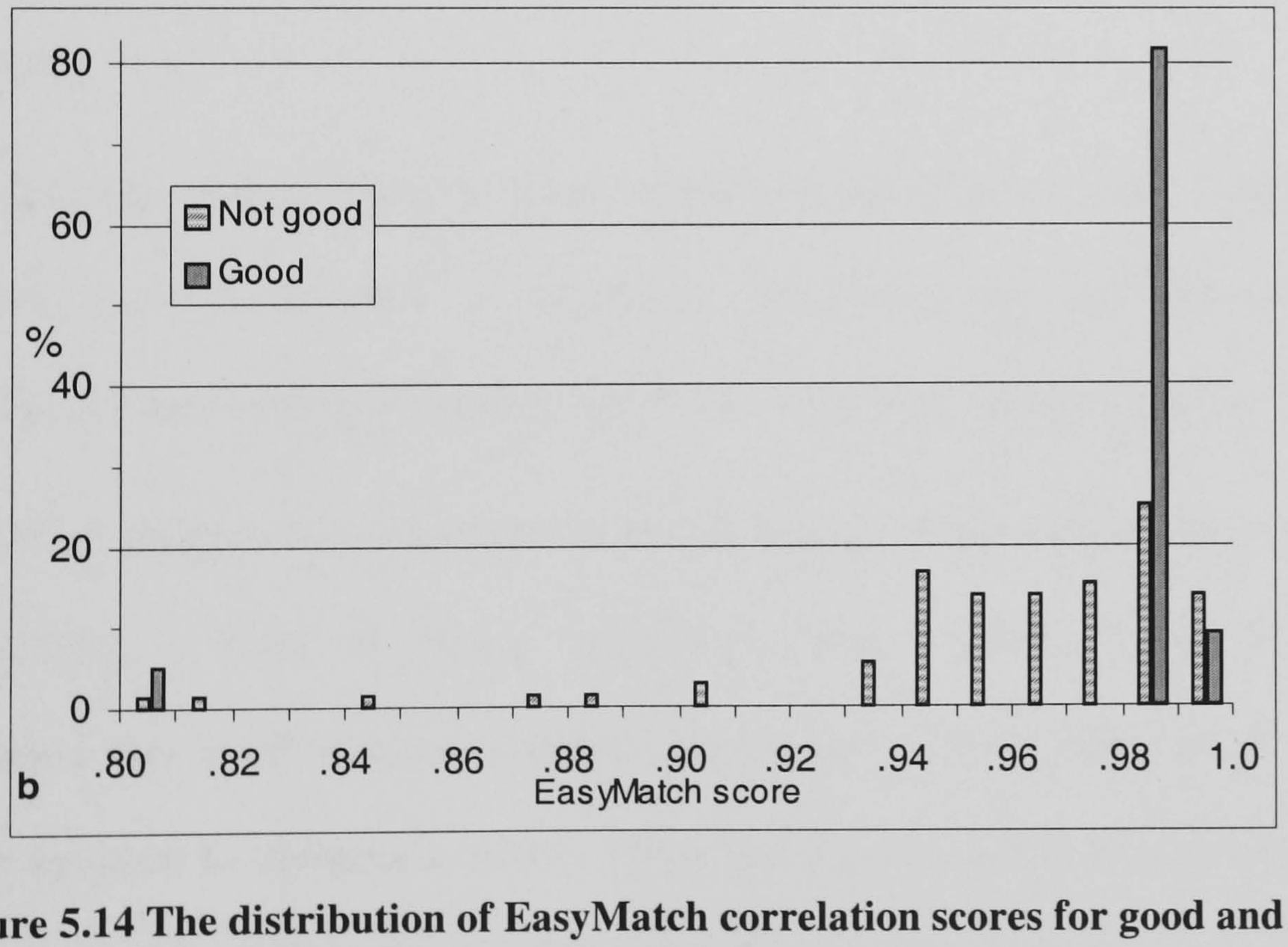

Figure 5.14 The distribution of EasyMatch correlation scores for good and bad graphics for test A

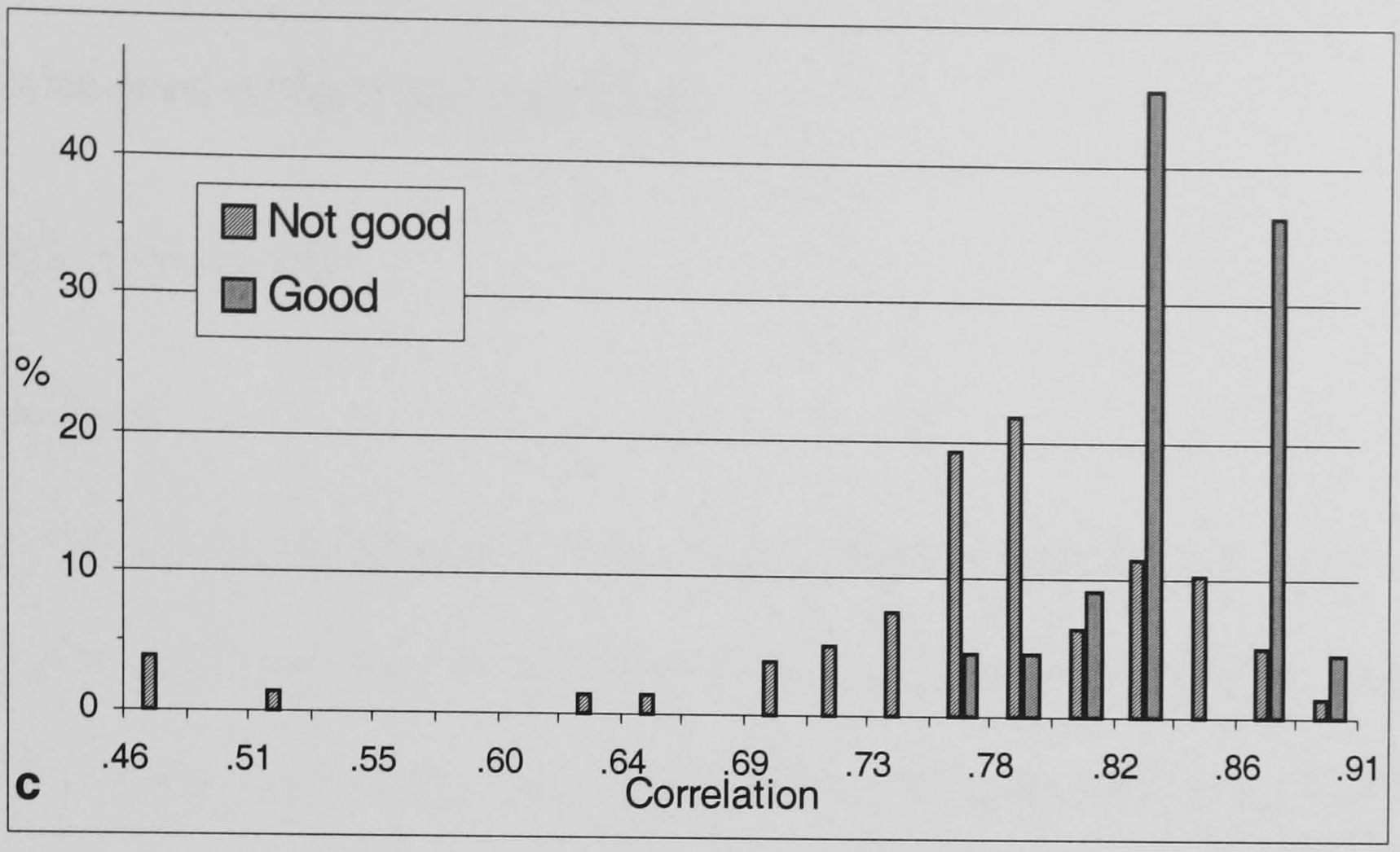

Figure 5.15 The distribution of template-correlations for good and bad graphics for test B

5.6 Summary

1 The IPPdiagnosis system using a linear correlation algorithm (LCA) correctly identified the printing error in 85-90% of laboratory specimens, but was unacceptably slow. Artificial neural networks gave interesting results when they replaced parts of the LCA.

2 The IPPimage program was reworked in Visual Basic to reduce development time and aid maintainability. Tests of image acquisition and processing on real specimens demonstrated that good and bad graphics can be successfully partitioned – a '*redlight*' alerts the operator to erroneous prints. False positives occurred in approximately 8% of cases with a small sample set. Allowing for the low-specification hardware used in the tests IPPimage performed too slowly.

Example images of faults, with their 'inverted ghosts' are in Appendix I.

6 The cliché-pad-substrate interface

6.1 Graphic distortion

6.1.1 Introduction

Pad printing requires the deformation of a silicon rubber applicator, first onto a flat cliché to pick-up ink then onto a substrate which may be flat or curved to deposit the ink. The pattern of ink should appear undistorted and free from errors upon being to transferred to the substrate. However, at the start of the project if the substrate was intricately shaped, contained small radius curves (for example 15mm) or was deformable then there was always some distortion. Much of the literature related to pad printing does not deal with the fundamental process and so does not discuss this aspect [Slade, 1997] [Truchetet *et al*, 1997]. Two papers deal with graphic distortion, albeit qualitatively [Scher, 1997] [Kiddell, 199#].

Kiddell discusses the importance of selecting the correct printing pad, and points out that the pad hardness is usually controlled by the proportion of silicon oil in the rubber. The shape of the pad is singled out as the most important factor in maintaining printing quality. The correct shape is said to produce a "rolling" action so that air is not trapped either during ink pickup on the cliché or release on the substrate. It is implied that this rolling action involves contact between the pad and a surface starting at the centre and working out, and is rolling as opposed to sliding. The printing surface of the pad should not be flat, but neither should it be too pointed. Similarly, the pad should not be so small that the graphic lies close to its edge, nor too large for a particular application. In general minimal force should be applied to totally transfer the print as a larger force leads to distortion. Two common pad shapes are round with a curved conical head, shown in Figure 6.1 and rectangular with a rounded pyramid. Pads

based on these forms are used for the majority of printing, and although customised shapes are produced it is not economical for a factory to use many.

Kiddell describes the "last resort" as *pre-distorting* the cliché image to compensate, but Scher accepts it is inevitable that distortion will occur when pad printing on curved products [Scher, 1997] [Kiddell, 199#]. If a line is to be straight after pad printing but is found to "smile" it can be pre-distorted such that a "frown" on the cliché produces the desired linear effect.

Various methods are given to produce the compensatory distortion of which the first is using three-dimensional graphics software [Scher, 1997]. Some packages are suited to modelling graphics on curved surfaces and apparently calculate stresses and strains. However, as will be demonstrated, rubber printing pads are complex non-linear solids suited to finite element analysis, and the literature makes no reference to the use of FEA. Another method is *grid pattern matching* where a standard grid is printed and the result is used to calculate pre-distortion. Trial and error printing with the desired graphic can be performed and metrology used to find the distortion. Finally, the image may be divided up with each segment being printed individually, though this needs substantial planning and is often not practical on a production line.

It can be seen that distortion is a significant problem. It is preferable to use one of a standard range of pads and find some way to pre-distort the cliché image, which must already be unique to a graphic and substrate. The work presented here uses finite element analysis to model the

interaction between a pad, cliché and substrate in order to understand the pad printing process.

The results were used to investigate pre-distortion graphics.

To achieve this the objectives were to:

1. Investigate the behaviour of the rubber by measuring its deformation characteristics and material properties

2. Produce a Finite Element Model of a printing pad and simulate deformation against flat and curved surfaces

3. Test the correlation between the computer model and physical data from pad tests

4. Use the model to calculate the distortion of a graphic during the printing process

5. Develop a method for pre-deforming the cliché so that the print shows minimum distortion

Research was carried out at the University of Birmingham [Morison *et al*, 1998].

6.2 Finite Element Modelling applied to pad printing

6.2.1 Material tests

Silicon rubber is an elastomer which exhibits non-linear visco-elastic behaviour. Having low rigidity it undergoes larger strains than many materials (20-50% strain in compression or shear) and its stress-strain relationship is more complex, for example the shear modulus varies with strain. As it is generally not possible to characterise rubbers by a unique combination of moduli the modelling and design of rubber products requires the choice of a suitable strain-energy function containing the correct constants.

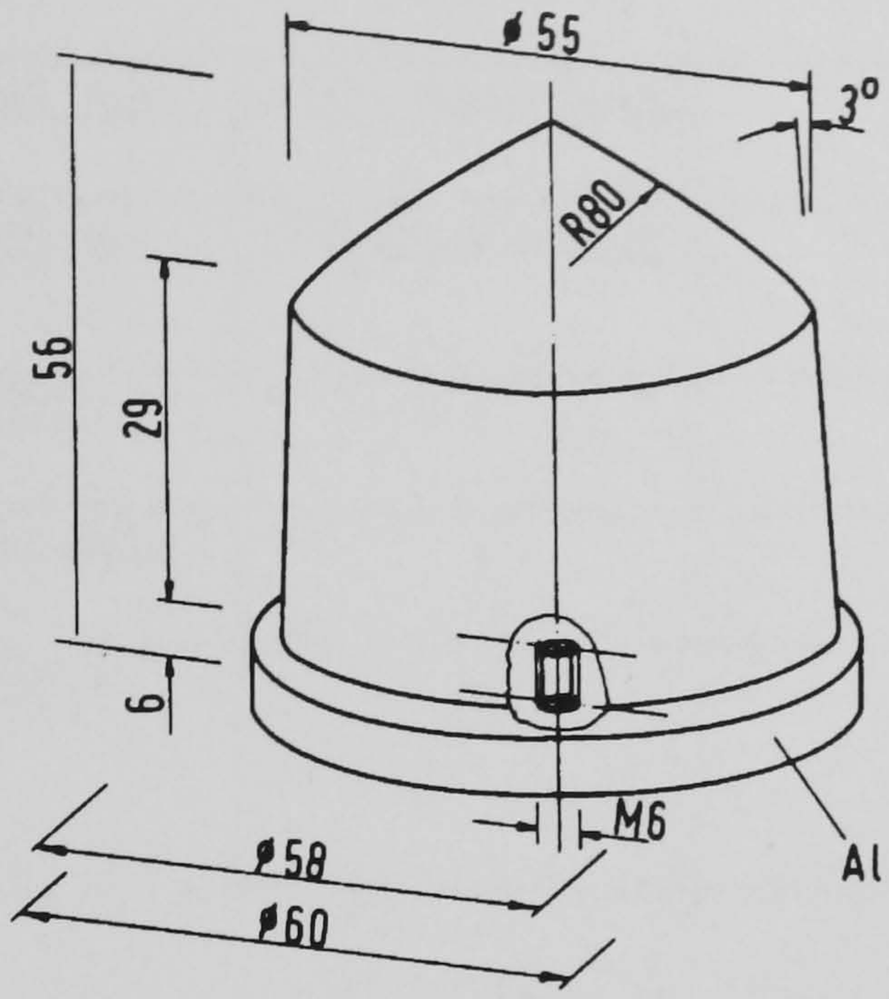

Figure 6.1Tampoprint's '410' pad [Tampoprint, 1996]

Testing procedures have been developed which produce non-linear data for many different loading conditions Uni-axial tension and compression, simple shear and volumetric tests were chosen in this case and they were performed on a Lloyd Instruments material testing machine using a 1kN load-cell. [MARC, 1997]. Rubber can be described by its indentation hardness as measured by a Shore A-type durometer and its quality, Q, which denotes to what applications it is suited. 0 Shore corresponds to the full protrusion of 2.50 +- 0.04mm (a soft rubber) of the indentor beyond the pressure foot (the base) of the meter and 100 Shore for no protrusion (glass) [BSI, 1989]. Tampoprint combines numbers representing hardness and quality with a mould number to identify a specific design of printing pad (Appendix II). Four permutations of silicon rubber were tested from 6 and 12 Shore, and qualities 1 and 3. All tests were performed at room temperature with a cross-head speed of 5.08 mm/ minute.

Table 6.1 Material test conditions

	Test sample size, mm	Cross-head speed		Other
Tension	ASTM Die C dumb-bell	5.08mm/ minute		–
Compression	dia. 17.8 x 25.3(T)	"		2 pre-conditioning cycles
Simple shear	40(L) x 16(W) x 5(T)	"		–
Volumetric	dia. 17.8 x 25.3(T)	"		Silicone oil lubricant, 3 pre-conditioning cycles (aim: 25% deflection)

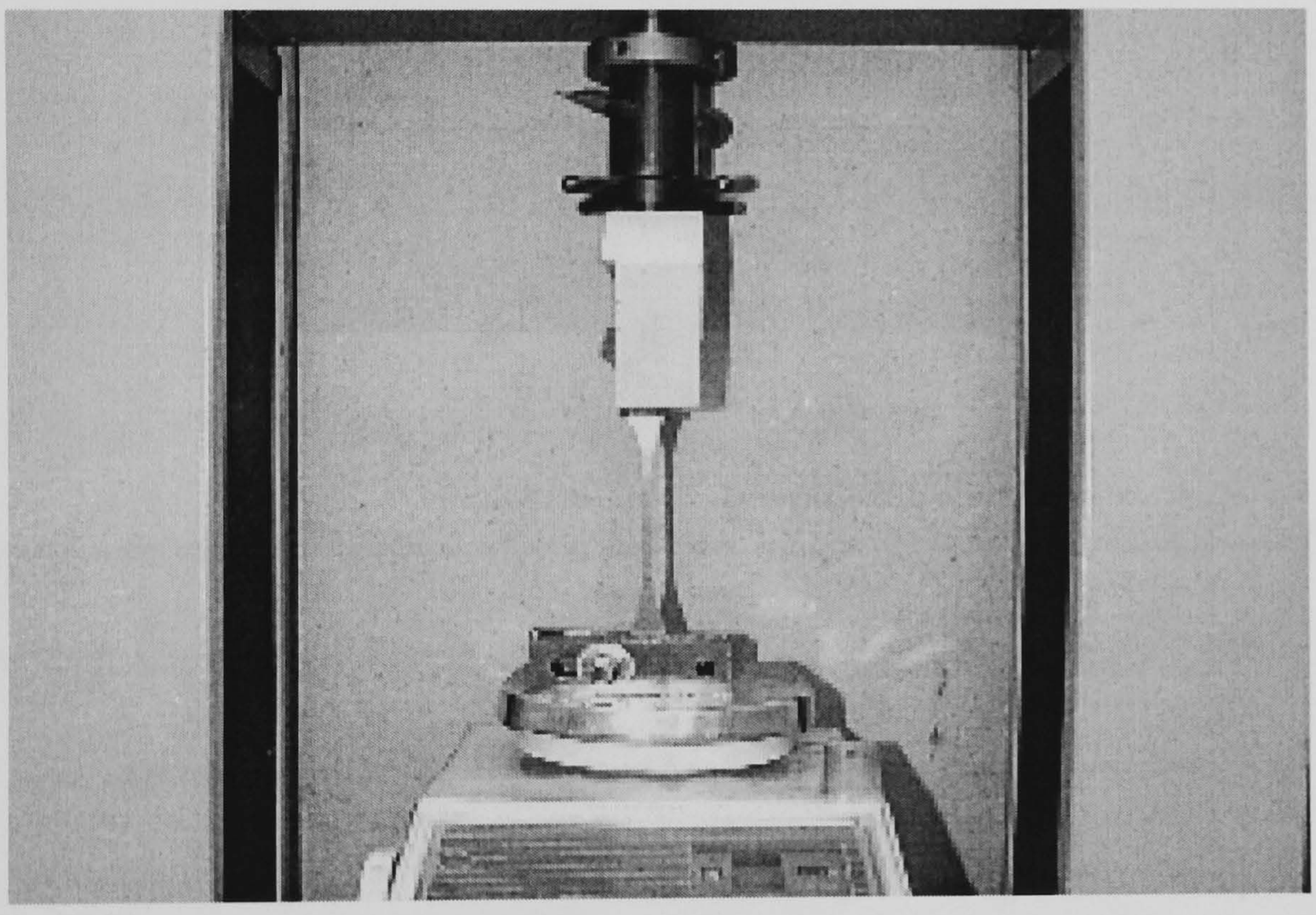

Figure 6.2 A silicon rubber sample undergoing uni-axial tension.

The uni-axial tension test setup is shown in Figure 6.2 and the quad-lap rig containing 4 equally dimensioned rubber samples is shown in Figure 6.3 (a). Using an alternative load-cell the volumetric test used a die-set like that shown in Figure 6.3 (b). This resulted in the samples being crushed in the die (Figure 6.4) at 10kN with only 5% strain. The conclusion was that the rubbers under test were virtually incompressible and this test was discontinued.

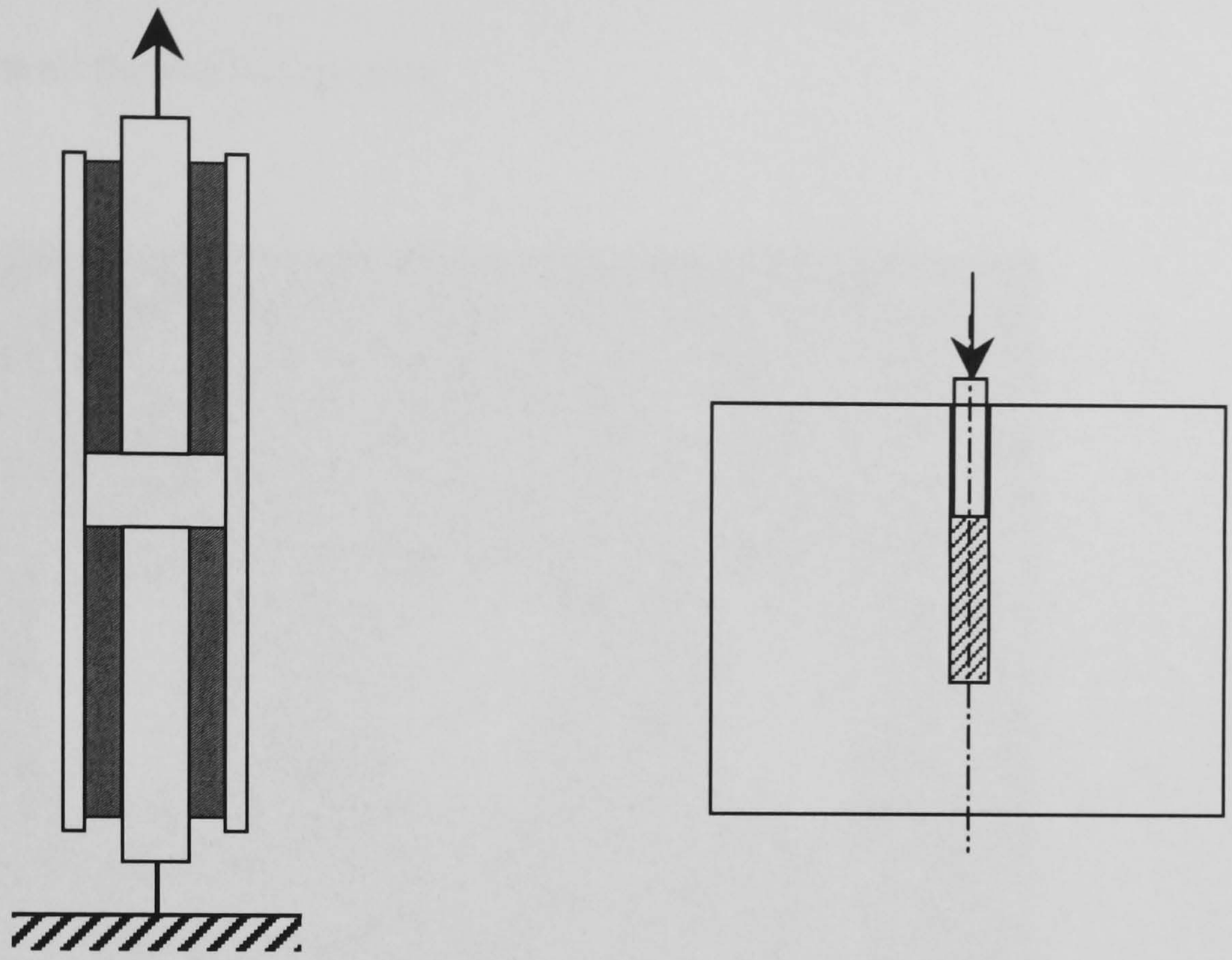

Figure 6.3 Quad lap shear test specimen and die set for volumetric compression tests.

6.2.2 Curve fitting and the initial Finite Element model

The non-linear finite element software MARC and its pre and post-processor MENTAT were used to model the pad printing process. It contains a curve-fitting program, and using the compression and shear test-data the constants were obtained for the Mooney-Rivlin (two and three term), Signorini, 3rd order, 4th order and Ogden strain-energy functions (Table 6.2). Finite element models of the tension, compression and shear material tests were set up using regular two-dimensional meshes and the different sets of constants were tried. As MARC states, the Mooney model contains the assumption that the material is incompressible (isochoric) whereas the Ogden model implies that the elastomer is compressible [MARC, 1997]. As it has already been demonstrated that the silicon rubbers were incompressible the Mooney model was favoured. Displacement-load graphs for the different rubbers show that the closest correlation between the tests and their models was when using the two-term

Mooney constants C_{10} = 0.02805 MPa and C_{01} = 0.010912 MPa for the Q3 i5 6 Shore rubber, and these were used in all the following tests.

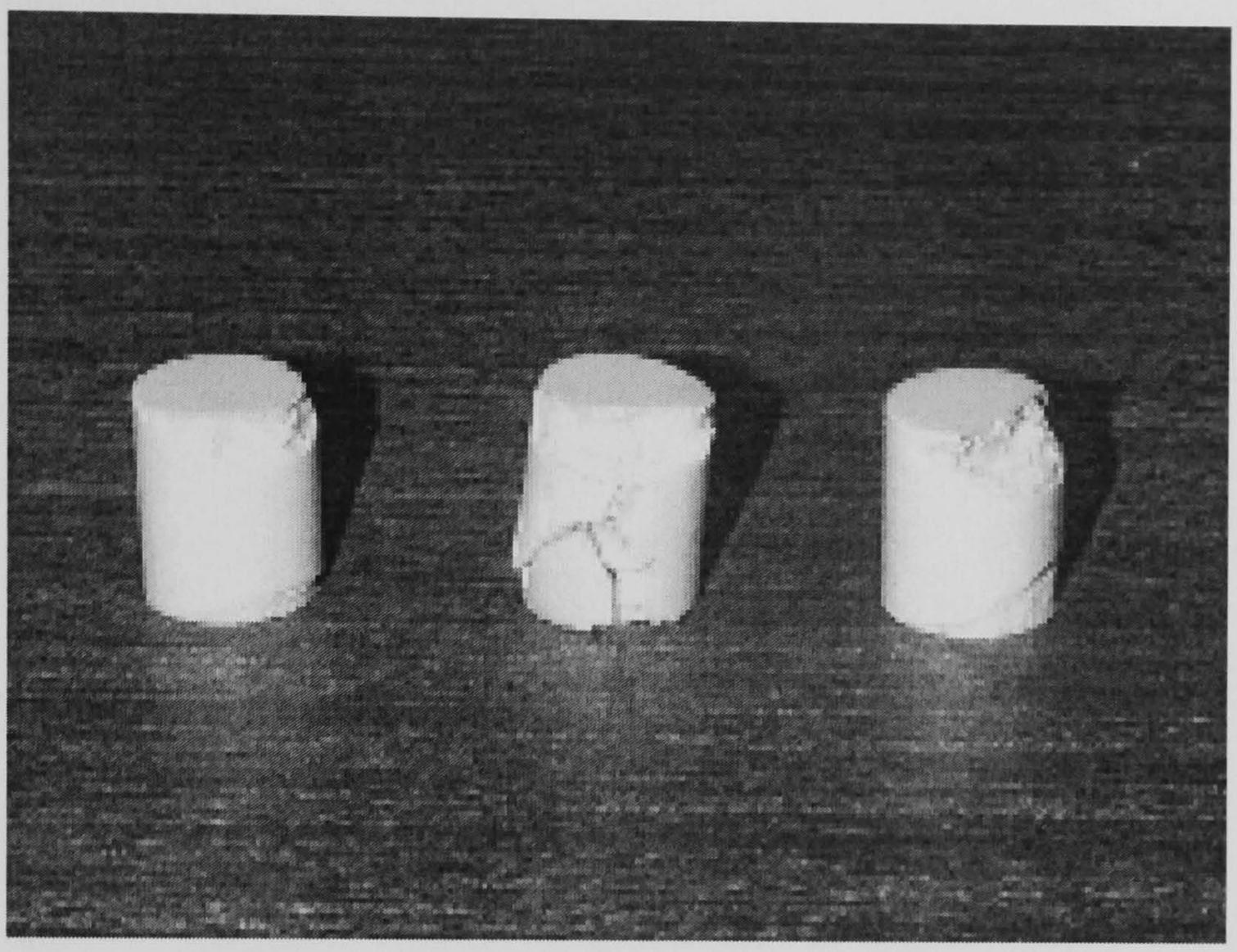

Figure 6.4 Crushed silicon rubber samples following volumetric testing – demonstrating incompressibility.

Table 6.2 Mooney-Rivlin, Signorini, 3rd order and 4th order constants for rubber Q3i5 6 shore.

Model	C_{10} (MPa)	C_{01} (MPa)	C_{11} (MPa)	C_{20} (MPa)	C_{30} (MPa)
Mooney(2)	0.02805	0.010912			
Mooney(3)	0.04016	-2.031E-4	0.00134		
Signorini	0.040813	-0.002236		0.004531	
3rd Order	0.0344022	0.0067123	0.00230805	-0.0051454	
4th Order	0.025788	0.014135	-0.011822	0.010539	0.00389

Table 6.3 Ogden constants for rubber Q3i5 6 shore.

	Term 1	Term 2	Bulk Modulus
Moduli (MPa)	0.596225	-0.00212398	0.158149E+6

Alpha	2.52216	-3.65901	

Thus far the pad used in printing had been considered a static system, when it could be modelled as a mass-spring-damper dynamic system. Two simulations of the rubber samples were run with the rate of pad compression two orders of magnitude apart and with all other parameters the same. A comparison of the load-displacement graphs for these models showed little difference in their shape, so that modelling the system as static can be considered a good approximation.

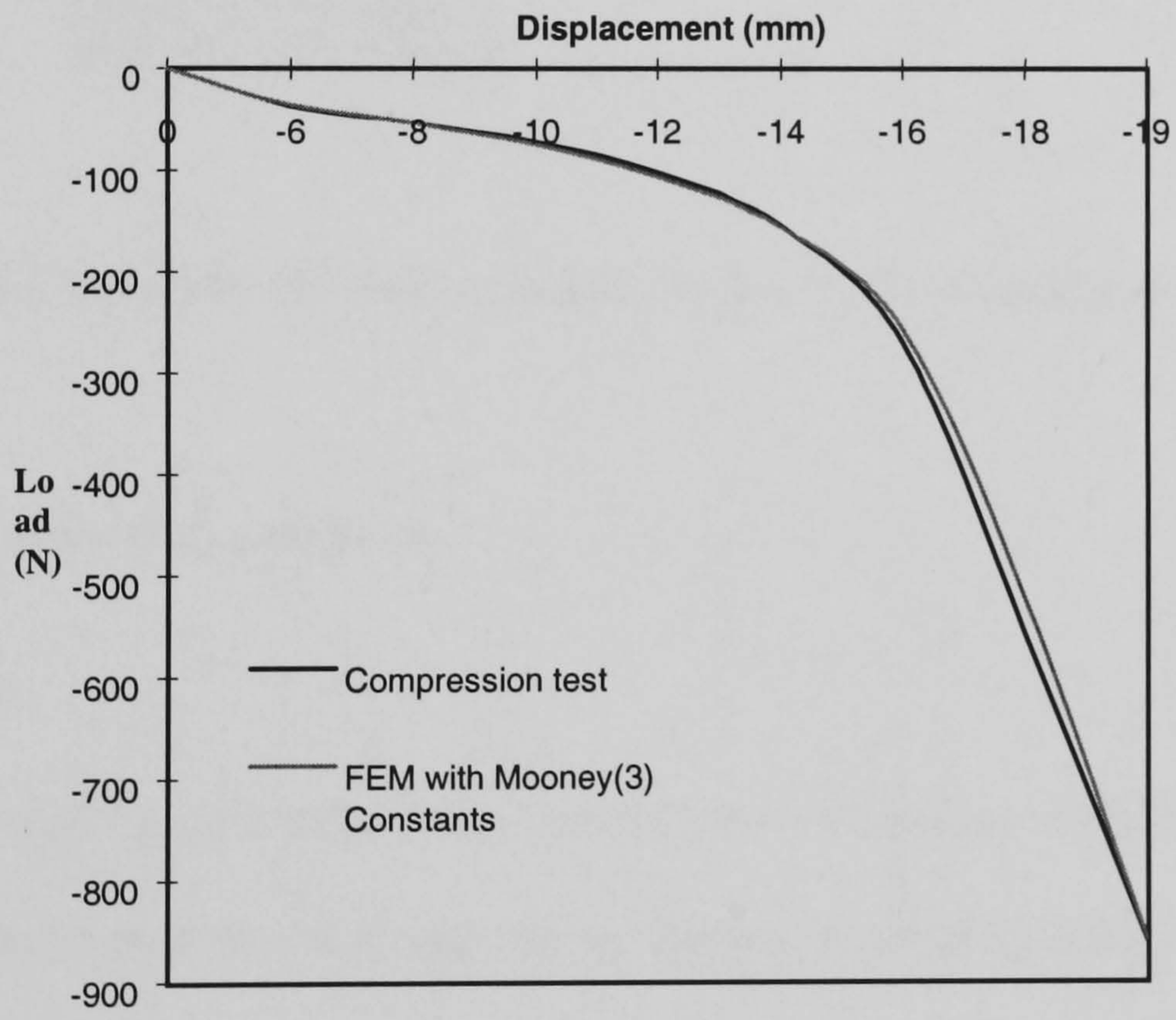

Figure 6.5 The load-displacement graph for the compression test and its FEM model for the Q3 i 12 Shore rubber.

The initial model of a printing pad (Model I) employed an axis-symmetric conical pad-geometry denoted '410' and with the material properties above the notation from Tampoprint is 07–4–410. By utilising the geometry in the pad to reduce the number of elements a two-dimensional model was produced representing half the pad's cross-section. Its elements were constrained horizontally (radially) along the x-axis on the left and vertically (axially) along the

base. A flat horizontal rigid surface was defined to represent the cliché or substrate and this moved down during modelling to represent the printing process.

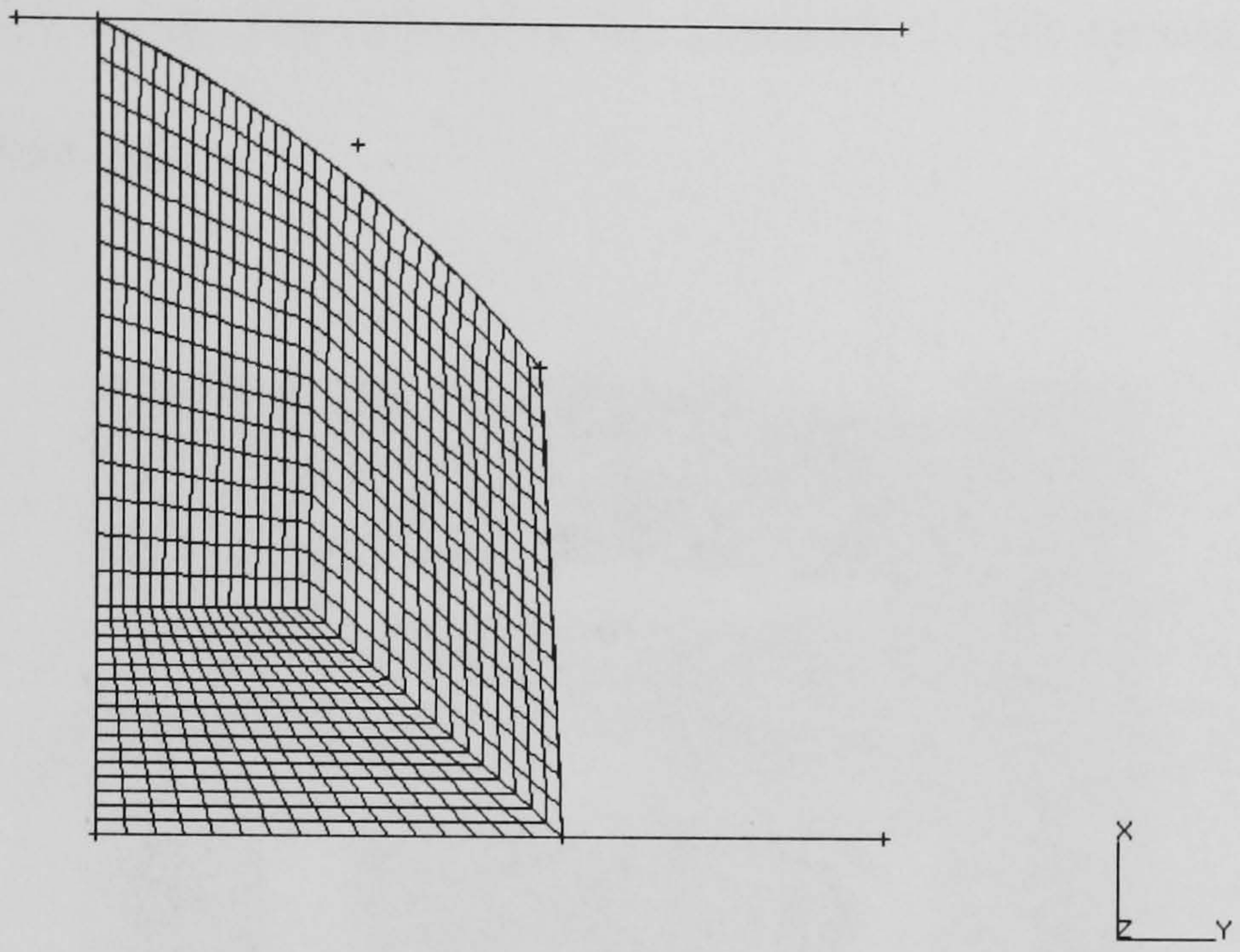

Figure 6.6 Initial 2D mesh representing the '410' printing pad.

6.2.3 Correlation of data with pad tests

6.2.3.1 LiMMS test

Pad-tests were performed for correlation with finite element analysis and as feasibility studies. The first tests were performed on the Linear Motor Motion System (LiMMS) at Philips CFT. This is an experimental machine which can simulate the motions of the Tampoprint '*hermetic 61'* closed-cup printer. The pad and cliché are moved by computer-controlled linear motors, which means that the time-displacement curves used can be widely adjusted. The purpose of the LiMMS or 'footprint' tests was to measure the size of a sample image on a flat substrate under a range of loads [Freear, Li and Shippen, 1997]. The pad used was a type 07-4-410 to match the finite element model. LIMMS accurately controlled the displacement but not the load on the pad during printing, and the Lloyd material-testing machine was used to measure

the load on the pad at the different displacements. The mean graphic-diameters (read from a Carl Zeis/ Jena MP320 measuring projector) and load for the tests and the model were plotted against displacement. The graph from first-pass Finite element modelling with 192 elements consisted of a stepped curve, but increasing the elements to 768 elements produced a close correlation with the test-data.

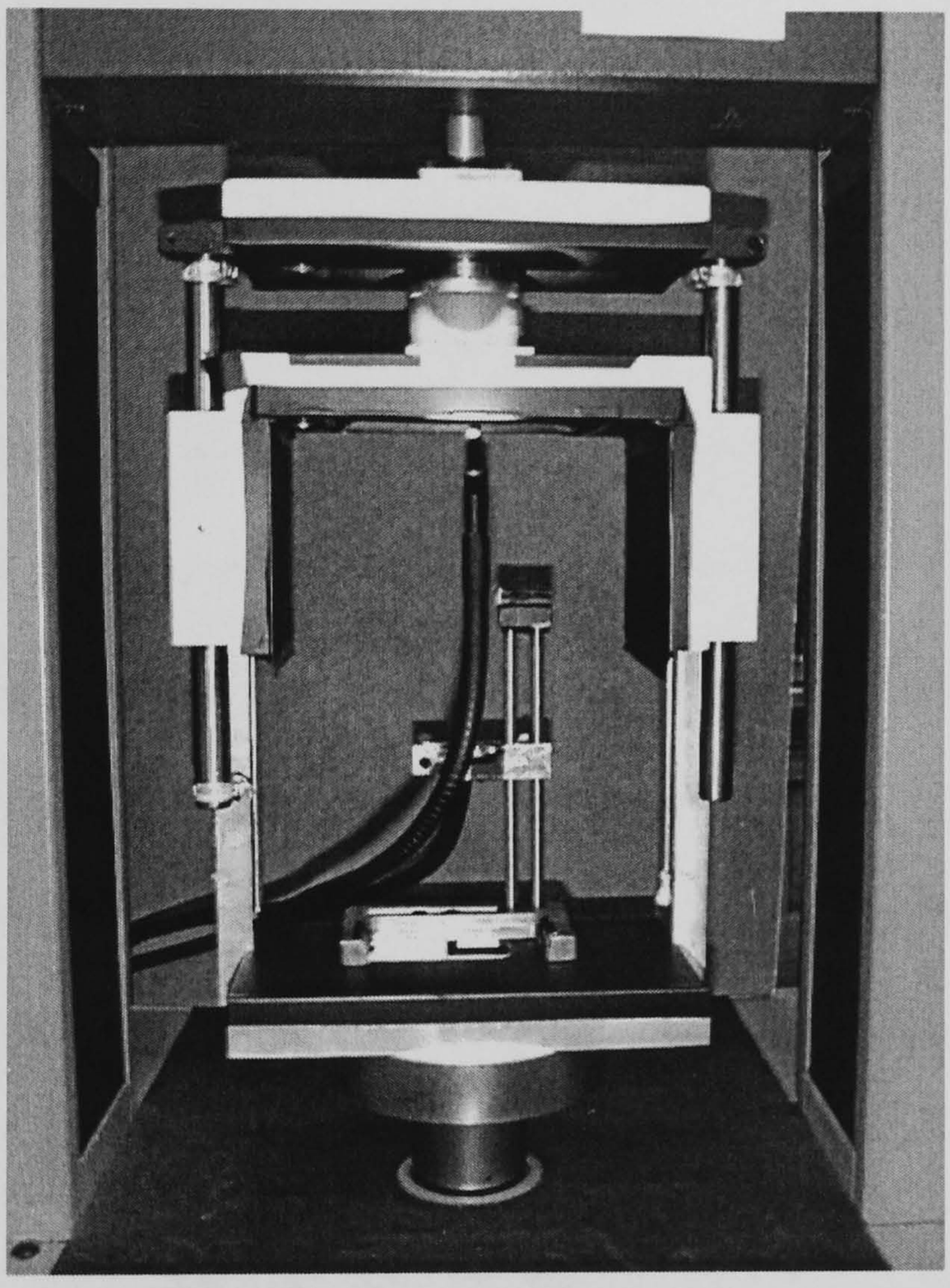

Figure 6.7 The photographic test-rig (camera not shown)

6.2.4 Photographic test

Having simulated and measured the size of the graphic for a pad displacement, we wished to measure the deformation of a pad under load. This lead to photographic tests on a conical 07-4-492 pad laser etched with a 1mm square grid. A die-set shown in Figure 6.7 was produced incorporating linear bearings and it can be free standing or placed within a material-testing

machine which controls the motion and measures the load. The rig contains a glass window which acts as a substrate with the pad being compressed against it on one side and the camera and light-source on the other. A Kodak DC120 digital still camera was used with +1, +2 and +4 close-up lens. The preliminary results were encouraging and the technique can be used to find the distortion of the printing pad, but only on a flat substrate.

6.2.5 Endurance test

The life of printing pads during production is unknown, and uncertainty about when pad-wear affects quality leads to subjective decisions regarding when a pad is discarded. However as the quality of printing depends on many factors, directly measuring quality using the methods discussed later without closely controlling the process would not provide meaningful data. This resulted in endurance tests, the object of which was to measure the life of a pad of a specific hardness, quality and geometry and to determine the area of maximum wear. Wear was taken as the reduction in depth of a grid or mesh laser etched on the pad due to removal of rubber, which is analogous to the reduction in depth of a tread on a tyre with use.

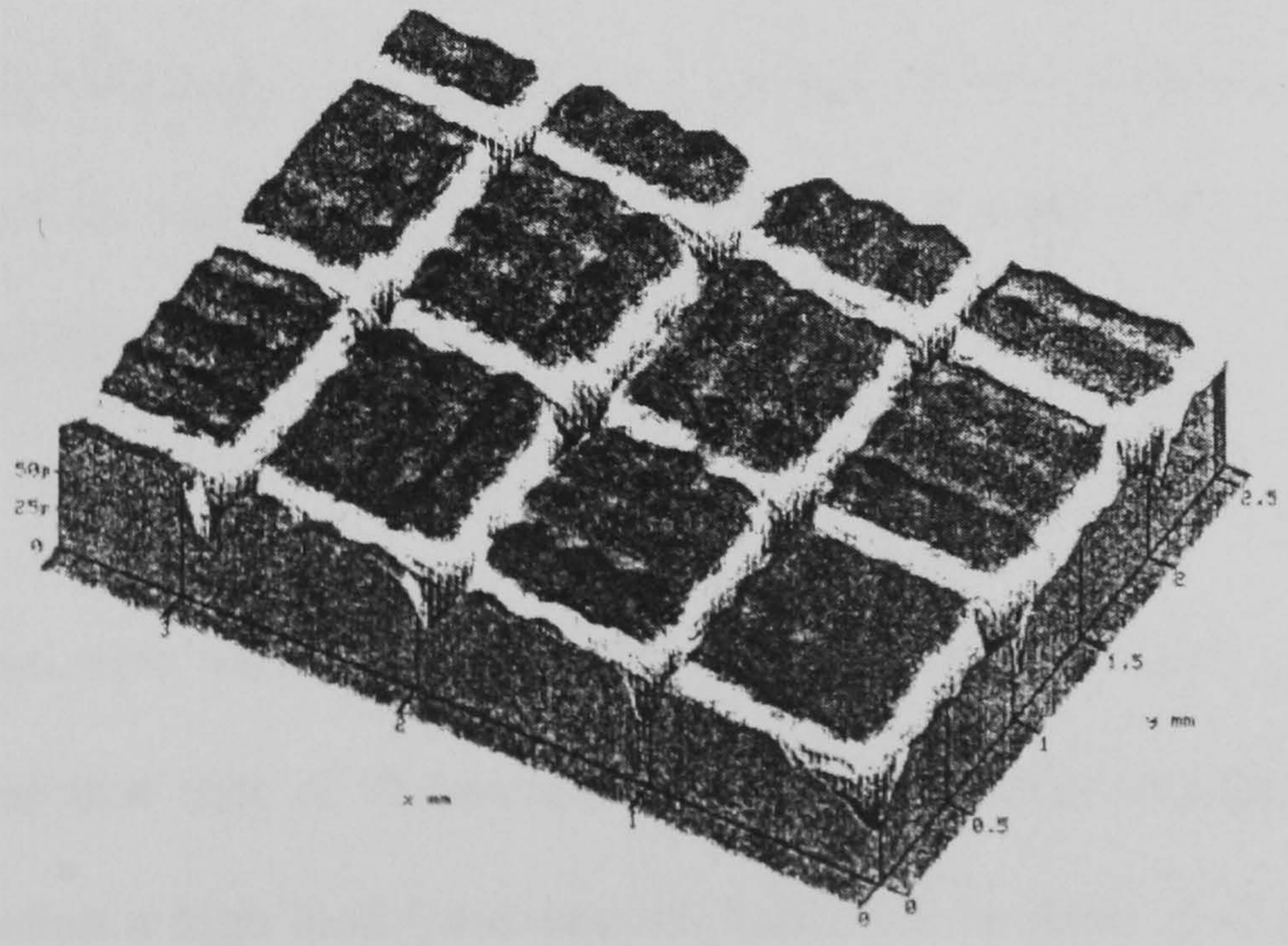

Figure 6.8 The topography of part of a printing pad after endurance testing.

The rig comprised an electromechanical counter recording the number of cycles performed by a pneumatic ram acting with a constant maximum pressure. The quality of the surface against which the pad was deformed and presence of ink was significant. For the feasibility study a smooth flat plate was used to imitate both the cliché and substrate in dry conditions, with a 08-5-048 pad which was rectangular and had a hardness of 12 Shore. (Where the substrate is flat, wear was thought to be the result of deformation against the etched cliché.)

The surface topography of the pad can be measured using three-dimensional surface measurement where parallel two-dimensional profiles of a surface are taken at intervals of several microns. This relatively recent technique was developed to overcome the disadvantages of two-dimensional stylus profilometry (measuring a surface with a 'needle').

However the vertical range of the instruments available was insufficient to cope with the curvature of the contact surface of the pad, the size of the stylus tip does not provide significant error in the 'valleys' or grid, and the deflection of the pad did not conform to the readings. This last problem lead to replication of the pad surface using Technovit 3040, a two-part acrylic resin, with the benefits that the test can continue after a brief pause and a permanent record of the pad wear exists.

After 6000 cycles no wear was visible on the pad surface: and there was no debris in the test-rig. This suggested that tens of thousands of cycles were required before significant wear takes place, even when a high load (in excess of 3kN) was applied. In Figure 6.8 after 2000

cycles the laser-etched mesh is visible but wear is not. At this trial stage a greater number of cycles was not undertaken.

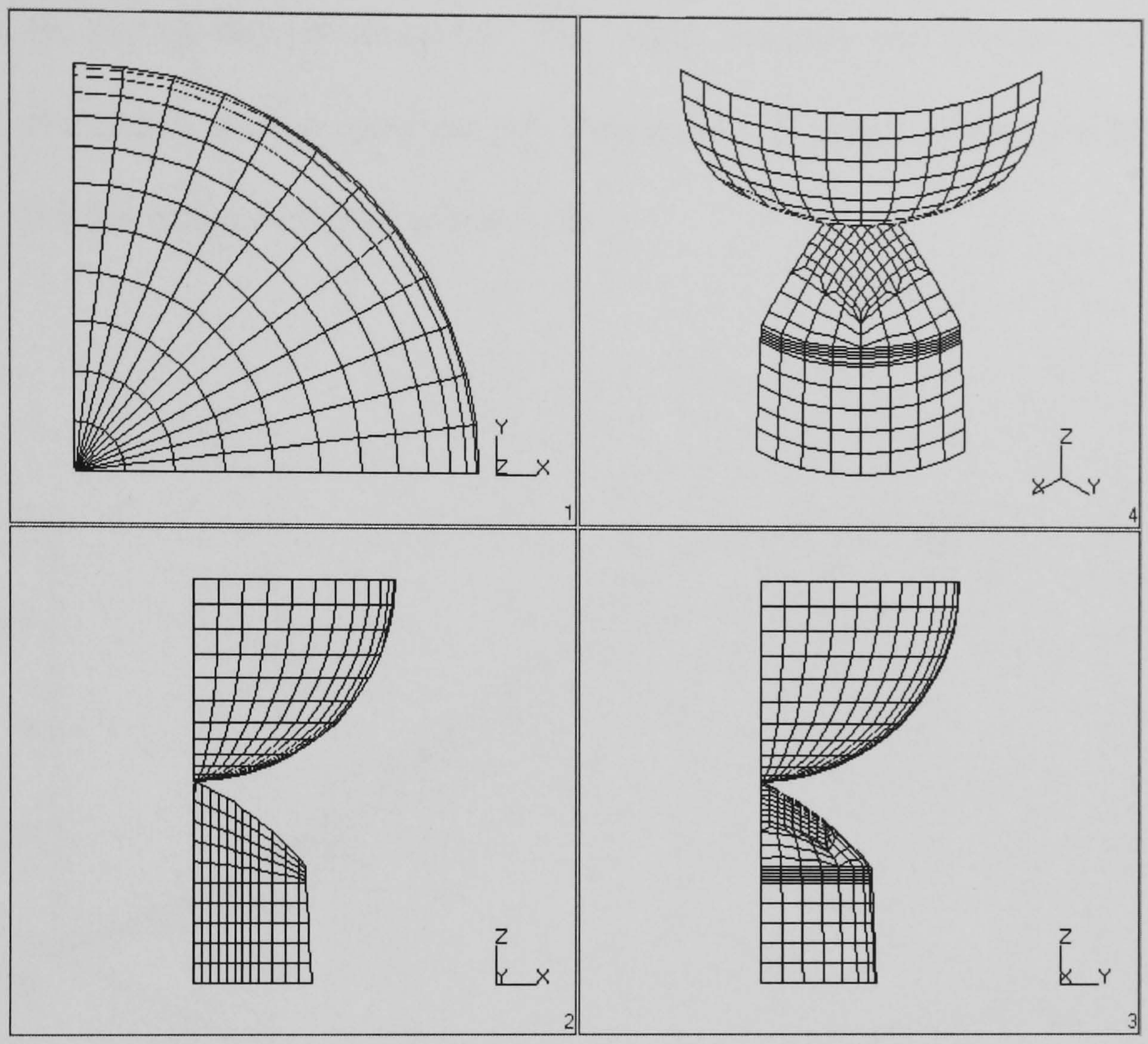

Figure 6.9 3-dimensional models of the '410' printing pad (Model II a,b), and the spherical surface.

6.3 Flat, spherical and saddle surfaces

6.3.1 Development of 3-dimensional meshs

Having demonstrated the feasibility of finite element modelling and the accuracy of the material parameters the next stage was to use the method to model deformation of a printing pad against curved surfaces. The surfaces chosen were a convex hemisphere and a saddle surface. The saddle surface was an area of a paraboloid defined by the equation:

$$z = sin(x \,.\, \pi/n) - sin(y \,.\, \pi/m) \qquad (1)$$

where x and y are coordinates on a plane perpendicular to the principal axis which is perpendicular to the surface through its centre. The '*sadl2*' function was written in MATLAB to generate part of a saddle surface using the equation above. Figure 6.10 shows a MATLAB mesh produced with the shape constants $m = n = 50$.

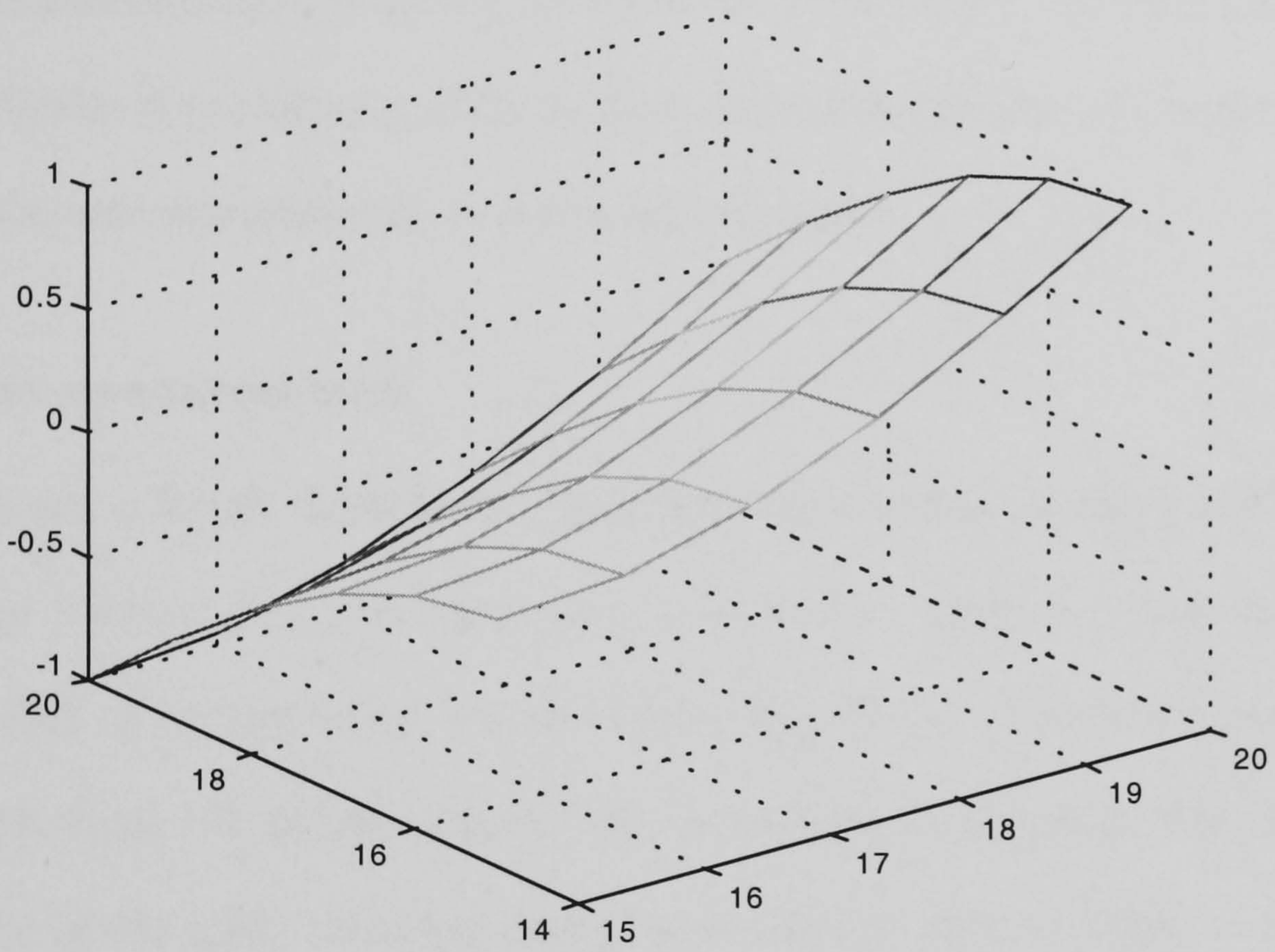

Figure 6.10 Example of a saddle surface created in MATLAB and used in FEA modelling.

A 07-4-410 pad was again modelled, but as the saddle surface is not symmetrical along both lateral axes the model needed to be three-dimensional. In order to minimise the number of elements a quarter of the pad was modelled and the corresponding quarters of the hemispherical and saddle substrates were defined. The initial three-dimensional mesh was formed of incompressible hexi-hedral elements each having eight nodes. The lower portion of the pad is an undistorted mesh, while the upper area is quite distorted. Looking down the

pad's axis the circumference is uniformly segmented. An alternative was developed with the lower part as before, but more finely divided towards the top. Looking down the pad's axis, the top region is a regular square mesh in the centre, married to segments which follow the circumference of the pad. The purpose of the square mesh on the printing surface was to directly produce distorted coordinates for a grid pattern.

The three-dimensional models predicted the distortion on the saddle and spherical substrates. Due to the difficulty of producing undistorted three-dimensional models of complex forms like printing pads the next step refined the two-dimensional model.

6.3.2 Distortion on a square mesh

Model 1 employed a simple automatically generated two-dimensional mesh, and was a good first attempt at a model of a pad which gave a satisfactory correlation with the pad tests. However the first refinement which was to increase the number of elements uniformly over the whole mesh (from 192 to 768) increased the computation time dramatically. Moreover in various regions of the mesh, including critical ones like the contact surface of the pad, the elements are distorted and this can lead to inaccuracies in the results.

LEGO provided a hemispherical plastic substrate with a radius of 15.71mm. Philips CFT produced distortion data for a grid comprising 1mm squares printed onto this substrate using a 410 pad. This can be modelled using the same type of two-dimensional mesh as used in Model I making it more straightforward to produce a good mesh and also with significantly reduced computation time compared with three-dimensional models used previously.

To generate the mesh, curves were used to define the outline of half the cross-section of the pad, based on dimensions in Tampoprint's catalogue [Tampoprint, 1996] [Morison, 1998]. The Mentat function '*Advancing front auto mesh*' was used to create the mesh with the curves divided into lengths of approximately 1.8mm. A greater number of nodes is necessary along the printing surface of the pad to model the distortion of the graphic due to printing, so each element in that area was divided into four. A transition region was then required between the areas containing coarse and fine meshes. The model used quadrilateral axis-symmetric solid elements throughout as required. Few of the elements were severely distorted and none of those were on the printing surface of the un-deformed model.

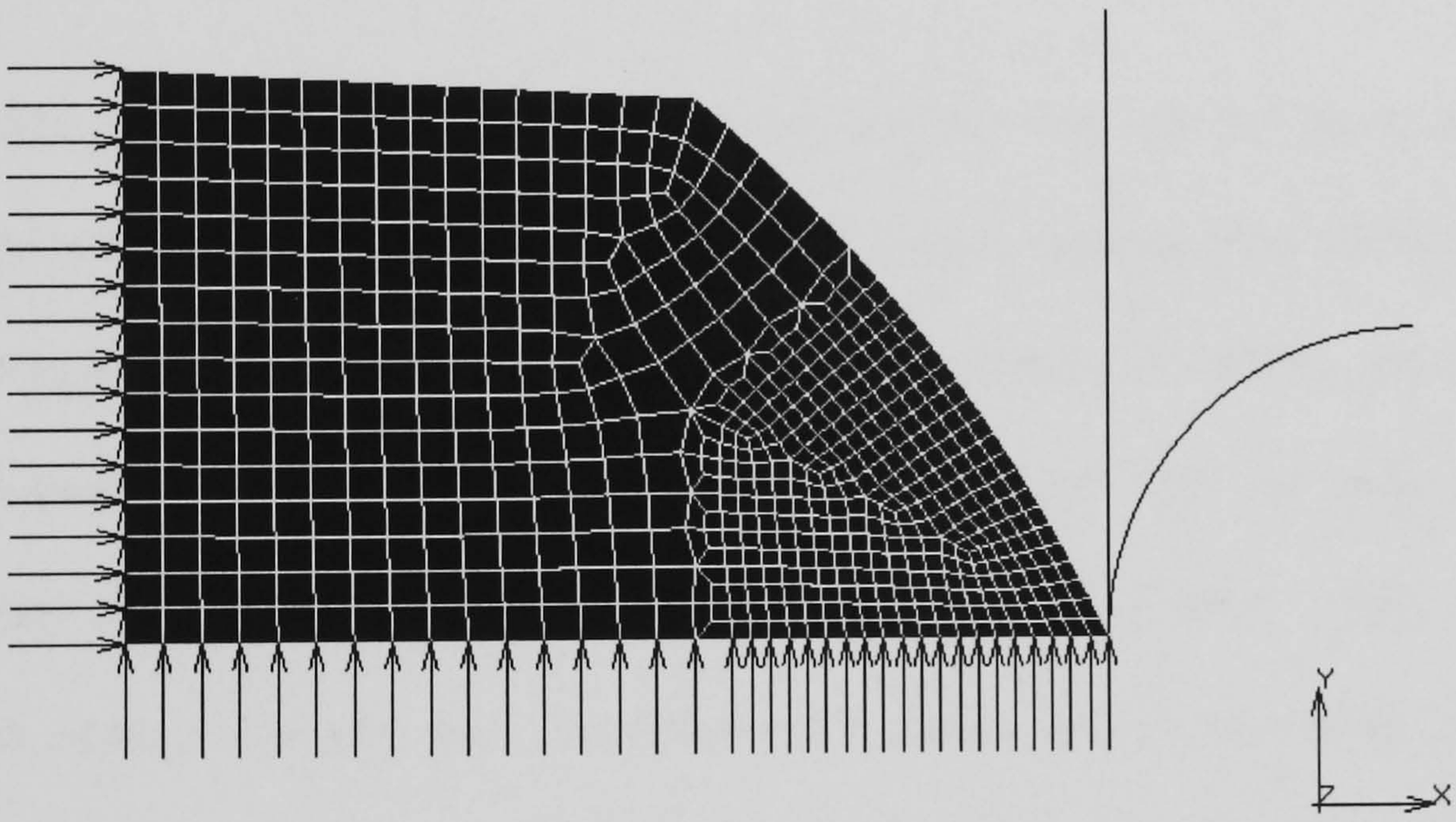

Figure 6.11 FEA model III of a '410' pad, showing boundary conditions and the two contact bodies. The fine mesh and transition region are evident near the contact surface.

The boundary conditions were applied as they had been in Model I. The nodes along the base of the pad were constrained longitudinally (x) and radially (laterally y). As required by the symmetry of the pad the nodes along the longitudinal (x) axis of the pad were free to move axially and constrained radially, as indicated by the arrows in Figure 6.11. As with previous models the two-term Mooney-Rivlin material constants C_{01} and C_{10} were employed.

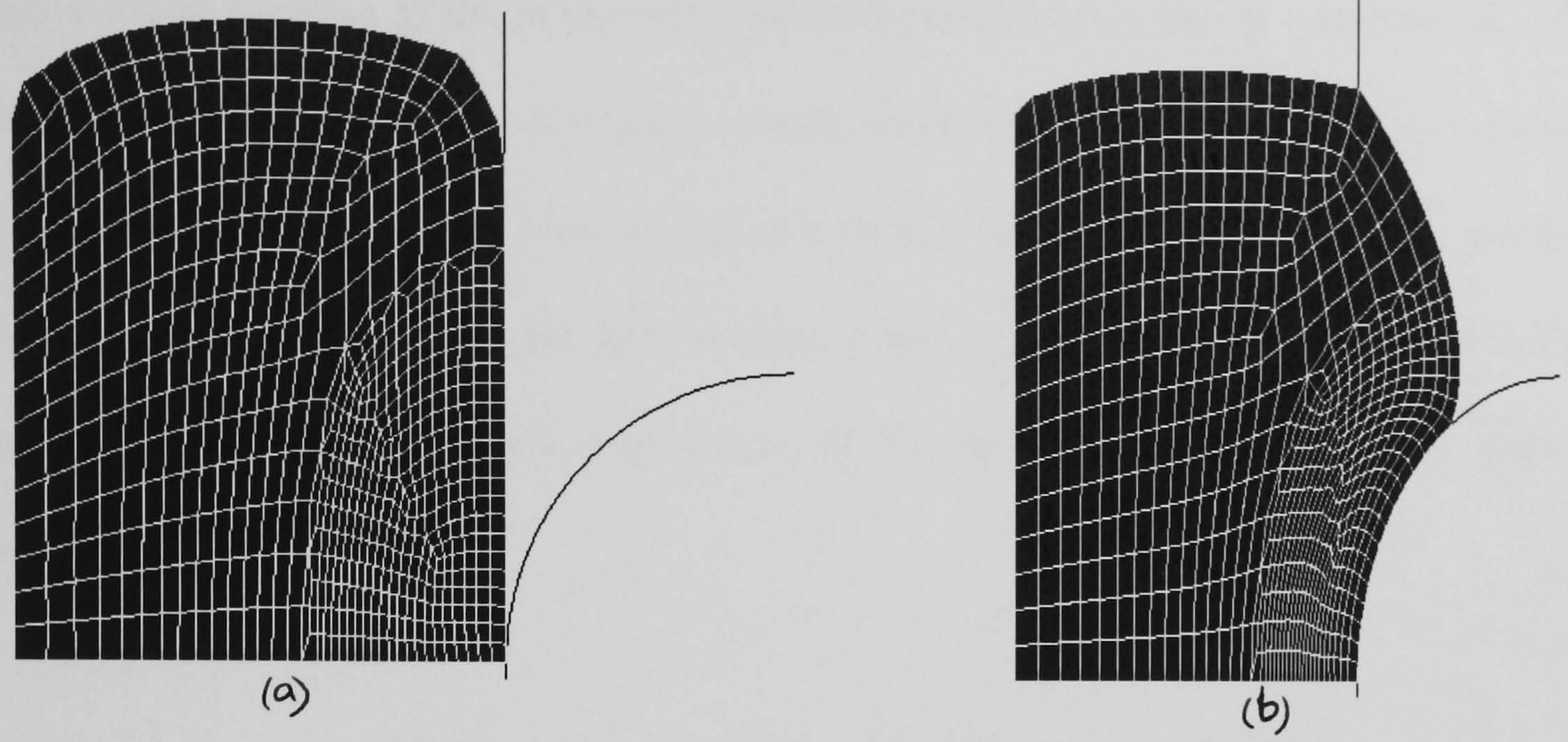

Figure 6.12 Model III compressed against a) the cliché and b) a spherical substrate.

MARC requires that the deformable body should be the first contact body defined. The second and third bodies defined were a rigid straight line to represent the cliché and a quarter of a circle to represent the substrate. Both were defined to move at –50m/s in the X direction. At each increment MARC tests if any nodes in the deformable body are encroaching on the rigid body they are prevented from moving during future increments. Two scenarios are defined in the same model and each is controlled by means of a contact table. In the second scenario the cliché replaces the substrate in the simulation. Each of the two load-cases specifies which boundary conditions are allowed, which contact table to use, and the type of solution, in this case static mechanical. Also defined are the test for convergence, and the length of time for the simulation (0.47s) which produced 23.5mm deflection of the pad onto the cliché and substrate. Fifty increments were specified and this was found to produce acceptable convergence in a reasonable time; more increments did not improve the accuracy of the results.

The final position of the nodes that contact the rigid bodies are significant, and if there was no change in radial position of the nodes when in contact with the substrate compared to when in contact with the cliché then no distortion would occur during printing. The files containing node numbers and co-ordinates were analysed by a MATLAB script and the data was entered in two matrices. Unless the nodes were in close proximity to the substrate, that is at a radius of approximately 15.71mm from the centre of the hemispherical rigid body, they were ignored.

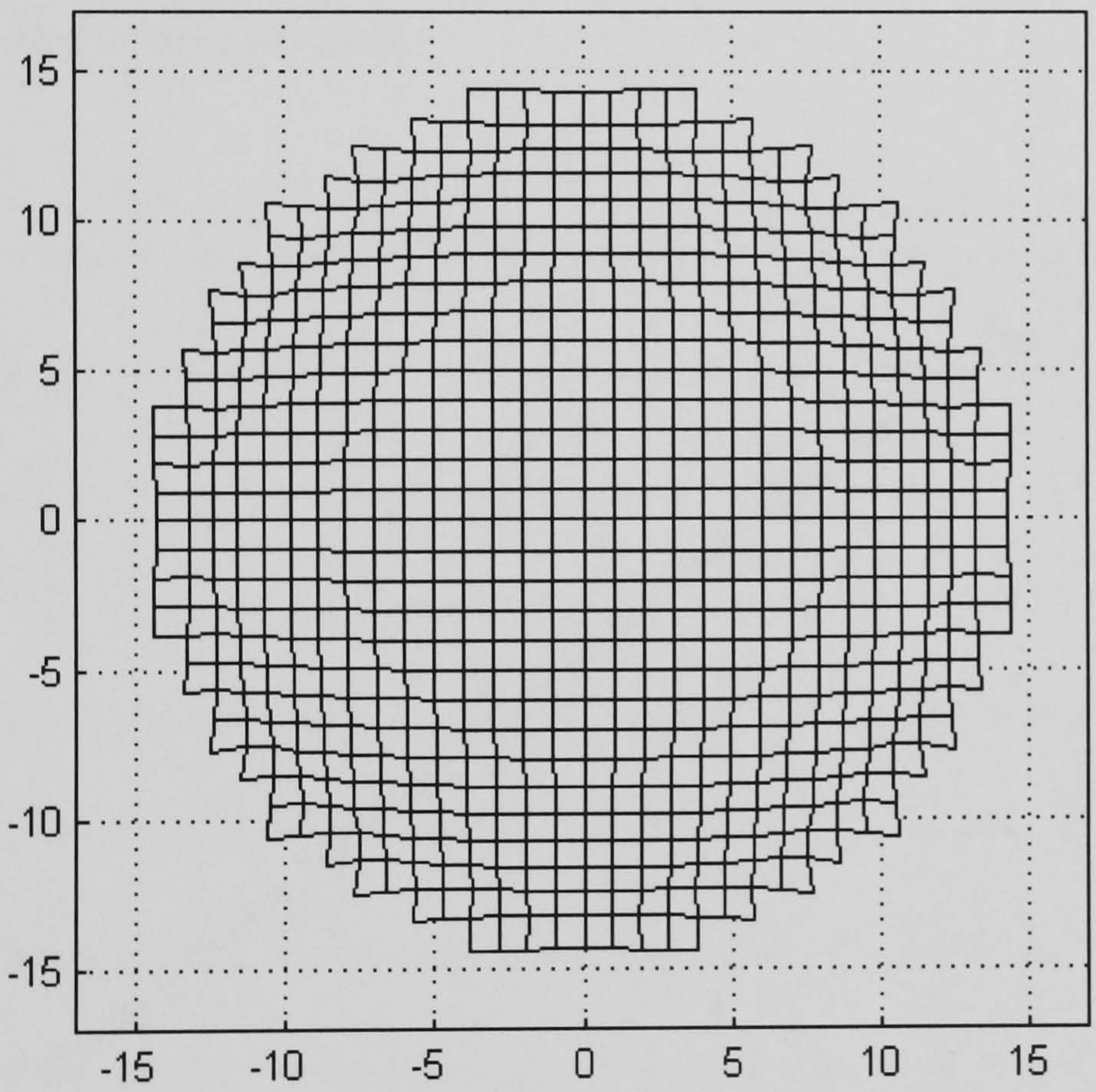

Figure 6.13 Distortion resulting from printing with a regular 1mm grid cliché on a convex spherical substrate.

6.3.3 Distortion transfer function

The MATLAB one-dimensional interpolation function '*interp1*' was used with the cubic spline method to produce a distortion transfer function. This was rotated into two dimensions by converting X and Y co-ordinates into radius and angle pairs. By calculating the new radius

after deformation of the mesh on the second rigid body the distortion of a grid of 1mm squares was found. Philips CFT produced physical data based on the mean of measurements in the positive and negative, X and Y directions. There was not a good correlation between the simulated 'no friction' data and the test data and the supposition was that this was due to a lack of friction. The analysis was re-run with 'glue' friction where nodes that contact the rigid body are locked in both directions until the end of the simulation. This 'infinite friction' makes a great difference as shown in Figure 6.15. Having simulated Coulomb friction with coefficients of zero and infinity, a coefficient of 4.5 was found to give the best correlation as judged from the overall shape of the data.

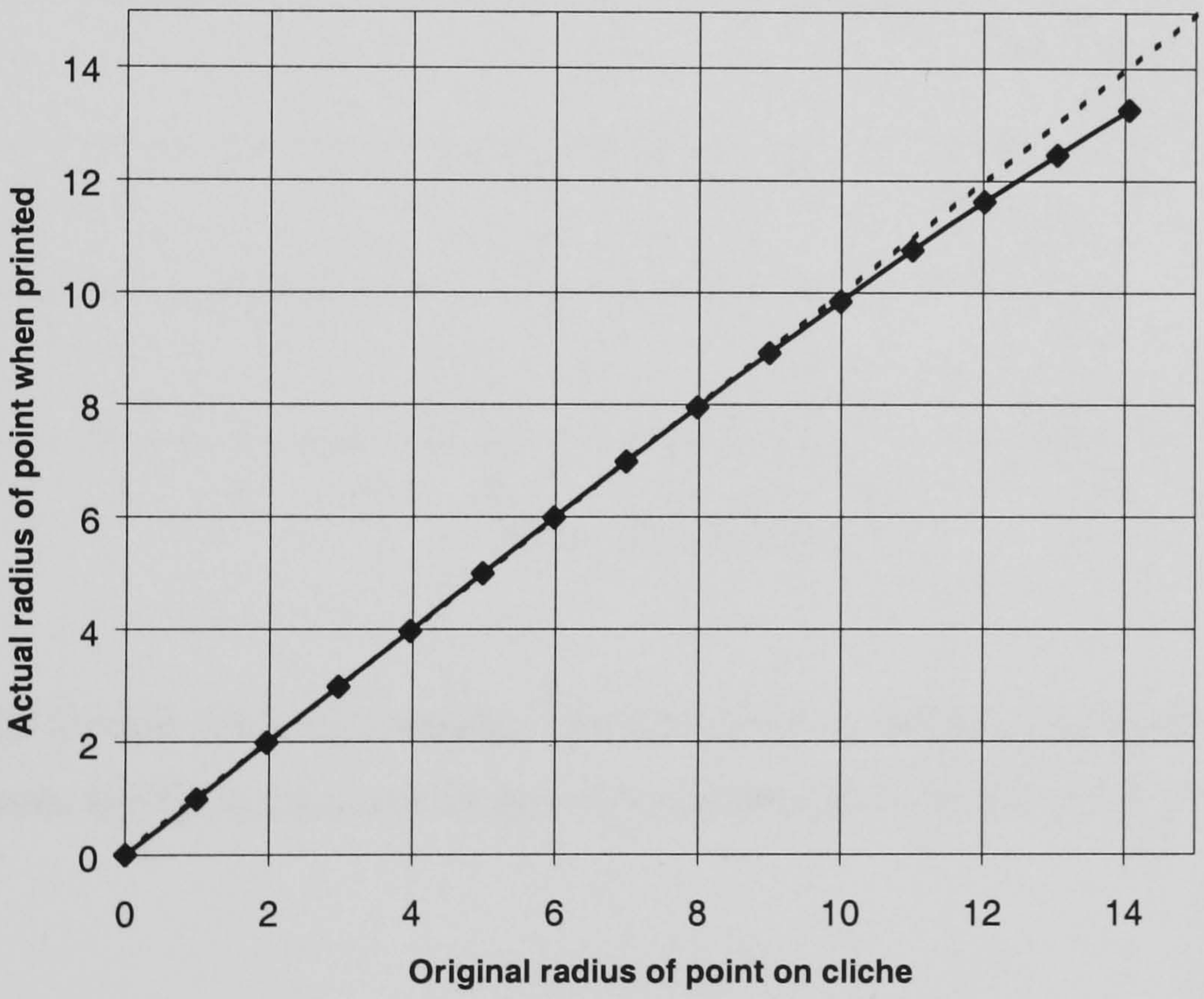

Figure 6.14 The *cliché-to-substrate* transfer function (units, mm).

The radial friction and reaction forces and nodal velocities were plotted for the duration of the simulation and Morison suggested that the uneven spacing of the co-ordinates was caused by *stick-slip* [Morison *et al*, 1998]. When a node in the model first contacts a surface the reaction and friction forces are zero. The node decelerates and sticks as the reaction and friction forces

rise, but simultaneously the internal stress behind that node rises rapidly as the material is virtually incompressible. When the internal stress reaches a threshold the node slips relieving the internal stress, and the node then sticks because of the friction. A cycle occupies hundredths of second and the process repeats with neighbouring nodes in contact with the rigid body oscillating out of phase with each other.

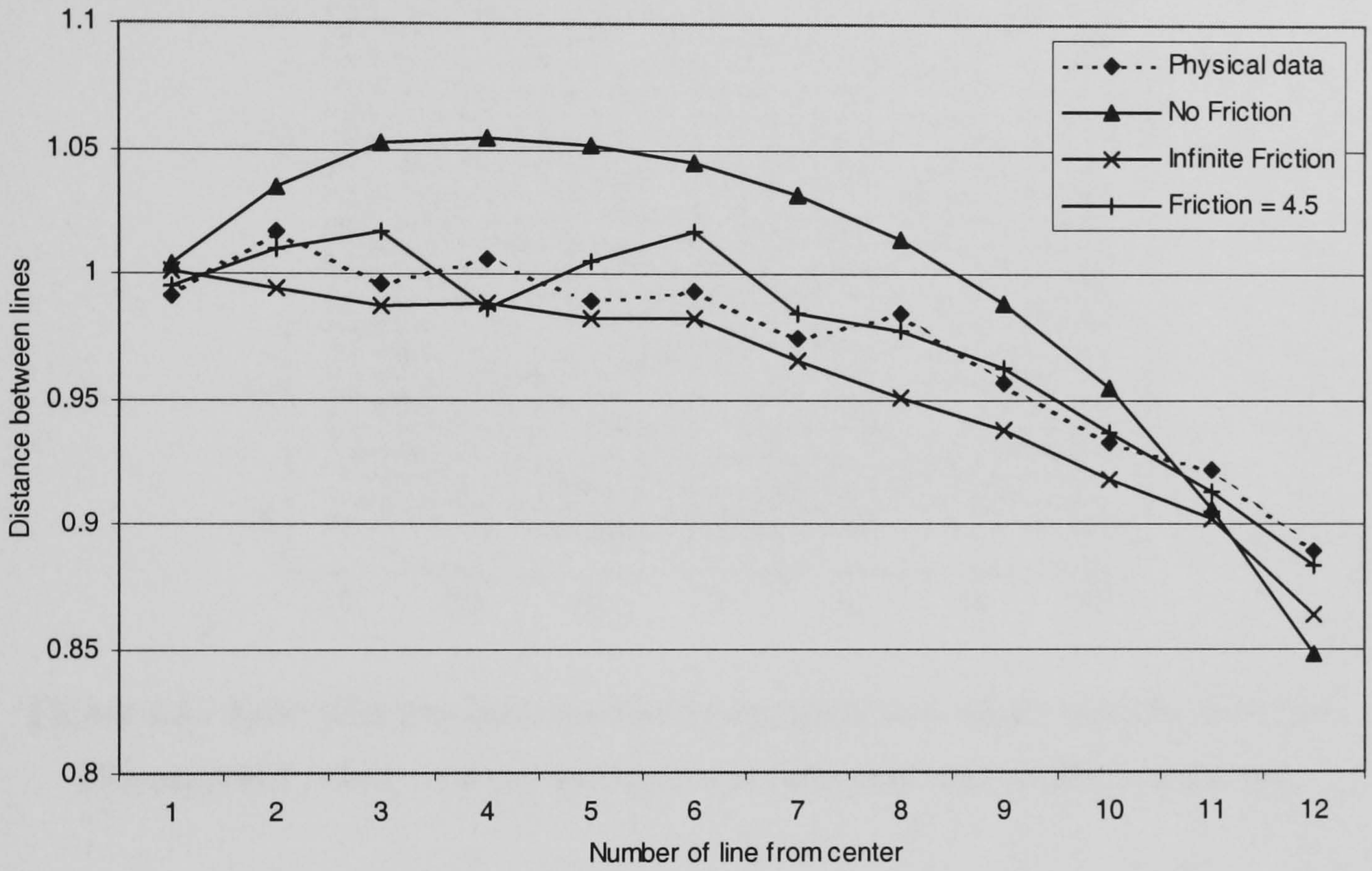

Figure 6.15 Graph showing measured distances between the projected grid points resulting from the finite element model compared to the results of the physical tests.

6.3.4 Pre-distortion

With the correlation between the Finite Element Analysis and the physical data for printing on a curved surface found to be acceptable, the next stage was to calculate the pre-deformation of the cliché pattern. The *cliché to substrate* transfer function was inverted and this was used to calculate the necessary radius of a point on the cliché so that when printed it would appear at

the correct radius and the graphic would be undistorted. The pre-deformation of the grid was found using this the *graphic to cliché* transfer function.

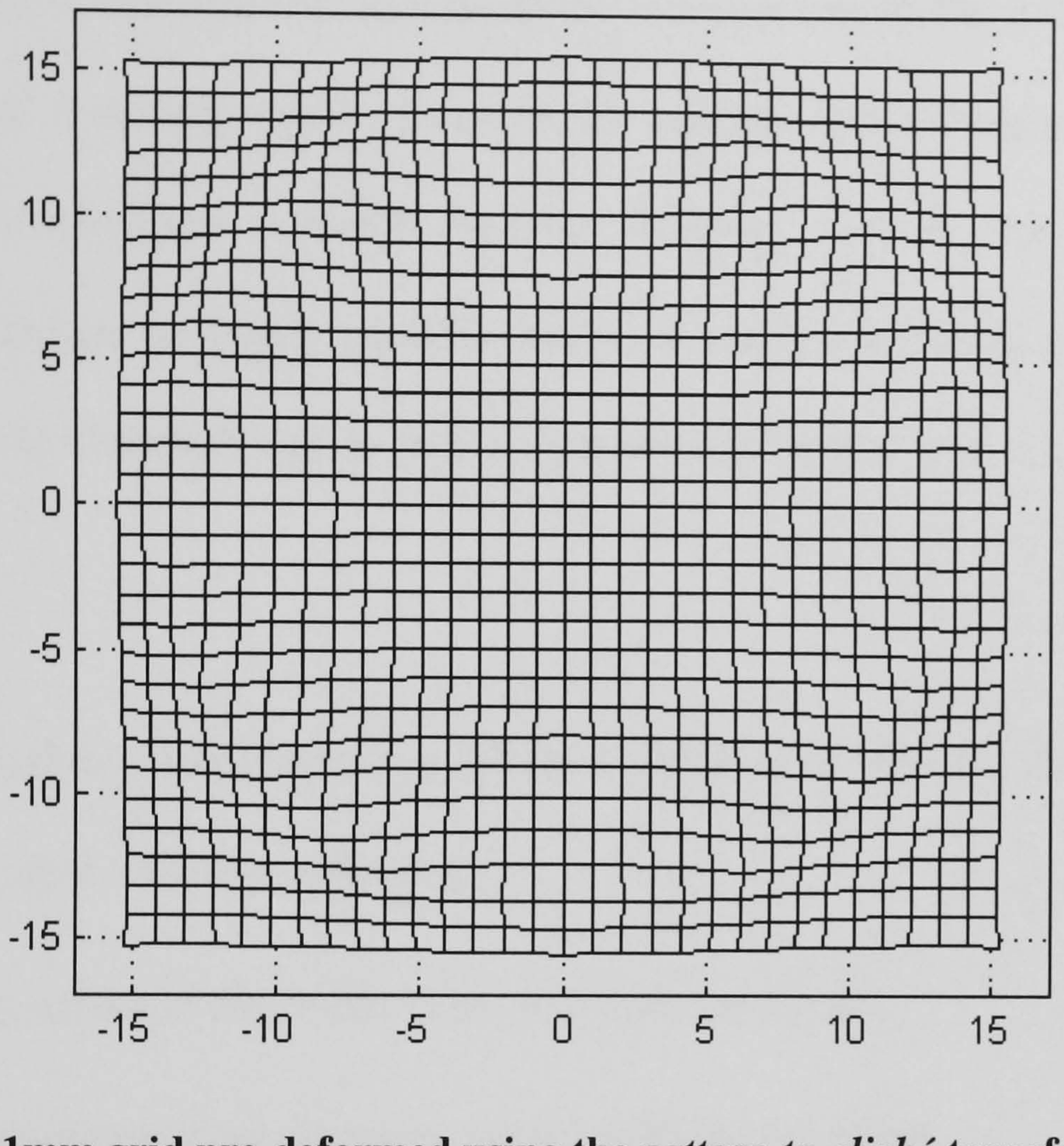

Figure 6.16 1mm grid pre-deformed using the *pattern-to-cliché* transfer function. The expected result on a convex spherical substrate is an undistorted print.

The method developed by Morison at Birmingham to calculate the pre-distortion of an arbitrary cliché pattern is independent of the source of data used for the calculation. Data required are the co-ordinates of the intersections of a standard grid printed on the substrate which can then be interpolated. There are a number of techniques which can be used to produce this data: metrology, image processing and Finite Element Analysis.

Metrology involves producing test prints of the standard grid on the substrate, and using a measuring projector to read the co-ordinates of the intersections on the substrate. This requires operator input but the equipment exists and relatively little skill is necessary. Disadvantages of the metrology technique are that the pad and substrate must have been

produced and the printing parameters must be optimised and reproducible. This process can be automated by using image processing, where a camera would capture the printed grid and software can be used to measure the location of the intersections of the grid. This the still has the disadvantages of metrology but in place of the operator input there is a requirement for further software development. Finite Element Analysis can be used and this has the overwhelming advantage of being possible before a pad or substrate is produced and is potentially faster; the disadvantage is that a powerful computer and a skilled operator are required.

Central to the method to extrapolate a pre-distorted cliché is the MATLAB function 'interp1'. This requires three input vectors containing:

1. radial positions of the nodes in contact with the cliché,
2. radial positions of the nodes in contact with the substrate,
3. input radii for which the output radii are to be returned,

and the interpolation method which was 'spline' for non-linear cubic spline.

For the method developed at Birmingham to work for arbitrary clichés it needs to be applied to images. In pad printing only one colour can be printed at a time so multi-colour printing uses multiple clichés which must be pre-distorted. The separation of colours aids the pre-distortion process. The difficulty lies in the discrete nature of digital images where two pixels may try to occupy the same space after transformation to the pre-distorted image. The simplest way around this uses a nearest-neighbour rule, though the weighted mean across a neighbourhood may be preferable.

Table 6.4 Comparison of the merits of metrology, imaging and finite element analysis (FEA) for producing distortion data (a high number (4) and 'No' are preferable)

Criteria/ requirements	Metrology		Imaging		FEA	
1. Equipment	Measuring projector, pad printer	**3**	Camera, powerful computer, pad printer	**1**	Powerful computer, software	**2**
2. Requires pad geometry	(Yes)	**2**	(Yes)	**2**	Yes	**1**
3. Requires pad	Yes	**1**	Yes	**1**	No	**4**
4. Requires substrate geometry	(Yes)	**2**	(Yes)	**2**	Yes	**1**
5. Requires substrate	Yes	**1**	Yes	**1**	No	**4**
6. Requires optimum printing	Yes	**1**	Yes	**1**	No	**4**
7. Time to use (rank)	(Equal)	**2**	(Equal)	**2**	Most	**1**
8. Operator experience / skill	No	**1**	(Yes)	**3**	Yes	**4**
9. Requires prior research	(No)	**3**	(Yes)	**2**	Yes	**1**
10. More software development	No	**4**	Yes	**1**	Yes	**1**
Rank | Total		**20**	**Best ?**	**16**	**Worst ?**	**23**

6.3.5 Summary

1. A Mooney-Rivlin two-term material model of silicon rubber, found from curve-fitting, was found to give the closest correlation between material tests and models of those tests. In particular it modelled the incompressible nature of the silicon rubber.

2. Foot-print tests and feasibility studies of endurance and photographic tests were performed on on printing pads and wear was found to be minimal.

3. A two-dimensional model of a pad deforming against a flat substrate was validated against data from pad tests.

4. The feasibility of various three-dimensional meshes to model deformation of quarter-pads against spherical and saddle-substrates was explored. There was success, but also difficulty in producing undistorted 3-dimensional models of conical pads.

5. An improved two-dimensional mesh was developed and deformed against a cliché and axi-symmetric curved substrate. The cliché-to-substrate transfer function was found for a regular grid of 1mm squares superimposed on this model.

6. The simulation of pad printing without friction did not give a good correlation with physical data. A friction coefficient of 4.5 was found to produce a match within approximately 5% and a *stick-slip* model was proposed for friction.

7. This lead to computation of a pattern-to-cliché transfer function, which was used to interpolate a pre-distorted grid to be used on the cliché.

8. A comparison was made of using finite element analysis, metrology and image processing to produce pre-distorted clichés. FEA requires experienced personnel but can be used to model the interaction of a pad, cliché and substrate before these components are produced.

9. Future work should include printing with the pre-distorted clichés produced from FEA and metrology.

7 The Intelpadrint system

7.1 Introduction

Components of the Intelpadprint system that were contributed by the other consortium partners are discussed here. The development of new inks, clichés and the new printers are presented.

7.2 Ink development

As an ink-supplier the role of Marabu in the Intelpadprint consortium was the development of new inks, and this was a key requirement of the specification. Better quality inks require less process control, lead to less waste and produce a more desirable product. Marabu evaluates inks on the basis of *printability*, which is judged by viscosity and ink release from the pad; and *visual quality*: ink opacity, colour strength, gloss, shadow, sharpness, and print completeness. Opacity was measured using a new spectrometer, while completeness is related to ink-release. Other tests are chemical resistance to ethanol and white spirit, and the level of mechanical adhesion. New equipment was used to measure the surface tension of plastic substrates, with and without pre-treatment, as in general high surface tension improves adhesion of the ink.

A solvent-based ink consists of finely rolled pigment powders, which contribute the colour; mixed with a binder which acts as a matrix to hold the dry ink to the printed surface. A solvent carries the ink when wet and all the solvent is lost through evaporation and absorption during drying, when the binder undergoes a chemical

reaction. (True *lacquers* contain binders that do not chemically change and so the drying process can be reversed with the correct solvent.) Fillers, stabilisers and other additives prevent the solids settling in the wet ink and improve printability.

Table 7.1Wear and chemical resistance tests for an experimental solvent ink printed at 1500 and 6000 parts/h

1500 prints/h 6004/ 435 95 73 black ink	Substrate plastic							
	PS	ABS	PC	ABS/PC	PA	ABS	PPO	PP
Adhesion test	0	0	0	0	-	0	0	2
Cross-hatch tape test	0	0	0	0	-	0	0	3
Rhc, ethanol*	2	1	2	2	-	2	2	3
Rhc, white spirit	2	1	1	1	-	> 1	< 1	3

6000 prints/h 6004/ 435 95 73 black ink	Substrate plastic							
	PS	ABS	PC	ABS/PC	PA	ABS	PPO	PP
Adhesion test	0	0	0	0	-	0	0	2
Cross-hatch tape test	0	0	0	0	-	0	0	2
Rhc, ethanol*	< 1	< 1	< 1	< 1	-	< 1	< 1	3
Rhc, white spirit	< 1	1	1	< 1	-	< 1	< 1	3

In the first year of the project existing Marabu inks were analysed, and it was found that two-component inks produced the best results. However they had a short life in the ink-cup of the printer and this was against the project specification. As expected ink-opacity increased with repeated printing of the same substrate, but because of the law of diminishing returns only double-printing is worthwhile. Opacity can also be increased by adding more pigment or titanium oxide, but increasing the amount of filling powders was

found to reduce the gloss of the print without improving opacity. There is a limit to the proportion of pigment powders that can be absorbed by a binder system, and because of the difficulty of printing white on dark backgrounds white inks are near this limit. The differences in formulation between different coloured inks can affect printing.

New inks with an improved binder were developed, and the best single-component ink was optimised in year two for high printing rates and became the prototype ink '14.20'. This ink was produced in a number of colours for testing by the end-users on standard printers and the pre-prototype. They were designated '6004/ XXX'. LEGO printed 22,000 Intelpadprint parts and 100,000 of their own substrate. The prototype inks were used at high speed and, after adopting a slower evaporating solvent, better results were reported for adhesion and printability than with their existing inks. A mechanical tumbler with a control chamber containing just printed substrates, and a test chamber containing substrates and polycarbonate granules, was used to test for adhesion. It was found that the ink contained no heavy metals and this is particularly vital in the toy-manufacturing sector occupied by LEGO. Philips performed printing tests at low speeds and found that the ink-release was better with the existing Marabu inks than with the prototype.

Polypropylene is a commonly used plastic and gave better results with corona pre-treatment and hot-air drying. PA needs pre-treatment after which the dispersed component of surface tension is low while the polar part becomes very high. PPO gave worse adhesion following hot-air post-treatment. The white and red prototype inks had the same rheology while the black ink had a different viscosity curve, but they were all

found to behave comparably during printing. Wetting and dispersing agents were used to minimise ink build-up around the rim of the ink-pot.

The one-component prototype was a useful compromise and had a longer pot-life but also a low chemical resistance. Therefore, it was decided to develop an ultraviolet cured ink in parallel with further solvent-based development. UV inks are beneficial for workers and the environment as they are solvent-free. Potentially, this would save LEGO 5500 kg/year (50 DKK/kg) 'waste' in solvents on an ink-consumption of 6000 kg/year. Though UV inks are widespread in the screen-printing sector they have not been successfully used for pad printing.

Initially tests were performed on existing '6001' and 'UVPK39' UV inks, but neither showed evidence of good adhesion or chemical resistance. '6001' gave better looking prints so it was modified but did not reach the Intelpadprint targets. In order to design a completely new ink, UV-curable raw materials and thermoplastic resins were investigated. The next step was to test the solubility of the thermoplastics in different resins, then the resulting product and UV-curable resins were combined to form binders, and complete inks.

Adhesion was tested on various substrates, then the best inks were evaluated on standard pad printers at Marabu and Philips. Some of the UV formulations showed good adhesion (except on difficult substrates) and moderate chemical resistance. These were modified with other monomers, but with no improvement in chemical resistance. Elastomers can be added to solvent-based inks to improve adhesion on difficult substrates, but in tests

they did not improve UV-inks. The best inks did not completely release from the pad leading to ink build-up and shadows on the substrates. Small proportions of thinners were added to eradicate this problem. Various metal-salt extenders were evaluated and some were found to improve the printability of the UV-ink.

At the conclusion of Intelpadprint development and testing of UV-curable inks were incomplete and continuing. The best UV-ink showed good chemical resistance and adhesion, and quite good printability. Large scale testing of the latest UV and solvent based inks on the demonstration printing system had not taken place by the end of the project because the it was not operational. The Intelpadprint solvent-based inks improve substantially on existing products, meet the project objectives (except that they contain solvents) and are optimised for high production rates.

7.3 The pad printing cliché

The clichés for Intelpadprint were developed jointly by Tampoprint and Philips CFT. Prior to the Intelpadprint project the majority of *clichés* were photo-chemically etched, thick stainless steel plates. The steel is expensive and is chosen to be hard-wearing and give a high resistance to corrosion by the ink. Etching is a manual process which requires a photographic negative of the design to produce a photo-resist mask on the blank cliché.

The *etch factor* is a function of the material and the etching time, which typically varies from twenty seconds to ten minutes. It is given by

$$f_{etch} = \frac{2D}{U-P} \qquad (1.)$$

where D is the line depth, P is the line width of the photo-resist mask, and U is the resultant line width on the cliché and is greater than P. An objective of the project was to reduce the minimum line width from 100μm to 30μm while doubling the maximum dry ink thickness from 5μm to 12μm. This can be achieved by improving the inks and by increasing the maximum cliché depth from 18μm to 35μm. As Figure 7.1 shows, to achieve the desired dry ink-layer thickness of 10μm requires a cliché depth in excess of 50μm. Philips performed etching experiments, and as Table 7.2 demonstrates phosphor bronze has a higher etch factor for a given etching time making it more suitable. In general, increasing the etching time increases the width as well as the depth of the line, and it is not possible to produce the depth-width combination demanded by Intelpadprint on a hard-wearing material using etching.

Table 7.2 The etch factor for four materials with a mask line width, P = 20μm.

Material	Cliché line width, U/ μm	Line depth, D/ μm	Etch factor, f
Stainless steel	35	18.5	2.5
Anodised aluminium	35	19	2.5
Phosphor bronze	31	17.5	3.2
Fernico N042, $t = 4min$	50	17	1.1
Fernico N042, $t = 5min$	56	19	1.0

The alternative to etching is laser engraving, which because it does not use corrosive chemicals has less impact on the environment. The cliché can be produced automatically from the design on a computer to the laser engraving, without intermediate steps or operator input. The disadvantage of laser engraving for Tampoprint was the initial high cost of the laser system, a lack of expertise and the limitation that a raster was not possible. Tampoprint performed initial tests on aluminium clichés with an aluminium oxide (*aloxid*) layer. The clichés could be produced at low cost in-house, but the quality depended on selection of the correct laser parameters and the evenness of the oxide layer. The laser produced lines with a minimum width of 50µm and a maximum depth of 20µm, which does not meet the project objectives.

Laser engraved ceramic clichés were produced with a very long life in service (millions of prints) and the quality only depends on the laser settings because the material is homogeneous. The difficulty was finding blank clichés of sufficient size: the maximum available was 110 x 215mm whereas Intelpadprint required 150 x 300mm. Initial tests using smaller white ceramic clichés produced low quality prints. The reason was found to be small cavity holes produced during manufacture and obscured with dust during grinding. A new black ceramic was developed by Tampoprint and their supplier which eradicated this defect and gave better laser absorption. Engraving time was reduced by a factor of five and sharper edges were achieved.

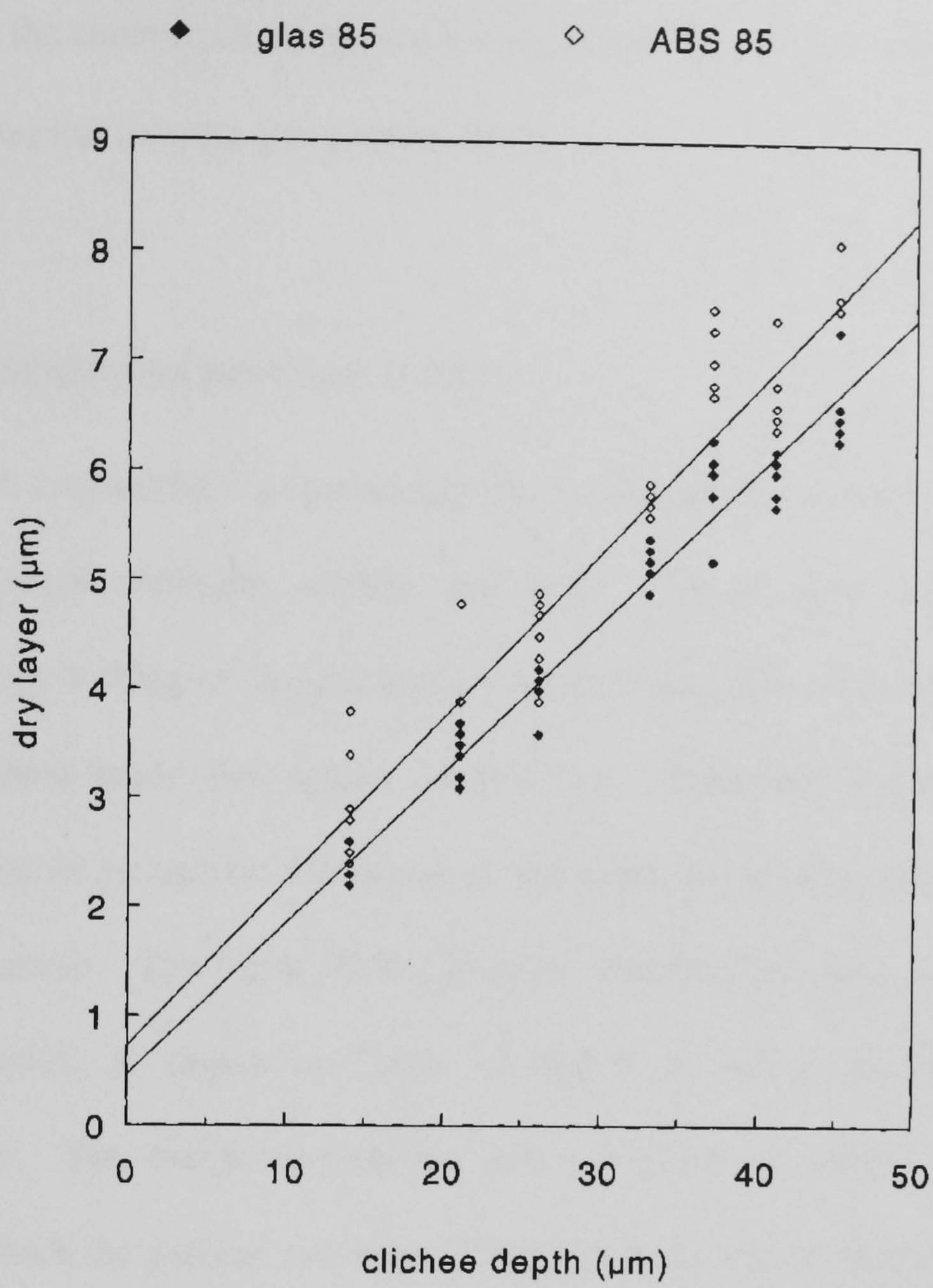

Figure 7.1 Dry layer ink thickness related to cliché depth for 2 polymer substrates [Philips CFT]

Philips has vast experience of lasers and tests were performed to optimise a laser set-up for Intelpadprint clichés. A second harmonic *Nd:YAG* (neodymium: yttrium aluminium garnet) commercial laser with a wavelength of 532nm was used for initial tests on metal and ceramic blanks. A minimum line width of 40µm was achieved with a depth of 10µm on metal and water-cooling was required to prevent burrs. A line depth of 50µm with a width of 80µm was the result of fifty scans with 1.5mJ/ pulse energy. Fifty scans at

1.5mJ/ pulse on the ceramic cliché gave a line depth of 280μm with a width of 60μm, and water-cooling was not necessary to prevent burrs.

7.4 Pre-prototype pad printing system

Tampoprint was responsible for producing the Intelpadprint printing machine, steering and process control software, clichés and pads. Mechanical cam actuation was considered, but the linking of the pad and cliché motions, and inflexibility in the motion of each component made this option unattractive. Therefore, there was the choice between electrical or pneumatic drives and at this point the existing range of Tampoprint printers was assessed. The *rapid 2000/130* is an advanced machine that is close to the project specification, as shown by Table 7.3 and it is used as the basis for the pre-prototype printer. The maximum printing rate would be increased to 7200/h and the range through which the pad can move was extended from 160 to 180mm. Standard parts were used where possible to reduce costs, and parameters were adjusted using an industrial keyboard and displayed on a small monitor. The need for flexibility in the acceleration curves for the pad and cliché and in the length of dwell and motion periods, lead to the choice of a PC over a *programmable logic controller* (PLC).

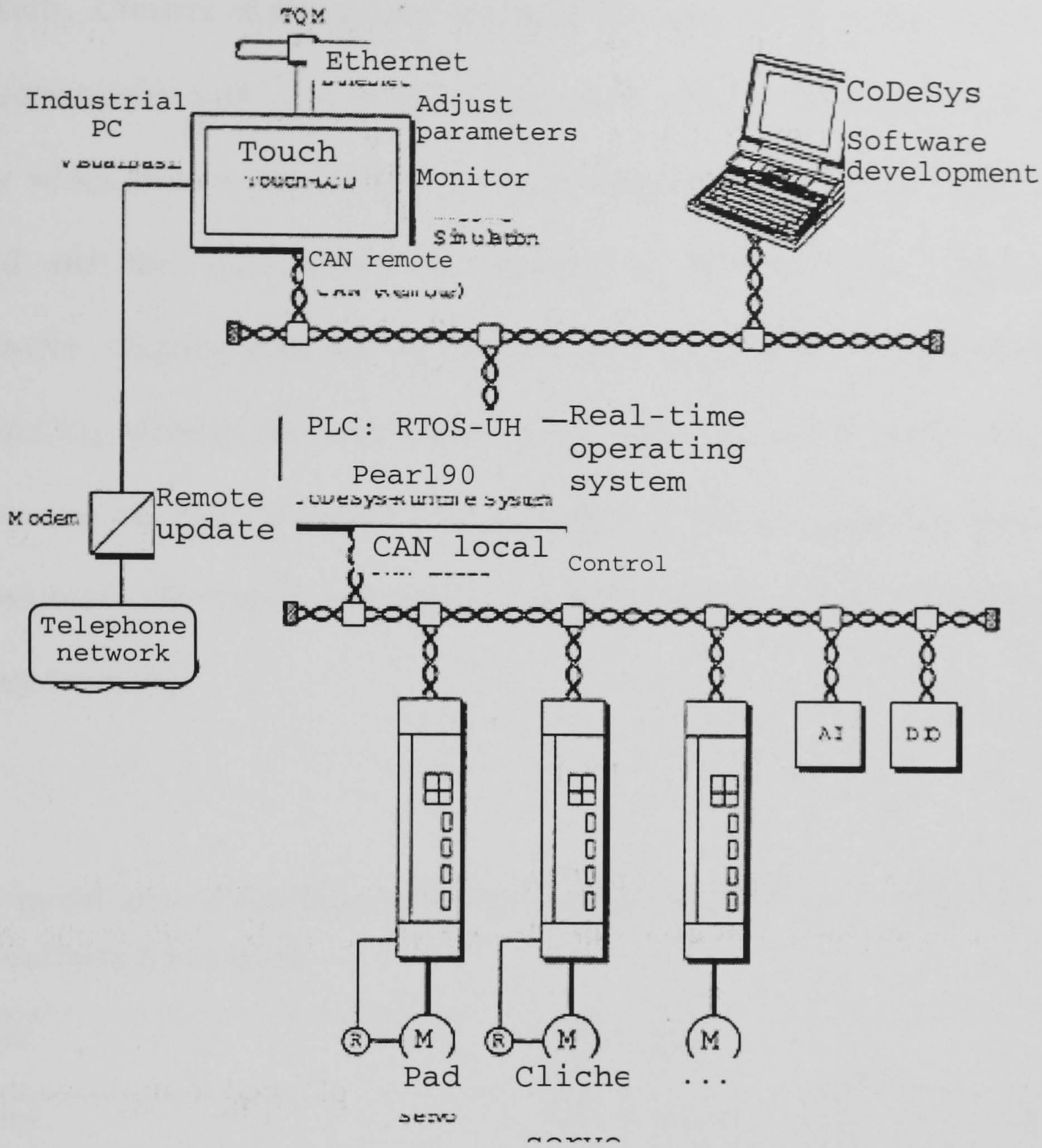

Figure 7.2 The *Intelpadprint* demonstration system CAN-buses [courtesy of esd]

Controller area network (CAN) was developed by Bosch to enable simpler communication between the increasing number of automotive electronic systems, for functions such as engine timing and throttle. CAN is a broadcast communications protocol which is now standardised (ISO 11898) and used in motor vehicles, domestic appliance such as washing machines and production facilities [ODVA, 1999] [Carsten, 1997]. The widespread use of an open standard has reduced the cost of chips. For real-time applications, high speed CAN operates at 200Kbits/s to 1Mbits/s, and the cable specified is a shielded twisted pair which is makes it suitable for noisy electronic

environments. Clusters of sensors and actuators are connected locally to a CAN module which communicates with other peers in the network. Each module has a high degree of autonomy which reduces the load on the controlling computer. Input-output lines are eliminated and the 'hard wiring' is replaced by flexible nodes, which are re-programmable. Simultaneous transmission conflicts are resolved under CAN with bit-wise arbitration, whereby the higher priority node has a lower identifier and does not have to re-send its data. Figure 7.2 is a diagram of the *Intelpadprint* demonstration system CAN-buses showing the industrial PC, the programmable logic controller (PLC) and the primary actuators.

Table 7.3 Specification of the Tampoprint *rapid 2000/130* pad printer on which the *Intelpadprint* system was based.

Parameter		**Parameter**	
Single print	✓	Diameter of ink-cup	130mm
Double print	✓	Maximum print diameter	120mm
Continuous operation	✓	Pad stroke	160mm
Cycles counter	✓	Maximum pad load	2kN
Continuously variable printing rate	✓	Drive	electro-mechanical
Printing rate	1700 – 4500 cycles/h	Power output	1kW
Cliché size	150 x 300mm	Control	PLC

Tampoprint engaged *esd*, an electronic system design-consultancy and CAN-bus specialist, as a contractor to develop low-level controllers for Intelpadprint. The pre-prototype scheme for the Tampoprint/ esd machine and process control system for Intelpadprint is shown in figure 5.4. The printer sensors and actuators are connected via the *local* high speed CAN-bus to the programmable logic controller (PLC). The PLC contains a real-time operating system (RTOS) in which interrupts are guaranteed to be handled in a specified maximum time. The industrial PC provides an interface with the user and is connected to the PLC on the *remote* CAN-bus. Software can be updated on-site over the remote CAN-bus or remotely via a modem, and *total quality management* (TQM) data is transmitted over an Ethernet connection.

Figure 7.3 contains plan and elevation drawings of the Tampoprint pre-prototype system which show the loading and unloading points, carousel, camera and printer.

The pre-prototype printer was evaluated at Philips and LEGO and feedback was provided, with most criticism reserved for the ink-pot and viscometer. A change in the design of the machine was needed to allow easier changing of the ink-pot and cliché, and the pot was awkward to clean. In order that the viscometer can operate with less ink in the pot the viscometer spindle needed to be closer to the cliché, and the bearings and seals on the viscometer were required to be resistant to thinner. The pre-prototype contained a system to add thinner to the ink-pot, but it was not possible to graduate the thinner and the change of ink-viscosity which resulted was invariably too great. The connection between the thinner-metering system and the ink-pot was inadequate, and the

end-users requested a feasibility study of a system to allow ink to be added through the top of the ink-pot.

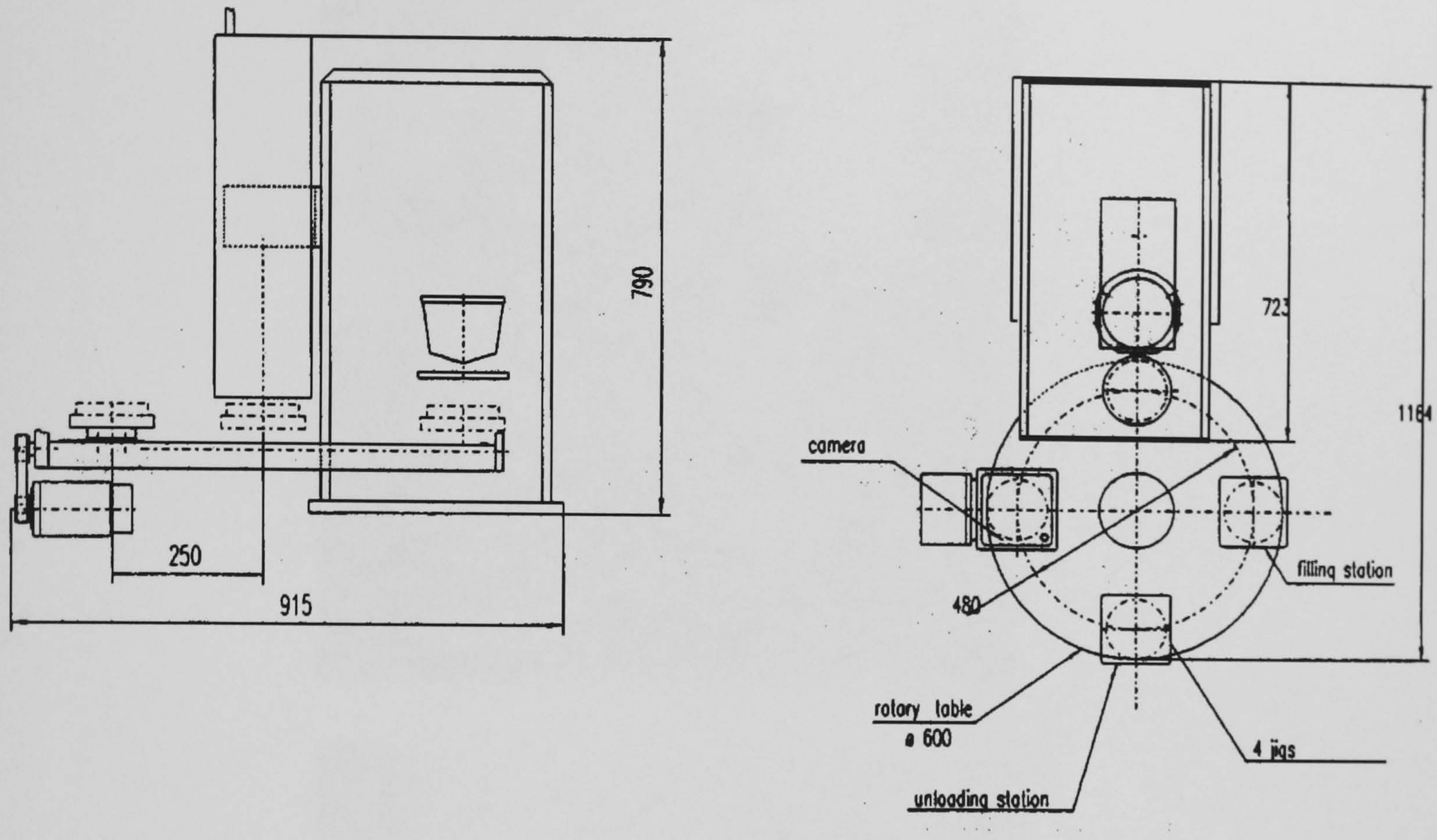

Figure 7.3 Plan and elevation drawings of the pre-prototype system

The system that fed substrates to the carousel was awkward to load. Temperature, relative humidity and ink-level sensors were not included, and the pre-prototype was not capable of double-printing. The minimum load between the ink-pot and the cliché needed to be less than 70N, particularly when a polymer cliché was in use and the system was at rest. Excessive ink was found outside the rim of the ink-pot and this may have been caused by a poor surface finish on the laser-engraved clichés. Machine vibrations produced an unacceptable noise level of 81dB (75dB is a desirable limit) and the pre-prototype printer only achieved a top printing rate of 5100/h.

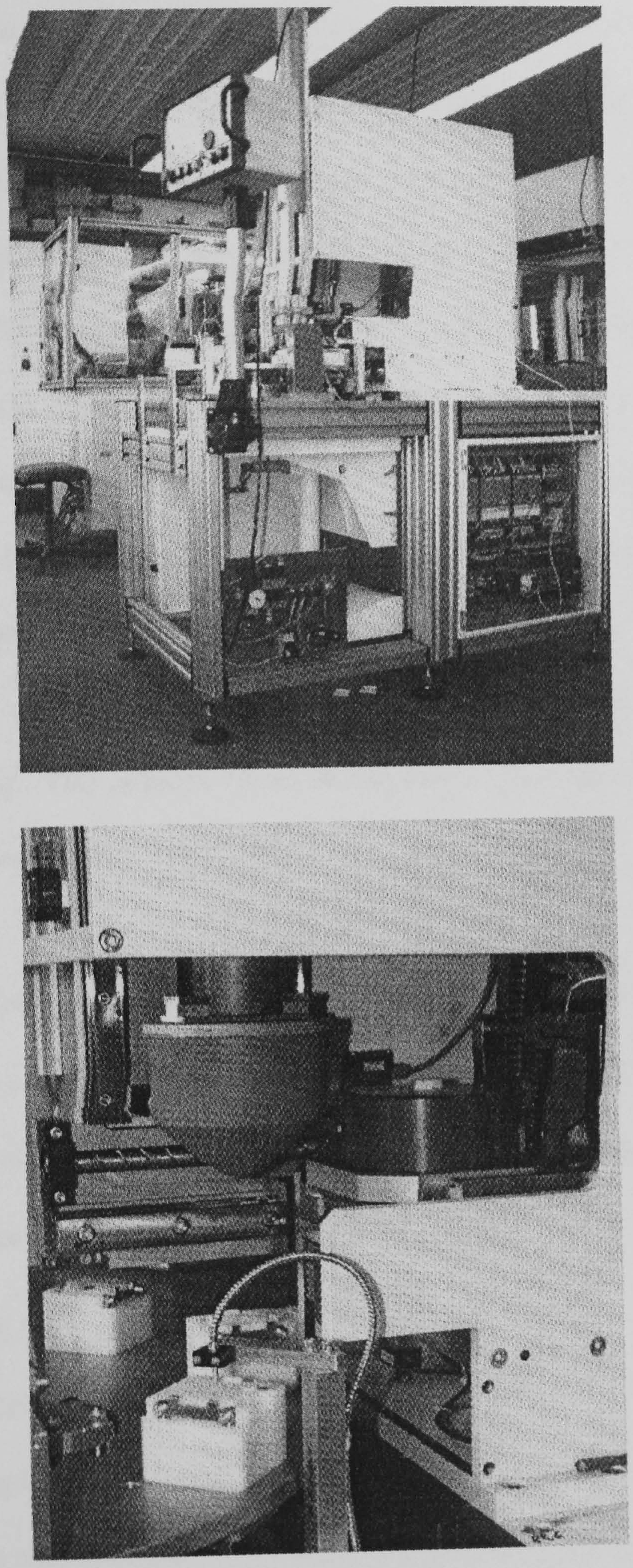

Figure 7.4 The pre-prototype printer, a) the complete system and b) the printing pad.

Improvements such as the ability to double-print were introduced in software on the pre-prototype, but fundamental points including the maximum printing rate and excessive noise would be addressed in preparations for the demonstration printing-system. *Linear motors* were investigated but none were found that could simultaneously achieve the high speed and force (2000N) that were required. The models that approached the necessary performance contained cooling systems that were larger than the pre-prototype printer. Instead, stronger faster servomotors and improved linear guides were specified for the demonstration model, and the manufacturer Lenze agreed to release the source code for their 'electronic cam' firmware. The sophisticated cam models used to control the motors contain no acceleration discontinuities and finite *jerk* or second acceleration [Shigley *et al*, 1995]. This reduces vibration and wear, and makes the lower noise level possible at high speeds.

Problems were encountered. When printing at 7200/h the time available to the processor in the Lenze motor-units was 1000μs in each cycle. Operating system processes and the calculation of the velocity curves to be followed by the motor occupy all but 17μs of that period and there was no time available for the other tasks:

1. operating system O/S	390 μs
2. run-time curve calculation	593 μs
3. run-time waiting time calculation, SPC	70 μs
4. reading position signal, SPC1	70 μs
5. recall of measured values, OSZ	80 μs
	1203 μs

It was calculated by *esd* that 150 to 200µs of processor time in the motor-unit could be saved by transferring the servo calculations to the PLC. The CAN-CBM-PLC/331 processor to be used on the demonstration system had a 50% greater clock speed than that used on the pre-prototype. This processor was a prototype, and the memory requirements of the modified real-time operating system and the user specific code were unpredictable. The 1MB of static memory (SRAM) was insufficient and the only available solution was to optimise the RTOS to be faster and use fewer resources. This solution required the CoDeSys real-time programming tool, which was not entirely compatible with CAN-bus. Eventually a new PLC processor with 2MB of memory and a higher speed became available, and this solution was pursued in parallel with the optimised operating system.

At the completion of the project the demonstration printing system was built but not operational, due to the software problems outlined above. The use of unproven PLC processors and the lengthy redevelopment of the PLC operating system were necessitated by the high printing rate demanded by Intelpadprint. They carried high technical and time risks which were realised, but given further development after the project the system will function. The resulting pad printer will achieve a higher production rate than any machine currently available, with a long life in service and acceptable noise levels during operation. The system will provide more flexibility and control than current pad printers.

7.5 Summary

1 Marabu developed solvent-based inks, which improved substantially on existing products, have a longer pot-life and are optimised for high production rates.

2 By the end of the Intelpadprint project ultraviolet-cured inks with good chemical resistance and adhesion, and adequate printability had been achieved – the research is ongoing.

3 Following research ceramic and metal clichés produced laser engraving meet the project target for the minimum line width and dry ink thickness.

4 The pre-prototype printing system produced by Tampoprint used the CAN-bus communication network and achieved a printing rate of 5100/h. It was successfully tested, but produced an unacceptable noise level and the ink-pot and cliché were difficult for the operator to change.

5 The demonstration printing system had a higher-specification printing-rate and increased flexibility, but fundamental problems with Programmable Logic Controller delayed testing.

8 Conclusion

8.1 Discussion

The aim of the Intelpadprint project was to improve pad printing and the 6 members of the consortium were responsible for developing different components that would achieve this. Tampoprint developed and built new printers. Tampoprint and Philips CFT developed innovative printing clichés, and Marabu researched new pad printing inks. The University of Birmingham and Philips CFT researched print distortion, and Birmingham developed the first models of printing-pad compression and devised a method to minimise print distortion by pre-distorting the cliché-graphic. The Universities of Birmingham and Maastricht were responsible for developing an automated visual inspection and control system. This would identify faults on products immediately following pad printing, sense whether printing parameters such as ink viscosity were out of the desired range and adjust the process to eradicate the faults. The machine vision part of this system presented the greatest challenge, so this was where most of the research was focused. The OCAP document (section 3.3, page 62) contains the first comprehensive library of pad printing errors, their causes and cures in the published literature.

It was proposed in section 3.4 that the OCAP faults could be categorised based on where they occur in relation to the printed boundary. Six generalised positions denoted $\Gamma 1$ to $\Gamma 6$ were identified where one-dimensional collections of contiguous pixels could be extracted in relation to the boundary. For example, $\Gamma 4$ "parallel to the border close outside the printed area" is a suitable curve on which to find OCAP fault 1, hairs. This was a novel starting point for pattern recognition and formed the basis for the Linear Correlation Algorithm.

The LCA algorithm was quite successful under laboratory conditions identifying 84% of the OCAP specimens with a quality $q > 1$. For each specimen the algorithm produced the probability that it contained each of the OCAP faults and a quality $q = 1$ would mean that the 2 greatest probabilities were equal. One of the algorithms chief disadvantages was that it used only 1-dimensional data, so that faults such as *ink missing* and *air bubbles* could not be distinguished (section 5.2). A number of approaches using 2-dimensional data were tried, including a neural network that achieved 80% success.

Acquiring the image of a printed product and locating the print and any errors on the product were identified as key steps whose success affected the success of subsequent fault diagnosis steps. This was the main subject of the thesis. During the first tests of the pre-prototype system at LEGO poor quality images were acquired. This was found to be due to the illumination, which took the form of a ring-light shining directly down onto the product. Diffuse light reflected from a white circular screen around the subject was found to produce far better quality images. The histogram in Figure 4.7 a) shows a much wider distribution of intensity for the poor quality image (approximately 3% of pixels occupy the two peaks), whereas the good quality image (b) resulted in more than 10% of pixels precisely occupying the maximum intensities. A novel adapter for the existing fibre-optic ring-light produced a compact source from which light shone radially out to reflect off the screen (section 4.2.4).

A form of template matching was proposed to locate the printed graphic and any faults in the image. The approach described in section 4.1.5 was termed Local Corner Matching and used small 5x5 templates representing the corners in the graphic. If no printing faults were present then the location of 3 corners would determine the position, orientation and scale of the graphic relative to a template-image of the whole graphic. To allow for faults a minimum of 4

or 5 corners were tested. By predetermining the expected position of all corners one could find relationships between corners (for the example on pp. 96 , C3 should be –23 pixels vertically from C2 within a tolerance of X pixels, and 0 pixels vertically from C4). During printing ('on line') the predetermined values were compared with calculated values to find the position of the suspect graphic. Although the example only calculates positions to whole-pixel accuracy the approach can be extended to the sub-pixel level. A box of 16 x 16 pixels around each expected position was searched and if no match was found there was considered to be a printing fault at that corner and it was disregarded.

The LCM technique had a number of advantages over other segmentation methods. It was computationally efficient in that only areas of the image containing useful features were matched. This was possible because the product was imaged in a holder so the position of the graphic was known within a small tolerance – if the features in the graphic were not present within their respective search boxes it could be concluded that the graphic or the product were missing. The method is suitable for other printing and production techniques where the approximate position of the subject is known. It is not suited to products that could be at widely differing positions or angles, for example on a conveyor belt. The process was able to handle erroneous features in an absolute way, they were filtered out and therefore did not affect the overall computation. This can be contrasted with other template matching techniques where printing errors are 'averaged' into the calculation, thereby affecting the values computed for position, scale and orientation.

The Local Corner Matching approach can be compared with the 'coarse-fine' technique, which was used for the tests described in section 5.5. The algorithm used a coarse template calculated from the means of small neighbourhoods in the fine template. The coarse template

was matched with a coarse version of the suspect image to find the approximate position of the subject. This required fewer calculations. Then the fine template was matched with the a sub-image around the approximate position to compute the position, scale and accuracy to sub-pixel accuracy. The tests demonstrated that bad graphics can be partitioned from good graphics in 90% of cases. The classification was based purely on a threshold applied to the sum of the absolute difference of the sample image with a reference and there was some overlap between the 2 sets (8% false positive on a small sample set). The threshold is sensitive to light and noise conditions so that a means to calibrate the system is required.

The 'coarse-fine' approach is general-purpose, and is most suited to a large image that can contain a relatively small subject at one of many positions. In this scenario it substantially reduces the number of calculations required, and therefore the time taken. However, in the situation provided by Intelpadprint the subject is large relative to the image, so that it becomes less efficient. The coarse-fine algorithm for Intelpadprint can be improved using a template of part of the graphic and matching it with a sub-image, which would comprise the central part of the main image. This would reduce the number of calculations.

Any future tests on the LCM algorithm could use a free image processing software library such as the IPL98 library, written in C++ from the University of Southern Denmark [Eriksen, 2001]. Future work should take advantage of the reusability and data-hiding features of the *object-oriented* paradigm, as demonstrated by Figure 8.1.

8.2 Conclusion

- Using laser engraving of metal and ceramic clichés, a minimum line width approaching the Intelpadprint-target of 30μm was achieved by Philips CFT and Tampoprint. This can be combined with a cliché depth that will produce the desired dry ink thickness of 10μm.

- Low-solvent inks have been developed by Marabu, which are optimised for high production rates (6000/h) and achieved the high (0 Rhc) chemical resistance required on most of the test plastics. Ultraviolet-cured inks were developed which contain no solvent and they showed improved chemical resistance and printability.

- Finite element analysis and pre-distortion of cliché artwork are tools that have been proved. Further development will lead to working systems, which can reduce the waste, cost and time to develop new pads and clichés.

- In the pre-prototype, Tampoprint realised a more flexible pad printer that achieved higher printing rates (5100 prints/h). The demonstration system would have reached project target-rate of 7200/h and solved design issues present in the pre-prototype. However, memory and operating system deficiencies in the programmable logic controllers delayed development.

- The visual fault diagnosis system was developed from the pre-prototype *linear correlation algorithm*. It used fractal wavelet analysis and was 95% successful. It was found to be sensitive to the quality of images resulting from the matching process.

- The *local corner matching* algorithm was proved to work, and tests using the *coarse-fine* approach achieved 90% success. This was the 'red-light' system, which alerted the

operator when it found a fault. The coarse-fine algorithm is more widely applicable, but the corner matching approach proves to be faster and more suited to pad printing.

8.3 Future work

More tests are required on the effectiveness of the Local Corner Matching algorithm. Further development work is necessary to find and reduce bottle-necks in the machine vision system and so achieve the required speed. The LCM algorithm is novel and has potential for many decorating and production applications. Screen printing shares similarities with pad printing in that it is used to print in colour on non-paper substrates and it has the same quality control issues. A form of pad printing is also used to decorate domestic ceramic products.

Other research can focus on integrating the machine vision system with control of the pad printer. A database system was specified during the project to collect all possible data during printing. This included data from sensors such as the ink-viscosity meter, the velocity curves used for the motion of the pad and cliché, measures of graphic quality from the machine vision system, results from the fault diagnosis system and changes made to the semi-automated process by the operator. The database would be 'mined' by the control system to find the correct parameters to use for a fully automated printer.

Further development, testing and evaluation in a production environment (*alpha testing*) is required to determine if the low reject rate of 0.1% is achievable. The project consortium has made the leap from human-controlled pad printing to 'computer-assisted' pad printing. The final steps required to achieve automated pad printing are the development and integration of the expert controller, the visual fault diagnosis system and the printing system.

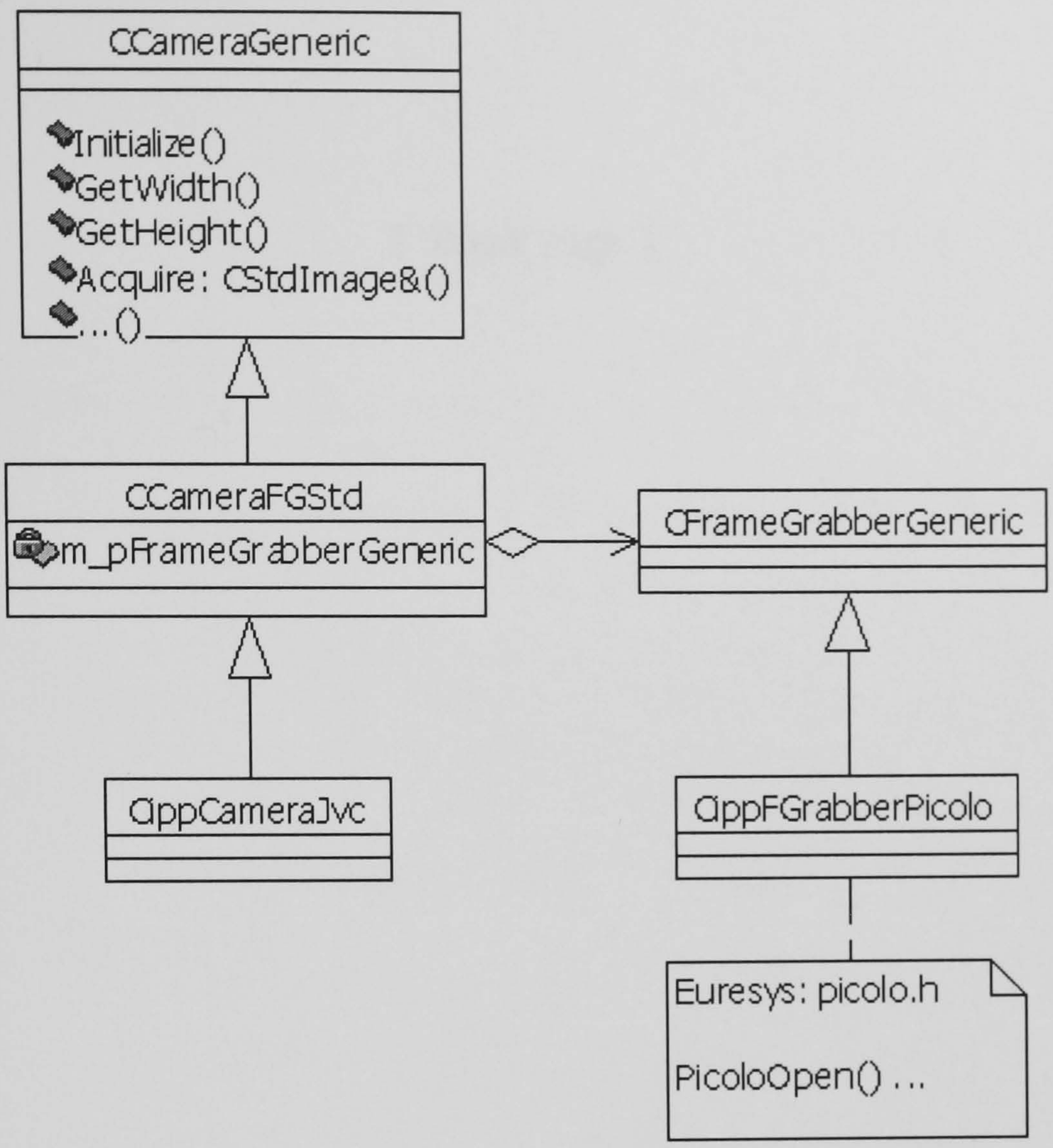

Figure 8.1 A Unified Modelling Language (UML) diagram of the IPP frame-grabber and camera C++ classes within the IPL98 framework.

[Blank page]

References

Abdou, I.E. and Pratt, W.K. (1979). Quantitative design and evaluation of enhancement/ thresholding edge detectors. *Proceedings of the IEEE,* 67, pp 753-763

Al-Kindi, G.A., Baul, R.M. and Gill, K.F. (1991). An example of automatic two-dimensional component inspection using computer vision. *B: J Eng. Manufacture, Proc Instn Mech Engrs*, 205, pp. 71-83.

AMI (1997). *AMI's 1997 West European Plastics Industry Report.* Bristol: Applied Market Information Ltd., 3rd ed, ISBN: 1-871463-52-1.

Anglim, P. (1997). Identification and classification of printing faults on the production line. *In* ERA. *Conference on 'web inspection for printing and packaging'.*, ... 2.1-2.14.

Apostolico, A., Galil, Z. [ed.] (1997). *Pattern Matching Algorithms.* (11 papers) Oxford University Press.

Årzén, K.-E. (1989). An Architecture for Expert system based feedback control. *Automatica*, 25, 6, pp. 813-827.

Åström K.J, Anton, J.J. and Årzén, K.-E. (1986). Expert Control. *Automatica*, 22, 3, pp. 277-286.

Åström K.J. (1989). Toward Intelligent Control. *IEEE Control Systems Magazine*, 9, 3, April, pp. 60-64.

Åström K.J. and McAvoy, T.J. (1992). Intelligent Control: An Overview and Evaluation. *In* White, D.A. and Sofge, D.A. [eds.] (1992). *Handbook of Intelligent Control: neural, fuzzy and adaptive approaches.* NY: Van Nostrad Reinhold, pp. 3-34.

Ballard, D.H. (1981). Generalizing the Hough Transform to detect arbitrary shapes. *Pattern Recognition*, 13, 2, pp. 111-122.

Barlow, R.J. (1989). *Statistics: A Guide to the Use of Statistical Methods in the Physical Sciences.* (The Manchester Physics Series) Chichester, UK: John Wiley and Sons.

Batchelor, B.G. and Whelan, P.F. (1994). Programming Fast Colour Recognition Hardware by Symbolic Reasoning in a Prolog Program. *SPIE*, 2298, pp. 581-592.

Beale, R. and Jackson, T. (1990). *Neural Computing: An Introduction.* London/ Bristol: Institute of Physics Publishing Ltd.

Berthod, M. and Maroy, J.P. (1979). Learning in syntactic recognition of symbols drawn on a template (OCR). *Comp. Graph. Image Process.* 9, pp. 166-182. IRIA France

Beyer, M. and Lohmar, J. (2000). Attractive and Robust: protective and decorative films based on Polyamides. *Kunstoffe plast europe*, 84, 1, July, pp. (translation) 44-46/ (DE) 98-101.

Bezdek, J.C. and Pal, S.K. [eds.] (1992). *Fuzzy Models for Pattern Recognition.* NY: IEEE Press.

Bobrow, D.G. (1984). Qualitative Reasoning about Physical Systems: An Introduction. *Artificial Intelligence*, 24, 3, pp. 1-5.

BPF (1996). *BPF 1996 Statistics Handbook.* London: British Plastics Federation, ISSN: 1351-5594.

Bretschi, J. (1981). *Automated Inspection Systems for Industry.* IFS Publications Ltd, Bedford, UK

BSI (1989). *Methods of testing vulcanized rubber. Part A57: Determination of indentation hardness by means of pocket hardness meters.* British Standards Institute, BS 903 : Part A57 : 1989/ ISO 7619-1986.

Burnside, C. (1994). Cliché Selection for Pad Printing. *Screen Printing*, November, pp. 122- [WWW] http://www.padprint1.com/articles/cliche.html

Calway, A.D. and Wilson, R. (1994). Curve Extraction in Images Using a Multiresolution Framework. *Image Understanding*, 59, 3, pp. 359-366.

Carsten (1999). *Controller Area Network: A Serial Bus System - Not Just For Vehicles.* esd GmbH, Hannover, DE [WWW] http://www.esd-electronics.com/PDF-file/CAN/Englisch/intro-e.pdf (3/10/00)

Chabat, F., Yang, G.Z. and Hansell, D.M. (1999). A corner orientation detector. *Image and Vision Computing*, 17, pp. 761-769.

Chan, J. (1997). Learning method for the inspection of non-precise repeating patterns. *In* ERA. *Conference on 'web inspection for printing and packaging'.*, ..., 7.1-7.10.

Chaplin, R.I., Hodgson, R.M. and Guntelike, S. (1999). Towards the Use of Problem Knowledge in Training Neural Networks for Image Processing Tasks. *7th Internat Conf Image Processing and its Applications*, IEE 465, 1, pp. 62-66.

Chiu, S., Cheng, J.J., Sitter, C. and Fooks, E. (1995). Perspectives on the Industrial Application of Intelligent Control. *Proc 34th Conf Decision and Control, IEEE*, pp. 757-761.

Chiu, S., Cheng, J.J., Sitter, C. and Fooks, E. (1995). Perspectives on the Industrial Applications of Intelligent Control. *Proc. 34th Conf. Decision Control*, part 1 of 4, pp. 757-761.

Daley, S. and Gill, K.F. (1989). Comparison of a fuzzy logic controller with a P + D control law. *Trans. ASME, J. Dynamical Systems, Measurement and Control*, 111: 128-137, June

Daubechies, I. (1990). The Wavelet Transform, Time-Frequency Localization and Signal Analysis. *IEEE Trans Information Theory*, 36, 5, September, pp. 961-1005.

Davies, E.R. (1988). Tradeoffs between speed and accuracy in two-stage template matching. *Signal Process.* 15, pp. 351-363.

Davies, E.R. (1997). *Machine Vision: Theory, Algorithms, Practicalities.* 2nd ed. (1990), Academic Press, Harcourt Brace Javonich, London.

Deans, S.R. (1981). Hough Transform from the Radon Transform. *IEEE Trans Pattern Analysis and Machine Intelligence*, PAMI-3, 2, pp 185-188.

Demuth, H. and Beale, M. (1994). *Neural Network Toolbox User's Guide: for use with MATLAB.* MA: The Mathworks Inc.

Devore, R.A., Lucier, B.J. (1992). Wavelets. *Acta Numerica*, A. Iserles, ed., Cambridge University Press, v. 1 (1992), pp. 1-56.

Dolan-Jenner (1995). *Illumination for Machine Vision* (Dolan-Jenner Industries. Inc.: Lawrence MA. USA)

Domino (2001 a). *Laser Printing*. Domino UK Ltd. [WWW] http://domino.netxtra.net/technology/laserprint.html (21 December 2001)

Domino (2001 b). *Inkjet Printing*. Domino UK Ltd. [WWW] http://domino.netxtra.net/technology/inkjetprint.html (21 December 2001)

Dorf, R.C. and Bishop, R.H. (1998). *Modern Control Systems*. 8th ed. Addison Wesley Longman.

Duda, R.O and Hart, P.E. (1972). Use of the Hough transformation to detect lines and curves in pictures, *Commun ACM*, v 15, n 1, January, pp. 11-15

Du-Ming Tsai (1997). An improved generalized Hough transform for the recognition of overlapping objects, *Image and Vision Computing* (15) 12, pp. 877-888

Eklundh, J-O. [Ed.] (1994). *Computer Vision – ECCV '94*: Third European Conference on Computer Vision, Stockholm, Sweden, May 2-6, 1994, Proceedings, Volume I. Springer-Verlag

Emzivat, D., Gagnadre, C. and Martin, E. (1999). Vision Sensor for the Industrial Quality Control. *7th Internat Conf Image Processing and its Applications*, IEE 465, 1, pp. 127-132.

ERA (1997, January). *Conference on 'web inspection for printing and packaging'*. Leatherhead, UK: ERA Technology Ltd., ERA Report 97-0230. ISBN 0 7008 0611 3,

Eriksen, R.D. (2001). *IPL98 Image Processing Library*. University of Southern Denmark [WWW] http://www.mip.sdu.dk/ipl98 (21 December 2001)

esd GmbH (1999). *Controller Area Network, CAN: A Serial Bus System – Not Just For Cars*. esd GmbH/ CiA – CAN in Automation [WWW] http://www.esd-electronics.com/PDF-file/CAN/Englisch/intro-e.pdf (6 May 1999)

Euresys S.A. (1999) *EureCard Picolo* [WWW] http://www.euresys.com/VisionBoards/Picolo/Picolo.htm (26 April 1999)

Euresys S.A. (1999) *eVision EasyMatch* [WWW] http://www.euresys.com/SoftwareTools/EasyMatch.htm (26 April 1999)

Fernengel, R. (1994). A Concept for Modern Injection Moulding Production. *Kunstoffe plast europe*. 84, October, pp. (translation) 22-25/ (DE) pp. 1361-1367.

Finlayson, G.D. (1996). Color in Perspective. *IEEE Trans Pattern Analysis and Machine Intelligence*, 18, 10, pp 1034-1038.

Finlayson, G.D. and Hordley, S (1999). Selection for Gamut Mapping Colour Constancy. *Image and Vision Computing*, 17, 8, pp. 597-604. (*British Machine Vision Conference*)

Fisher, R., Perkins, S., Walker, A. and Wolfart, E. (1994) Hough Transform, HIPR – *The Hypermedia Image Processing Reference*, Universiy of Edinburgh [WWW] http://www.cee.hw.ac.uk/hipr/html/hough.html (26 August 2000)

Forsyth, D, Mundy, J.L., Zisserman, A., Coehlo, C., Heller, A. and Rotherwell, C. (1991). Invariant Descriptors for 3D Object Recognition and Pose. *IEEE Trans. Pattern Analysis and Machine Intelligence*, 13, 10, pp. 971-991.

Freear, N.D., Li, W. and Shippen, J.M. (1997). *Determination of Material Parameters for Silicon Rubber, Correlations between Finite Element models and Pad Tests, Endurance Tests, and Vision Fault Detection.* Report Tasks 2.1–2.2, September, Intelpadprint/ Birmingham University.

Freear, N.D. (1998a). Deformation Analysis of the Pad Printing Process by Finite Element Analysis. See:. Morison, C.N. *et al.*, 1998.

Freear, N.D. (1998b). Machine vision for Quality control of Intelligent Pad printing. *Proceedings of the Fourth Annual Research Symposium of Postgraduate Research.* Birmingham: University of Birmingham, ISBN 070 441 934 3, May, pp 46-50.

Freear, N.D. (1998c). Deformation Analysis of the Pad Printing Process by Finite Element Analysis. See:. Morison, C.N. *et al.*, 1998.

Freear, N.D. (1999a). Implementing Intelligent visual Inspection for Pad Printing, *Proceedings of the Fifth Annual Research Symposium of Postgraduate Research.* Birmingham: University of Birmingham, ISBN: 07044 20376, May, pp 36-40.

Freear, N.D, Shippen, J.M. and Westra, R.L (1999b). Applying Neural Networks to Fault Classification in Image Data. *7th European Congress on Intelligent Techniques and Soft Computing* (EUFIT), Aachen, DE, pp 118-.

Freear, N.D. (1999c). A Parallel Hardware Multiple Microprocessor Asynchronous Neural Network Architecture for Control Applications. See: Shippen, J.M. *et al.*, 1999.

Freear, N.D. (1999d). Printing Quality Control Using Template Independent Neuro-Fuzzy Defect Classification. See:. Westra, R.L. *et al.*, 1999.

Freear, N.D. (2000). *Intelpadprint, Final Project Report.* See:. Legierse, P.E.J. [ed.], 2000.

Funt, B.V. and Finlayson, G.D. (1995). Color Constant Color Indexing. *IEEE Trans Pattern Analysis and Machine Intelligence*, 17, 5, pp 522-529.

Gonzalez, R.C. and Woods, R.E. (1992). *Digital Image Processing.* USA: Addison-Wesley.

Gregory, R.L. (1970). *The Intelligent Eye.* McGraw-Hill/ Weidenfeld & N.

Gregory, R.L. (1972). *Eye and Brain: the psychology of seeing.* (1992, Princeton University Press).

Griffin, P.J. (1999). New methods for decorating moulded parts. *Machine Design*, 71, 8, April, pp. 56-62.

Haralick, R.M. (1980). Edge and region analysis for digital image data. *Comput. Graph. Image Process.* 12, pp. 60-73.

Hardt, D.E. (1993). Modeling and Control of Manufacturing Processes: getting more involved. *Trans ASME: J. Dynamic Systems, Measurement and Control*, June, 115, pp. 291-300.

Hebb, D.O. (1949). *The Organisation of Behavior.* John Wiley & Sons, New York.

Hensel, T.L. (2000). The Future Role of the Plastics Producers: strategic decisions at the start of the 21st century. *Kunststoffe Plast Europe,* 90, 1, pp. (translation) 11-15/ (DE) pp. 34-38.

Herkt-Maetzky and Robers, W. (1994). White on Black, Laser Inscription. *Kunstoffe plast europe*, 84, July, pp. (translation) 12-25/ (DE) pp. 872-875.

Hess, M, Hamburg, H.R. and Morgan, W.M. (1979). *Hess's Paint Film Defects: their causes and cures.* 3rd English ed. (1938, German), London: Chapman and Hall. (*Häufige Austrihmängel und Austrichschäden*).

Hillestad, K. (1998). Plastics Decorating Technology Provides Many Processing Options. *Modern Plastics Encyclopedia*, 75, 12 -November, 1998, pp. F7-8.

Hansen, K. and Andersen, J.D. (1997). Understanding the Hough transform: Hough cell support and its utilisation, *Image and Vision Computing* (15) 3, pp. 205-218. (Klaus Hansen and Jens Damgaard Andersen)

Hough, P.V.C. (1959). Machine Analysis of Bubble Chamber Pictures, *International Conference on High Energy Accelerators and Instrumentation*, CERN.

Hough, P.V.C. (1962). *Method and means for Recognising complex patterns*, US Patent no. 3069654

Howitt, S. [ed] (1995). *A Market Sector Overview: Plastics Processing.* Middlesex: Key Note Ltd., ISBN: 1-85765-384-X.

Howitt, S. [ed] (2000). *Printing: 2000 Market Report.* Middlesex: Key Note Ltd., 6th ed., ISBN: 1-84168-028-1.

Hunt, D. (1999). Understanding the Mechanism: the essence of process control. *SGIA Journal*, 3rd *Quarter '99*, Screen Printing Technical Foundation, pp.51-55 [& WWW] http://www.sgia.org/../pcontrol.pdf.

Hunt, K.J., Sbardo, D., Zbikowski, R. and Ganthrop, P.J. (1994). Neural Networks for control systems: A survey. *In* Gupta, M.M and Rao, D.H. [eds.] *Neuro-Control Systems: Theory and Applications*, 171-200, IEEE Press, Piscataway, NJ.

Janco, R.A. (1996). Different ways of decorating plastics. *Injection Molding*, 4, 10, October, pp. 94-95.

Jawerth, B. and Sweldens, W. (1994) *An Overview of Wavelet Based Multiresolution Analysis.* SIAM Review, v 36, n 3, September, p 377-412. [& WWW] overview.pdf.

Jeng, S.-C., Tsai, W.-H. (1991). Scale- and orientation-invariant generalised Hough transform – a new approach. Pattern Recognition, 24 (11) pp.1037-1051.

Jenkins, F.A. and White, H.E. (1981). *Fundamentals of Optics.* Singapore: McGraw-Hill Book Co. (Physics Series), international 4th edition

Johnson, S.C. and Moler, C. (1994). Compiling Matlab. *Usenix conference on Very High Level Languages*, Santa Fe, New Mexico, updated Nov 1995.

Jones, S. (1997). Video web inspection – past, present and future. *In* ERA (1997). *Conference on 'web inspection for printing and packaging'.*, ..., 1.1-1.11.

Kahn, J.E. [ed] (1989). *Reader's Digest Reverse Dictionary*, 1st edition, The Reader's Digest Association Ltd, London, pp. 399-400.

Kassim, A.A., T. Tan and K.H. Tan (1999). A comparative study of efficient generalised Hough transform techniques, *Image and Vision Computing,* (17) 10, pp. 737-748.

Kepf, H.-P. (1995). Non-Abrasive Imprinting on Curved Plastics Surfaces. *Kunststoffe Plast Europe,* 85, 7, July, pp. (translation) 13-15/ (DE) pp. 906-909.

Kesidis, A.L. and Papamarkos, N. (2000). On the gray-scale inverse Hough transform, *Image and Vision Computing* (18) 8, pp. 607-618,

Kiddell, P (199#). Understanding the pad in pad printing. [WWW] http://www.padprint1.com/articles/thepad.html (accessed January 2000)

Kiddell, P (1994). Pad Printing: controlling ambient conditions for better quality. *Screen Printing*, July, pp. 94- [WWW] http://www.padprint1.com/articles/ambient.html

Kiddell, P. (1996). Choosing a pad printing machine. *British Plastics and Rubber*, January, pp. 21-27 [+WWW] http://www.padprint1.com/articles/choosemachine.html

King, T.G. and Tao, L.G. (1994). An incremental real-time pattern tracking algorithm for line-scan camera applications. *Mechatronics*, Vol. 4, 5, pp. 503-516.

Kisworo, M., Venkatesh, S. and West, G. (1994). Modeling Edges at Subpixel Accuracy Using the Local Energy Approach. . *IEEE Trans Pattern Analysis and Machine Intelligence*, 16, 4, pp 405-410.

Kurfess, T.R. (1992). Predictive Control of a Robotic Grinding System. *Trans ASME: J. Engineering for Industry*, November, 114, pp. 412-420.

Lan, M.S., Lin, P., Bain, J. (1994). Modeling and control of the lithographic offset color printing process using artificial neural networks. *Trans. of ASME, Journal of Engineering for Industry*, vol. 116, pp.274-276, May 1994.

Langari, R. and Berenji, H.R. (1992). Fuzzy Logic in Control Engineering. *In* White, D.A. and Sofge, D.A. [eds.] (1992). *Handbook of Intelligent Control: neural, fuzzy and adaptive approaches*. NY: Van Nostrad Reinhold.

Langari, R., Berenji, H.R. (1992). Fuzzy logic in control engineering. *In* White, D.A., Sofge, D.A. [eds.] (1992) *Handbook of Intelligent Control: neural, fuzzy and adaptive approaches*, Van Nostrand Reinhold, NY, pp.93-140.

Leavers, V.F. (1992). *Shape detection in computer vision using the Hough transform.* London: Springer-Verlag.

Lee, M., Kittler, J., Wong, K.C. (1992). Generalised Hough transform in object recognition. Proc. 11th IAPR Int. Conf. on Pattern Recognition, IEEE Computer Society Press, vol. 3, pp.285-289.

Legierse, P.E.J. [ed.] (2000). *Intelpadprint, Final Project Report*, Brite/Euram, European Union DG XII, grant BE3180.

Legierse, P.E.J. Witgrefe, F. (1995). *Intelpadprint, the development of an intelligent padprinting system*, project proposal Brite/Euram, European Union DG XII, grant BE3180.

Li, Y.F. and Lau, C.C. (1989). Development of Fuzzy Algorithms for Servo Systems. *IEEE Control Systems Magazine*, 9, 3, April, pp. 65-71.

Lindeberg, T. (1998). Edge Detection and Ridge Detection with Automatic Scale Selection. Internat. J. Computer Vis., 30(2), pp. 117-154.

Lippmann, R.P. (1987). An Introduction to Computing with Neural Nets. *In* Bezdek and Pal, 5.1 pp.417-435, and *IEEE ASSP Mag*., April, pp.4-22.

Liu, G.P., Kadirkamanathan, V. and Billings, S.A. (1998). Predictive Control for non-linear systems using neural networks. *Int J. Control*, 71, 6, pp. 1119-1132.

Long, G. (1997). Keynote Address. *In* ERA (1997). *Conference on 'web inspection for printing and packaging'*., ..., C.1-2

Ma, D., Chen, X. (1988). Hough transform using slope and curvature as local properties to detect arbitrary shapes. *Proc. 9th Int. Conf. on Pattern Recognition*, pp.511-513.

Mallat, S.G. (1989). A Theory for Multiresolution Signal Decomposition: the Wavelet Representation. *IEEE Trans. Pattern Analysis and Machine Intelligence*, 11, 7, July, pp. 674-692.

MARC (1996). *Nonlinear Finite Element Analysis of Elastomers*. MARC Analysis Research Corporation, Palo Alto, CA.

MARC (1997). *Volume A: Theory and User Information*. MARC Analysis Research Corporation, Palo Alto, CA. (Version K7, RF-3001-07).

Margolis, J.M. [ed.] (1986) *Decorating Plastics*. Hanser Publishers, ISBN 3-446-14698-9.

Massopust P.R. (1994). *Fractal Functions, Fractal Surfaces and Wavelets*.

Mathworks Inc. (1993). *MATLAB Image Processing Toolbox User's Guide*. MA: The Mathworks Inc.

McCulloch, W.S., Pitts, W. (1943). A Logical Calculus of the Ideas Imminent in Nervous Activity. *Bulletin of Mathematical Biophysics*, 5, pp.115-133.

McMahon, D. (2000). *Rapid Application Development with Visual C++*. McGraw-Hill.

McQueen, M.P.C. (1981). A generalization of Template Matching for recognition of real objects. *Pattern Recognition*, 13, 2, pp. 139-145.

Milgram, M., Dubuisson, B. and Vachon, B. (1977). A computationally efficient clustering algorithm. *IEEE Trans. Systems Man Cybern.* 7, pp. ?.

Morison, C.N., Li, W., Freear, N.D., Shippen, J.M. (1998). Deformation Analysis of the Pad Printing Process by Finite Element Methods. *Unpublished paper*

Morrison, L. [ed] (1999). *Printing: 1999 Market Report*. Middlesex: Key Note Ltd., 5th ed.

Morton, R.A. [ed.] (1984). *Photography for the Scientist*. 2nd edition, London: Academic Press, Harcourt Brace Jovanovich Publishers.

Mottram, J.T. and Shaw, C.T. (1996) *Using Finite Element Analysis in Mechanical Design*. inter lib

Nagao, M. and Matsuyama, T. (1979). Edge preserving smoothing. *Comput. Graph. Image Process.* 9, pp. 394-407.

Nagel, R.N. and Rosenfield, A. (1972). Ordered Search Techniques in Template Matching. *Proc. IEEE*, 60, pp. 242-244.

Nayar, S.K., Fang, Y,-S., Boult T. (1997). Separation of Reflection Components Using Color and Polarisation. *International Journal of Computer Vision*, Kluwer Academic: The Netherlands, 21(3), pp.163-186.

OCCAA (1984). *Surface Coatings: volume 2: paints and their applications*. Tafe Educational Books, Randwick, Australia, 2nd ed. Prepared by the Oil and Colour Chemist's Assoc., Australia.

ODVA (1997). *What is the* [sic] *DeviceNet?* Open DeviceNet Vendor Association. devnet1.htm

ODVA (1999). *CAN and DeviceNet,* Florida: Open DeviceNet Vendors Association, Inc. [WWW] http://www.odva.org/ABOUTDN/over6.htm (6 May 1999)

Paler, K., Foglein, J., Illingworth, J. and Kittler, J. (1984). Local ordered grey levels as an aid to corner detection. *Pattern Recogn.* 17, pp. 535-543.

Parker, E. (1997). *A new technique to measure the dynamic elastic constants of rubber under load.* Birmingham: University of Birmingham, PhD (839), Electronic and Electrical Engineering.

Passino, K.M. and Yurkovich, S. (1998). *Fuzzy Control.* California: Addison Wesley Longman.

Paton, K. (1979). Line Detection by Local Methods. *Computer Graphics and Image Processing*, 9. pp. 316-332.

Pattison, T. (1998). *Programming Distributed Applications with COM and Microsoft Visual Basic 6.0.* Microsoft Press, [E-mail attachment] indistri.chm.

Philipp, Wilfried (1984). *Tampondruckmaschine*. Patent no. (Anmeldenummer) 84111505.8 (Veröffentlichungsnummer: 0140165), European Patent Office, DE.

Phillips, M. (1997, 810). *Caching for Image Processing*. Birmingham: University of Birmingham, PhD, Electronic and Electrical Engineering.

Pitas, I. (1993). *Digital Image Processing Algorithms*. London: Prentice Hall

Pratt, P.J. and Adamski, J.J. (1994). *Database Systems: management and design*. MA: Boyd and fraser, 3rd ed.

Pugh, S. (1991). *Total Design*. Prentice Hall.

Ray, S.F. (1984). Photographic Optics. *In* Morton, R.A. [ed.]. *Photography for the Scientist*. 2nd edition, London: Academic Press, Harcourt Brace Jovanovich Publishers, part 2, 87-167.

Ray, S.F. (1994). *Applied Photographic Optics: lenses and optical systems for photography, film, video and electronic imaging*. 2nd ed. (1988), Focal Press (Reed Elsevier), Oxford.

Reichmann, R. (2000). Product printing: its your choice. *British Plastics and Rubber*, January, pp. 12-13.

Roberts, G. (1995). *Mastering Photography.* Macmillan Publishers.

Rosenfeld, A. (1979). Fuzzy Digital Topology. *Inform. Control*, vol. 40, no. 1, pp.76-87, January *& In* Bezdek, Pal [eds.] (1992).

Rosenfield, A. and VandeBrug, G.J. (1977). Coarse-fine template matching. *IEEE Trans. Systems Man Cybern.* 7, pp. 104-107.

Russell and Wong, (1989). An application of computer vision to lace cutting. *Robotics and Autonomous Systems*, Vol. 5, pp. 91-96.

Scher, D. (1997). How to print flat artwork on to curved objects. *British Plastics and Rubber*, January, pp. 25-27.

Ser, P.-K., Siu, W.-C, (1994). Non-analytic object recognition using the Hough transform with matching technique. IEE Proc. Part E, Computers and Digital Techniques, 141 (1) pp. 11-16.

Ser, P.-K., Siu, W.-C. (1992). A rotation invariant generalized Hough transform for image recognition. IEE Proc. Comput. Digit. Tech., pp.231-235.

Sherman, L.M. (1996). Printing on parts. *Plastics Technology*, 42, 4, April, pp. 68-71.

Shippen, J.M., Westra, R.L. and Freear, N.D. (1999). A Parallel Hardware Multiple Microprocessor Asynchronous Neural Network Architecture for Control Applications. *7th European Congress on Intelligent Techniques and Soft Computing* (EUFIT), Aachen, DE, p116.

Shoureshi, R. (1993). Intelligent Control Systems: are they for real?. *Trans ASME: J. Dynamic Systems, Measurement and Control,* June, 115, pp. 393-401.

Slade, A. (1993). *Mechatronics Applied to Scale Model Decoration.* MPhil thesis, University of Loughborough, Department of Mechanical Engineering (NAFEMS).

Smith, J.R. (1997). Shine a light. *Image Processing,* April '97, 20-23.

Sonka, M., Hlavac, V. and Boyle, R. (1993). *Image Processing, Analysis and Machine Vision.* London: Chapman and Hall.

Stroustrup, B. (1991). *The C++ Programming Language.* New Jersey: AT&T Bell Laboratories, 2nd ed.

Sutton, R. and Jess, I.M. (1991). A design study of a self-organizing fuzzy autopilot for ship control. *I: J. Systems and Control Engineering, Proc Instn Mech Engrs*, 205, pp. 35-47

Tabanis, K., Tsai, R.Y. and Allen, P.K. (1994). Analytical Characterization of the Feature Detectability Constraints of Resolution, Focus, and Field-of-View for Vision Sensor Planning. *Image Understanding*, 59, 3, pp. 340-358.

Tampoprint (1996). *Tamponliste (catalogue of rubber printing pads).* Tampoprint GmbH, Germany.

Theuwissen, A.J.P. (1994). CCD imaging. *Philips J. Res.* 48, pp 147-158.

Thomas, A.D.H. (1993). Compressing the parameter space of the generalised Hough transform. *Pattern Recognition Letters*, 13 (2) pp.107-112.

Truchetet, F. and Cholley, J.P. (1997). Tampoprint Quality Control By Artificial Vision. *Materials Evaluation*, 55 (12), pp. 1361-1366.

Ulsoy, A. Galip and Koren, Y. (1993). Control of Machining Processes. *Trans ASME: J. Dynamic Systems, Measurement and Control*, June, 115, pp. 301-308.

Vandebrug, G.F. and Rosenfeld, A. (1977). Two-Stage Template Matching. *IEEE Trans. Computers*, C-26, 4, pp. 384-393.

Vernon, D. (1991). *Machine Vision – Automated Visual Inspection and Robot Vision,* Prentice-Hall International: London.

Vetter, J.P. (1984). Photomicropgraphy. *In* Morton, R.A. (ed.) *Photography for the Scientist.* 2nd edition, London: Academic Press, Harcourt Brace Jovanovich Publishers, 8, pp.393.

Westra, R.L, Freear, N.D, and Shippen, J.M. (1999). Printing Quality Control Using Template Independent Neuro-Fuzzy Defect Classification. *7th European Congress on Intelligent Techniques and Soft Computing* (EUFIT), Aachen, DE, p117.

Westra, R.L. (2001). *Real-time Quality Control using Interactive Vision.* PhD thesis, University of Maastricht, Netherlands, ISBN 90-5278-326-8.

Wetherill, G.B. and Brown, D.W. (1992). *Statistical Process Control: theory and practice.* London: Chapman and Hall.

White, D.A., Sofge, D.A. (1992). *Handbook of Intelligent Control: neural fuzzy and adaptive approaches*, Van Nostrand Reinhold, NY.

Williams, A.R. (1984). Close-up Photography and Photomacrography. *In* Morton, R.A. [ed.] *Photography for the Scientist.* 2nd edition, London: Academic Press, Harcourt Brace Jovanovich Publishers, 7, pp. 355-391.

Window, A.L. and Holister, G.S. (eds.) (1982). *Strain Gauge Technology*. Essex: Applied Science Publishers Ltd.

Yang, G. Z.; Burger, P.; Firmin, D. N.; Underwood, S. R. (1996). Structure adaptive anisotropic image filtering. *Image and Vision Computing*, v 14, 2, March, pp. 135-145.

Zadeh, L.A. (1965). Fuzzy Sets. *Inform. Control*, vol. 8, no. 1, pp. 338-353 *& In* Bezdek, Pal [eds.], 1992.

Zak, S.H. and Blouin, E.E. (1993). Ripple-Free Deadbeat Control. *IEEE Control Systems Magazine*, August, pp. 51-56.

[171]

Appendix I: Example images of test B printing faults with inverted ghosts

The format of the filename is: xxxxx-OCAP_NO-SAMPLE_NO.jpg

The 'score' is: $\frac{1}{N\,M}\sum\sum|R-I|$

IPPtestB-00-00.jpg score: 0.93851

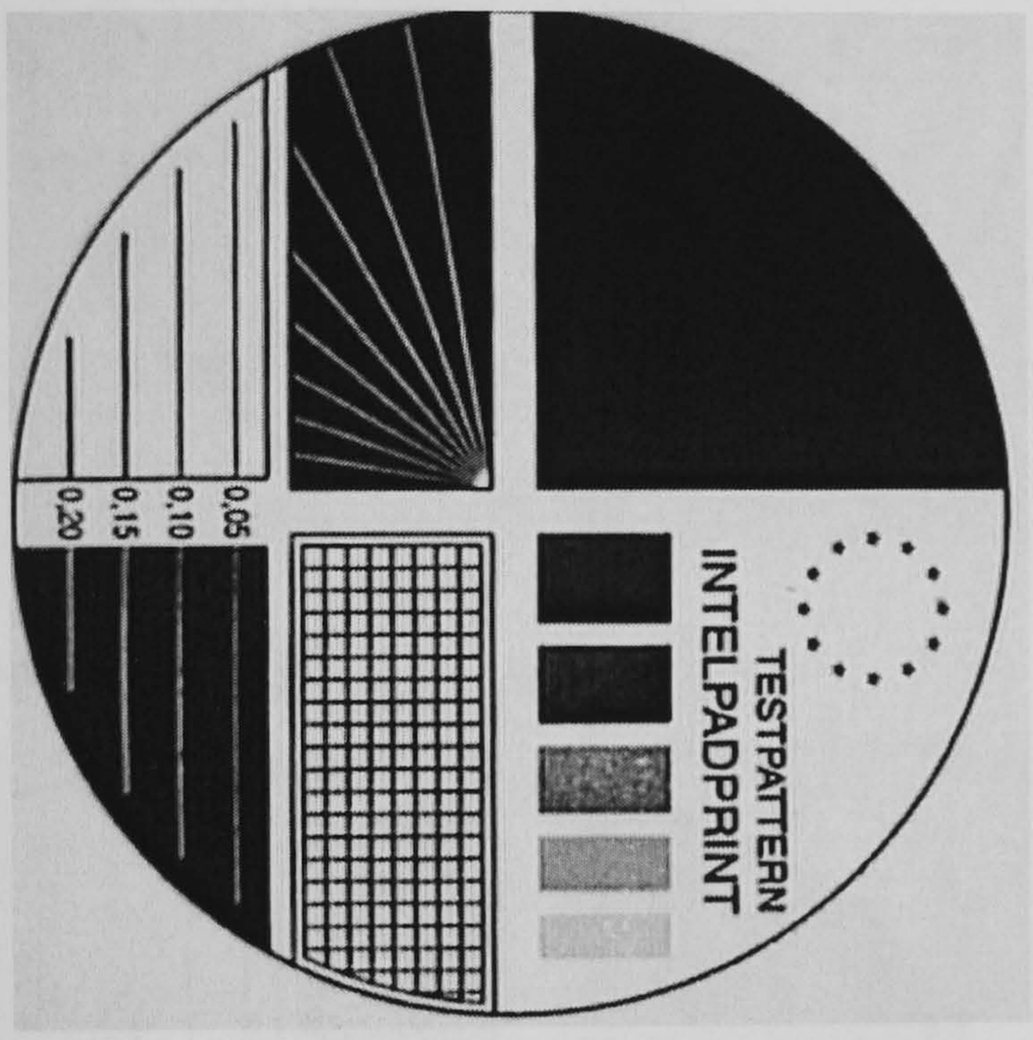

Good graphic

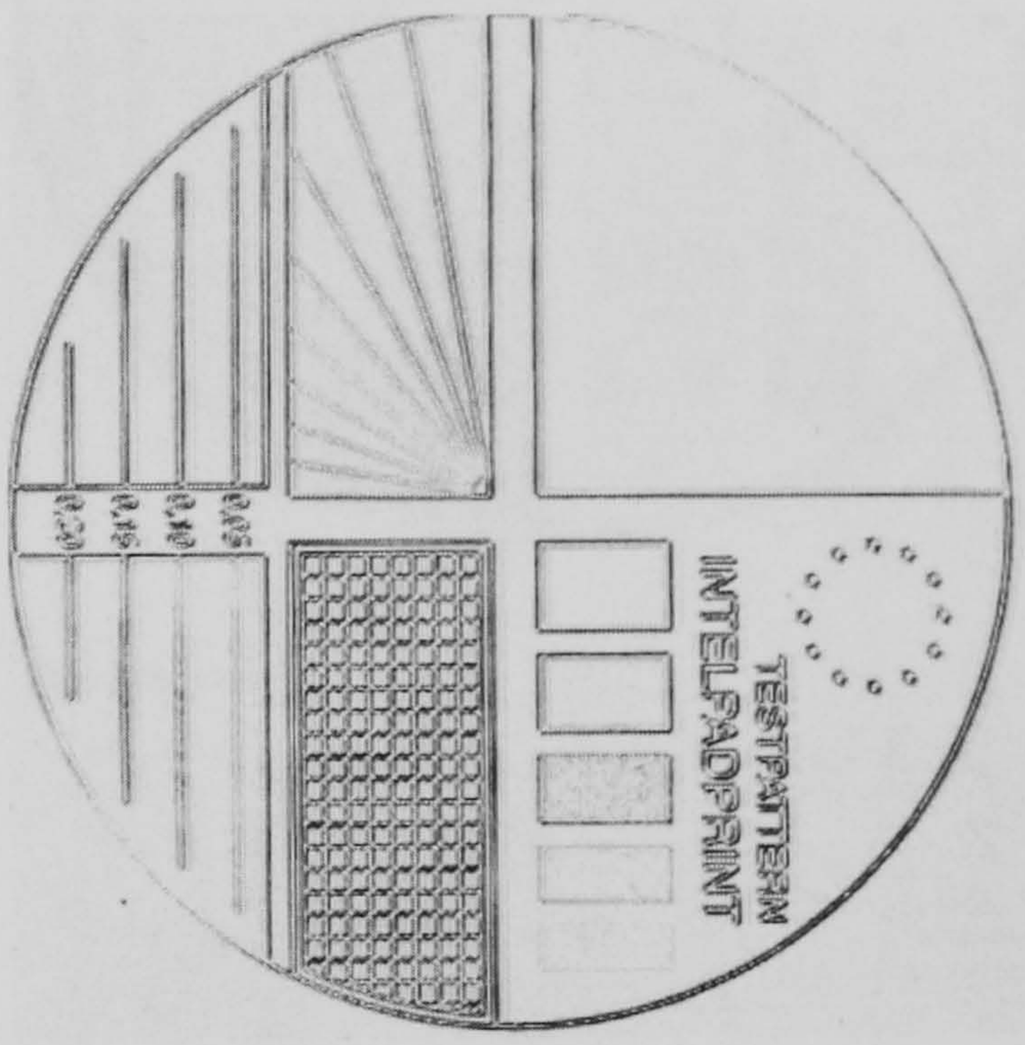

IPPtestB-01-00.jpg score: 0.89202

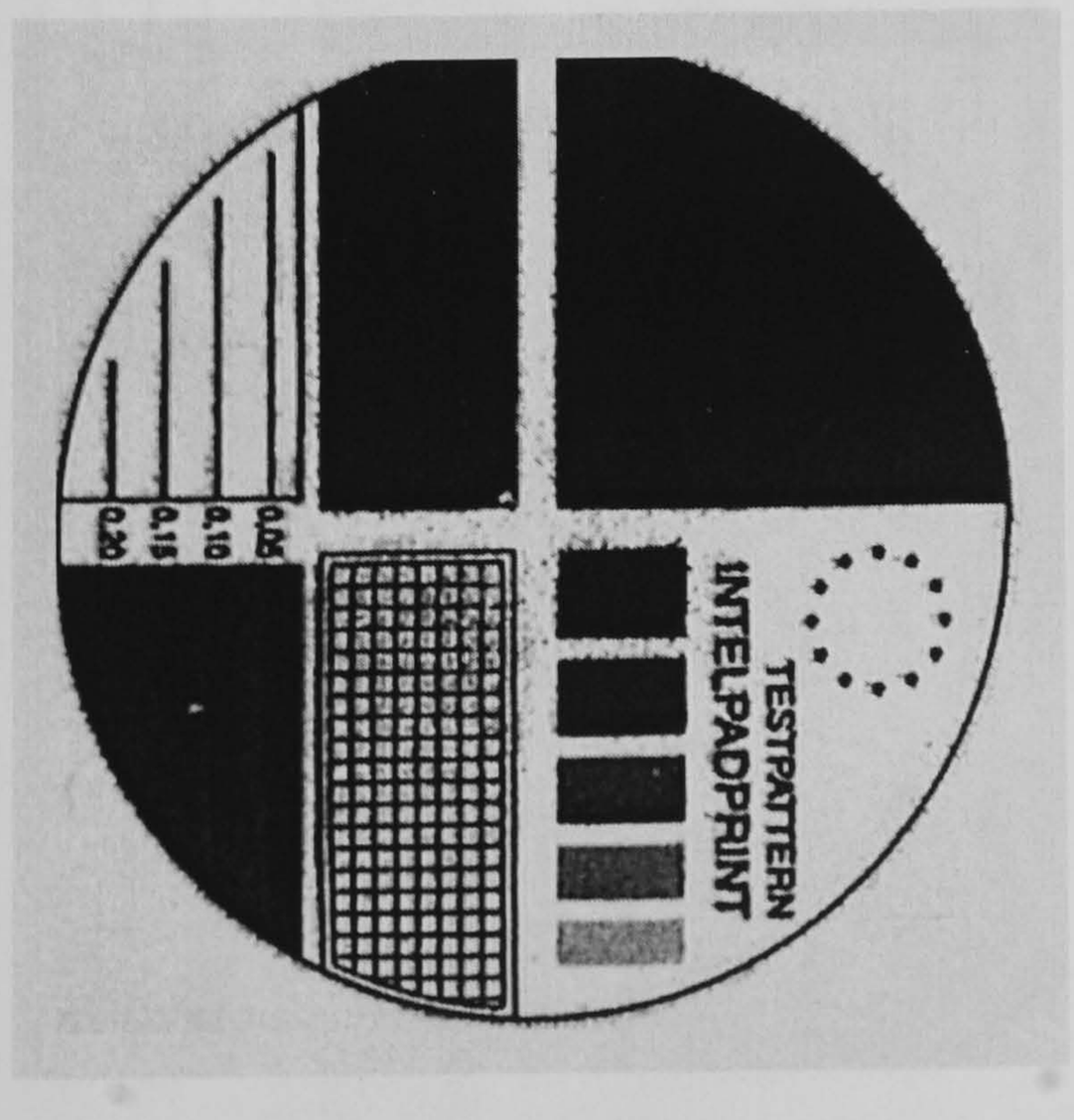

Hairs

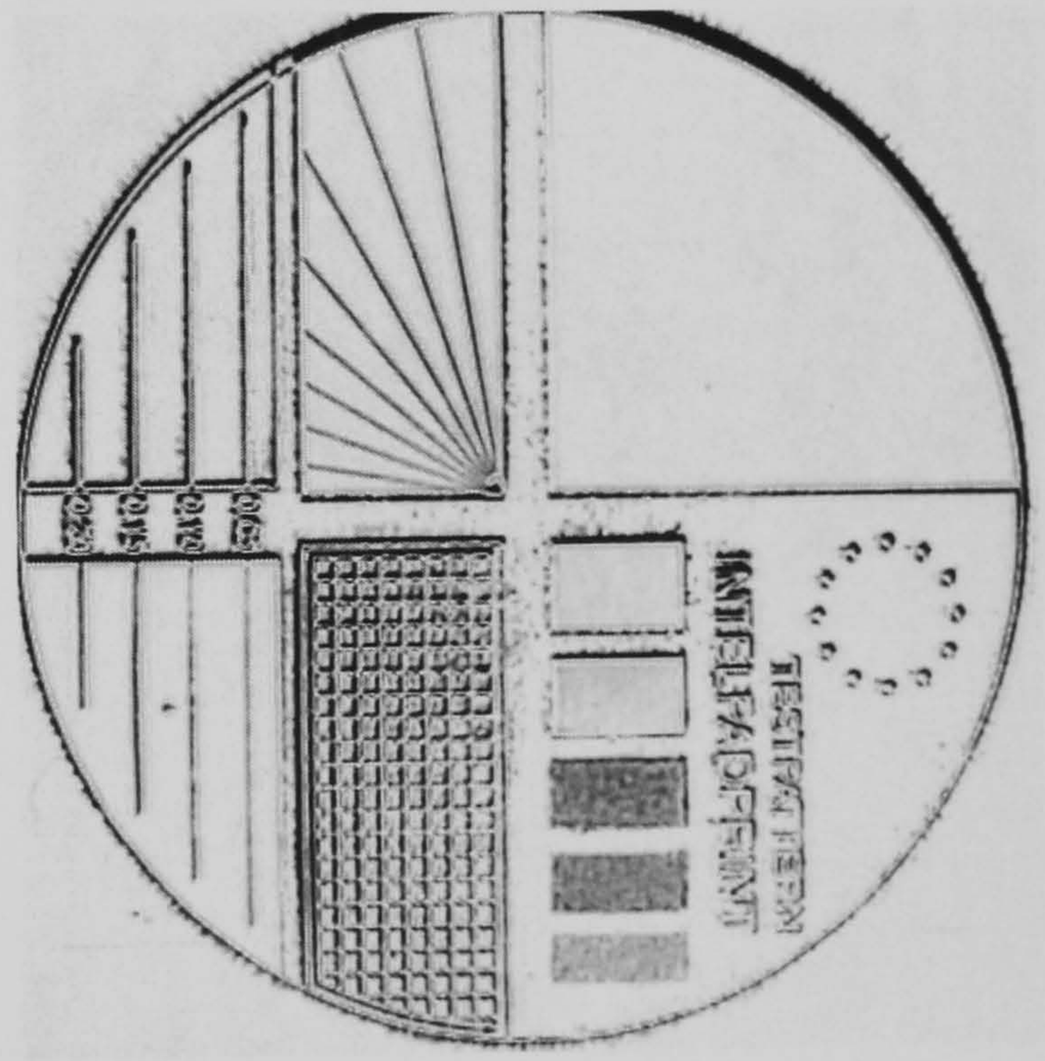

IPPtestB-02-01.jpg score: 0.86947

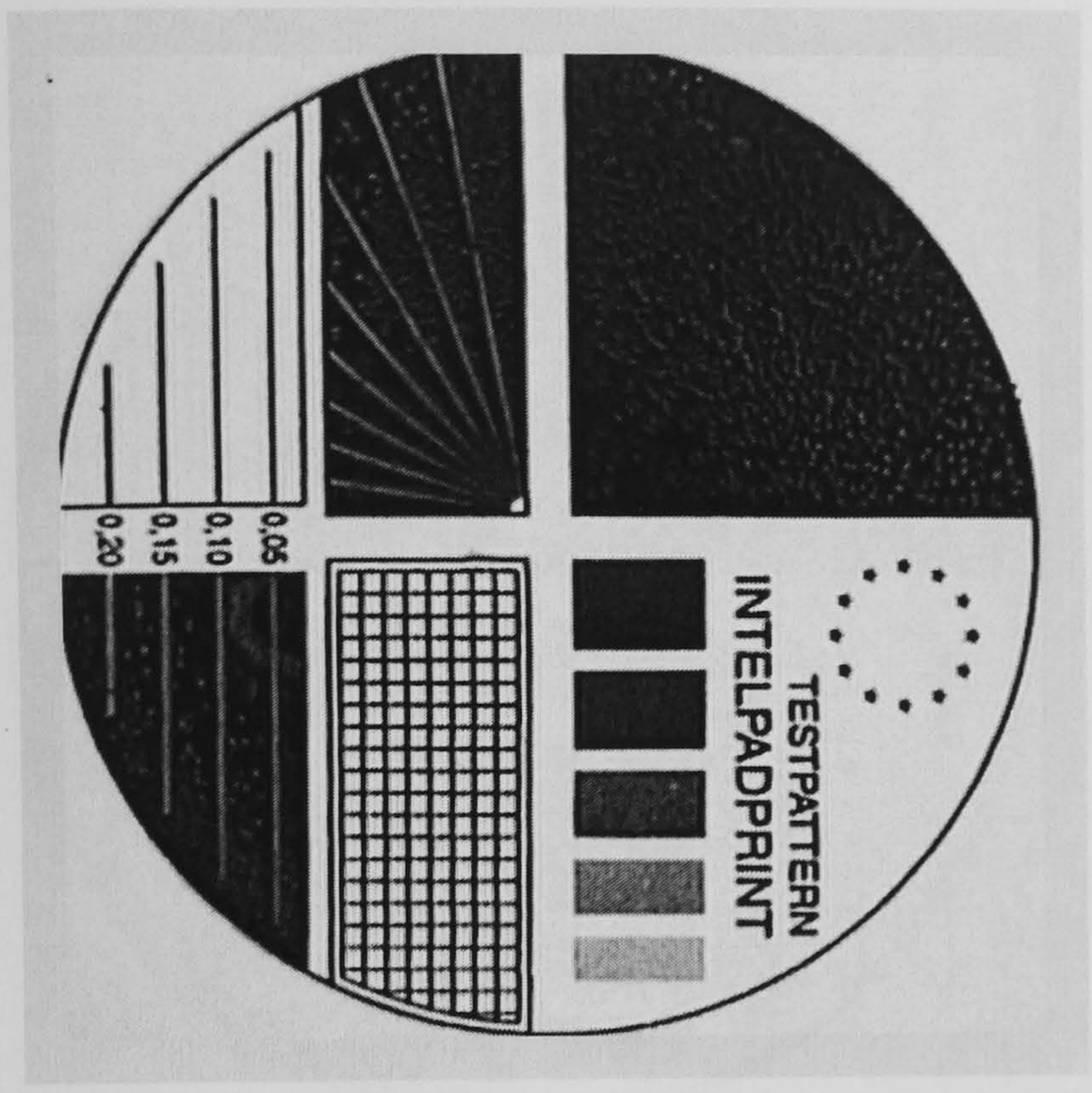

Air bubbles

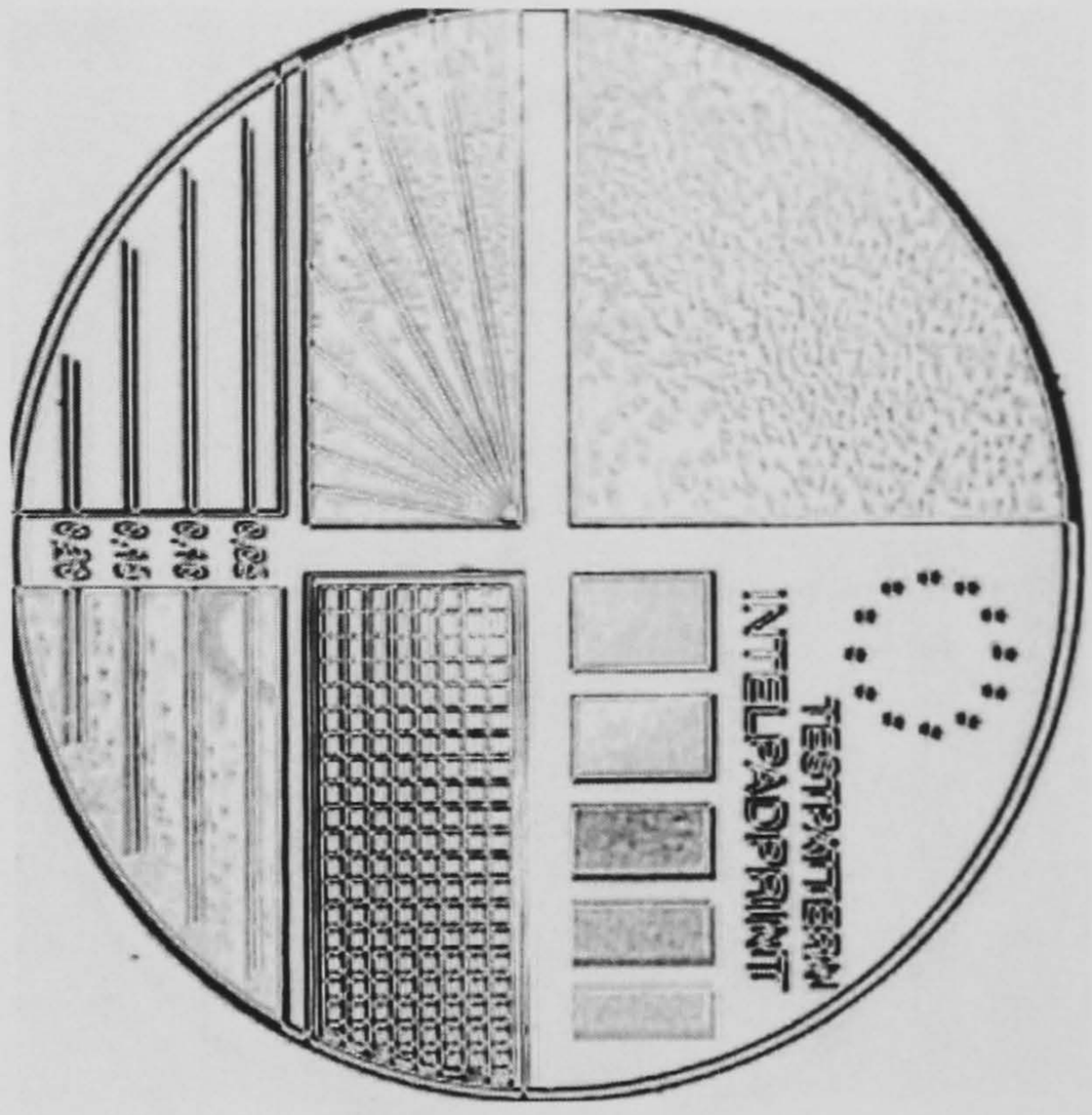

IPPtestB-05-00.jpg score: 0.91733

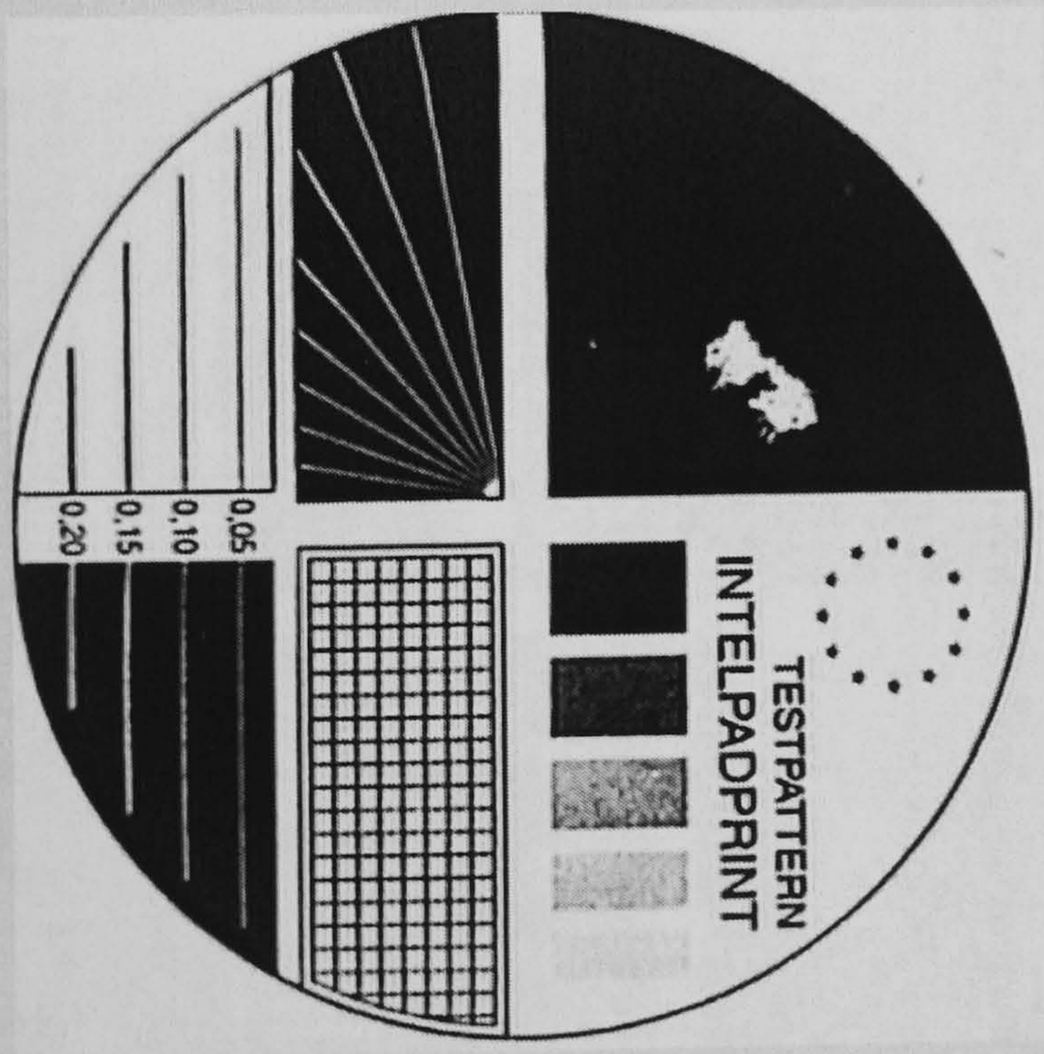

Ink missing

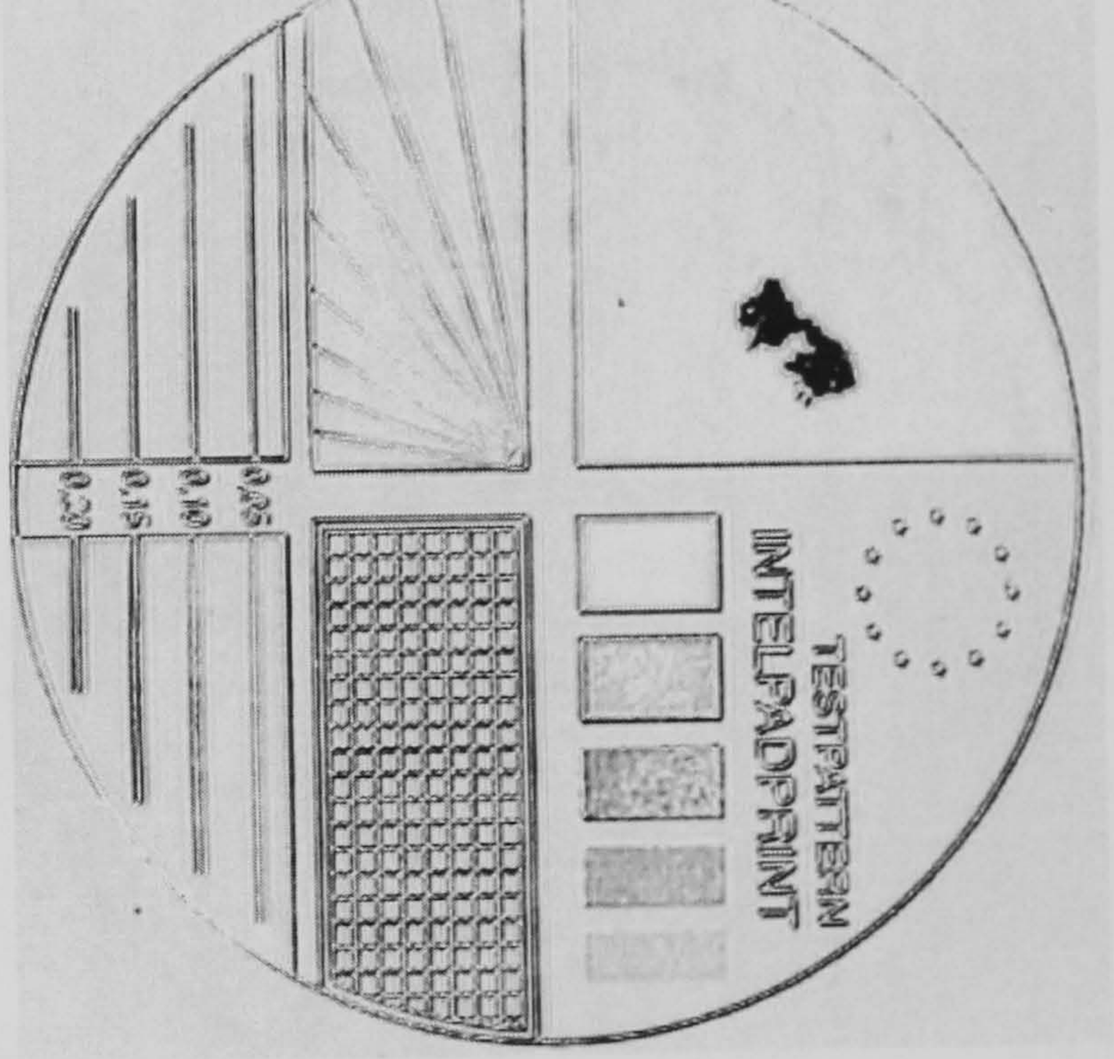

IPPtestB-07-00.jpg score: 0.86957

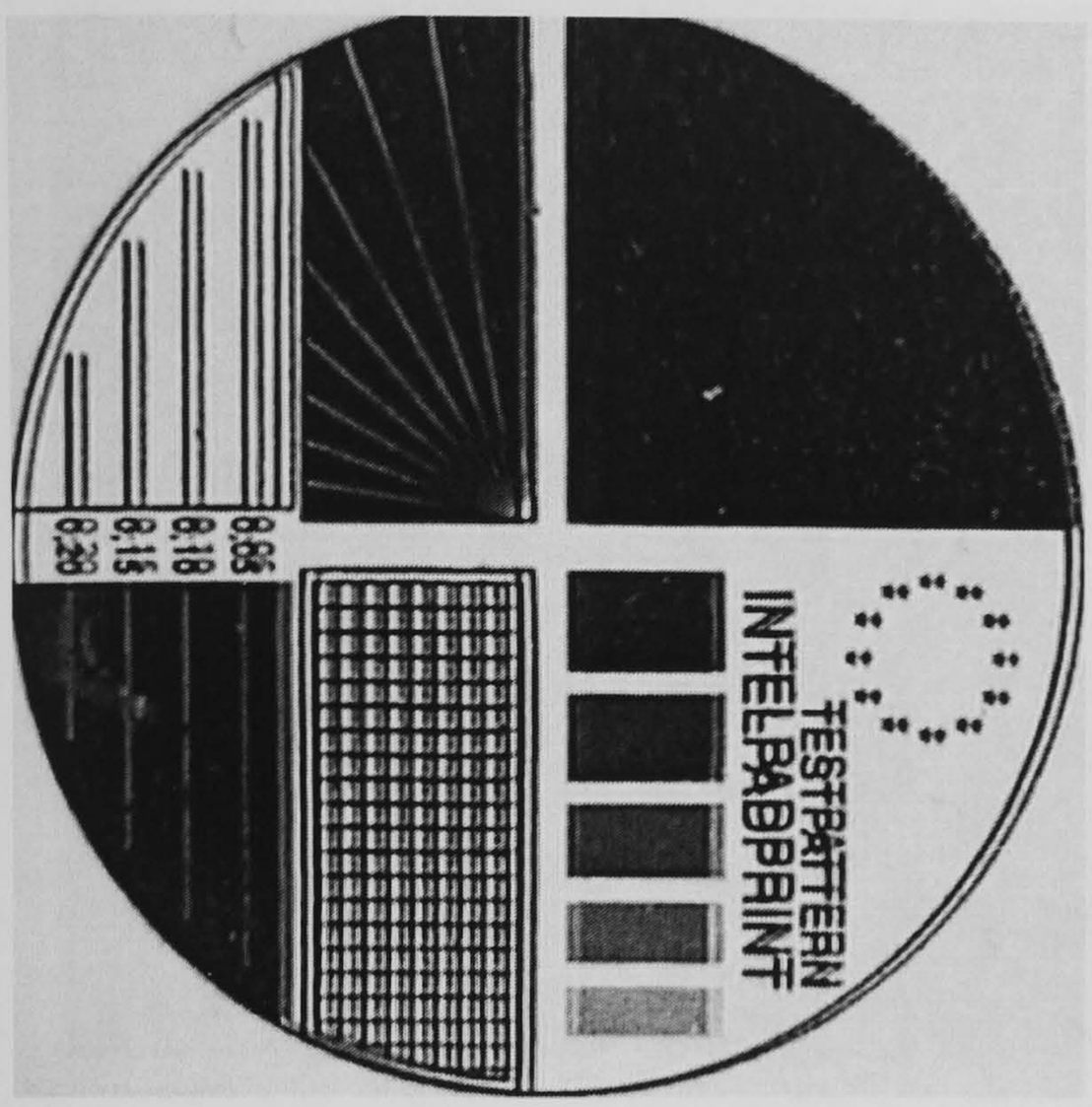

Dirt particles (also mis-registration of double print)

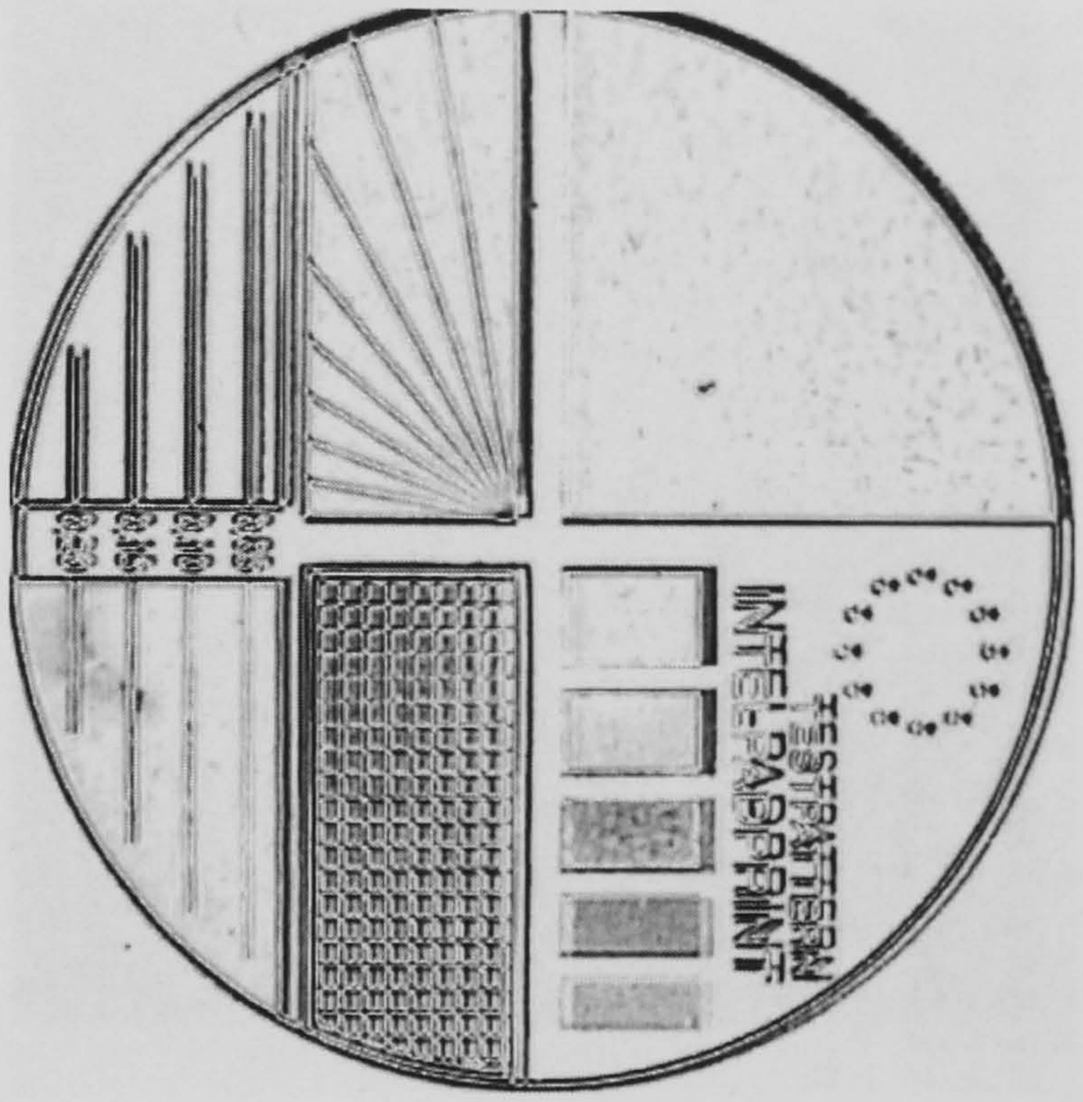

IPPtestB-10-00.jpg score: 0.8949

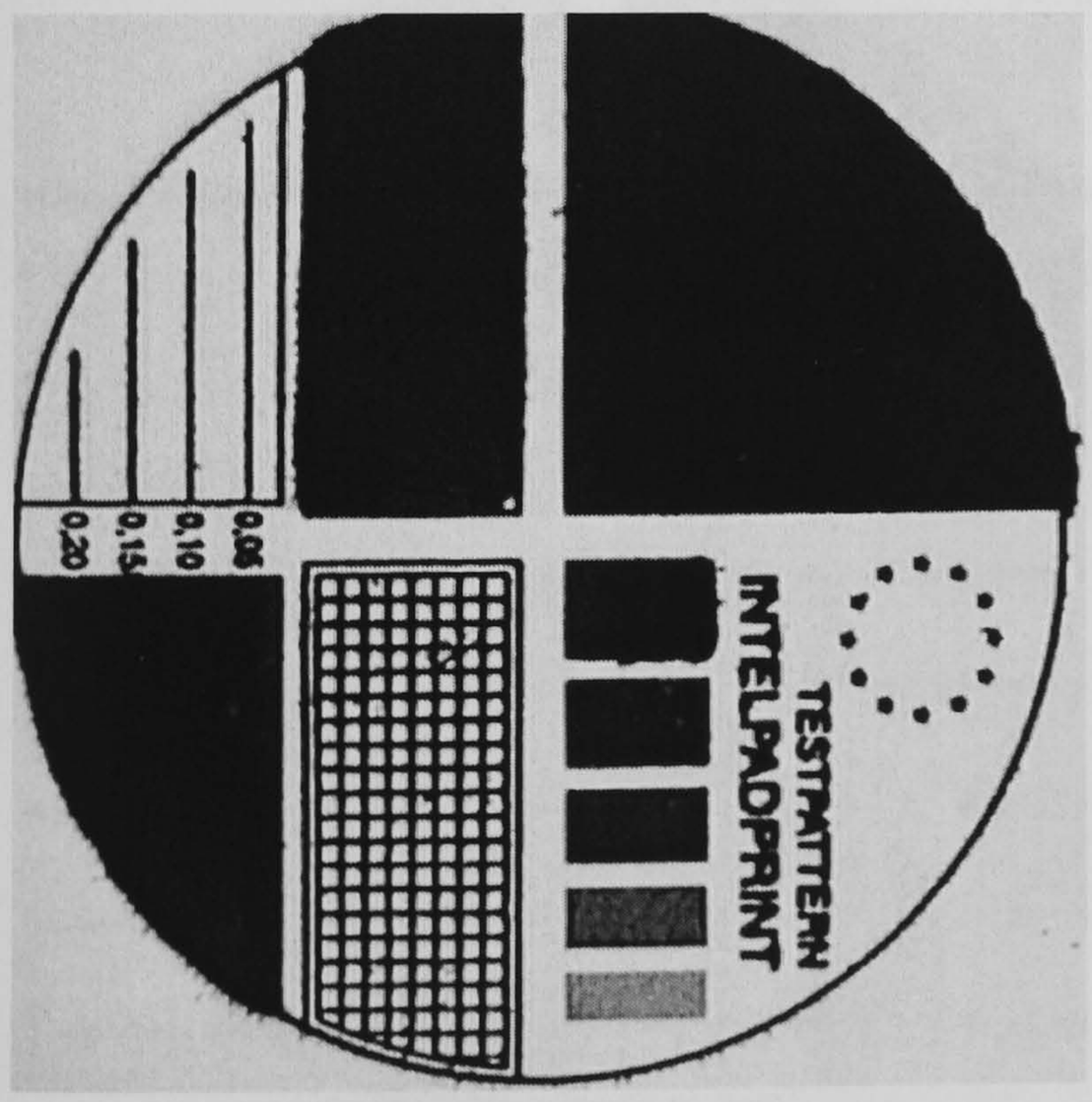

Smearing

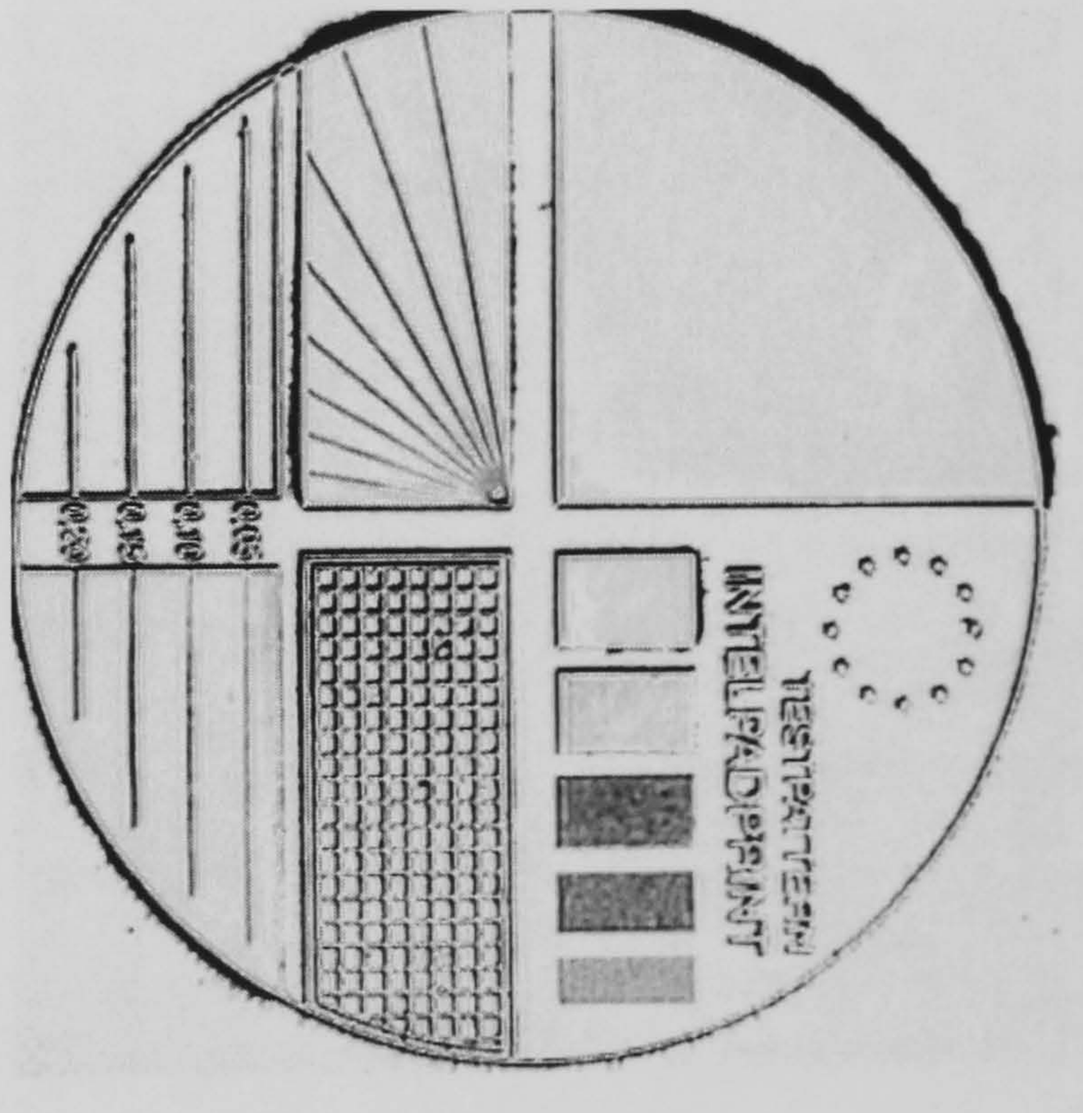

IPPtestB-12-12.jpg score: 0.73174

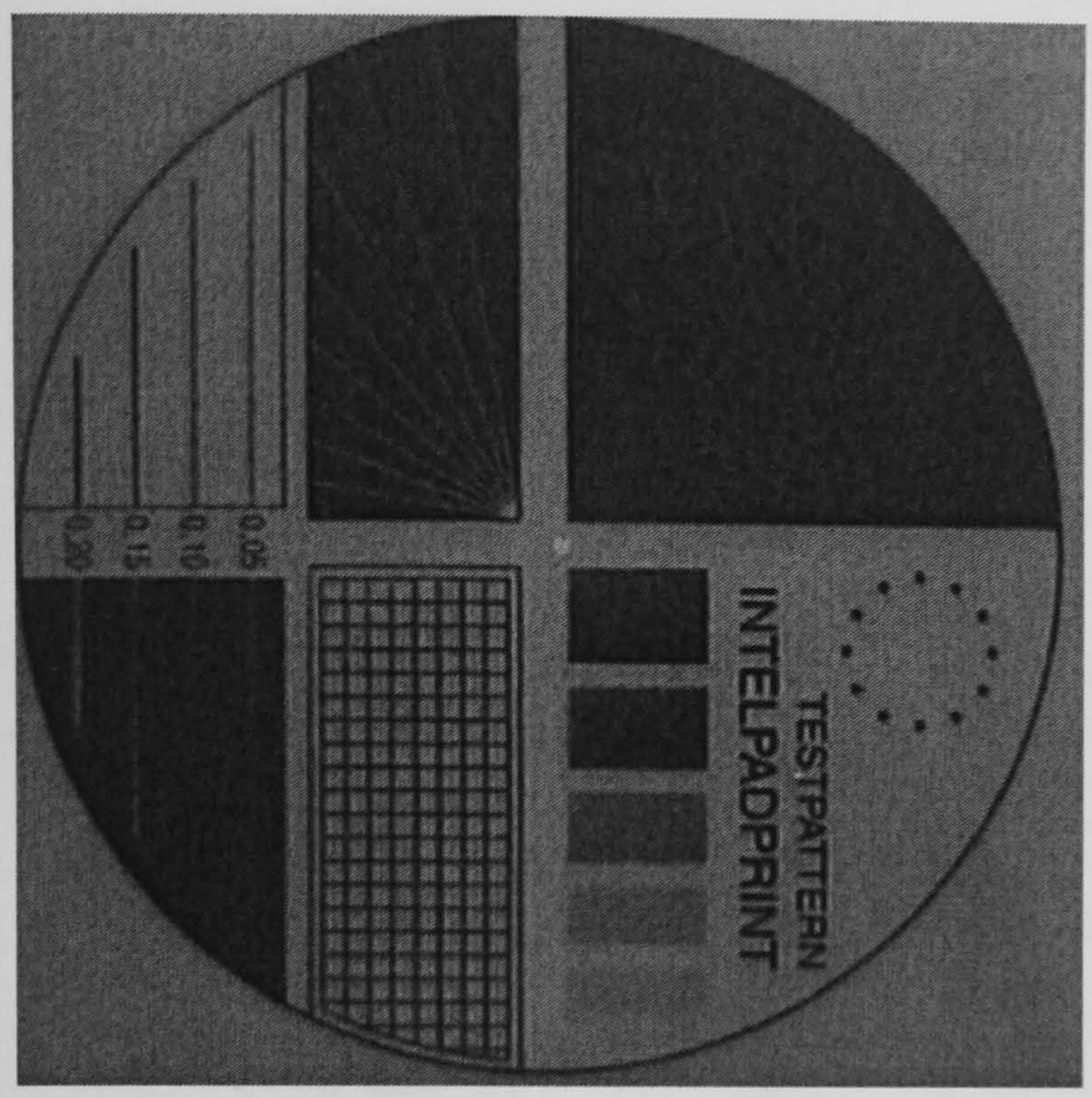

Colour differences (? – wrong substrate colour)

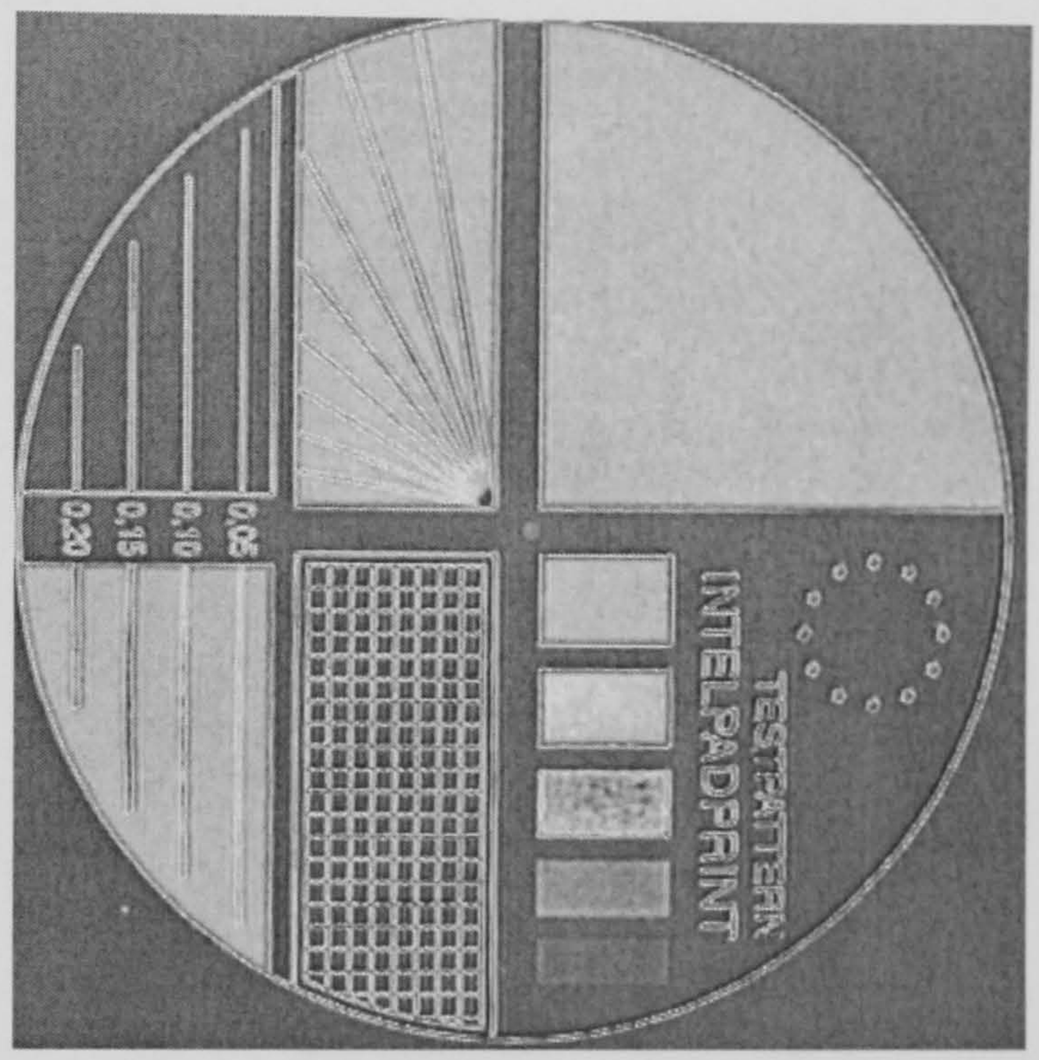

IPPtestB-15-00.jpg score: 0.84377

Streaks

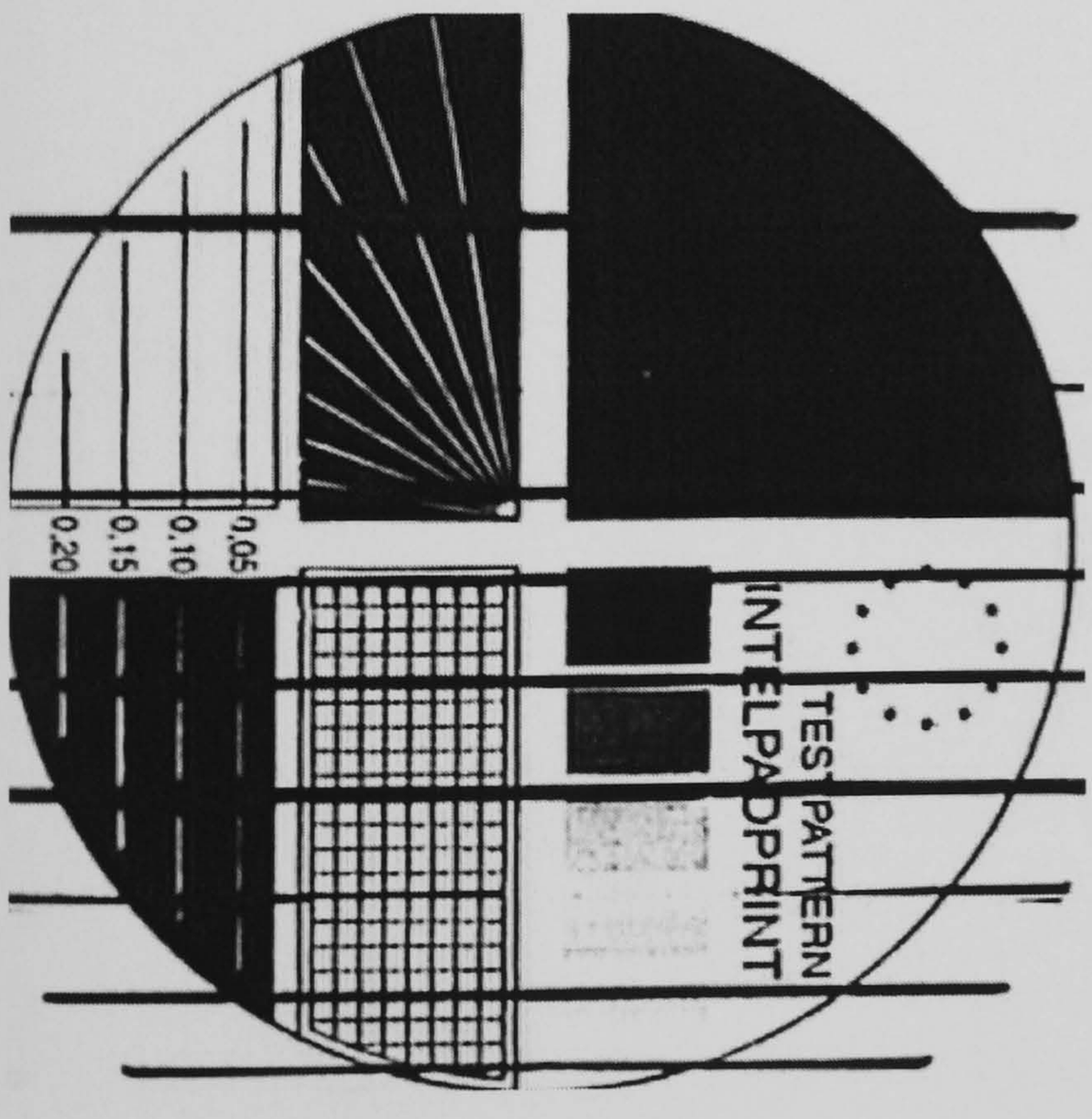

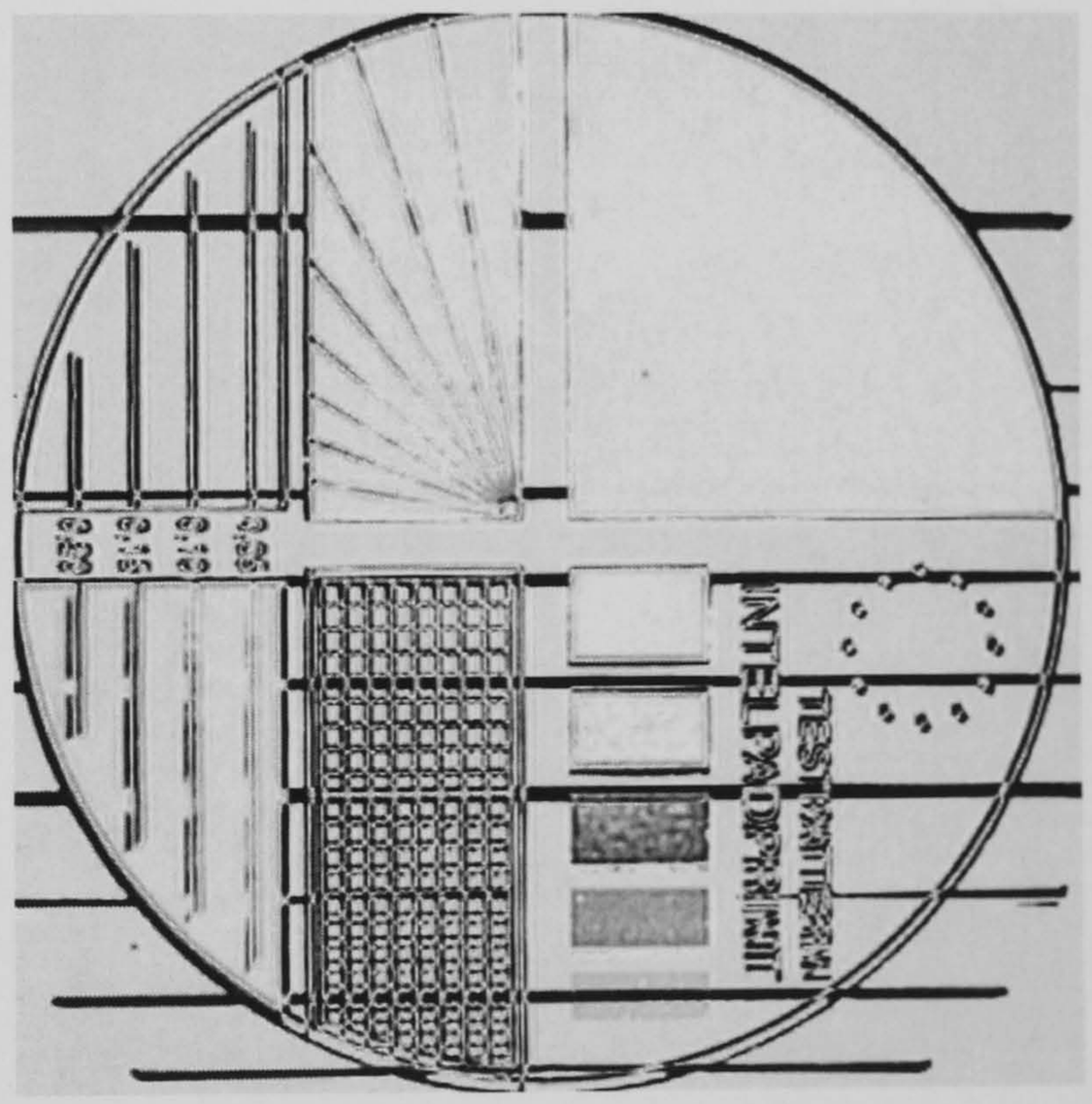

IPPtestB-16-00.jpg score: 0.85128

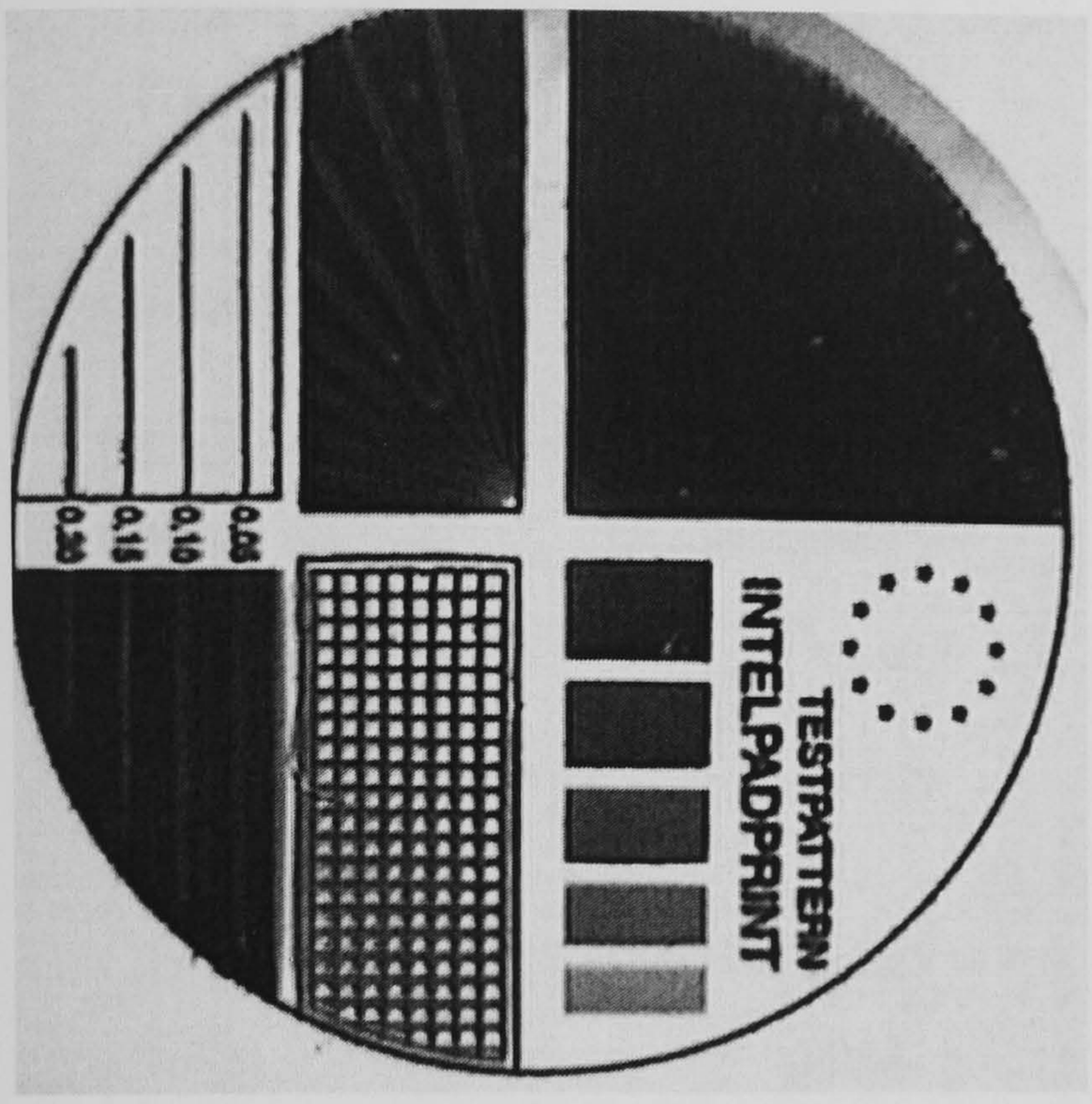

Haze

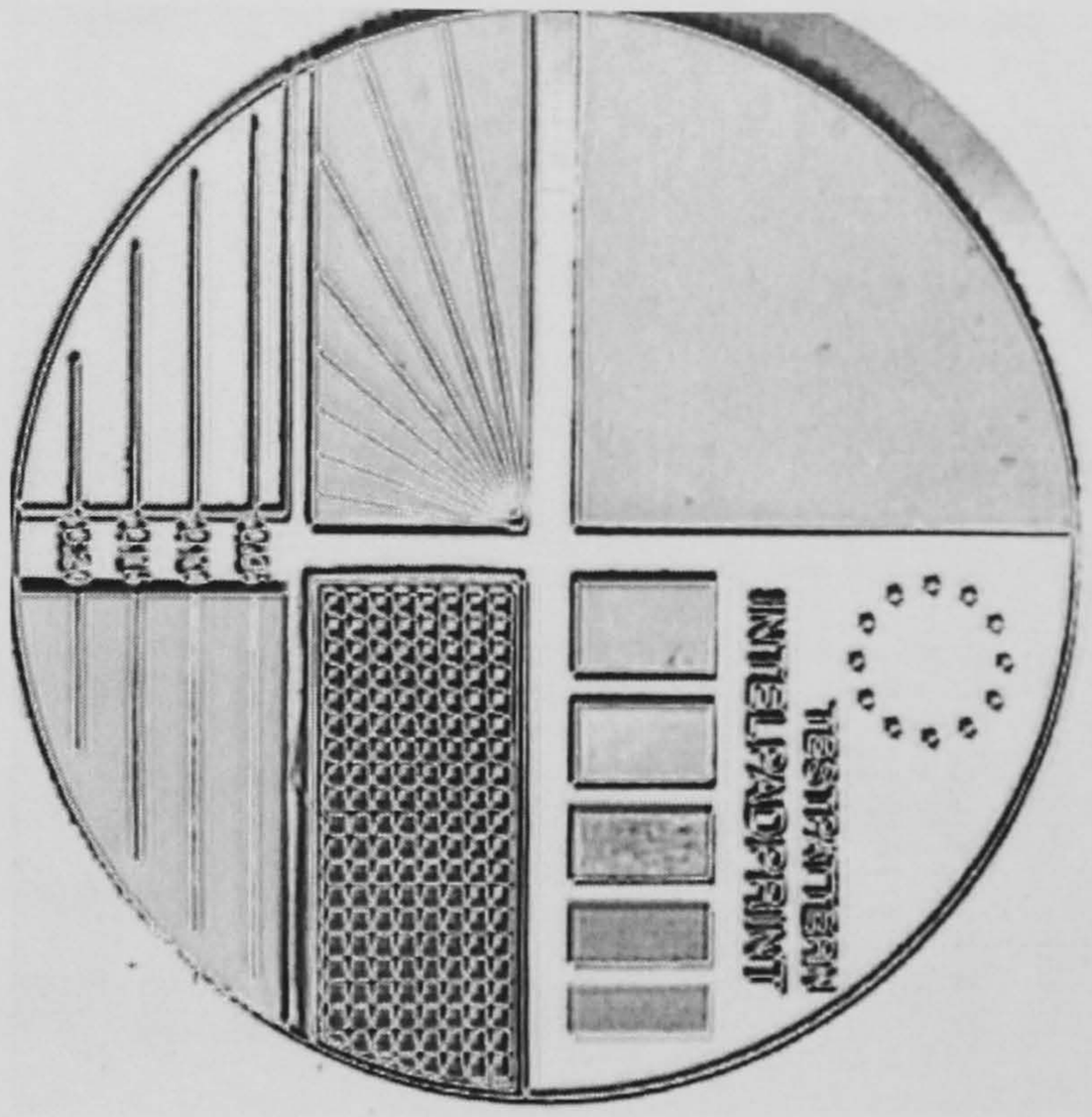

Appendix II: Tampoprint's pad-coding system

Printing pad article number: 0X–X–XXX (quality equiv.)–(hardness equiv.)–Mould no

[Tampoprint, 1996]

Quality (attribute)

Component of article no	Quality	Rubber colour	Suitability
05 –	Q 1	Yellow	Standard printing
06 –	Q 2	White	Aggressive colours, limited mech. endurance
07 –	Q 3	Red-brown	Maximum mechanical endurance
08 –	Q 4	Black	Low static charge, as Q 3

Shore hardness

Component of article no	Approximate Shore A	Base colour	Suitability	Availability
– 2 –	~ 1	Blue		Q 1, 3, 4
– 3 –	~ 3	Red	Delicate substrates	Q 1, 3, 4
– 4 –	~ 6	Green	Standard	Q 1 - 4
– 5 –	~12	White	Parts with textured surfaces	Q 1 - 4
– 6 –	~18	Black	Flat tampons, large parts	Q 2 - 4

Mould number

Component of article no	Shape, dimensions	Pad base – see tampon list

– XXX	See tampon list	AP aluminium, HP wooden

Examples comparing Tampoprint material test-sample designations with equivalent article numbers:

Q3 i5 6 (Shore)	07–4–XXX
Q1 i 12 (Shore)	05–5–XXX